KU Leuven
Biomedical Sciences Group
Faculty of Movement and Rehabilitation Sciences
Department of Movement Sciences

IDENTIFYING THE LIMITATIONS IN BALANCE CONTROL OF ELDERLY USING PREDICTIVE SIMULATIONS OF HUMAN POSTURE AND GAIT

Maarten Afschrift

Jury:

Promoter:	Prof. dr. I. Jonkers
Co-promoter:	Prof. dr. F. De Groote,
	Prof. dr. J. De Schutter
Jury members:	Prof. dr. J.Orban de Xivry
	Prof. dr. B. Vanwanseele
	Prof. dr. S. Verschueren
	Prof. dr. L. Ting
Chair:	Prof. dr. F. Boen
Secretary:	Prof. dr. E. Boffé

Dissertation presented in partial fulfilment of the requirements for the degree of Doctor in biomedical sciences

August 2018

Table of contents

1 Summary **5**

2 General introduction **13**

Reactive control of balance 14

Strategies for reactive control of balance during standing and walking 17

Effects of aging on reactive balance control strategies - experimental studies 18

Effects of aging on reactive balance control strategies - simulation studies 20

Objectives 22

3 General methodology **27**

4 Mechanical effort predicts the selection of ankle over hip strategies in non-stepping postural responses **43**

5 Modulation of gluteus medius activity reflects the potential of the muscle to meet the mechanical demands during perturbed walking **63**

6 Increased sensory noise and not muscle weakness explains changes in non-stepping postural responses following stance perturbations in healthy elderly **83**

7 Increased use of stepping strategy in response to medio-lateral perturbations in the elderly relates to altered reactive tibialis anterior and not gluteus medius activity **95**

8 General discussion **111**

Specific conclusions 113

General discussion and conclusions 118

Limitations 124

Future work 127

9 Dankwoord **131**

10 General appendix **135**

11 Appendix: simulation standing balance control **149**

12 Appendix: simulation walking balance control **165**

13 Appendix: the effect of muscle weakness on the capability gap during gross motor function: a simulation study supporting design criteria for exoskeletons of the lower limb **175**

Chapter 1

Summary

To most of us, standing and walking are easy. This is remarkable, given the fact that standing and walking are highly unstable and therefore require active control. This becomes apparent in the elderly. There is a high incidence of falls in the elderly, often resulting in significant injuries and loss of independence. Deterioration in balance control may contribute to increased fall risk in older adults. However, correlations between age-related decrease in balance performance and the incidence of falling only provide limited insight in the underlying mechanisms by which aging alters balance control. An improved understanding of age-related changes in balance control and the contribution of changes in the neural and muscular system to balance control could improve therapeutic approaches aiming at fall prevention. These insights may then steer neuromuscular training programs to target the age-related changes that affect balance control most.

The main aim of this PhD was to identify the changes in sensory and muscle function that contribute most to the observed differences in balance control in perturbed standing and walking in older compared to young adults. To this aim, a blended experimental and computational approach was used. An experimental perturbation protocol was used to evaluate the balance recovery of young and older subjects in response to a perturbation in different planes during standing and walking. Predictive simulations were used to causally relate age-specific changes in muscle and sensory function to altered control of balance during standing and walking.

The first objective was to identify which neuromechanical factors can explain the experimentally observed kinematic responses to perturbations of standing and walking in healthy adults.

In study 1, we evaluated if a simple neuromechanical model could predict the measured postural responses to a backward support surface translation in a group of young subjects. Non-stepping postural responses to a backward support surface translation were measured in a group of young subjects (n=10). A continuum of ankle (i.e. rigid rotation around the ankle joint) and hip strategies (i.e. counter rotation leg and trunk) was observed to control balance in response to this perturbation. In simulation, the postural response to the perturbation was predicted using a linearized torque driven double inverted pendulum model with full state feedback. Other researchers previously showed that feedback control models that minimize effort can predict reactive muscle activity in response to a backward surface translation. We therefore hypothesized that the relative importance of minimizing effort versus postural instability can explain the continuum of observed non-stepping postural responses. We confirmed this hypothesis and showed that effort minimization induced an ankle strategy whereas instability minimization induced a hip strategy. Hence, the relative importance of minimizing effort versus instability can explain the continuum of postural responses observed in healthy young subjects. In addition, our neuromechanical model predicted the measured shift from an ankle towards a hip strategy when the base of support was decreased, which indicates that the model can be used to predict postural response in novel mechanical contexts.

In study 2, we investigated the mechanism behind the modulation of reactive gluteus medius

activity during perturbed walking in young subjects. Joint kinematics and reactive gluteus medius activity in response to a medio-lateral translation of the treadmill with onset during different phases of the gait cycle were measured in a group of 18 young subjects. In accordance with previous studies, we observed that the magnitude of reactive gluteus medius activity depends on the phase of the gait cycle in which the perturbation is applied. In a forward simulation, we evaluated the isolated effect of the perturbation (i.e. passive response), and the perturbation in combination with reactive gluteus medius activity on the kinematics of balance control (i.e. active response). Results from the simulated passive response showed that the platform translation perturbed stability during all phases of the gait cycle and that an active response is needed to control balance. In addition, the influence of the platform translation on the inter-foot distance (related to the risk for inter-limb collision) and the margin of stability varied during the gait cycle. Hence, the mechanical demands imposed by the perturbation vary during the gait cycle. Results from the active response showed that the potential of gluteus medius to adjust lateral foot placement and prevent collisions during swing varied during the gait cycle. The increase in stance, swing or stance and swing gluteus medius activity all caused an outward foot placement and could therefore compensate for the loss of stability caused by a perturbation early in the gait cycle. Gluteus medius activity of the swing leg in response to a platform translation late in the gait cycle counteracted foot placement, but prevented collision of the swing foot with the stance leg. In conclusion, using this novel blended experimental and simulation approach, we showed that the previously reported gluteus medius activity modulation during the gait cycle can be explained through altered mechanical demands imposed by the perturbation as well as altered muscle potential to control balance throughout the gait cycle.

The second objective was to evaluate the influence of aging on the dominant neuromechanical factors affecting balance control during standing and walking in the elderly.

In study 3, we investigated the mechanisms behind the age-related changes in standing balance control. It is unclear which age-related changes in sensory and muscle function cause the increased occurrence of hip and stepping strategies in the elderly. Previously, a decrease in muscle strength in the older adults has been suggested to contribute to these observations. However, since age-related changes in both muscle and sensory function occur simultaneously, it is hard to identify the individual contribution of altered muscle and sensory function to balance control. Age-related changes in muscle function (i.e. maximal joint torques, rate of joint torques), base of support size and sensory noise were introduced into the neuromechanical model of standing balance control (study 1) to evaluate their effects on the model response. First, we compared the measured postural response of healthy young and older adults to a backward support surface translation. Consistent with previous studies, we found that the older adults relied more on a hip strategy than the young subjects to control balance. Second, in simulation, an increase in sensory noise resulted in a shift from ankle to hip strategies, similarly to the observed increased use of hip strategies in the elderly. However, limiting the maximal (rate of) joint torque or functional base of support to the values measured during balance control in the elderly, did not predict the observed shift from ankle to hip strategy with

aging. In contrast, the addition of noise to the sensory information could explain the observed increased incidence of hip strategies in the elderly, whereas changes in muscle function could not. Our results suggest that fall prevention that rely on isolated strength training programs only may not be most sufficient to improve standing balance control in the elderly. The addition of proprioceptive training or sensory cues in the environment, seems important to deliver efficient training programs.

In study 4, we evaluated how aging influences balance control in response to sagittal and especially frontal plane perturbations during walking and if changes in kinematic strategies could be related to altered reactive activity of muscles around the ankle or hip joint. In balance control during walking, it remains unclear how aging influences the reactive muscle activity and kinematics in response to perturbations. The influence of aging on balance control has been mainly investigated in the sagittal plane, whereas balance control in the frontal plane is largely unexplored. This is remarkable, given that walking mainly requires active control in the frontal plane. In healthy young subjects, reactive activity of the gluteus medius and tibialis anterior has been reported in response to frontal plane perturbations administered during different phases of the gait cycle. This suggests that both muscles have an important contribution in balance control during walking. We hypothesized that the older adults will switch from a lateral ankle towards a stepping strategy for lower perturbation magnitudes (i.e. similar as in standing balance control), and that this switch could be related to reduced ankle and hip muscle reactive activity. In partial agreement, we found that reactive muscle activity and kinematic strategies differed between the young and older adults but only for a small subset of perturbations. When perturbation magnitude increased, the older adults relied more on a stepping strategy for inward directed perturbations and for sagittal plane perturbations with onset just before heel strike. We found that reduced reactive activity of the tibialis anterior and not gluteus medius contributed to the shift in balance control strategy in the elderly. Tibialis anterior activity increased less in the older compared to the young subjects when perturbation magnitude increased, whereas a similar gluteus medius response was observed in the young and older adults independent of the perturbation magnitude. In simulation, we showed that the tibialis anterior had an important contribution to the lateral ankle strategy. Hence, the reduced reactive tibialis anterior activity measured in the elderly might predispose them to use stepping strategies more than ankle strategies in response to more challenging perturbations. Furthermore, this indicates that altered tibialis anterior, and not gluteus medius reactive activity, causes changes in balance control during walking. Therefore, our results suggest that gait perturbation paradigms for training of reactive recovery responses might benefit from an increased focus on reactive tibialis anterior activity.

The unique insights gained in this work depended on the use of a blended computational and experimental approach. This approach allowed us to conclude that for lower perturbation magnitudes, elderly shift towards a strategy that is more robust against perturbations and therefore provides an increased ability to compensate for perturbations. In standing balance control, we showed that sensory noise and not muscle weakness can explain the shift from

the more efficient ankle strategy to the more robust hip strategy in the elderly. In walking balance control, we showed that reduced reactive tibialis anterior activity predisposed elderly to stepping rather than ankle strategies in response to more challenging perturbations. Hence, therapeutic approaches aiming at fall prevention might benefit from an increased focus on sensory function, in addition to strength training of the distal muscles.

Samenvatting

Gaan en staan is voor de meeste mensen eenvoudig. Dit is opvallend, daar zowel gaan als staan onstabiel zijn en actieve controle vereisen. Dit wordt duidelijk bij ouderen. Er is een hoge incidentie van vallen bij oudere mensen, met verwondingen en een verlies van zelfstandigheid tot gevolg. Verminderde evenwichtscontrole draagt mogelijk bij tot dit verhoogde valrisico. Correlatie tussen veroudering-gerelateerde veranderingen in evenwichtscontrole en de kans op vallen draagt echter weinig bij tot het identificeren van de mechanismen die verstoorde evenwichtscontrole veroorzaken. Betere kennis van de bijdrage van verouderingsgerelateerde veranderingen in het musculoskeletaal en sensorische systeem in evenwichtscontrole kan valpreventie-therapie verbeteren. Op basis van deze kennis kan neuromusculaire training gericht worden op de veranderingen die het grootste effect hebben op evenwichtscontrole. Het doel van dit doctoraat was het identificeren van de verandering in het sensorische en musculaire systeem, met de grootste bijdrage in de verminderde evenwichtscontrole tijdens gaan en staan bij ouderen. Een combinatie van een experimentele benadering én simulatie benadering is gebruikt om dit doel te bereiken. Een experimenteel perturbatie-protocol is gebruikt om evenwichtscontrole na een verstoring tijdens gaan en staan te meten bij jongere en oudere proefpersonen. Voorspellende simulaties zijn gebruikt om het causale verband te onderzoeken tussen leeftijds-gerelateerde veranderingen in spierfunctie, sensorische functie en evenwichtscontrole tijdens gaan en staan.

De eerste doelstelling was het identificeren van de neuromechanische factoren die de veranderingen in kinematische evenwicht strategieën bij staan en gaan tussen jong en oud kunnen verklaren.

In studie 1 werd geëvalueerd of een eenvoudig neuromechanisch model de houdingscontrole na een achterwaartse platformtranslatie kan voorspellen bij jonge proefpersonen. Houdingscontrole zonder stappen, na een achterwaartse platformtranslatie, werd gemeten bij 10 jonge proefpersonen. Een continuüm van enkel- (rotatie rond de enkel) en heupstrategieën (tegengestelde rotatie van benen en romp) werd vastgesteld in de houdingscontrole in reactie op de perturbatie. Bij simulatie werd de houdingscontrole na de perturbatie voorspeld op basis van een moment gedreven omgekeerde dubbele slinger model met volledige toestand feedback. Andere onderzoekers toonden aan dat feedback gecontroleerde modellen, die inspanning minimaliseren, spieractivatie kunnen voorspellen na een achterwaartse platformtranslatie. Onze hypothese was daarom dat het relatieve belang van het minimaliseren van inspanning ten opzichte van het minimaliseren van instabiliteit, het continuüm van enkel- en heupstrategieën kan verklaren. Deze studie bevestigde de hypothese. We toonden aan dat minimaliseren van inspanning resulteert in een enkelstrategie en dat het minimaliseren van instabiliteit resulteert in een heupstrategie. Bovendien kon dit neuromechanisch model de opgemeten verandering van enkel- naar heupstrategie voorspellen als de steunbasis verkleinde. Dit suggereert dat het model gebruikt kan worden om houdingscontrole te voorspellen in een andere mechanische context.

In studie 2 werd het mechanisme onderzocht dat het moduleren van reactieve gluteus medius activiteit tijdens gaan met verstoring van evenwicht veroorzaakt. Gewrichtskinematica en reactieve gluteus medius activiteit werden onderzocht na een translatie van de loopband in medio-laterale richting tijdens verschillende fases van de gangcyclus bij 18 jonge proefpersonen. In overeenstemming met andere onderzoeken, stelden we vast dat de grootte van de reactieve gluteus medius activiteit afhankelijk is van de fase van de gangcylus waarin het evenwicht werd verstoord. In een voorwaartse simulatie onderzochten we het geïsoleerde effect van de verstoring (passieve reactie) en de verstoring in combinatie met de reactieve gluteus medius activiteit (actieve reactie) op evenwichtscontrole. Resultaten van de gesimuleerde passieve reactie toonden aan dat de platformtranslatie evenwicht verstoort tijdens alle fases van de gangcyclus. Dit wijst erop dat een actieve reactie nodig is om evenwicht te behouden. Bovendien varieert de invloed van de perturbatie op de afstand tussen het zwaai en steunbeen tijdens de gangcyclus. De mechanische vereisten voor evenwichtscontrole veranderen dus tijdens de gangcyclus na perturbatie. De gesimuleerde actieve reactie toonde aan dat het potentieel van de gluteus medius om zijwaartse voetplaatsing aan te passen en het haken van de voeten te verhinderen varieert tijdens de gangcyclus. De toename in gluteus medius activiteit van het steun- en zwaaibeen veroorzaakte een zijwaartse voetplaatsing en compenseerde zo de instabiliteit veroorzaakt door een perturbatie vroeg in de gangcyclus. Gluteus medius activiteit van het zwaaibeen in reactie op de platform translatie op het einde van de gangcyclus werkte de verandering van voetplaatsing tegen, maar verhinderde het haken van de voeten tijdens de zwaaifase. Op basis van een nieuwe methode, die experimenten combineert met simulatie, hebben we aangetoond dat modulatie van gluteus medius activiteit kan verklaard worden door de veranderingen in mechanische vereisten veroorzaakt door de perturbatie, en door de veranderingen in het potentieel van de spier om evenwicht te controleren.

De tweede doelstelling was het evalueren van veroudering op de dominante neuromechanische factoren die evenwichtscontrole beïnvloeden tijdens staan en gaan. In studie 3 werd bij ouderen het mechanisme onderzocht dat de leeftijds-gerelateerde verandering in houdingscontrole veroorzaakt. De leeftijds-gerelateerde verandering in sensorische en musculaire functie die de toename in gebruik van heup- en stapstrategieën veroorzaken zijn onduidelijk. Enkele studies suggereerden dat een daling in spierkracht de veranderingen in evenwichtscontrole veroorzaakt. Het identificeren van de individuele bijdrage van leeftijds-gerelateerde verandering in spierfunctie en sensorische functie in evenwichtscontrole is echter moeilijk, aangezien die veranderingen simultaan gebeuren. Veranderingen in spierfunctie (maximaal gewrichtsmoment, snelheid van gewrichtsmoment), in grootte van de steunbasis en in sensorische ruis werden geïntroduceerd in het neuromechanische model van staand evenwicht, dit om het geïsoleerde effect op evenwichtscontrole te kunnen identificeren. In dit onderzoek werd de houdingscontrole gemeten bij jongere en oudere proefpersonen in reactie op een achterwaartse platform translatie. In overeenstemming met andere onderzoeken, stelden we vast dat ouderen meer gebruik maakten van een heupstrategie dan jongeren. In simulatie werd de toename in heupstrategie voorspeld als sensorische ruis werd toegevoegd aan het model van staand evenwicht. Het beperken van de maximale gewrichtsmomenten, de snelheid van gewrichtsmomenten en de

functionele steunbasis kon de toename in heupstrategieën niet verklaren. Onze resultaten suggereren daarom dat valpreventie-training, enkel gebaseerd is op krachttraining, mogelijk niet de beste interventie is om houdingscontrole te verbeteren. Het toevoegen van proprioceptie oefeningen aan valpreventie-training lijkt belangrijk.

In studie 4 werd geëvalueerd hoe veroudering de evenwichtscontrole beïnvloedt in reactie op perturbaties in het sagittale en vooral in het frontale vlak. Bovendien werd onderzocht of de verandering in kinematische strategieën voor evenwichtscontrole gerelateerd zijn aan veranderde reactieve activiteit van enkel- en heupspieren. Bij evenwichtscontrole tijdens gaan is het nog onduidelijk of veroudering een invloed heeft op reactieve spieractiviteit en kinematica in reactie op perturbaties in het frontale vlak. De invloed van veroudering op evenwichtscontrole is hoofdzakelijk onderzocht in het sagittale vlak, terwijl in het in frontale vlak het onderzoek eerder beperkt is. Dit is opvallend, aangezien wandelen voornamelijk onstabiel is in het frontale vlak. Bij jongere proefpersonen werd tijdens het gaan activiteit van de tibialis anterior en gluteus medius gerapporteerd in reactie op perturbaties in het frontale vlak. Dit suggereert dat beide spieren een belangrijke bijdrage leveren aan de controle van evenwicht. Onze hypothese was dat ouderen sneller overschakelen van een enkel- naar een stapstrategie en dat deze verandering gepaard gaat met een verminderede reactieve activiteit van de enkel- en heupspieren. In gedeeltelijke overeenstemming met de hypothese vonden we dat reactieve spieractiviteit en kinematica veranderden bij ouderen, maar uitsluitend bij specifieke perturbaties. Bij een toenemende perturbatie grootte maakten de oudere proefpersonen meer gebruik van een stapstrategie in reactie op naar binnen gerichte perturbaties en in reactie op perturbaties in het sagittale vlak met aanvang net vóór de voetplaatsing. We stelden vast dat de gereduceerde activiteit van de tibialis anterior en niet van de gluteus medius in reactie op de perturbatie gerelateerd is aan de toename van stapstrategie. Een kleinere toename in activiteit van de tibialis anterior werd gemeten bij de ouderen in vergelijking met de jongeren als de perturbatie grootte toenam, terwijl een gelijkaardige toename in activiteit van de gluteus medius werd gemeten bij jongeren en ouderen. Door middel van simulatie toonden we aan dat de tibialis anterior activiteit een belangrijke bijdrage levert tot de enkelstrategie. Dus de verminderde tibialis anterior activiteit veroorzaakt mogelijk de toename in stapstrategieën bij de ouderen in reactie op moeilijkere perturbaties. Dit suggereert dat programma's om reactieve evenwichtscontrole te trainen mogelijk baat hebben bij een toegenomen focus op reactieve tibialis anterior activiteit.

De inzichten, die verworven zijn in dit werk, zijn afhankelijk van het gebruik van een methode die simulatie en experimenten combineert. Deze benadering laat ons toe te concluderen dat ouderen overschakelen naar een strategie die meer robuust is en dus beter bestand tegen een perturbatie. Bij staand evenwicht toonden we aan dat sensorische ruis, en niet spierzwakte, de verandering van een meer efficiënte enkelstrategie naar een meer robuuste heup strategie bij de ouderen kan verklaren. Bij evenwichtscontrole tijdens wandelen toonden we aan dat de verminderde reactieve tibialis anterior activiteit gerelateerd is aan de overschakeling van enkel- naar stapstrategie. Valpreventie-therapie heeft dus mogelijk baat bij een toegenomen focus op sensorische functie, in combinatie met krachttraining van de distale spieren.

Chapter 2

General introduction

To most of us, standing and walking are easy. This is remarkable, given the fact that from a mechanical point of view walking is highly unstable and therefore requires well-coordinated active control. This becomes apparent in the elderly. There is a high incidence of falls in the elderly, often resulting in significant injuries and loss of independence [1]. Falling does not only undermine the safety and therefore independency of the elderly, but also imposes a high burden of fall-related costs on society [1]. More than 25% of fall-related injuries in older adults occur during locomotion [1]. Slipping and tripping during walking are the most common causes of falls among older adults, sometimes resulting in hip fractures [1]. More than 90% of hip fractures occur as a result of a fall [2].

Deterioration of balance control may contribute to increased fall risk in older adults. Impaired balance was indeed correlated with an increased risk of falls [3]. Simple tests, such as standing on a narrow beam or a near-tandem standing test with eyes open and closed can differentiate between elderly with and without a history of falls [4]. During these tasks, larger corrective movements have been recorded in fallers compared to non-fallers. Therefore, the inability to control balance during standing has been reported as a significant risk factor for future falls in older adults.

However, correlations between age-related decrease in balance performance and the incidence of falling only provide limited insight in the underlying mechanisms by which aging alters balance control. An improved understanding of age-related changes in balance control and the contribution of changes in the neural and muscular system to the control of balance could improve therapeutic approaches aiming at fall prevention. For example, these insights may steer neuromuscular training programs to target the age-related changes that affect balance control most efficiently.

Reactive control of balance

The human musculoskeletal system is mechanically unstable because of its many degrees of freedom combined with the high location of the center of mass (COM) above a small base of support. Reactive and anticipatory mechanisms contribute to the control of balance during standing and walking. We focused on the influence of aging on the reactive control of balance [5]. Reactive control of balance relies on different components of the neuro-musculoskeletal system including (1) the musculoskeletal system, (2) the sensory system, and (3) sensory and cognitive processing in the nervous system [5].

The musculoskeletal system consists of the skeletal structure, actuated by muscles. In a static situation, the musculoskeletal system is stable if the projection of the center of mass position is within the base of support. The conditions for stability are more complex during dynamic tasks. The extrapolated center of mass (Xcom) [6] or capture point [7] was introduced to extend the static definition of stability by correcting the COM position with the COM velocity [6]. The Xcom is derived from a linear inverted pendulum model and represents the point on the ground where the center of pressure (COP) has to be placed to result in a vertical

position of the inverted pendulum (i.e. kinetic energy is transferred into potential energy). The distance between the Xcom and the boundaries of the base of support can be used to quantify the stability of the skeletal system under the inverted pendulum assumption and is referred to as margin of stability [6]. Both active (muscle activity) and passive (e.g. passive muscle properties, ligaments) musculoskeletal components contribute to balance control as they provide resistance to perturbations and assist in keeping the Xcom position within the base of support. Using the passive and active muscle properties, stability of the skeletal system can be maintained in the presence of internal and external perturbations by adjusting stiffness and damping in the joints (i.e. mechanical impedance). Muscle force is controlled by the nervous system to compensate for instability of the skeletal system. Muscle strength, joint range of motion and segmental inertial and kinematic properties are referred to as musculoskeletal constraints for balance control [5].

The sensory systems involved in the control of balance are the visual, vestibular and somatosensory systems, which provide information about the state of the musculoskeletal system. The somatosensory system consists of muscle splindles, Golgi tendon organs, cutaneous receptors and other mechanoreceptors that provide the centeral nervous system with tactile, proprioceptive and kinesthetic information [8]. The vestibular system provides information about the tilt of the head with respect to gravity and its angular acceleration [9]. The visual system provides information about the body orientation with respect to the environment. Sensory integration is important in balance control and can be defined as the fusion of information from visual, vestibular and somatosensory systems to estimate the current orientation of the body in space [8]. Several studies described that the relative importance of visual, somatosensory and vestibular information in the sensory integration process varies when the sensory environment changes (i.e. sensory reweighting) [8]. For example, Peterka et al. estimated that healthy young subjects rely on somatosensory (70%), vision (10%), and vestibular (20%) information to control balance during standing [10]. When the sensory environment was manipulated by means of a non-rigid support surface, the subjects decreased their dependence on the unreliable somatosensory inputs and therefore relied more on visual and vestibular information [10]. The mechanism of reweighting redundant sensory information improves the accuracy of the estimation of the current orientation of the body in space in the presence of noise in the sensory system.

Sensory information is processed by the central nervous system to generate motor commands. Several studies suggested that sensory information is integrated based on an internal model of the musculoskeletal system to estimate the current orientation of the body in space (i.e. state estimation) [8]. This internal model represents the relationship between motor commands and their effect on the limbs movements [8,11]. The internal model therefore does not only describe the kinematics of the musculoskeletal system, but also considers the inertial properties of each segment [8]. Discrepancies between the desired and estimated state induce efferent signals to the muscles to control balance.

A model describing the different subcomponents and their interactions can be used to gain

insights in the control of balance (Figure 2.1). Reactive control of balance is often described as a delayed feedback control system in which noisy sensory information from vestibular, somatosensory and visual systems is integrated to estimate the state of the internal model [10, 12–15]. Motor commands are then generated in the task-level controller as differences between the desired and estimated state of the internal model. The task-level controller induces reactive muscle activity to control task-level variables such as effort and instability. These motor commands are subjected to signal-dependent noise due to the size principle (i.e. larger commands results in less accurate control of muscle force due to the recruitment of larger motor units) [16]. The resulting motor command is not a simple mono-synaptic reflex but relies on integration of sensory information from different systems [14]. Therefore, we will refer to the motor command as an automatic response, which can be interpreted as a long latency reflex (i.e. time delay between 80-120ms) [14]. These automatic respones, also referred to as balance-correcting responses [17], then serve as input to the musculoskeletal system. Late action (>300ms) were not analysed in this PhD since it is unclear if these actions can be described as reactive control strategies.

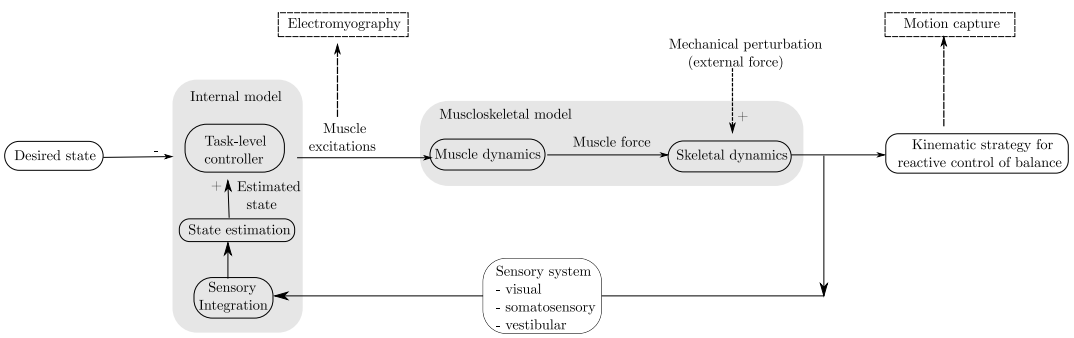

Figure 2.1: **Reactive control of balance modeled as a delayed feedback control system.** Noisy sensory information from vestibular, somatosensory and visual systems is integrated to estimate the state of the internal model. The difference between the estimated and desired state is used as feedback information in the task-level controller that controls task level variables such as effort and instability. The resulting muscle excitations drive the musculoskeletal model resulting in a kinematic strategy for balance control. Perturbations are commonly used to gain insight in the control of balance. In this PhD, mechanical perturbations are used to excite the feedback control of balance. The corrective motor responses to the perturbation can be measured with electromyography and the resulting kinematic strategy with 3D motion capture. This figure is based on the feedback control of balance proposed by [16]

.

Experimental perturbation protocols are commonly used to gain insight in the reactive control of balance during standing and walking [14,17–20]. A perturbation excites the feedback control loop and generates a corrective response, which can be described using electromyographic and kinematic variables (Figure 2.1). Both mechanical and sensory perturbations have been used to gain insight in the control of balance. During a mechanical perturbation, the state of the musculoskeletal model is perturbed by means of an external force (i.e. slip, trip, push perturbations). This approach is commonly used to evaluate the ability to control balance

in patient populations [21]. During a sensory perturbation, the visual, somatosensory or vestibular feedback information is perturbed by means of changes in the visual field (i.e. virtual reality) [22], muscle vibration [23], and galvanic stimulation [24]. These perturbations were used to identify the relative importance of the different components of the sensory system in balance control [23].

Strategies for reactive control of balance during standing and walking

Kinematic strategies to control balance during perturbed standing and walking differ between individuals, depending on context and age [20, 25–27].

During standing balance control, kinematic strategies can be subdivided into stepping and non-stepping postural strategies. The ankle and hip strategies are the two extremes in the continuum of non-stepping postural responses. The ankle strategy is characterized by a rigid rotation of the legs and trunk around the ankle joint [25]. The ankle muscles rotate the stance leg, which causes a shift of the COP in the foot. The hip strategy is characterized by large hip angle excursions and counter-rotation of the trunk with respect to the legs [25]. The angular acceleration of the large upper body inertia influences horizontal ground reaction forces and the linear motion the center of mass. During a stepping strategy, foot position and therefore the base of support is adjusted to control balance. The selection of a strategy depends on the perturbation magnitude, experience, adaptation, and fear of falling [26, 27]. The ankle strategy is mainly used to cope with small perturbations. In more challenging conditions, subjects gradually switch their postural response from an ankle towards a hip and stepping strategy [20, 26]. Examples of more challenging conditions are an increased perturbation magnitude or a reduced base of support, e.g. when standing on a narrow beam. It was suggested that an ankle strategy is advantageous to maintain an upright pose with minimal head movements. This is thought to improve sensory feedback from the vestibular and visual systems [28]. On the other hand, Kuo and Zajac showed that a hip strategy increases the ability to accelerate the center of mass (COM) without stepping and that the instantaneous muscle activity for a desired COM acceleration is lower during a hip than during an ankle strategy [29].

During walking, kinematic strategies can also be subdivided into stepping and non-stepping strategies. Since gait is mainly unstable in the frontal plane [30], kinematic strategies for balance control were mainly described in the frontal plane. The stepping strategy is the main kinematic strategy for medio-lateral control of balance. In a stepping strategy during walking, the location of foot placement of normal walking is adjusted to affect the location of the COP and therefore control balance. Hof et al. showed that foot placement is adjusted in the direction of the perturbation (i.e. instability) to keep the distance between the Xcom and COP constant [18]. Activity of the swing leg gluteus medius is considered to be the main contributor to the stepping strategy. It was suggested that activity of the swing leg gluteus

medius abducts the hip and therefore controls the medio-lateral position of the foot. Increased stance leg gluteus medius activity in response to a perturbation was observed as well [17, 19], but the contribution to foot placement and gait stability is not well understood. In addition, the magnitude of the reactive activity of the stance and swing leg gluteus medius changes during the gait cycle (i.e. modulation). However, the mechanisms behind this modulation are yet unclear. Reiman et al. showed that the stepping strategy is often used in combination with a lateral ankle strategy [31]. The lateral ankle strategy is characterized by a medio-lateral shift of the COP in the foot, which is mainly controlled by tibialis anterior, soleus and peroneus muscle activity. It was suggested that tibialis and peroneus activity control respectively the lateral and medial position of the COP in the foot and that soleus activity is needed to counteract the dorsiflexion torque generated by tibialis anterior [32]. The corrective effect of the lateral ankle strategy is smaller compared to the stepping strategy, because the COP excursion is constrained by the border of the foot. However, the lateral ankle strategy has a direct effect on the center of mass movement, whereas the stepping strategy has no effect before foot-ground contact.

Effects of aging on reactive balance control strategies - experimental studies

During perturbed standing in response to backward support surface translations, healthy older adults rely more on a hip and stepping strategy than young subjects to control balance [20]. Other studies found an increase in center of mass movement after a sudden release from an inclined lean angle [33]. During perturbed walking, older subjects needed more steps to return to a stable gait pattern [34], had larger center of mass movements after perturbation and a smaller margin of stability [35]. In addition, a higher incidence of falls in response to a laboratory based trip perturbation was reported in the elderly compared to the young [21].

Age-related changes in both the musculoskeletal and sensory systems have been related to the changes in reactive balance control strategy and the high incidence of falls in the elderly as described below.

Age-related changes in the musculoskeletal system

Deficits in balance control in the elderly have been related to changes in muscle function. Altered muscle function in the elderly is the result of changes in fiber type composition [36], number of muscle fibers [37, 38], activation and deactivation dynamics [39], and tendon stiffness [40]. These structural changes result in slower activation and deactivation of muscles, decreased maximal isometric force, reduced maximal contraction velocity and rate of force development and therefore potentially alter balance control [41].

Several experimental studies suggested that the aforementioned changes in muscle properties

cause different behavioural changes, limit balance control and cause falls in the elderly. First, lower limb muscle weakness is a major risk factor for falling in older adults [9]. Reduced ankle dorsiflexion, knee extension and hip abduction strength was found to correlate with an increased risk of falls [9]. In addition, changes in muscle properties, such as increased intramuscular adipose tissue, were observed in fallers compared to non-fallers [42]. Second, muscle strength was related to changes in balance control strategies in response to perturbations. During perturbed standing, the increased occurrence of hip and stepping strategies was related to reduced maximal ankle dorsiflexion torque [20, 43], reduced rate of change in ankle joint torque [20, 44], and reduced maximal hip abduction torque [45]. During perturbed walking, reduced leg extension strength and maximal jump height was related to an increased occurrence of falls in response to a trip perturbation during walking [46]. This suggests that the age-related changes in muscle mechanics may affect, and potentially limit, balance control during standing and walking.

Age-related changes in the sensory system

Deficits in balance control was also related to changes in sensory function [47]. Structural changes in both visual, somatosensory and vestibular systems potentially contribute to deficits in balance control in the elderly [9]. First, structural changes in muscle spindles and Golgi tendon organs cause a deterioration of sensory information in the elderly [48], which has was related to a decrease in position and movement sense [48–51]. Second, visual acuity and contrast sensitivity declines in the elderly [9]. Finally, the number of vestibular hair cells decreases in the elderly, which might affect vestibular function [8].

Experimental studies where sensory function is altered by means of a perturbation or in the context of a specific pathology have provided more information on the isolated contribution of changes in the sensory system on balance control. First, studies in specific patient populations showed that reduced sensory function is related to a decreased ability to control balance [52–55]: (1) Individuals with peripheral nerve dysfunction, such as patients with diabetes mellitus and peripheral neuropathy, are at greater risk of falling [55], (2) changes in strategies to control balance were found in patients with bilateral vestibular loss [54]. Second, experimental blocking or perturbing of sensory information showed that proprioception is important to control balance: (1) changes in standing balance control strategies were observed after hypoxic anesthesia of the feet and ankles (i.e. loss of somatosensory information) [54], (2) muscle vibration studies showed that perturbation of the muscle spindle and Golgi tendon organ information causes reactive muscle activity, therefore indicating the important contribution of proprioceptive feedback to postural control [56], (3) compensatory muscle activity in response to a perturbation decreased when plantar skin sensory input was inhibited by hypothermia [52]. Finally, in animal studies (cats), the automatic muscle response to perturbations was delayed and no initial burst of reactive muscle activity was observed when somatosensory information was impaired by injection of pyridoxine [57, 58].

Age-related changes in cognitive processing of the central nervous system

Besides changes in muscle and sensory function, age-related changes in cognitive processing in the central nervous system might also cause deficits in balance control. Many cognitive resources are required to process the sensory information for the control of balance [5]. Therefore, age-related capacity problems at the central nervous system [59] and slower neural transmission due to loss of myelination may cause a decrease in reaction time following a perturbation [9, 60, 61].

Experimental studies where a cognitive task is added to a balance perturbation experiment (i.e. dual task paradigm) have provided more information about the cognitive load related to the control of balance. Dual-task studies showed that the control of balance is affected more in older adults compared to young adults when the complexity of the balance task was increased (for review: [59]). Similarly, a recent study showed that reaction time during walking incrased in the elderly when the stepping task involved decision making [62]. Hence, these dual-task studies suggested that the cognitive processing saturates in the elderly, which causes a delay in reactive balance control. This might be the result of an increased need for cognitive processing to cope with sensory noise in the elderly [59].

Effects of aging on reactive balance control strategies - simulation studies

Age-related changes in muscle and sensory function occur simultaneously, which impedes the experimental determination of their individual contribution to balance control. Furthermore, it is hard to independently manipulate muscle and sensory function in experiments on human subjects, which makes it hard to establish causal realtions between age-related changes and the control of balance. In contrast, simulations allow investigating the effect of isolated changes in the musculoskeletal and neural control system on balance control. In a simulation, the musculoskeletal and motor control systems are described by equations. Simulations of balance control during standing and walking typically rely on a neuromechanical models that incorporate both the musculoskeletal mechanics and neural control of movement [15, 63].

Neuromechanical models of standing are typically used in combination with experiments of perturbed standing to gain insight in the neural control. Due to the limited movement in standing balance control, musculoskeletal dynamics are commonly simplified to torque or muscle driven single and double inverted pendulum models with delayed feedback from somatosensory, visual and vestibular information [11, 13–15, 64, 65]. Lockhart et al. showed that an inverted pendulum model with delayed center of mass position, velocity and acceleration feedback can reproduce measured reactive muscle activity in response to forward and backward support surface translation [58]. It remains currently unknown if center of mass feedback can

also reconstruct the kinematics of a hip strategy.

Neuromechanical models of perturbed standing can be used to predict the balance control strategy when changes in the sensory and musculoskeletal system are imposed. Peterka et al. predicted that balance control in response to more challenging perturbations is impossible when vestibular information is absent. This is consistent with responses observed in patients with vestibular loss [66]. Kuo et al. showed that when perturbation magnitude increased, the postural response shifted from an ankle strategy towards a hip or stepping strategy [67]. In addition, they found that the continuum of ankle and hip strategies can be explained by minimizing postural instability versus upright posture [15]. Currently, it remains unclear if other task-level goals, such as minimizing effort, can also explain the continuum of ankle and hip strategies.

Musculoskeletal models of walking are mainly used to gain insights in the musculoskeletal mechanics during locomotion. Measured kinematics and external forces are often combined in these models to estimate parameters that are hard to measure experimentally, such as (1) joint torques, (2) muscle forces, and (3) joint contact forces [68]. The computation of muscle forces that can reproduce the measured kinematics and external forces involves solving a redundant problem (i.e. muscle redundancy) and typically relies on the minimization of an effort or fatigue related objective [69]. However, this inverse approach to analyse musculoskeletal dynamics does not allow model-based predictions of kinematic trajectories. Model-based predictions of walking are currently limited by high computational costs and by over-simplifications of motor control. Hence, these models can only reproduce a measured movement or reconstruct a movement based on measured motor control and cannot predict the effect of changes in the musculoskeletal system on balance control.

Neuromechanical models of standing have the potential to evaluate the mathematical relation between isolated changes in the neuro-musculoskeletal system and the control of balance. Hence, causal relations between age-related changes in the neuro-musculoskeletal system and the control of balance can be established within the limitations of the model. Nevertheless, these models have not been used to evaluate the effect of aging on balance control. Therefore, currently it remains unclear to what extent changes in muscle function or changes in sensory function can explain the shift from ankle towards hip and stepping strategies in the elderly. In contrast with the models of standing, the state of the art in predictive simulations of walking does not yet allow to use these models to predict the influence of aging on balance. Nevertheless, these models can at least in theory be used to gain insight in the contribution of reactive muscle activity to kinematic strategies in response to perturbation of walking balance.

Objectives

The main aim of this PhD was to identify to which extent changes in sensory and muscle function contribute to the observed differences in balance control in perturbed standing and walking in elderly. An experimental perturbation protocol was used to evaluate the recovery response of young and older subjects to a perturbation during standing and walking, imposed in different planes and at different timings. Experimental data was combined with predictive simulations to causally relate age-related changes in muscle and sensory function to altered balance control during standing and walking.

To this aim, two main objectives were defined:

1. To identify which neuromechanical factors can explain the experimentally observed kinematic responses to perturbations of standing and walking in healthy adults.
2. To evaluate the influence of aging on the dominant neuromechanical factors affecting balance control during standing and walking in the elderly.

Objective 1: To identify which neuromechanical factors can explain the experimentally observed kinematic responses to perturbations of standing and walking in healthy adults.

It is unclear to date, which neuromechanical factors determine the selection of a specific postural response in perturbed standing and walking. The identification of the neuromechanical factors that contribute to the control of balance is needed to evaluate their role in age-related changes in balance control.

In standing balance control, it is unclear whether and how effort minimization influences the selection of a postural response to perturbation. It was shown that feedback control models that minimize effort can predict reactive muscle activity in response to a backward surface translation [58], but it is unclear if minimizing effort can also predict the continuum of ankle and hip strategies.

Study 1 aimed to evaluate if the relative importance of minimizing instability versus minimizing effort (i.e. task level goal) can explain the selection of a postural response in the observed continuum of ankle and hip strategies in perturbed standing. To this aim, a simple predictive simulation model was developed that can explain the range of observed non-stepping postural control strategies in response to backward support surface translations in healthy individuals. Predicted postural responses were compared to measured responses in a group of 10 healthy young adults.

Hypothesis study 1: The relative importance of minimizing effort versus postural instability can explain the continuum of observed postural responses.

In walking balance control, reactive activity of the hip and ankle muscles has been observed in response to medio-lateral perturbation [17, 19]. However, it is currently unknown to which extent the automatic response of both ankle and hip muscles contributes to kinematic requirements for balance control during walking. The adjustment of foot placement is the main kinematic strategy to control balance. Therefore the contribution of the hip abductor muscles (i.e. gluteus medius) to the adjustment of foot placement and prevention of inter-limb collision during swing is most important in the identification of neuromechanical factors for balance control in healthy adults. The contribution of the lateral ankle strategy and the response of ankle muscles (i.e. tibialis anterior) will be discussed in the second objective to evaluate the influence of aging on the control of balance during walking.

Study 2 aimed to identify the contribution of reactive stance and swing leg gluteus medius activity to walking balance control. To gain insights into these mechanisms, it is important to unravel the individual contribution of stance and swing leg gluteus medius activity to the mechanics of perturbed walking. Therefore, we developed a forward simulation of perturbed walking that allows us to quantify the influence of the perturbation force on the mechanics of gait stability and the isolated contribution of a measured individual muscle response to the stepping strategy. Reactive muscle activity in response to medio-lateral perturbation was

measured in 18 healthy young subjects. Experimental data was combined with forward simulations to evaluate the causal relations between reactive gluteus medius activity of the stance and swing limb and the kinematic response to medio-lateral perturbations of walking.

Hypothesis study 2: The potential of the stance and swing leg gluteus medius to (1) adjust lateral foot placement and (2) prevent collisions during swing varies during the gait cycle and explains the observed modulation in reactive gluteus medius activity.

Objective 2: To evaluate the influence of aging on the dominant neuromechanical factors affecting balance control during standing and walking in the elderly

Currently, it is unclear how specific age-related changes in muscle and sensory function influence the control of balance in perturbed standing and walking. Correlations between experimentally observed measures of muscle and sensory function and the control of balance provide important insights, but have only a limited capacity to unravel the mechanisms due to the multi-factorial influence of aging on sensory and muscular function. The simulation methods developed in study 1 and 2 will be used to causally relate changes in sensory and muscle function with the control of balance during standing (study 3) and walking (study 4).

In standing balance control, it is unclear which age-related changes in sensory and muscle function (i.e. muscle strength, rate of force development) cause the increased occurrence of hip and stepping strategies in the elderly. Previously, a decrease in muscle strength in the older adults was suggested to contribute to these observations [20]. However, since the age-related changes occur simultaneously, it is hard to identify the individual contribution of altered muscle and sensory function to balance control.

Study 3 aimed to evaluate the effect of isolated age-related changes in muscular and sensory function on the postural response to a backward support surface translation. We assessed if either a decrease in muscle function or an increase in sensory noise could explain the increased occurrence of hip strategies in older versus young adults. The neuromechanical model to simulate standing balance control developed in study 1, was used to evaluate the influence of age-related decrease in sensory and muscle function on the selection of a postural response from the potential postural responses. Predicted postural responses were therefore compared to measured kinematic responses following a backward surface translation in a group of 10 healthy young and 10 healthy older adults.

Hypothesis study 3: Sensory noise, impaired muscle function and a smaller base of support can explain the observed shift in postural strategy from an ankle towards a hip strategy in healthy older versus young adults in standing balance control.

In balance control during walking, it is unclear how aging influences the reactive muscle activity, kinematics in response to perturbations. The influence of aging on balance control was mainly investigated in the sagittal plane, whereas balance control in the frontal plane is largely unexplored. This is remarkable, given that walking mainly requires active control in the frontal plane. In healthy young subjects, reactive activity of the gluteus medius and tibialis anterior was reported in response to frontal plane perturbations administered during different phases of the gait cycle [17, 32]. This suggests that ankle and hip strategies are used by the young and older subjects and that both muscles have an important contribution in balance control during walking.

Study 4 aimed to evaluate (1) if there are differences in kinematic strategy to control balance during perturbed walking in a group of young and older adults, and (2) if the differences in kinematics are related to changes in reactive activity of ankle or hip muscles. To this aim, we measured the reactive muscle activity and kinematics in response to multi-directional perturbations with onset during different phases of the gait cycle in a group of 18 healthy young and 10 healthy older adults. The influence of age-related changes in reactive muscle activity on the mechanics of walking was evaluated using the predictive simulation method developed in study 2.

Hypothesis study 4: Elderly shift earlier from a lateral ankle to a stepping strategy in response to a perturbation during walking, which can be related to concurrent alterations in reactive muscle activity of the tibialis anterior or gluteus medius.

Chapter 3

General methodology

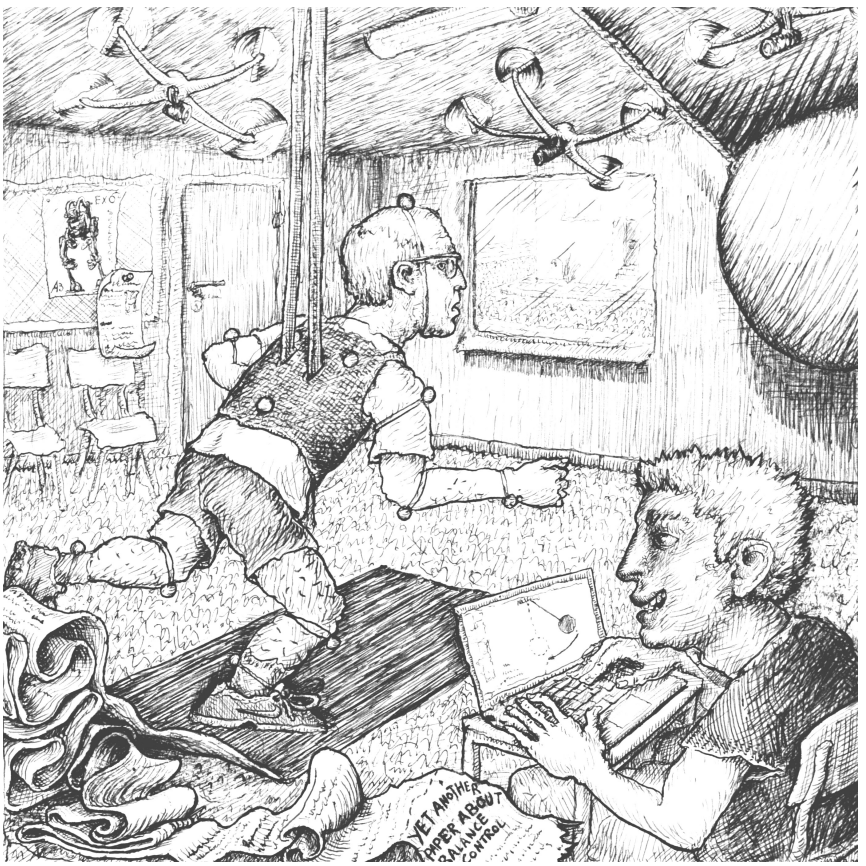

A blended experimental and simulation approach was used to evaluate the influence of aging on the control of balance during standing and walking. This chapter contains a summary of the experimental and simulation methods used in the four studies (Figure 3.1).

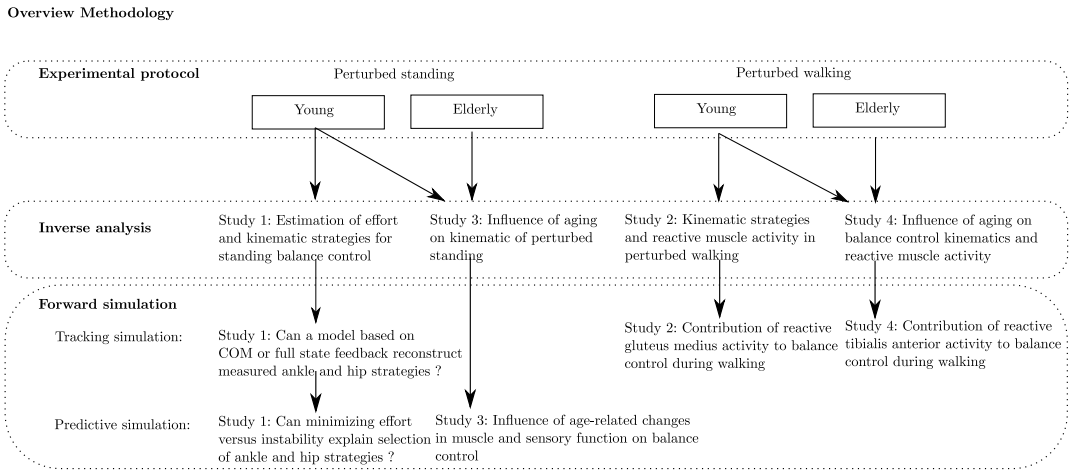

Figure 3.1: **Overview Methodology.** Kinematics and reactive muscle activity was measured in response to perturbations during standing and walking in young and older subjects. The measured data was used in combination with simulations with neuromechanical model in the four studies.

Subjects

For study one and three, ten healthy young (21 ± 2 std (standard deviation) years) and ten healthy older adults (67 ± 3 std years) were recruited in Leuven. All subjects volunteered to participate after receiving a flyer during classes at Cardiff University and at sport and leisure activities organized for elderly. Inclusion criteria were: (1) age between 18 and 25 years for the young subjects and between 60 and 80 years for the older subjects, (2) no history of falling, (3) free of any acute and chronic low back and lower limb injuries in the last 6 months.

For study two and four, eighteen healthy young (age 21 ± 2 std years) and ten older adults (age 71 ± 4 std years) were recruited in Cardiff. All subjects volunteered to participate after receiving a flyer during classes (young, physiotherapy student) and at sport and leisure activities organized for elderly (yoga, dancing, play at cards). Similar inclusion criteria as in study 1-2 were used: (1) age between 18 and 26 years for the young subjects and between 65 and 80 years for the older subjects, (2) no history of falling, (3) free of any acute and chronic low back and lower limb injuries in the last 6 months.

Data collection

Integrated 3D motion capture was used to measure the response to perturbations during standing and walking in a group of young and older adults.

Experiments of perturbed standing, KU Leuven

Subjects stood at stance width equal to their shoulder width on a moving platform (Carenbase, Motekforce Link, Netherlands). Subjects were informed that the platform would randomly move in multiple directions and were instructed to maintain stability without stepping (Figure 3.2). We analysed perturbed standing in response to backward platform translations (0.16 m total excursion) administered within three blocks of randomized perturbations in anterior-posterior and medio-lateral directions with respectively fast, medium and slow acceleration profiles (1.1 m/s^2, 0.8 m/s^2 and 0.6 m/s^2 peak acceleration). These acceleration profiles elicited a wide range of postural responses. Two trials per acceleration profile were analysed, resulting in six trials per subject.

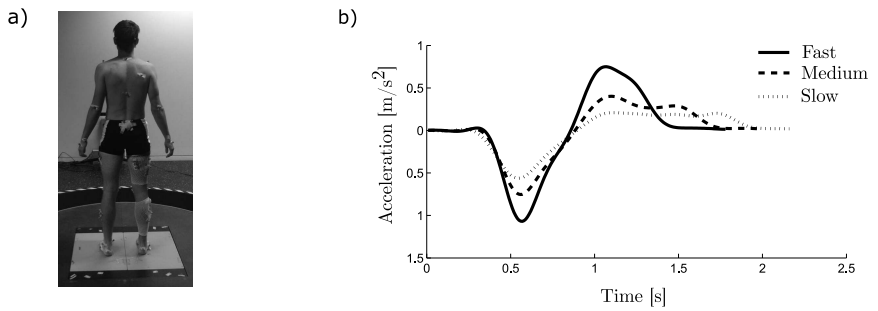

Figure 3.2: **Experiments on perturbed standing.** Upright posture was perturbed by means of a sudden backward support surface translation of 0.16 m with three accelerations profiles.

Whole-body motion was recorded using 3D motion capture with an extended plug in gait marker set (48 makers) at 100Hz using a motion capture system (Vicon, Oxford Metrics, Oxford, UK, 7 cameras). Ground reaction forces were collected at 1000 Hz from two AMTI force plates (AMTI, Watertown USA).

Experiments of perturbed gait, Cardiff University

Subjects walked for two minutes on a split-belt treadmill (Grail, MotekForceLink) at a fixed speed of 1.1 m/s to adapt to the treadmill. The perturbation protocol consisted of 48 randomized unique perturbations per session. Each session was repeated three times with five minutes rest in between. The set of 48 unique perturbations consisted of three different perturbation magnitudes, four directions and four onset timings in the gait cycle (Figure 3.3). In the elderly, only the small and large perturbation amplitudes were applied, resulting in a total of 32 perturbation. Sudden platform translation to the left or right were used for the medio-lateral perturbation direction and a sudden increase or decrease in the speed of both belts was used for the anterior-posterior perturbations. The perturbation was applied immediately after left heelstrike (7.5% gait cycle, first double support), during early midstance (22.5% gait cycle), late midstance (37.5% gait cycle) and push-off (52.5% gait cycle, second double support). Details on the perturbation properties can be found in figure 3.3. The next perturbation was applied only when the subjects reached steady state walking (i.e. the

standard deviation of the stride time of the last 5 strides was below 0.05) and the operator indicated that it was safe to apply the perturbation.

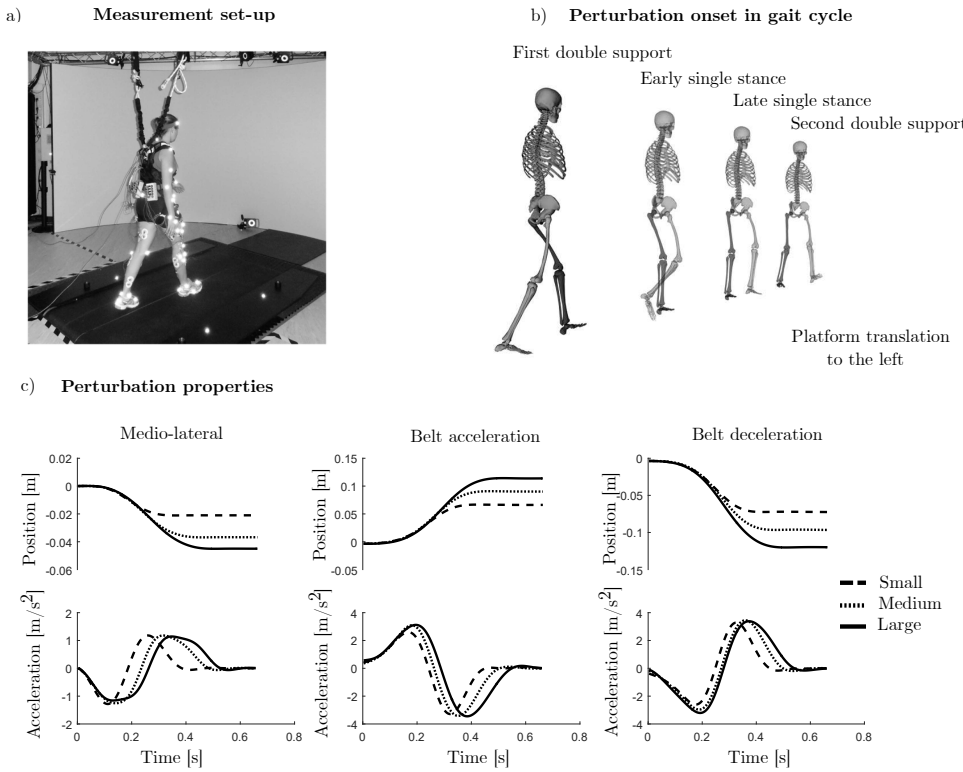

Figure 3.3: **Experiments on perturbed walking.** The treadmill-based perturbation protocol consisted of medio-lateral platform translations and sudden increases or decreases in the speed of both belts (a). The perturbations were applied in four phases of the gait cycle with three different magnitudes (c). An integrated 3D motion capture system was used to measure the kinematics and muscle activity (using EMG) in response to the perturbation

An integrated 3D motion capture system was used to measure the kinematics in response to the perturbations. 12 Vicon T20 cameras (Vicon, Oxford) measured the trajectories of 48 retroflective markers in an extended plug in gait marker protocol at 200 Hz. Ground reaction forces were collected on a split-belt treadmill with a sampling frequency of 1000Hz (MotekForceLink). Muscle activity of the left and right gluteus medius, gastrocnemius, soleus, tibialis anterior, rectus femoris, vastus lateralis and biceps femoris was measured using surface electromyography (Bortec Octopus 8 channel EMG) at 1000Hz.

Simulation

Model-based simulations were used to gain insight in the neuromechanics of balance control. Simulations are based on the assumption that human movement can be described in mathematical equations that can be combined into neuromechanical models. A neuromechanical model consists of equations that describe human skeletal, muscular and neural control

systems.

Inverse analyses and forward simulations were used to answer research questions on the control of balance during walking and standing (Figure 3.4). In an inverse analysis, parameters that are difficult to measure are estimated from the experimental data (e.g. muscle forces, joint loading,...). Inverse analyses were used to evaluate if the older adults use a different kinematic strategy to control balance compared to the young subjects. More specifically, joint kinematics, location of the center of mass with respect to the base of support and the underlying muscle excitations were estimated using inverse analysis techniques in the four studies. An inverse analysis consists of an inverse kinematic procedure that computes joint kinematics from the recorded marker positions and an inverse dynamics procedure that computes joint kinetics from the joint kinematics and recorded external forces.

In a forward simulation, joint kinematics are computed from muscle excitations using the neuromechanical model. This direct relation between muscle excitations, model properties and the resulting kinematics was used to evaluate the isolated effect of age-related changes in muscle and sensory function on the kinematics of balance control. Hence, this model allows to decouple the concomitant effect of age-related changes in muscle and sensory function on balance control.

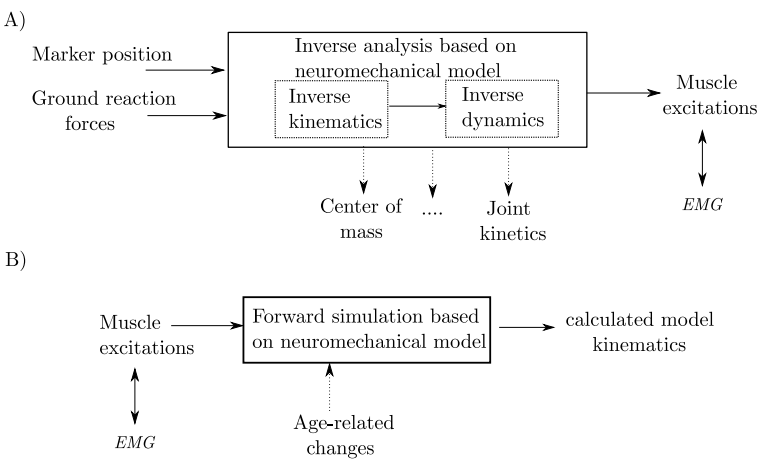

Figure 3.4: **Inverse analysis and forward simulation.** In an inverse analysis, parameters that are difficult to measure are estimated from the experimental data (motion capture). In a forward simulation, joint kinematics are computed from muscle excitations.

Neuromechanical models

Throughout this work, different levels of detail have were used to describe the skeletal, muscular and neural control systems in the neuromechanical models of standing and walking.

Standing balance

In standing balance control, a torque driven double inverted pendulum with full state feedback was adopted from [13] and used to simulate the response to a backward surface translation (Figure 3.5). Skeletal dynamics were described by applying the Euler-Lagrange formalism:

$$\boldsymbol{M(q)\ddot{q} + B(q,\dot{q}) - S(q)W_{ext} - T = 0} \tag{3.1}$$

Where $\boldsymbol{q}$ is a vector containing the generalized coordinates, $\boldsymbol{M(q)}$ is the generalized inertia matrix, $\boldsymbol{B(q,\dot{q})}$ is the vector of generalized Coriolis, centrifugal and gravitational forces. $\boldsymbol{W_{ext}}$ contains the external forces due to ground contact and the perturbation, $\boldsymbol{S(q)}$ transforms the external forces to joint forces. $\boldsymbol{T}$ is a vector containing joint torques. A detailed formulation of the equations of motion of the double inverted pendulum model can be found in the appendix.

The state ($\boldsymbol{x}$) of the double inverted pendulum model consists of the ankel and hip joint angles and angular velocities:

$$\boldsymbol{x} = \begin{bmatrix} \boldsymbol{q} & \boldsymbol{\dot{q}} \end{bmatrix}^T \tag{3.2}$$

The double inverted pendulum model was controlled using feedback. In this feedback controller, sensory information was either modelled as linear full state or linear center of mass position and velocity feedback. Hence, the joint moments were the result of full state feedback:

$$\boldsymbol{T = Kx} \tag{3.3}$$

where $\boldsymbol{K}$ is a matrix of feedback gains, which were computed by minimizing the difference between measured and simulated kinematics in a tracking simulation or by minimizing a specific task in a predictive simulation (described below).

Since the ankle was welded to the ground in this model, unrealistically high torques could be generated around the ankle. The movement of the COP was constrained based on the measured size of the base of support (i.e. dimensions of the foot). Therefore, the ankle joint moment was constrained by the base of support:

$$m(\ddot{com}_y + g)COP_{min} < T_{ankle} < m(\ddot{com}_y + g)COP_{max} \tag{3.4}$$

where m is the mass of the subjects, $\ddot{com}_y$ is the vertical acceleration of the center of mass, COP_{min} and COP_{max} represent the border of the foot (i.e. base of support).

Walking balance

In walking balance control, a musculoskeletal model with 23 degrees of freedom and 92 Hill-type muscles was used to simulate perturbed and unperturbed walking (figure 3.7).

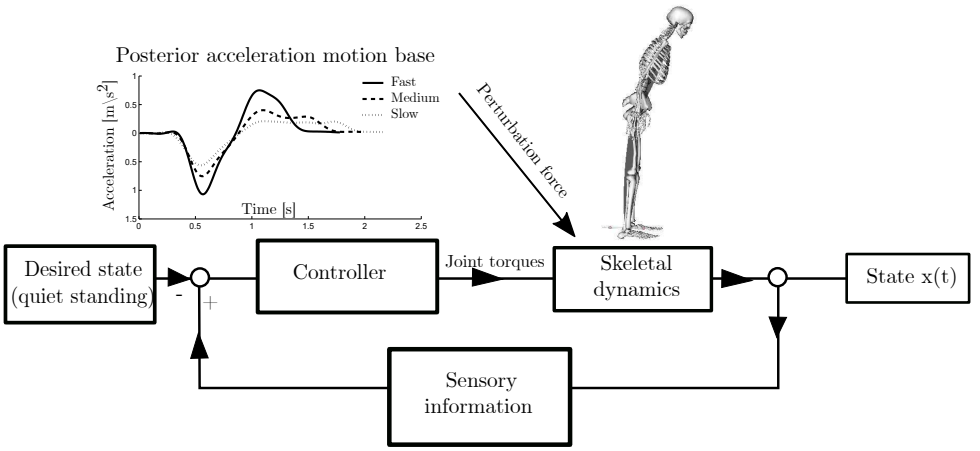

Figure 3.5: **Neuromechanical model of standing.** The feedback control model is similar to the model of Park et al. [13]. In the sensory information block, the full state of the model (ankle and hip joint angles and angular velocities) was used as sensory information. The sensory information is compared to the desired state of quiet standing. The error on the desired state is multiplied by a feedback gain matrix K to compute the ankle and hip joint torques. The different acceleration profiles of the platform as a function of time were approximated by cubic splines and imposed as external forces acting on the skeletal model.

Skeletal dynamics of this complex 3D model were derived in OpenSim (equation 3.1). Ground reaction forces were computed based on a Hunt–Crossley based contact model. Four contact spheres were added to both feet to simulate ground reaction forces (heel, metatarsal head 1-3-5). Vertical reaction force F_y acting on each sphere was computed based on the indentation and indentation velocity of the contact sphere with the ground [70].

$$F_y = \begin{cases} (10^6 k\sqrt{r}(y-r)^3)(1+c\dot{y}), & y \geq 0 \\ 0, & y < 0 \end{cases} \tag{3.5}$$

where k is the stiffness parameter, r is the radius of the sphere, y is the indentation of the sphere in the ground, c is the damping parameter and $\dot{y}$ is the indentation velocity of the sphere in the ground. The contact properties were adapted from [71] and are explained in detail in the appendix.

Friction forces (F_z) were computed as a function of the vertical ground reaction force and the horizontal velocity of the contact sphere.

$$F_z = F_y tanh(10\dot{z}) \tag{3.6}$$

where F_z is the friction force, $\dot{z}$ is the velocity of the contact sphere in the horizontal plane.

Muscle dynamics were described by activation and contraction dynamics. First, activation dynamics models the slow electro-chemical process to activate a muscle based on a neural

excitation and was formulated as a first order differential equation [41, 72]:

$$\frac{da_j}{dt} = \begin{cases} (u_j - a_j)(\frac{u_j}{\tau_a} + \frac{1-u_j}{\tau_d}), & u_j \geq a_j \\ \frac{u_j - a_j}{\tau_d}, & u_j < a_j \end{cases} \tag{3.7}$$

where a_j is the activity of muscle j, u_j is the muscle excitation, $\tau_a = 15ms$ is the activation time constant and $\tau_d = 60ms$ is the deactivation time constant.

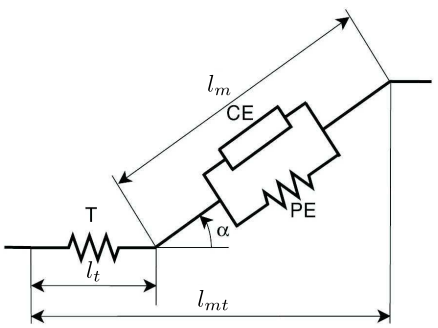

Figure 3.6: **Schematic representation of the Hill model [69].** The muscle-tendon actuator, of length l_{mt}, comprises a tendon in series with a pennate muscle. The tendon is modelled as a nonlinear spring of length l_t. The muscle, of length l_m, consists of a contractile element (CE) parallel to a passive element (PE). The pennation angle α is the angle between the orientation of the muscle fibers and the tendon.

Muscle contraction dynamics was described based on Hill's model [69]. The muscle-tendon actuator is modelled as a tendon in series with a muscle fiber. Five parameters influence the contraction dynamics for a specific muscle: optimal fiber length l_m^0, maximal muscle fiber velocity v_m^{max}, peak isometric muscle force F_m^0 tendon slack length l_t^s and pennation angle at optimal fiber length α_0. Muscle force depends on the activity trough active force-length and force-velocity characteristics and the force-length characteristics of a parallel passive element.

$$F_m = F_m^0[af_{act}(\tilde{l}_m)f_v(\tilde{V}_m) + f_{pas}(\tilde{l}_m)] \tag{3.8}$$

where F_m is the muscle force, F_m^0 is the maximal isometric muscle force , $\tilde{l}_m$ is the normalized fiber length ($\tilde{l}_m = l_m/l_m^0$) and l_m^0 is the optimal fiber length , ($\tilde{V}_m$) is the normalized fiber velocity and f_{act}, f_{pas} and f_v are respectively the active and passive force-length and force-velocity characteristics. The tendon was modelled as a non-linear spring:

$$F_t = f(\tilde{l}_t) \tag{3.9}$$

where F_t is the force in the tendon and $\tilde{l}_t$ is normalized tendon length $\tilde{l}_t = l_t/l_t^s$. The interaction between the tendon and the muscle is described as:

$$F_t = cos(\alpha)F_m \tag{3.10}$$

$$l_{mt} = l_t + l_m cos(\alpha) \tag{3.11}$$

$$l_m sin\alpha = l_m^0 sin\alpha_0 \tag{3.12}$$

where l_{mt} is the muscle-tendon length.

Passive joint moments were added to the ankle, knee, hip and lumbar joints to simulate joint capsule and ligament forces. Passive joint torques were modelled as coordinate limit forces in OpenSim:

$$P_i = k_1 e^{k_2(q_i - \theta_2)} + k_3 e^{k_4(q_i - \theta_1)} - c\dot{q}_i \tag{3.13}$$

where P_i is the passive joint torque of the joint angle i, k_{1-4} and θ_{1-2} are coefficients describing the force-angle and force-angular velocity characteristics. Coefficients were selected for each joint and were based on [73] and can be found in the appendix.

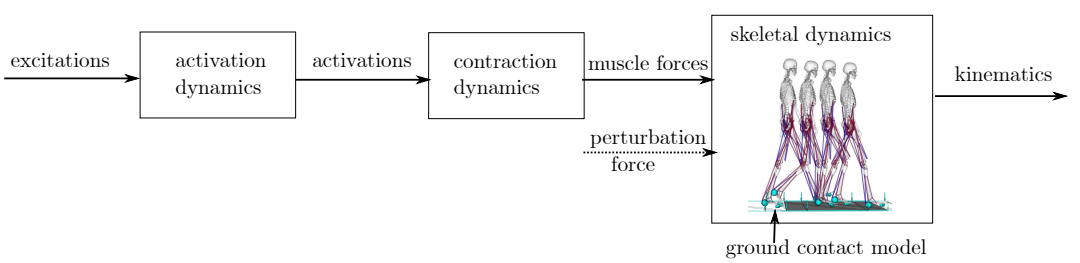

Figure 3.7: **Neuromechanical model of walking.** Excitations are input to the dynamics of the model. Activation, contraction and skeletal dynamics are integrated in a forward simulation to compute the resulting kinematics. The influence of measured reactive muscle activity on the resulting joint kinematics was evaluated by adding the reactive muscle excitations to the simulated excitations of unperturbed walking. The influence of the platform translation on joint kinematics was evaluated by adding the perturbation as an external force to the skeletal dynamics.

Both neuromechanical models of standing and walking were used in inverse analyses and forward simulations.

Inverse analysis

An inverse analysis consists of an inverse kinematic and inverse dynamic analysis (Figure 3.8). In an inverse kinematic analysis, measured marker position are given and joint kinematics are computed based on the skeletal model. In an inverse dynamic analysis, joint kinematics and external forces are given and joint torques or muscle excitations are computed based on the

muscloskeletal dynamics. Inverse analyses are mainly used to estimate variables that are difficult to measure directly such as joint kinematics, joint kinetics, muscle excitations and metabolic energy consumption. We used this method, in combination with a generic musculoskeletal model with 23 degrees of freedom and 92 Hill-type muscles (gait 2392) in OpenSim. This model was scaled to the anthropometry and mass of the subject based on the marker positions and ground reaction forces in the static trials. Joint kinematics of the scaled model were computed from the recorded marker trajectories using a Kalman smoothing algorithm [74]. Joint kinetics were computed based on the equations of motion of the model with OpenSim's inverse dynamics tool (equation 3.1). The underlying muscles forces were computed based on the joint kinematics, joint kinetics, muscle geometry and muscle dynamics. Since there are more muscles than degrees of freedom in the muscloskeletal system, muscle forces are not uniquely defined by joint torques (i.e muscle redundancy problem). Optimization methods were used to solve this redundancy under the assumption that muscle coordiation is produced by optimizing some performance criteria [69]. In standing balance control (study 1 and 3), muscle activations and forces were estimated from the joint kinematics and kinetics using static optimization. Static optimization simplifies the computation of muscle forces by assuming rigid tendons. Under the assumption of rigid tendons, muscle-tendon length and velocity can be computed from the skeletal kinematics, thereby allowing algebraic solution of the contraction dynamics [72]. Static optimization solves the muscle redundancy problem at each time frame independently by minimizing muscle activity squared [69]. In walking balance control (study 2 and 4), the muscle redundancy problem was solved using a recently developed optimization approach that accounts for Hill-type muscle dynamics and minimizes muscle excitations squared [72]. This approach was used instead of static optimization because modeling of muscle dynamics with non-rigid tendons is more important in faster motions (i.e. walking instead of standing) [72]. Metabolic energy consumption was then estimated from the joint kinematics and simulated muscle activity using the equations proposed by [75] implemented in OpenSim (Umberger2010MetabolicProbes).

Forward simulations

In a forward simulation, muscle excitations are prescribed and activation, contraction and skeletal dynamics are integrated to compute the joint kinematics from measured (i.e EMG) or pre-defined muscle excitations (Figure 3.9). Forward simulations have the potential to evaluate the influence of isolated changes in inputs (e.g. muscle excitations, feedback gains), external forces (e.g. perturbation forces) and changes in model parameters on joint kinematics. There are multiple methods to estimate the muscle excitations that drive the forward simulation including tracking simulations and predictive simulations.

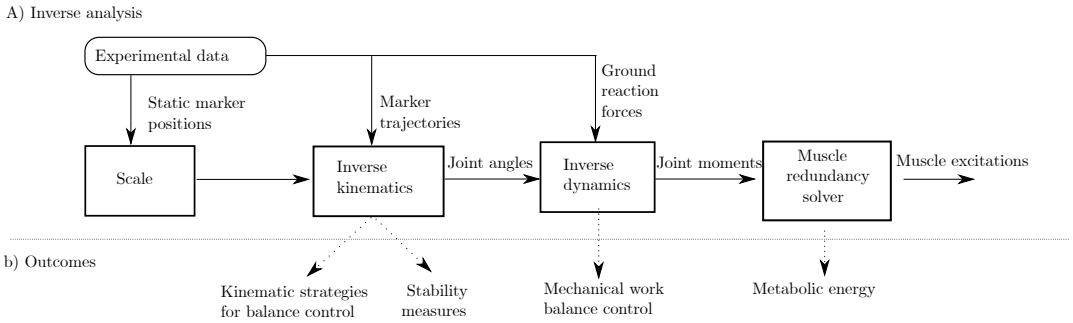

Figure 3.8: **Inverse analysis of the experimental data.** In an inverse analysis, measured marker position and external forces are given and joint kinematics, joint torques and muscle excitations are computed using respectively inverse kinematics, inverse dynamic and muscle redundancy analyses based on parts of the musculoskeletal model. For these analyses, the generic musculoskeletal model (OpenSim Gait2392) was scaled to the anthropometry of the subjects using the static marker positions. Joint kinematics were used to evaluate the kinematic strategies and compute stability measures. Joint moments were used in combination with the joint kinematics to compute joint power squared (an estimate of effort). Finally, computed muscle excitations were used to estimate metabolic energy (another estimate of effort).

Tracking simulation

In a tracking simulation, controls (i.e. muscle excitations) are selected that minimize the difference between the recorded kinematics and kinetics and the results of a forward simulation. Therefore, this method is mainly used to compute muscle excitations for a forward simulation. In addition, the difference between the measured and computed joint kinematics shows if the neuromechanical model can describe the measured data.

In perturbed standing (study 1), tracking simulations were used to evaluate if linear full state feedback or linear center of mass position and velocity feedback in a double inverted pendulum model can reconstruct observed continuum of ankle and hip strategies in perturbed standing. The feedback gains of the double inverted pendulum with center of mass or full state feedback were optimized to minimize the difference between the measured and predicted joint angles:

$$J(K) = \int_{t_0}^{t_{end}} (\hat{\boldsymbol{x}} - \boldsymbol{x})^2 dt \tag{3.14}$$

where t_0 is the onset of the platform translation and $t_{end} = t_0 + 2s$ corresponds to the end of the response.

Hence, this method evaluates the ability of the feedback-controlled double inverted pendulum model to describe the joint kinematics of non-stepping postural responses to the perturbation.

In simulations of walking (study 2 and 4), tracking simulations were used to compute muscle excitations that can reconstruct the measured joint kinematics, kinetics and ground reaction

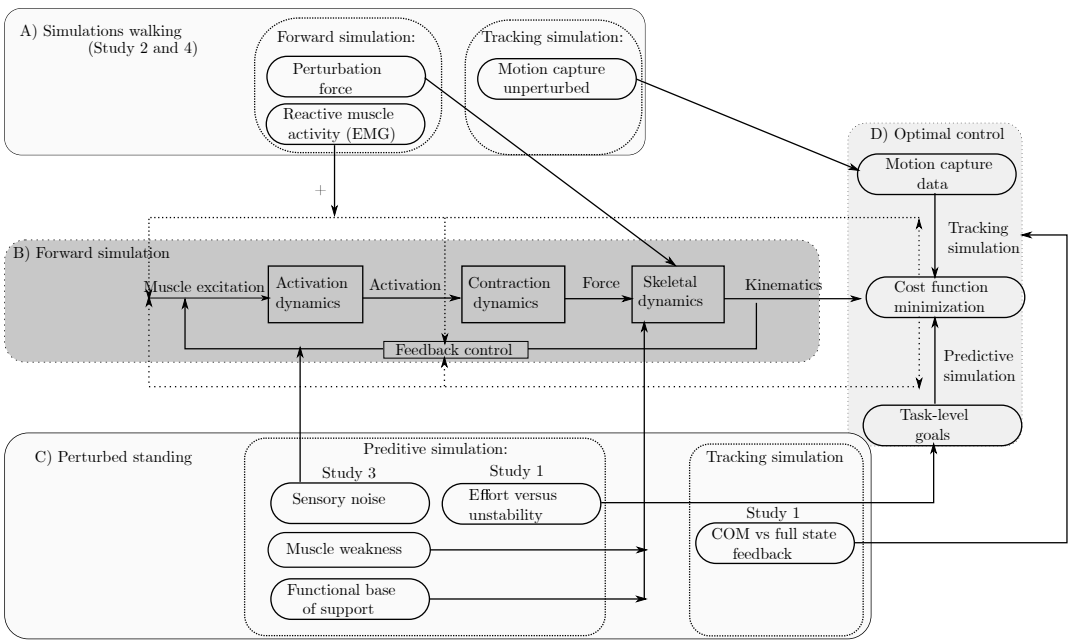

Figure 3.9: **Forward simulation.** In a forward simulation (Pane B), activation, contraction and skeletal dynamics are integrated to compute the joint kinematics from muscle excitations. Muscle excitations and/or feedback gains are commonly computed using tracking simulations and predictive simulations. In both tracking and predictive simulations, muscle excitations and/or feedback gains are optimize to minimize a specific cost function (i.e. optimal control problem). In a tracking simulation, the muscle excitations or feedback gains are optimized to track the measured joint kinematics, kinetics and muscle activity in a forward simulation. In a predictive simulation, the muscle excitations or feedback gains are optimized to minimize task level goals (i.e. performance criteria such as effort, instability, fatigue). In walking balance control (Pane A), tracking simulations were used to create pre-defined (open-loop) muscle excitations that can reconstruct the measured unperturbed walking kinematics and kinetics in a forward simulation (i.e. cost function: minimizing difference between measured and predicted movement). A perturbation force was added to the forward integration of unperturbed walking to simulate the passive response of the model to the perturbation. The active response was simulated by adding the reactive muscle activity to the pre-defined muscle excitations and the perturbation force the to skeletal dynamics in the forward simulation. In standing balance control (Pane C), Tracking simulations were used to evaluate if a torque driven double inverted pendulum model with center of mass position and velocity feedback can reconstruct the measured data. Predictive simulations were used to evaluate if the continuum of ankle and hip strategies can be predicted by minimizing effort and postural instability (i.e. cost function: minimizing effort and instability). In the third study of this PhD, age-related changes in sensory and muscle function were imposed to the predictive simulation with effort-instability task level goal to evaluate which age-related changes can predict the shift from ankle towards hip strategies in the elderly.

forces in a forward simulation. First, we solved for the joint torques that, when input to the skeleton dynamics, minimized the difference between simulated and measured movement (details below). Next, we solved for the muscle excitations that produced these joint torques by solving the muscle redundancy problem. Muscle-tendon actuators were replaced by joint actuators in the first step. Model inputs (joint torques) were optimized to minimize the difference between the measured and simulated marker positions, ground reaction forces and joint torques:

$$J = \int_{t_0}^{t_{end}} \|(\boldsymbol{p(q)} - \hat{\boldsymbol{p}}\|_2^2 + w_1 \sum_{j}^{nF} (\boldsymbol{F(x)_j} - \hat{\boldsymbol{F}}_{\boldsymbol{j}})^2 + w_2 \|\boldsymbol{T} - \hat{\boldsymbol{T}}\|_2^2 dt \tag{3.15}$$

where t_0 is the time of left heelstrike and t_{end} the time of the consecutive left heelstrike, $\boldsymbol{p(q)}$ is the vector containing the modeled marker positions, $\hat{\boldsymbol{p}}$ is a vector with the corresponding measured marker coordinates, $\boldsymbol{F(x)}$ and $\hat{\boldsymbol{F}}$ are vectors containing respectively the simulated and measured ground contact forces and moments and nF equals two (ground reaction force under left and right foot). $\hat{\boldsymbol{T}}$ is a vector containing the inverse dynamic joint torques based on the measured kinematics and ground reaction forces, $\boldsymbol{T}$ is a vector containing the corresponding simulated joint torques. The optimization was subject to skeleton dynamics.

In a second step, the simulated muscle excitations that generate the inverse dynamic joint torques were computed using dynamic optimization. We modified the dynamic optimization approach proposed by [72] to include tracking of the measured electromyography data of the gluteus medius (study 2). The objective function contains a part that minimizes muscle excitations squared, a second part the minimizes the differences between the measured (EMG) and simulated excitations and a third part that minimizes the torque generated by ideal torque actuators (Equation 3.16).

$$J = \int_{t_0}^{t_{end}} \sum_{i}^{nMus} e_i^2 + w_1 (s\hat{e}_{EMG} - e_{EMG})^2 + w_2 \sum_{j}^{nDOF} e_{Tj} T_{max} dt \tag{3.16}$$

where nMus=92 is the number of muscles in the model, e_i is the simulated excitation of muscle i, $\hat{e}_{EMG}$ is the measured gluteus medius muscle excitation (EMG), s is an optimization variable that scales the EMG from voltage to muscle excitations, e_{EMG} is the simulated gluteus medius excitation. Reserve actuators were added to guarantee feasibility in the presence of fast changes in joint torques in the tracking simulation that can not be generated by the muscles. T_{max} equals 150Nm and is the reserve actuator action on degree of freedom j, e_{Tj} is the activation of the reserve actuator of DOF k. Note that the weight w_2 is high to penalize the use of the reserve actuators. This objective function was minimized subject to dynamic constraints following from muscle activation and contraction dynamics and to path constraints imposing that the model's actuators (muscles, passive torque, reserve actuators) should produce the inverse dynamics joint torques from the tracking simulation (step 1). The source code of the muscle redundancy solver can be found on the simtk project optcntrlmuscle.

Results of the tracking simulation were then used to evaluate the isolated contribution of reactive muscle activity and the perturbation force to the kinematics of balance control in a forward simulation (Figure 3.7). To this aim, the time series of simulated muscle excitation and the initial state of the model, computed in the tracking simulation, were used as input to a forward simulation to simulate the unperturbed gait pattern. The influence of the perturbation (passive response) and the combined influence of perturbation and muscle activity (active response) was simulated separately for all the measured perturbation trials. The passive response of the musculoskeletal model to the perturbation was simulated by imposing the platform translation to a muscle-driven forward simulation, controlled by the muscle excitations computed for unperturbed walking.

The platform translation was applied as an external force, equal to the segment mass times the platform accelerations, at the center of mass of all the segments during the forward simulation. The active response of the musculoskeletal model to the perturbation was simulated by imposing the platform translation and adding the measured individual change in gluteus medius activity to the muscle excitations of unperturbed walking.

Predictive simulations

In a predictive simulation, the joint kinematics are predicted without input from measured data (i.e. data-free simulation) and is based on the neural control and musculoskeletal system. Optimal (feedback) control is commonly used in perturbed standing to model the neural control system [13, 14]. Optimal control selects a movement strategy in the redundancy of all potential strategies [69]. This method assumes that the neural systems selects a neuromechanical strategy optimizing performance criteria. Different performance criteria were used in standing and walking including; minimization of center of mass movement, deviation from upright posture, effort and fatigue [15, 76, 77]. These performance criteria, also referred to as task-level goals, are defined as motor intention that cannot be directly mapped to a particular sensory input or a unique motor output [78]. By its formulation, this method can provide evidence that it is possible that the nervous system selects strategies based on specific task-level goal to (learn the) control of balance during standing and walking.

In standing balance control (Study 1 and 3), predictive simulations were used to evaluate if the continuum of ankle and hip strategies that are experimentally observed can be explained by the relative importance of minimizing instability and effort related performance criteria (study 1). Hence, the performance criteria (i.e. objective function):

$$J(K) = \int_{t_0}^{t_{end}} [w(Xcom)^2 + (1-w) \sum_{i}^{nDOF} (\dot{q}_i T_i)^2] dt \tag{3.17}$$

where Xcom is the extrapolated center of mas, $nDOF = 2$ and represent the ankle and hip joint angles in the double inverted pendulum and w is a weight that represents the relative importance of both terms in the objective function.

Predictive simulations were also used to evaluate the influence of age-related changes in muscle and sensory function on the control of balance (study 3). The properties of the model for standing balance control was adjusted to simulate age-related changes in muscle and sensory function. Therefore, constraints were imposed on the maximal (rate of) joint torques to simulate weakness [43] and on the maximal base of support to simulate a reduced functional base of support in the elderly [20, 79]. To exclude the effect of changes in task-level goals, we selected the weight w such that an ankle strategy was predicted for the model without age-related constraints. Therefore, changes in the predicted strategy can be solely attributed to changes in the parameters describing the musculoskeletal system. Furthermore, to assess the effect of age-related changes in sensory information, white Gaussian noise (i.e. with a normal distribution) was added to the sensed states in the feedback model. The modelled full state noise is a simplified representation of the integrated sensory information of the visual, vestibular and somatosensory system. A novel method was developed to find the optimal feedback gains in the presence of sensory noise. To avoid the simulation of responses that were tuned towards a specific noise signal, feedback gains that minimized the cost function for multiple random noise signals simultaneously were computed.

Numerical methods to solve optimal control problems

The tracking and predictive simulations require solving large optimization problems (i.e. optimal control problems). The differential equations for musculoskeletal dynamics are numerically stiff and highly nonlinear. As a result, forward integrations require small time steps [80], and the optimization is slow and sensitive to local minima [80]. In this PhD, numerical techniques were used to improve the convergence and reduce computation time for solving the optimal control problems.

First, all optimization problems for the tracking and predictive simulations were solved using a direct collocation approach. Using this approach, the states and controls trajectories are discretized on a mesh. The discretized states and controls are implemented as optimization variables and the muscloskeletal dynamics are implemented as dynamic constraints. Hence, direct collocation simulates the dynamic equations by solving all time frames simultaneously. This results in a large non-linear programming problem (NLP), which we solved using Ipopt [81]. The NLP was created using the direct collocation software GPOPS II [82]. Direction collocation was used instead of the commonly used shooting method to solve the optimal control problem. In a shooting method, the cost function is evaluated using time-marching (i.e. time frames are solved sequentially) to simulate the muscloskeletal dynamics. Given the stiff differential equations of the musculoskeletal system, time marching results in long computation times [73] and high sensitivity of the states to the controls [72].

Second, skeletal, activation and contraction dynamics were formulated implicitly. The implicit representation introduced additional controls, defined as the time derivatives of the states, allowing the to be imposed as algebraic path constraints, resulting in very simple dynamics equations [72] . The implicit formulation of muscle dynamics improved convergence and

decreased computation time in the muscle redundancy solver [72]. In addition, no inversion of the (ill-conditioned) mass matrix is needed when evaluating the skeletal dynamics implicitly, which may improve convergence and reduce computation time.

Third, automatic differentiation software Adigator was used in the simulations of standing balance control and in the muscle redundancy solver to produce analytic values for the derivatives that are required by the NLP solver (Ipopt) [81, 83]. Automatic differentiation generates analytic derivatives by applying differentiation rules (e.g. product, quotient, and chain rules) on the elementary function operations that underlie the code. De Groote et. al. showed that automatic differentation decreases the computation time when solving the muscle redundancy problem [72]. Since OpenSim does not support automatic differentiation, finite differences were used to compute the derivatives in the tracking simulations of walking.

Chapter 4

Mechanical effort predicts the selection of ankle over hip strategies in non-stepping postural responses

Maarten Afschrift, Ilse Jonkers, Joris De Schutter, Friedl De Groote

Published in *Journal of Neurophysiology*

Abstract

Experimental studies have shown that a continuum of ankle and hip strategies is used to restore posture following an external perturbation. Postural responses can be modeled by feedback control with feedback gains that optimize a specific objective. On the one hand, feedback gains that minimize effort have been used to predict muscle activity during perturbed standing. On the other hand, hip and ankle strategies have been predicted by minimizing postural instability and deviation from upright posture. It remains unclear, however, whether and how effort minimization influences the selection of a specific postural response. We hypothesize that the relative importance of minimizing effort versus postural instability influences the strategy used to restore upright posture. This hypothesis was investigated based on experiments and predictive simulations of the postural response following a backward support surface translation. Peak hip flexion angle was significantly correlated with three experimentally determined measures of effort, i.e. joint power squared, mean muscle activity and metabolic energy. Furthermore, a continuum of ankle and hip strategies was predicted in simulation when changing the relative importance of minimizing effort and postural instability, with increased weighting of effort resulting in an ankle strategy. In conclusion, the combination of experimental measurements and predictive simulations of the postural response to a backward support surface translation showed that the trade-off between effort and postural instability minimization can explain the selection of a specific postural response in the continuum of potential ankle and hip strategies.

New and Noteworthy: First, we investigated the relation between effort minimization and the selection of a postural response in the continuum of potential ankle and hip strategies. We found that ankle strategies can be explained by minimizing effort whereas hip strategies can be explained by minimizing instability. Second, although previous studies showed that center of mass (COM) feedback is important, our results indicate that a COM feedback controlled torque-driven model cannot accurately track the experimental hip strategies.

Keywords: Standing balance control, Postural responses, simulation, motor control

Introduction

An improved understanding of the neuromechanics of human balance control has the potential to improve the assessment and treatment of balance disorders. However, till to date, the factors determining postural control strategies in response to perturbations of standing remain unclear. Computer simulations are a useful tool to investigate causal relations that cannot be directly measured experimentally.

Ankle and hip strategies are the two main non-stepping postural responses to a perturbation of standing [26]. Using an ankle strategy, the postural equilibrium is maintained by rotating the body as a rigid segment around the ankle joint [26]. Using a hip strategy, the postural equilibrium is maintained by flexing the hips and plantar flexing the ankles [26]. Ankle and hip strategies are the extremes in the continuum of non-stepping postural responses [15, 26, 84, 85]. The ankle strategy is mainly used by healthy subjects to cope with small perturbations of balance [26] Runge et al., 1999). In more challenging conditions, subjects gradually switch their postural response from an ankle towards a hip strategy [26]. Examples of more challenging conditions are an increased perturbation magnitude [26] or a reduced base of support, e.g. when standing on a narrow beam [26]. The selection of a postural response not only depends on the perturbation conditions but is also influenced by experience, adaptation [86], and fear of falling [27]. However, the determinants for selecting an ankle or hip strategy remain unclear. It has been suggested that an ankle strategy is advantageous to maintain an upright pose with minimal head movements, which is thought to improve sensory feedback from the vestibular and visual systems [15, 87]. On the other hand, Kuo and Zajac showed that using a hip strategy increases the capability for accelerating the center of mass (COM) without stepping and that the instantaneous muscle activity for a desired COM acceleration is lower during a hip than during an ankle strategy [67]. This might explain why a hip strategy is used in more challenging conditions. However, only the instantaneous muscle activity needed to accelerate the center of mass was investigated. Therefore, it remains unclear whether the total muscle effort during the postural response is smaller for a hip strategy than for an ankle strategy.

Perturbed standing is controlled based on integrated feedback from visual, vestibular and somatosensory systems, and this complex feedback signal has been modelled in different ways. Park et al. used full state feedback to control a torque driven double inverted pendulum model [13, 64, 65]. They showed that this model could accurately track experimental kinematics and kinetics. Alternatively, Ting et al. used delayed COM position, velocity and acceleration feedback to control a muscle driven inverted pendulum model [58, 76]. They showed that for each muscle a set of feedback gains could be determined such that the model accurately reconstructed the measured muscle activity in response to forward and backward perturbations [76]. However, since COM and full state feedback are equivalent when controlling a single inverted pendulum, it is still unclear whether COM feedback is sufficient to control a model with more than one degree of freedom.

It has been suggested that in the aforementioned feedback models, a specific postural response is selected from a redundant set of responses by optimizing performance [15,58,88]. Different performance criteria have been used; including minimization of (1) center of mass movement (2) deviation from upright position (3) muscle activity squared. Kuo showed that minimizing COM movement of a double inverted pendulum model resulted in a hip strategy whereas minimizing deviation from the upright position resulted in an ankle strategy [29]. On the other hand, measured muscle activity and COM kinematics of a muscle driven inverted pendulum model can be predicted by minimizing the weighted sum of muscle activity squared (i.e. neural effort) and deviation from the upright position [58,76,86]. In addition, Welch and Ting (2014) showed that during adaptation to perturbations of standing, experimental muscle activity patterns shift closer towards the minimal muscle effort activity patterns. Furthermore, McKay and Ting (2012) showed that muscle activity and ground reaction forces can be predicted for perturbed standing in cats by a cost function that minimizes muscle activity squared while satisfying the measured forces and moments around the COM [88]. Hence, these studies suggest that postural responses are optimized to minimize neural effort, which is related to energy consumption. Although simulations showed that the optimization criterion influences the predicted strategy and that postural responses can be predicted by effort minimization, it is still unclear whether and how minimizing effort influences the selection of a specific postural response from the redundant set of ankle and hip strategies.

The main goal of this study was therefore to investigate whether the selection of a postural response to recover from a backward translation of the support surface can be explained by the trade-off between mechanical effort, and postural instability. Experiments and predictive simulations were combined to evaluate the correlation between the peak hip angle, indicative of the use of a hip strategy, and mechanical effort, muscle effort, and metabolic energy used by the subject. We hypothesized that the relative importance of minimizing effort versus postural instability can explain the continuum of observed postural responses. To test this hypothesis, kinematics predicted by an optimal feedback control model were compared to measured kinematics. In addition, two sensory architectures, i.e. COM feedback and full state feedback, and the effect of more demanding conditions, more specific a decreased base of support, on the postural response were evaluated.

Method

An overview of the hypothesis, research question and various methods can be found in figure 4.1.

Experiments

During the experiments, the posture of 10 healthy adults (21 ± 2 STD (standard deviation) years) was perturbed by a sudden backward translation of the motion base (MotekMedical, Netherlands). The measurement protocol was submitted to and approved by the commission

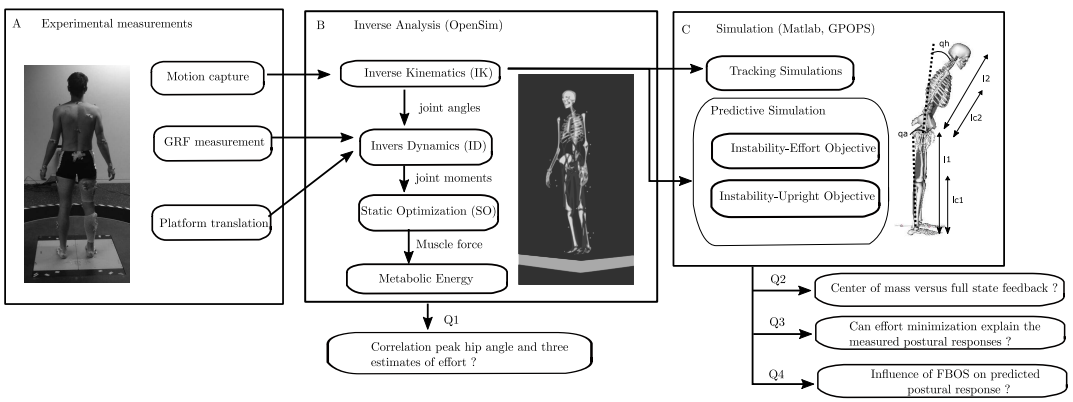

Figure 4.1: **Workflow.** Pane A shows the experimental measurements of the 10 healthy subjects where the posture was perturbed by means of a posterior platform translation. The motion capture and ground reaction forces (GRF) data was combined with a scaled musculoskeletal model to conduct the inverse analysis of the postural response (Pane B). Joint kinematics, joint moment, muscle forces and metabolic energy consumption were calculated to evaluate if three estimates of effort are correlated with the peak hip angle during the postural response (research question Q1). The computed joint kinematics were used in the tracking simulations (Pane C) to evaluate if COM feedback is sufficient to model the measured postural response (research question Q2). Furthermore, the joint kinematics prior to perturbation and after the perturbation were used to constrain the predictive simulations (Pane C). Predictive simulations were used to evaluate the influence of minimizing mechanical effort versus postural instability on the postural response (research question Q3). Minimizing mechanical effort was compared to an objective function proposed by Kuo et al. 1995 to evaluate if effort explains the ankle strategy as well as upright posture. Finally, predictive simulations were used to evaluate the influence of a reduced FBOS on the predicted postural response (research question Q4).

of medical ethics of KU Leuven, Belgium. All participants gave written informed consent before participating in the study. The subjects were instructed to stand on marked foot positions corresponding to a stance width that equaled their shoulder width. The subjects knew that the platform could move randomly in medio-lateral and anterior-posterior directions and were instructed to maintain stability without stepping. The data was controlled visually and automatically to exclude postural responses with heel-lift or stepping. The motion base translated in anterior-posterior or medio-lateral direction over a distance of 0.16m with three different acceleration profiles (figure 4.2). In order to minimize anticipation, the perturbation protocol was semi-randomized. Random perturbation directions were applied in the three blocks of respectively medium, fast and slow acceleration profiles. These acceleration profiles were sufficient to elicit a wide range of postural responses. Two trials were measured for each perturbation acceleration profile and direction. Only the posterior platform translations were used in the current study, resulting in a total of six trials for each subject. Integrated motion capture was used to measure the postural response of the subjects: 3D marker coordinate data and the ground reaction forces under both feet were measured using a Vicon system (100Hz) and two AMTI force plates (1000Hz). An extended plug in gait marker protocol (58 makers) was used to capture the full body movement ([89], appendix). The functional base of support (FBOS) was measured for each subject. To this aim the subjects were asked to move their trunk maximally anteriorly and posteriorly without lifting their feet. Subsequently, the extreme positions of the center of pressure (COP) with respect to the ankle quantified the FBOS.

Inverse analysis of the experimental data

The experimental data of each individual trial was analyzed in OpenSim [68] to evaluate the correlation between the peak hip flexion angle, characterizing the use of a hip strategy, and the mechanical effort, muscle effort and metabolic work used by the subject. A scaled skeletal model with 23 degrees of freedom and 92 hill-type muscles (Gait2392model) [68, 90] was used to calculate joint kinematics from the recorded marker trajectories using a Kalman smoothing algorithm [74]. Joint kinetics were calculated with the inverse dynamics tool.

Subsequently, muscle activations and forces were estimated using static optimization. Static optimization assumes that muscles are coordinated to optimize performance while satisfying the kinetic constraints of the movement. Static optimization solves the muscle redundancy problem at each time frame individually by minimizing muscle activity squared, a commonly used objective function [69]. Subsequently, three estimates of effort were computed over the duration of the postural response (2 seconds). First, the time integral of joint power squared, which accounts for the positive and negative mechanical work needed for balance control was computed from the measured joint kinematics and kinetics to estimate mechanical effort:

$$\text{mechanical effort} = \int_{t_0}^{t_{end}} \sum_{j=1}^{nDOF} (\dot{q}_j T_j)^2 dt \tag{4.1}$$

Where t_0 is the start of the perturbation, t_{end} is 2 seconds after the start of the perturbation, nDOF is the number of degrees of freedom (ankle, knee and hip joint angles in the sagittal plane), $\dot{q}_i$ is the joint angular velocity and T_i is the joint moment. Second, the increase in muscle activity was integrated over the duration of the postural response:

$$\text{Muscle Effort [-]} = \int_{t_0}^{t_{end}} \sum_{i=1}^{nMuscles} (a_i - a_{i,0}) dt \tag{4.2}$$

where Muscles = 92 is the number of muscles in the Gait2392Model, a_i is the computed muscle activity. Third, the increase in metabolic power was integrated over the duration of the postural response:

$$\text{Metabolic work [J]} = \int_{t_0}^{t_{end}} \sum_{i=1}^{nMuscles} (\dot{E}_i - \dot{E}_{i,0}) dt \tag{4.3}$$

The experimental data, models and simulations are available to the reader on the Simtk project "Mechanical work predicts non-stepping postural responses".

Simulation model

Forward simulations with a linearized double inverted pendulum model proposed by [13] were generated for each measured postural response (figure 4.2). The model has two rotational degrees of freedom, four states ($x = \begin{bmatrix} q_{ankle} & q_{hip} & \dot{q}_{ankle} & \dot{q}_{hip} \end{bmatrix}^T$, ankle and hip angle and angular velocity) and two controls (ankle joint moment and hip joint moment, $u = \begin{bmatrix} T_{ankle} & T_{hip} \end{bmatrix}^T$. The ankle joint angle is defined as the angle between the leg and the vertical, the hip joint angles is defined as the angle between the torso and the leg. The inertial parameters of the segments were derived from the scaled OpenSim models that were used to analyze the experimental data [90]. Acceleration of the motion base was implemented as an external force acting on the feet in the simulation. A feedback loop was added to model control of postural responses (figure 4.2). Two different sensory information architectures were evaluated. First, the four states were used as feedback signals [13]. Second, only COM position and velocity were used as feedback signals, similar to the work of Ting et al. [14, 58, 76, 86, 91]. Subsequently, the feedback signals were compared to the desired values corresponding to quiet upright standing and multiplied by a set of feedback gains to compute the ankle and hip joint moments that drive the model. The feedback gains K were selected through optimization as discussed below.

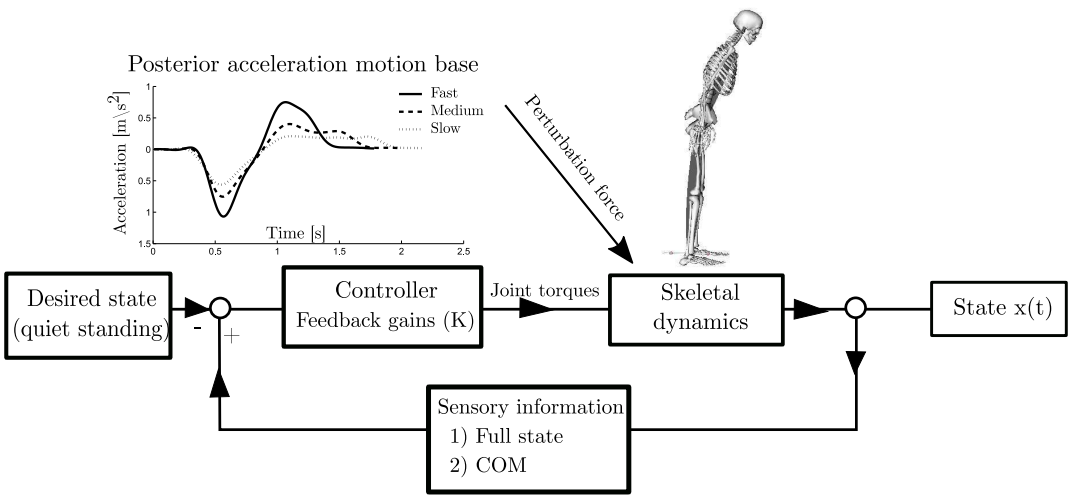

Figure 4.2: **Feedback control model.** The feedback control model is similar to the model of Park et al. [13]. In the sensory information block, either the full state of the model (ankle and hip joint angles and angular velocities) is used or only the COM position and velocity are used. The sensory information is compared to the desired values corresponding to quiet standing. The error on the desired state is multiplied by a feedback gain matrix K to compute the ankle and hip joint torque (eight feedback gains for full state feedback and four feedback gains for COM feedback). The different acceleration profiles of the platform as a function of time were approximated by cubic splines and imposed as external forces acting on the skeletal model. Appendix 1 contains detailed information on the skeletal dynamics, perturbation forces and feedback control system.

Optimization

To evaluate the ability of the feedback controlled double inverted pendulum model to describe non-stepping postural responses to perturbations of standing, feedback gains were determined for the full-state and COM feedback models by minimizing the difference between the experimental and simulated kinematics:

$$J(K) = \int_{t_0}^{t_{end}} (x - \hat{x})^2 dt \tag{4.4}$$

where t_0 is the onset of the platform translation and $t_{end} = t_0 + 2s$ corresponds to the end of the response. x and $\hat{x}$ are the simulated and measured joint kinematics respectively. These simulations will be referred to as tracking simulations. Predictive simulations with the double inverted pendulum model were used to evaluate the relative importance of mechanical effort versus postural stability. A first objective function consisted of a weighted sum of (1) the integral of the extrapolated center of mass position with respect to the quiet standing position, a measure of stability accounting for the COM velocity [6], and (2) the sum of ankle and hip joint power squared, a measure for the mechanical effort needed for postural control:

$$J(K) = \int_{t_0}^{t_{end}} [fw(Xcom - Xcom_0)^2 + (1-w) \sum_{i}^{nDOF} (\dot{q}_i T_i)^2] dt \tag{4.5}$$

where $f = 2e^5$ is a scale factor to account for the different magnitude of both parts of the objective. Xcom is the extrapolated center of mass [6] and $Xcom_0$ is the position of the extrapolated center of mass prior to perturbation. $\dot{q}$ is a vector containing the ankle and hip angular velocities, and w is the relative weight between both parts of the objective function. This value was varied between 0 and 1 in steps of 0.03 to investigate the influence of both terms of the objective function on the predicted kinematics. We will refer to this function as the instability-effort objective function. Note that $Xcom_0$ is equal to the center of mass and center of pressure position during quiet standing prior to perturbation. The deviation of the Xcom from the center of pressure during quiet standing and not from the instantaneous COP was minimized because the instantaneous COP might be close to the boundaries of the BOS and in that case, a Xcom close to the boundaries of the BOS and hence a small margin of stability would not be penalized. In addition, this modeling choice allows easy comparison with previous studies [15, 58, 76].

The weight (w) was varied between 0 and 1 in steps of 0.03 to investigate the influence of both terms of the objective function on the predicted kinematics. The weight that best predicted the measured joint kinematics was selected based on the root mean square difference between the experimental and measured joint angles.

A second objective function consisted of a weighted sum of (1) the integral of the extrapolated center of mass position with respect to the quiet standing position, a measure of stability and

(2) the integral of the ankle and hip joint angle, a measure for the deviation from upright posture:

$$J(K) = \int_{t_0}^{t_{end}} [2e^2 w(Xcom - Xcom_0)^2 + (1-w)(q)^2]dt \tag{4.6}$$

This objective function was used to investigate whether effort explains the selection of an ankle strategy as well as upright posture and is similar to the function proposed by [15]. We will refer to this function as the instability-upright objective function.

In order to provide a hot start for the optimization, the initial feedback gains were computed from the experimental joint kinematics and kinetics. For each joint, the feedback gains were computed by solving the linear set of equations expressing that the measured joint moments equal the measured states times the feedback gains:

$$K_0 \begin{bmatrix} \hat{x}_0 & \hat{x}_i & ... & \hat{x}_{end} \end{bmatrix} = \begin{bmatrix} \hat{T}_0 & \hat{T}_i & .... & \hat{T}_n \end{bmatrix} \tag{4.7}$$

where K_0 is the initial guess for the feedback gains, $\hat{x}$ are the experimental joint angles and velocities and $\hat{T}$ are experimental joint moments. This over determined set of equations was solved for K_0 in a least squares sense.

Task and physiological constraint

Constraints were added to make the simulation physiologically and mechanically more realistic. First, the movement of the COP was constrained based on the measured FBOS. As the feet were welded to the ground, the ankle joint moment was directly related to the distance between the COP and the ankle joint. Therefore, the FBOS of each subject was imposed by constraining the ankle joint moment during the simulation:

$$m(\ddot{com}_y + g)COP_{min} < T_{ankle} < m(\ddot{com}_y + g)COP_{max}$$

where m is the mass of the subject, $\ddot{com}$ is the vertical acceleration of the COM, COP_{max} and COP_{min} are respectively the measured maximal and minimal position of the COP with respect to the ankles. The influence of a reduced FBOS on the predicted kinematics was evaluated by decreasing the FBOS in steps of 3mm until no feasible solution could be found (i.e. the constraints could no longer be satisfied). These simulations were performed to evaluate if the predicted postural response shifts from an ankle towards a hip strategy in more demanding conditions. In this case, the weight w was kept constant to exclude the influence of a change in objective (w=0.1).

Second, the initial joint angles and joint moments of the model were constrained based on the experimental joint angles and moments prior to perturbation:

$$\hat{T}_{t_0} - 10Nm < T_{t_0} < \hat{T}_{t_0} + 10Nm \tag{4.8}$$

$$\hat{x}_{t_0} = x_{t_0} \tag{4.9}$$

This prevented the feedback controlled double inverted pendulum model to anticipate the perturbation and therefore models the anticipatory feed-forward control used by the subject. Third, the final state of the model was bounded based on the measured joint angles after perturbation:

$$\hat{x}_{t_{end}} - \begin{bmatrix} 5° & 5° & 20°s^{-1} & 20°s^{-1} \end{bmatrix} \leq x_{t_{end}} \leq \hat{x}_{t_{end}} + \begin{bmatrix} 5° & 5° & 20°s^{-1} & 20°s^{-1} \end{bmatrix} \tag{4.10}$$

Fourth, the feedback gains were constrained to result in a stable closed-loop system. A closed-loop system is stable if the real parts of the eigenvalues are negative. For numerical reasons, this condition was not directly imposed. Instead, the property that the states of a stable system are bounded over time was used. Therefore, an additional constraint was imposed that the ankle and hip joint angles returned within the boundaries of normal standing after 20s of simulation starting from six different initial body configurations (angle joint angles between -3 ° and 3 ° and hip joint angles between -6° and 6°). The real parts of the eigenvalues of the system matrix were calculated post-hoc to evaluate if this constraint resulted in a stable system. Finally, the rate of change of the ankle and hip joint moments was bounded between -250 Nm/s and 250 Nm/s. This value is similar to the average maximal rate of change in joint moments found in the experimental trials and resulted in the best prediction of joint moments.

All constrained dynamic optimization problems were solved using the direct collocation software GPOPS 2. The sensitivity of the optimized feedback gains to the initial guess was investigated using 150 simulations with random initial feedback gains. The random feedback gains were selected using latin hypercube sampling. The sensitivity of predicted postural response to a 10 % change in the optimal feedback gains was investigated to evaluate the robustness of the control strategy to parameter variations. More details on this sensitivity analysis and on the optimization problem can be found in the appendix

Statistical analysis

To evaluate if minimizing effort can explain the selection of a postural response in the continuum of potential ankle and hip strategies, statistical analyses on both the experimental and simulation results were conducted. A linear mixed-effect analysis was used to evaluate the correlation between the measured peak hip angle in each postural response and (1) the measured mechanical effort, (2) the estimated muscle activity, and (3) the estimated metabolic energy consumption (IBM SPSS Statistics for Windows, Armonk, NY, USA). The estimates of effort were used as a fixed effect and intercept and slope for each subject were used as

random effects, in order to account for subject variability. The same linear mixed model was used to evaluate the correlation between the optimal value of w and the measured peak hip angle. The optimal value of w that weights both parts of the instability-effort and instability-upright objective function was used as a fixed effect, the slope and intercept were used as random effect.

Results

Experimental data

The measured peak knee angle during the postural response was limited (5°+/- 3.8° STD). There were significant strong positive correlations between (a) the measured peak hip angle and joint power squared [F (1, 8.6) = 31.37, p<0.001], (b) the measured peak hip angle and the increase in muscle activity following the perturbation [F (1, 10.4) = 35.39, p<0.001], and (c) the measured peak hip angle and the metabolic work [F (1, 8.2) = 45.02, p<0.001] (figure 4.3).

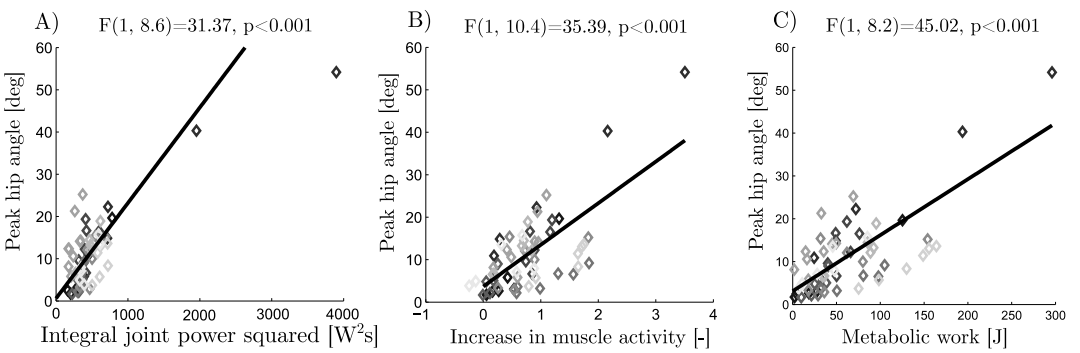

Figure 4.3: **Correlation between measured peak hip angle and the data-based approximations of effort used during the postural response.** Each point represents a single trial of a subject. Different shades of gray were used for each subject. Significant strong correlations were found between the measured hip range of motion and (A) mechanical effort, (B) increase in muscle activity, (C) metabolic work. The black line is constructed from the mean slope and mean intercept of the different subjects in the linear mixed model.

Sensitivity analysis

The sensitivity of the optimized feedback gains to the initial guess of the feedback gains showed that the initial guess influenced the optimization results due to local minima. However, the optimization starting from the hot start (i.e. computed from the recorded kinematics and kinetics) resulted in the minimal objective values. The sensitivity of predicted postural response to a 10 % change in the optimal feedback gains showed that for the predicted ankle strategies (i.e. minimizing effort) variations in the feedback gains of the ankle and hip joint angle have a strong impact on the predicted postural response and small variations

result in an unstable system. Variations in the optimal feedback gains of the predicted hip strategies (i.e. minimizing postural instability) on the other hand have a smaller impact on the predicted postural response. More information on this sensitivity analysis can be found in the appendix.

Tracking simulations

The RMS (root mean square) difference between the experimental and simulated joint angles was computed for each measured postural response. The average RMS difference of all measured postural responses was 1.1° (+/- 0.8 STD) for the tracking simulation with full state feedback. This RMS difference was 10.7° (+/- 15.1° STD) for the tracking simulations with center of mass feedback only. In the tracking simulation with center of mass feedback the RMS error increased with increasing peak hip angle during the response (figure 4.4, C). The results of the tracking simulation with full state feedback and with COM feedback for a randomly selected postural response are visualized in figure 4.4 (A, B).

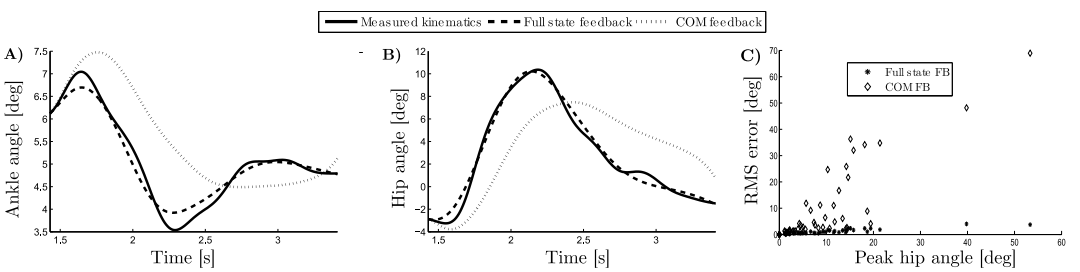

Figure 4.4: **Comparison of COM feedback and full state feedback.** Results of tracking simulation in a randomly selected postural response are shown for the ankle (A) and the hip angle (B). In this case, the RMS difference between the measured and simulated angles was 0.7° and 4.5° for the tracking simulation with full state feedback and COM feedback respectively. The RMS error as a function of the peak hip angle for all measured trials is shown in C. The RMS error for the simulations with COM feedback increases when the measured peak hip angle increases.

Predictive simulations

A low value of w (i.e. minimizing mechanical effort) predicted the experimental kinematics best when the subject used an ankle strategy, whereas a high value of w (i.e. minimizing postural instability) predicted the kinematics best when the subject used a hip strategy (figure 4.5). The RMS difference between the experimental and the simulated joint angles was 3.2° (+/- 2.4° STD) for the predictive simulations with instability-effort objective function with optimal weights. For the simulations with the upright-instability objective [29], the RMS difference between the experimental and the simulated joint angles was 3.9° (+/- 2.4° STD).

There was a clear correlation between the optimal value of w and the experimental peak hip angle for energy-postural instability objective ($F(1, 8.023) = 13.62$, $p=0.006$) and for

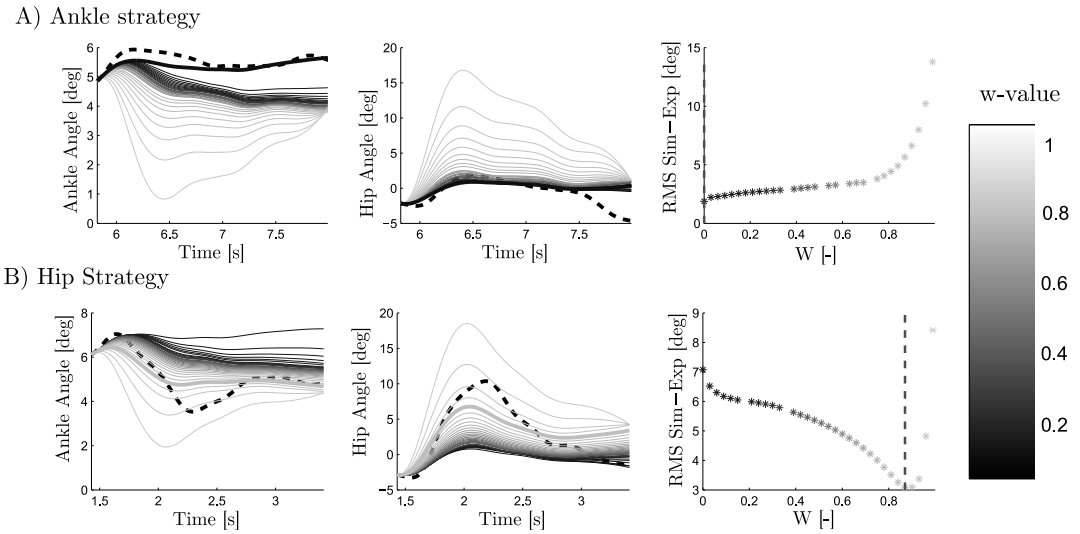

Figure 4.5: **Results of the predictive simulation for a typical measured (A) ankle strategy and (B) hip strategy.** The black dotted lines represent the experimentally measured joint angles of a single trial of one subject in response to the perturbation; the gray lines represent the results of the predictive simulations with various values of w. The left and middle graphs show respectively the ankle and hip joint angle as a function of time. The right graphs show the root mean square (RMS) difference between the experimental and simulated kinematics as a function of w. The predicted postural response with the lowest RMS difference is selected as and is highlighted with the red dotted line in the right graphs and as a bold line in the left and middle graphs. A typical ankle and hip strategy were selected based on the measured peak hip angle, which was respectively in the 25 and 75 percentile of the measured peak hip angles.

the upright posture-postural instability objective (F(1, 12.049) = 10.869, p=0.006) (figure 4.6).

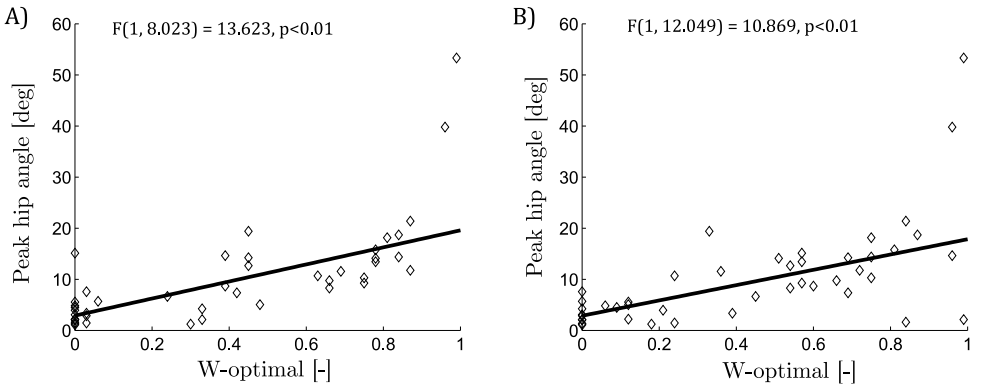

Figure 4.6: **Correlation between optimal weight and measured peak hip angle.** The optimal value of w that weights the two parts in the objective function was selected for each trial. Each dot represents the optimal value of w for an experimental perturbation trial. (A) Shows a significant correlation between the measured peak hip angle and optimal w for the instability-energy objective. (B) Shows a significant correlation between the measured peak hip angle and w-optimal for the instability-upright objective.

The predicted peak hip angle increased when the FBOS decreased (figure 4.7).

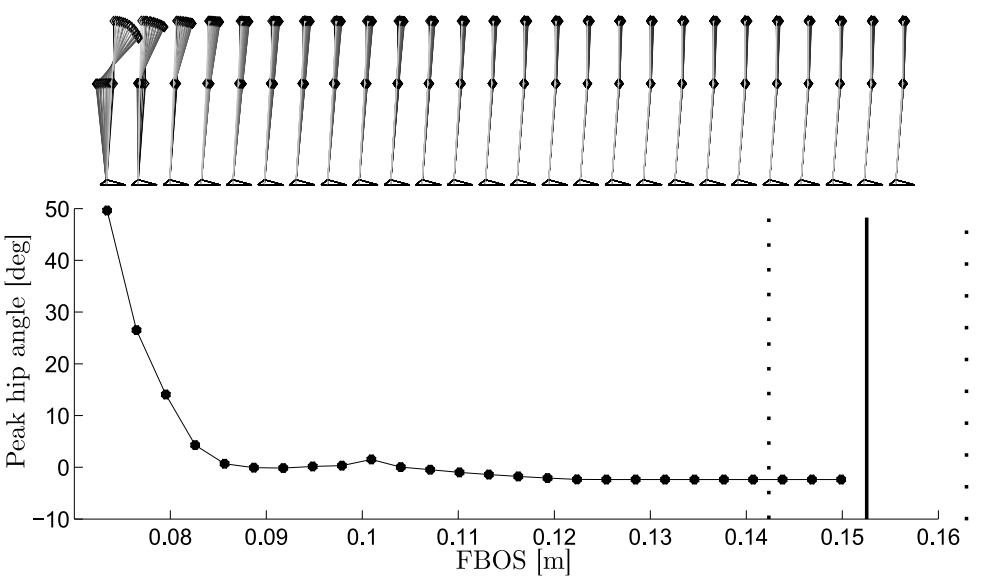

Figure 4.7: **Simulated peak hip angle as a function of the functional base of support.** Each dot represents the result of a predictive simulation with a different FBOS. The vertical black solid and dotted lines represent respectively the mean FBOS in the 10 subjects and the standard deviation. The stick figures show the postural response for each simulation.

Discussion

The aim of this study was to investigate if minimizing mechanical effort influences the selection of a postural response from the continuum of ankle and hip strategies capable of restoring balance after a posterior surface translation. The experimental results showed that there is a relation between peak hip angle and different measures of effort. The simulation results confirmed the hypothesis that the relative importance of mechanical effort versus postural instability influences the predicted peak hip angle during the postural response. Hence, our results demonstrated that the selection of a postural response can be explained by the trade-off between energy consumption and postural stability.

Tracking simulations

The low RMS error between the experimental and simulated kinematics of the tracking simulation with full state feedback confirmed the results of Park et al. [13]. It showed that this model can accurately describe a range of non-stepping postural responses to posterior support surface translations of different magnitudes in a control population. Although previous studies showed that COM feedback is important [76], the high RMS differences between the experimental and simulated kinematics in the tracking simulations with COM feedback, especially for high peak hip angles, indicate that COM feedback is not sufficient to track the full range of experimental postural responses using a torque-driven double inverted pendulum model. These results seem to contradict the study of Welch et al. who showed in a similar task that measured muscle activity can be modeled by delayed COM feedback of an inverted pendulum model driven by a single muscle [76]. Several factors might have influenced the finding that COM feedback is not sufficient to track the experimental kinematics. First, different acceleration profiles of the motion base were used to perturb the posture in our study compared to the study of Welch et al. Second, COM feedback and full state feedback are equivalent in a single inverted pendulum model, since COM position and velocity are linearly related to and fully determine the state. Nevertheless, Welch et al. demonstrated that COM kinematics explains to a large extent the experimental muscle activity, suggesting that COM feedback is of major importance during postural responses. Third, the RMS error in the tracking simulations with COM feedback was low for ankle strategies but increased with increasing peak hip angle, suggesting that COM feedback might be sufficient to explain ankle strategies. Fourth, the discrepancy between the current study and the results from the study of Welch et al. might also be explained by the contributions of muscle dynamics to the control of postural equilibrium. It is known that intrinsic muscle properties (such as force-length and force-velocity characteristics) and history-dependent muscle dynamics help stabilize dynamic movements [92]. In our simulations the states were linearly transformed to joint torques whereas muscles will non-linearly transform the feedback signals to joint torques. Finally, the properties of the feedback control system can also influence the postural response. Individual feedback gains for each muscle rather than joint level feedback gains will increase

the capability to control posture. More specific, individual control of bi-articular muscles allowing energy transfer between joints would influence the postural response [93]. Other researchers suggested that the central nervous system does not control muscles individually but by activating combinations of muscle synergies [94]. To study the influence of muscle dynamics and muscle control, more detailed musculoskeletal and control models, are needed. Hence, there are inherent limitations to the use of torque driven simulations that may limit the insights gained by the current study. Nevertheless, the low RMS error between the experimental and simulated kinematics indicates that this model can be used to predict ankle and hip kinematics during postural responses.

Predictive simulations

The significant positive correlations between the peak hip angle and estimates of effort in the experimental data (figure 4.3) and between the peak hip angle and the optimal weight in the predictive simulation (figure 4.5-4.6) confirmed the hypothesis that the relative importance of minimizing mechanical effort versus postural instability can explain the selection of a hip versus an ankle strategy. The predictive simulations allowed us to investigate cause-effect relationships between changes in the objective and postural responses without the influence of confounding variables. All possible confounding variables, such as FBOS, initial and final posture, were modeled and kept constant in the simulation, which is not possible in experimental conditions. Minimizing mechanical effort resulted in an ankle strategy whereas minimizing postural instability resulted in a hip strategy (figure 4.5). The finding that minimization of mechanical effort resulted in an ankle strategy seems to contradict the finding of Kuo et al. that less muscle effort is required for a given magnitude of horizontal acceleration when using a hip strategy [67]. This contradiction might be explained by the different definitions of effort. Kuo et. al. defined effort as the percentage of the feasible acceleration needed to restore posture. The feasible acceleration was computed based on maximal muscle activity taking into account heel lift and toe lift constraints. Hence, Kuo et al. used a relative measure of effort that does not account for the work needed for the postural response. Furthermore, there is a difference in time horizon of both analyses. Kuo et al. only evaluated the instantaneous effort whereas the current study evaluated effort over the duration of the postural response. Our results confirm the findings of Lockhart et al. that effort-related objective functions can be used to predict postural responses [58, 76]. Furthermore, by using a double instead of a single inverted pendulum, we showed that the relative importance of mechanical effort versus postural stability can explain the continuum of ankle and hip strategies. When using the upright-instability objective function that is similar to the objective proposed by Kuo, a similar correlation between the measured peak hip angle and the optimal weight was found (figure 4.6). This indicates that both upright posture and mechanical effort can explain the selection of a postural control strategy equally well.

The higher sensitivity of the postural response to a change in the optimal feedback gains in ankle strategies compared to hip strategies emphasizes the finding that hip strategies

are more stable postural responses [95]. These results suggest that hip strategies are more robust to inaccuracies and noise in the sensory system. This could be an additional reason for the increase in hip strategies in the elderly with age-related detoriation of the sensory system [48, 96]. However, additional experiments and simulations are needed to confirm this hypothesis.

To test if the model was able to predict a change in postural response following a change in the perturbation conditions, the influence of a decreased FBOS on the postural response was evaluated. A gradual shift towards a hip strategy was found with decreasing FBOS (figure 4.7). The shift from an ankle towards a hip strategy for a constant objective indicates that the ankle strategy is not a feasible solution when the FBOS decreases. This is in accordance with experimental studies that found an increased occurrence of hip strategies when balancing on a narrow beam [26]. Previous experimental studies showed a correlation between a decrease in FBOS and a reduced ability to restore balance without stepping [20]. This is highly relevant in understanding falling hazards in the elderly. Indeed, the FBOS is known to decrease with aging [79], reducing the balance restoring ability. It has been suggested that reduced ankle muscle strength contributes to a decreased FBOS and explains the increased number of stepping responses in the elderly [20]. Our results emphasize the importance of training the FBOS in non-stepping postural control. In conclusion, both the objective of the movement (i.e. relative importance of minimizing mechanical effort versus postural instability) and the FBOS influence the postural response. Hence, the modeling framework captures both the dependence of the selection of a postural response on the performance criteria (minimizing mechanical effort versus maximizing stability) and on changes in the perturbation conditions (modeled by the FBOS). As a result, the simulation method proposed in this study can be used to evaluate if a subject's postural response is the result of a decreased FBOS or rather a change in objective. Therefore, this method can be used to identify how the age-related reduction of the FBOS versus age-related changes in objective (e.g. as a result of fear of falling) contribute to the higher incidence of hip strategies in elderly and has therefore the potential to identify whether ankle strength training is needed.

Strengths, limitations and future directions

Although the cause-effect relationship between changes in the objective and the postural response was demonstrated, more complex biomechanical models and further experiments are needed to study control of posture in more detail. These results should therefore be interpreted within the limitations of the study. First, only three acceleration profiles of the motion base were used. Different profiles could elicit different responses. For example, higher perturbation velocities elicit hip flexion torques with increasing magnitudes [84]. Since measured peak hip flexion torques were small in this study, peak hip angles instead of peak hip flexion torques were used to classify hip and ankle strategy. Nevertheless, the range of acceleration profiles in the present study was sufficient to elicit a wide range of peak hip angles. Second, the simulations did not include a neural time delay and muscle dynamics. An effect of neglecting

time delay is that the maximal hip angle occurs faster in the predictive simulations compared to the tracking simulations (figure 4.3). Therefore, we expect the RMS differences between the measured and simulated kinematics to decrease when accounting for the neural time delay. However, without any muscle dynamics or passive joint stiffness, a neural time delay in torque driven simulations results in constant joint torques equaling the joint torques during quiet standing, and as a consequence unrealistically high angular accelerations during the first time interval after the perturbation. This contradicts the experimentally observed increase in joint moments during the first time interval after the perturbation. This initial response in joint moments could be caused by muscle force-length and force-velocity properties, tendon stiffness, short range stiffness [97, 98], and stretch reflexes. Third, we simplified the multi degree of freedom skeletal system to a model with two degrees of freedom. This simplification is motivated by the limited peak knee angle observed in the experimental data. Furthermore, the internal joint moments that would be required to stabilize the knee in the simulations are physiologically realistic and in the same order of magnitude as those observed in the experiments (appendix 1). Nevertheless, additional degrees of freedom (such as motion around the knee, lumbar and shoulder joint) will be considered in future research, especially to predict stepping postural responses. Therefore, we believe that future work should concentrate on implementing muscle dynamics and neural time delays as well as additional degrees of freedom in simulations of postural responses that allow stepping responses.

Conclusion

The combination of experimental measurements and predictive simulations of postural responses following a backward support surface translation suggests that effort minimization influences the selection of a postural response in the continuum of potential ankle and hip strategies. More specifically, the relative importance of minimizing postural instability versus mechanical effort is correlated with the peak hip angle used during the postural response. Hence the selection of an ankle or hip strategy can be explained by a trade-off between effort and stability.

Chapter 5

Modulation of gluteus medius activity reflects the potential of the muscle to meet the mechanical demands during perturbed walking

Maarten Afschrift, Lorenzo Pitto, Wouter Aerts, Robert van Deursen, Ilse Jonkers, Friedl De Groote

Published in *Scientific Reports*

Abstract

Mediolateral stability during walking can be controlled by adjustment of foot placement. Reactive activity of gluteus medius (GM) is modulated during the gait cycle. However, the mechanisms behind the modulation are yet unclear. We measured reactive GM activity and kinematics in response to a mediolateral platform translation during different phases of the gait cycle. Forward simulations of perturbed walking were used to evaluate the isolated effect of the perturbation and the GM response on gait stability. We showed that the potential of GM to adjust lateral foot placement and prevent collisions during swing varies during the gait cycle and explains the observed modulation. The observed increase in stance, swing or combined GM activity causes an outward foot placement and therefore compensates for the loss of stability caused by a perturbation early in the gait cycle. GM activity of the swing leg in response to a platform translation late in the gait cycle counteracts foot placement, but prevents collision of the swing foot with the stance leg. This study provides insights in the neuromechanics of reactive control of gait stability and proposes a novel method to distinguish between the effect of perturbation force and reactive muscle activity on gait stability.

Introduction

Falls in the elderly frequently occur during walking [99], often resulting in significant injuries and loss of independence. Bipedal walking stability is actively controlled in the frontal plane [30,100], whereas stability in the sagittal plane results to a larger extent from passive dynamics [101]. Active control of stability relies on the integration and processing of sensory information inducing muscle activation in response to a perturbation [22]. Active control of gait stability is commonly investigated by the use of sensory and mechanical perturbations to measure the corrective motor response [17, 19, 22, 32]. This response to perturbation is quantified using changes in electromyographic and kinematic variables [17, 22]. Adjustment of medio-lateral foot placement is the main kinematic strategy for medio-lateral control of stability following a perturbation during walking [17, 18, 22, 100]. Stepping in the direction of the perturbation, increases the width of the base of support to ensure that the margin of stability remains constant [18]. In addition, it is important to control that the swing foot does not collide with the ground or contra-lateral limb.

The gluteus medius (GM) is thought to play an important role in medio-lateral control of stability. Increased activity of the stance and swing leg GM has been observed in response to medio-lateral perturbations during walking [17, 19, 22]. Activity of the swing leg GM has been studied most frequently and is considered to be the main contributor to the stepping strategy after a medio-lateral perturbation during walking [17, 19, 22]. It has been suggested that activity of the swing leg GM abducts the hip and therefore controls the medio-lateral position of the foot [17]. This hypothesis is based on the positive correlation between swing leg GM activity and lateral foot placement during normal and perturbed walking [19]. Increased stance leg GM activity in response to a perturbation has been observed as well [17,19], but the contribution to contralateral foot placement and gait stability is not well understood. Hof et al. hypothesized that stance leg GM activity stabilizes the hip joint and provides additional floor clearance, but does not contribute to lateral foot placement [17].

The reactive response of both stance and swing leg GM is modulated during the gait cycle: Hof et al. found that the bilateral GM response magnitude to a lateral push perturbation depends on the timing of perturbation onset during the gait cycle [17]. Simultaneously, the timing of the perturbation influences the direction of the stepping strategy. After a perturbation that causes a loss of stability in the direction of the swing leg, the foot in swing phase is positioned more outwards, hence an outward strategy [17]. After a perturbation in the opposite direction, the swing foot is positioned more in the direction of the stance leg (i.e. inward strategy) (Figure 2).

The above suggests that both stance and swing leg GM muscles contribute to restoring stability after a medio-lateral perturbation during walking and that swing leg GM is important to adjust foot placement. Evidently, the muscle response is modulated depending on the perturbation timing during the gait cycle. However, the mechanisms behind this modulation are yet unclear. To gain insights into these mechanisms, it is important to unravel the in-

dividual contribution of stance and swing leg GM activity to the mechanics of the stepping strategy and to understand the potential of each muscle to influence stepping mechanics during the gait cycle (i.e. potential of the muscle to adjust foot placement and prevention of collision during swing). Correlations between changes in bilateral GM activity and changes in kinematics in response to the perturbation provide limited insight into these underlying mechanisms, because it is hard to separate the individual contribution of the perturbation force (passive response) and the action of individual muscles (active response) in relation to the mechanics and stability of perturbed walking.

Forward simulations with detailed models of the musculoskeletal system and corrective motor responses allow studying causal relations between muscle action and stability control. In simulation, the effect of the response of an isolated muscle on the kinematics can be computed. In addition, simulations can discriminate between the changes in kinematics caused by the perturbation and by the muscle response. Forward simulation has been successfully applied to study the contribution of muscle action to perturbed standing balance [76], but not in perturbed walking because of the more complex musculoskeletal dynamics.

The main goal of this study was to identify the contribution of stance and swing leg GM to the control of gait stability during different phases of the gait cycle. We hypothesized that the potential of both muscles to (1) adjust lateral foot placement and (2) prevent collisions during swing varies during the gait cycle and explains the observed modulation in stance and swing leg GM activity. A combined experimental and simulation approach was used to test the hypothesis.

Methods

An experimental perturbation protocol was used to measure the kinematics and bilateral GM activity in response to a medio-lateral platform translation during different phases of the gait cycle. Muscle driven forward simulations were developed to establish causal relations between measured GM activity and walking kinematics and derived stability measures. Forward simulations of unperturbed and perturbed walking were used to quantify (1) the influence of the perturbation force on the mechanics of stability control (i.e. passive response) and (2) the isolated contribution of a single measured muscle response to the stepping strategy (i.e. active response).

Experimental protocol

Eighteen healthy young subjects (age 21 $\pm$ 2 STD) without movement disorders participated in the study. The experimental protocol was approved by and performed in accordance with the relevant guidelines and regulations of the School ethics committee of the School of Healthcare Sciences, Cardiff University. All participants gave written informed consent before participating in the study.

First, the subjects walked for two minutes on a split-belt treadmill (Grail, MotekForceLink) at a fixed speed of 1.1 m/s. Second, 48 randomized unique perturbation were applied in a walking session. Each session was repeated three times with five minutes rest in between. The set of 48 unique perturbations consisted of three different magnitudes of perturbations (Figure 5.1c), four directions (i.e. platform translation to the left and right, increase and decrease of the speed of both belts) and in four phases of the gait cycle (Figure 5.1b). A gait cycle was defined as a complete left stride, starting at left heelstrike (0%) up to the next left heelstrike (100%). The perturbation was applied immediately after heelstrike (7.5% gait cycle, first double support), during early single stance (22.5% gait cycle), late single stance (37.5% gait cycle) and push-off (52.5% gait cycle, second double support).

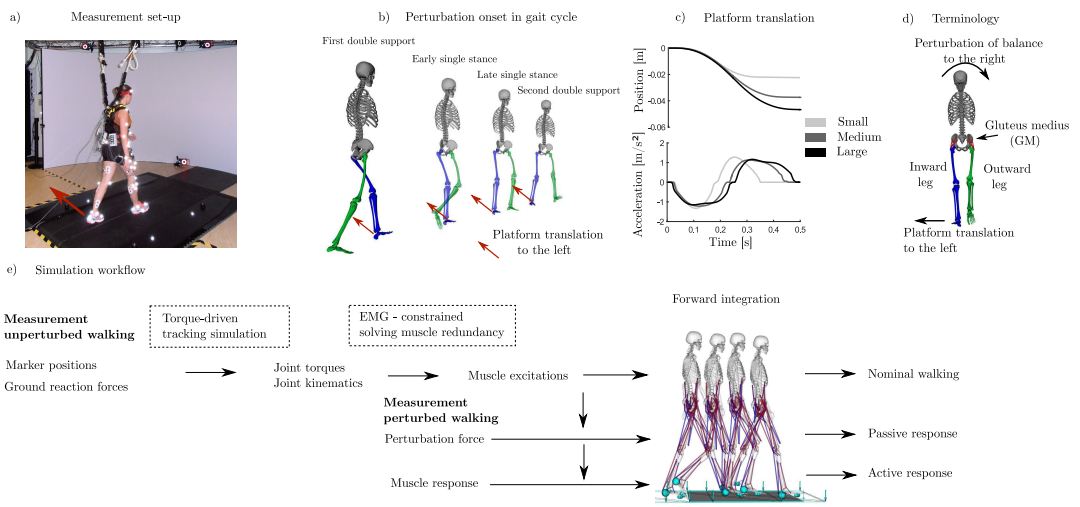

Figure 5.1: **Overview of the measurement protocol and simulation method.** Walking was perturbed by means of a platform translation to the left with onset at four different phases of the gait cycle (pane b) and three different amplitudes (pane c). The motion capture, ground reaction force and EMG data of unperturbed walking was used to generate a forward simulation of unperturbed walking (pane e). The platform translation was added as an external force to the forward simulation of the passive response. The platform translation and measured GM response (EMG) was added to the forward simulation of the active response

In this study, we focused on medio-lateral stability and therefore only analyzed the response to platform translations to the left during the stance phase of the left leg. The response to a platform translation to the left during the stance phase of the left leg and the response to a platform translation to the right during the stance phase of the right leg are symmetrical. To account for this symmetry in our terminology, we will refer to the left leg by inward leg and to the right leg by outward leg based on the terminology proposed by Hof [18]. A platform translation to the left causes a loss of stability towards the right that is counteracted by either outward placement of the right foot, hence termed the outward leg, or inward (cross-over) placement of the left foot, hence termed the inward leg (Figure 5.1d).

Measurements and data analysis

An integrated motion capture system was used to measure the response to the perturbations. 12 Vicon T20 cameras (Vicon, Oxford) measured the trajectories of 48 retroflective markers in an extended plug in gait marker protocol at 200 Hz. Ground reaction forces were collected on a split-belt treadmill with a sampling frequency of 1000Hz (MotekForceLink). Ground reaction forces and 3D marker coordinates were filtered with a 4th order low-pass Butterworth filter with a cutoff frequency of 8Hz. Muscle activity of the left and right GM was measured using surface electromyography (Bortec Octopus 8 channel EMG) at 1000Hz. The EMG data was filtered with a 4th order recursive Butterworth bandpass filter with cutoff frequencies of 20-400Hz. Subsequently, the filtered signals were rectified and a linear envelope was created with a 4th order recursive Butterworth low-pass filter with a cutoff frequency of 20 Hz.

Left and right heel strikes were determined from the ground reaction forces (Supplementary Section 6 Online). The muscle responses to the perturbation were quantified by comparing the muscle activity after perturbation with the muscle activity during unperturbed walking. The processed EMG data of the last 60 gait cycles during the two minutes of unperturbed walking and the gait cycles after the perturbation were interpolated to 100 data points between two consecutive heelstrikes. The change in muscle activity in response to a perturbation was computed by subtracting the average muscle activity during unperturbed walking from the activity after perturbation. The long latency muscle response was quantified as the time integral of the change in muscle activity during the first 300ms after perturbation onset [17].

3D marker coordinates were analyzed in OpenSim [68] to evaluate the kinematic strategy used by the subjects in response to the perturbation. A generic musculoskeletal model with 23 degrees of freedom was scaled to the subject's anthropometry and was used to calculate joint kinematics from the recorded marker trajectories using a Kalman smoothing algorithm [74]. Stride width was computed as the average distance in the frontal plane between the left and right ankle joint center during double support. Margin of stability was computed at left and right heel strike as the distance between the extrapolated center of mass [102] and respectively the left and right ankle joint center. A positive margin of stability indicates foot placement beyond the extrapolated center of mass in the direction of the perturbation (i.e. to the right).

Muscle driven forward dynamic simulation of gait

A muscle driven forward simulation of unperturbed gait was created for each subject (Figure 5.1e). The model was driven by 92 Hill-type muscle tendon actuators [90]. Four contact spheres were added to both feet to simulate ground reaction forces (heel, metatarsal head 1-3-5). Hunt–Crossley based contact model was used to simulate the ground contact forces, which depend on the indentation and indentation velocity of the contact spheres with respect to the ground [70] (Supplementary Section 1 Online). These simulations will be referred to as tracking simulations. The muscle excitations that drive the forward simulation of unper-

turbed walking were computed using a two-step optimization procedure. In the first step, we computed joint torques of a torque driven model that track the measured marker positions, joint torques and ground reaction forces for a representative gait cycle within the two minutes of unperturbed walking (equation 5.1) by minimizing:

$$J = \int_{t_0}^{t_{end}} \|(\boldsymbol{p} - \hat{\boldsymbol{p}}\|_2^2 + w_1 \sum_{j}^{nF} (\boldsymbol{F_j} - \hat{\boldsymbol{F}}_{\boldsymbol{j}})^2 + w_2 \|\boldsymbol{T} - \hat{\boldsymbol{T}}\|_2^2 dt \tag{5.1}$$

Where p is a vector containing the 3D coordinates of the markers, F_j is a vector containing the ground reaction forces and moments on the left and right foot (nF equals two), T is a vector containing the joint torques of the 23 generalized coordinates. Measured variables are labelled with the hat symbol. w1 and w2 are weights to scale the different orders of magnitude in the objective function and equal respectively 10^{-7} and 10^{-5}.

In the second step, muscle excitations that generate the simulated joint torques (step 1) were computed by solving the muscle redundancy problem [72]. The objective function was the weighted sum of muscle excitations squared, a term penalizing differences between computed and measured bilateral GM activity during unperturbed walking (equation 2, Supplementary Section 3 Online):

$$J = \int_{t_0}^{t_{end}} \sum_{i}^{nMus} e_i^2 + w_1 (s\hat{e}_{GM} - e_{GM})^2 + w_2 \sum_{j}^{nDOF} e_{Tj} T_{max} dt \tag{5.2}$$

where n=92 is the number of muscles in the model, e_i is the simulated excitation of muscle i, $\hat{e}_{GM}$ is the measured activity of the GM (processed EMG), and e_{GM} is the simulated GM excitation. s scales the measured excitation and is an optimization variable. Hence, we track the pattern but not the magnitude of the measured EMG signal.

The time series of simulated muscle excitation and the initial state of the model were used in a forward simulation to generate a simulated unperturbed gait pattern for every individual subject. To evaluate the influence of the perturbation and the isolated contribution of a muscle to the mechanics of perturbed walking, the influence of the perturbation (passive response) and the combined influence of perturbation and muscle activity (active response) was simulated separately for all the measured perturbation trials.

The passive response of the musculoskeletal model to the perturbation was simulated by imposing the platform translation to the muscle-driven forward simulation, controlled by the muscle excitations computed for unperturbed walking (Figure 5.1e). The platform translation was applied as an external force at the center of mass of all the segments in the forward simulation.

The active response of the musculoskeletal model to the perturbation was simulated by imposing the platform translation and adding the measured individual change in GM activity to the muscle excitations of unperturbed walking. The scaling factor (s) of the muscle redundancy

solver (equation 5.2) was use to scale the EMG (voltage) to the simulated muscle excitations. For every measured perturbation trial, we ran a simulation with modified GM activity of the (1) outward leg, (2) inward leg and (3) outward and inward leg.

The isolated contribution of the measured muscle activity to the mechanics of the stepping strategy was quantified by the difference between the passive and active simulated response. Since the stepping strategy depends on adequate lateral foot placement and the prevention of collisions during swing, we compared the (1) foot placement, (2) margin of stability at first heel strike after perturbation, (3) swing foot height, and (4) distance between both feet during mid-swing. The latency between the onset of the GM response and the adjustment of swing foot position was quantified as the time between perturbation onset and the time at which the difference in swing foot position between active and passive response exceeded 1cm.

All optimal control problems (tracking simulation, muscle redundancy problem) were solved using the direct collocation software GPOPS II (Supplementary Section 2 Online).

Outcome measures and statistical analysis

Two-way repeated measures analysis of variance (rmANOVA) was used to evaluate the main effect of perturbation onset timing (four levels) and perturbation magnitude (three levels) on measured stride width, margin of stability and bilateral GM activity. Post-hoc pairwise comparison was used to evaluate the response after perturbation compared to unperturbed walking using Tukey's Honest Significant Difference to correct for multiple comparisons. Shapiro–Wilk test was used to check the normality of the data. Linear regression (including Pearson's correlation coefficient) was used to compare changes in bilateral GM activity and changes in simulated stride width and margin of stability at the first heel strike after perturbation and foot height and inter-feet distance during the first mid-swing after perturbation. Correlation between the aforementioned outcome variables and the muscle response was reported by adjusted R squared values. The slope and intercept of the linear regression was computed for the different onset timings of the perturbation (Figure 1b). A two-sided confidence interval with an alpha level of 0.05 was used to define significance for all statistical tests.

The dataset and simulation software generated during the current study are available from the corresponding author on request.

Results

Experimental results

The onset timing of the perturbation had a significant effect on stride width ($F=59.82$; $p<0.001$) and margin of stability ($F=23.20$; $p<0.001$) at first heelstrike after perturbation.

An outward strategy, characterized by an increase in stride width, was observed when the platform translation started early in the gait cycle (7.5% and 22.5% gait cycle). For this timing of perturbation, the outward leg is in swing phase and therefore gait stability can be adjusted by outward foot placement (Figure 2c). An inward stepping strategy, characterized by a decrease in stride width, was observed when the perturbation started during second double support (i.e. 52.5% of the gait cycle) (Figure 5.2d). For this timing of perturbation, the outward leg is in stance phase and therefore stability can be restored by inward foot placement of the swing leg (Figure 5.2d).

The timing of the perturbation had a significant effect on GM activity in the inward [$F=11.47$, $p<0.001$] and outward leg [$F=9.55$, $p<0.001$] (Figure 5.3). A significant increase in GM activity of both the outward and inward leg was found in response to perturbations during first double support (7.5% gait cycle, Figure 5.3a). The bilateral GM response to perturbation during first double support differed substantially between subjects (Figure 3c), although the kinematic response of the outward stepping strategy was similar (Figure 5.2). The bilateral GM response was characterized by an increased GM activity of the inward, outward or a combination of both legs (Figure 5.4). Muscle responses to perturbations during midstance and push-off were similar between subjects (Figure 5.3c). Perturbations with onset at 22.5% of the gait cycle, when the inward leg is in early midstance and the outward leg is in midswing, caused a significant increase in GM activity of the outward leg (Figure 5.3a). Perturbations with onset at 37.5% and 52.5% of the gait cycle, when the inward leg transitions from stance to swing and the outward leg is in late swing or early stance, caused an increase in GM activity of the inward leg (Figure 5.3b).

An increased perturbation amplitude significantly increased stride width [$F=5.1$, $p=0.006$], but not the margin of stability [$F=0.57$, $p=0.56$] and GM activity of the inward [$F=1.31$, $p=0.26$] and outward leg [$F=2.55$, $p=0.08$] leg at first heel strike after perturbation.

Simulation results

The simulations of unperturbed walking were in agreement with the experimental data. The root-mean square error of the tracking simulation of unperturbed walking was 0.03 cm for the marker positions, 29N for the ground reaction forces and 6.7 Nm for the joint torques (For details, Supplementary Fig. 2-3 Online).

When adding the perturbation force to the simulation of unperturbed walking, without reactive muscle activity, we found that the perturbation had a destabilizing effect. The influence of the perturbation force on foot placement, margin of stability and collisions was visualized in Figure 5.5 as the intercept of the linear regression between the magnitude of the measured GM response and the three aforementioned outcome variables. Hence, the intercept shows the passive response simulation when the reactive muscle activity of the GM in response to the perturbation equals zero. First, a decrease in margin of stability was found in the passive response simulation for all onset timings of the perturbation. The negative

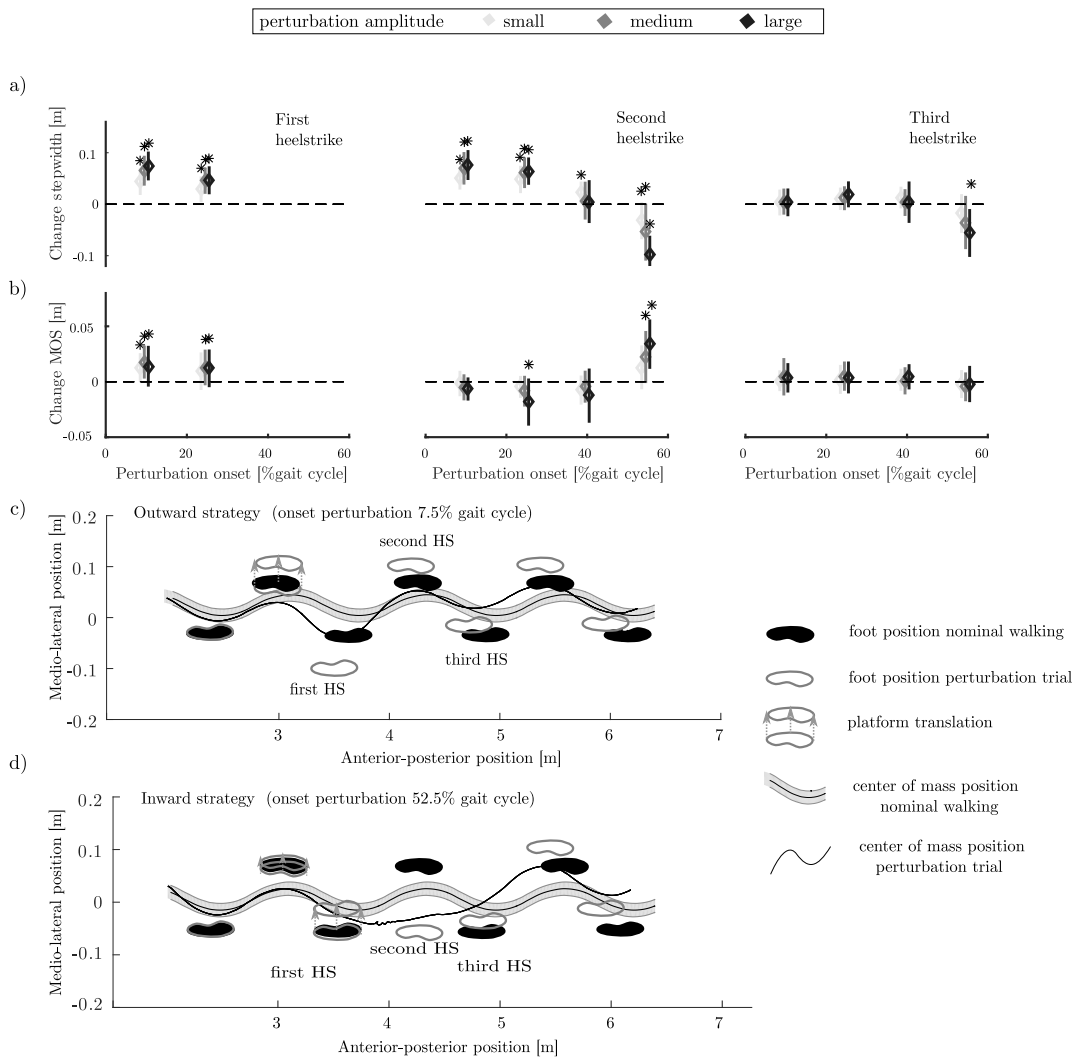

Figure 5.2: **Modulation of stepping strategy in response to platform translation to the left during the gait cycle.** Group mean ± standard deviation of change in step width (a) and margin of stability (b) at the first three heelstrikes after perturbation onset compared to unperturbed walking as a function of the onset timing of the platform translation. The stars indicate results significantly different from zero ($p<0.05$). An outward stepping strategy was used in response to the platform translation during first double support (c) (perturbation onset 7.5% gait cycle). An inward stepping strategy was used in response to the platform translation with onset during second double support (d) (perturbation onset 52.5% gait cycle).

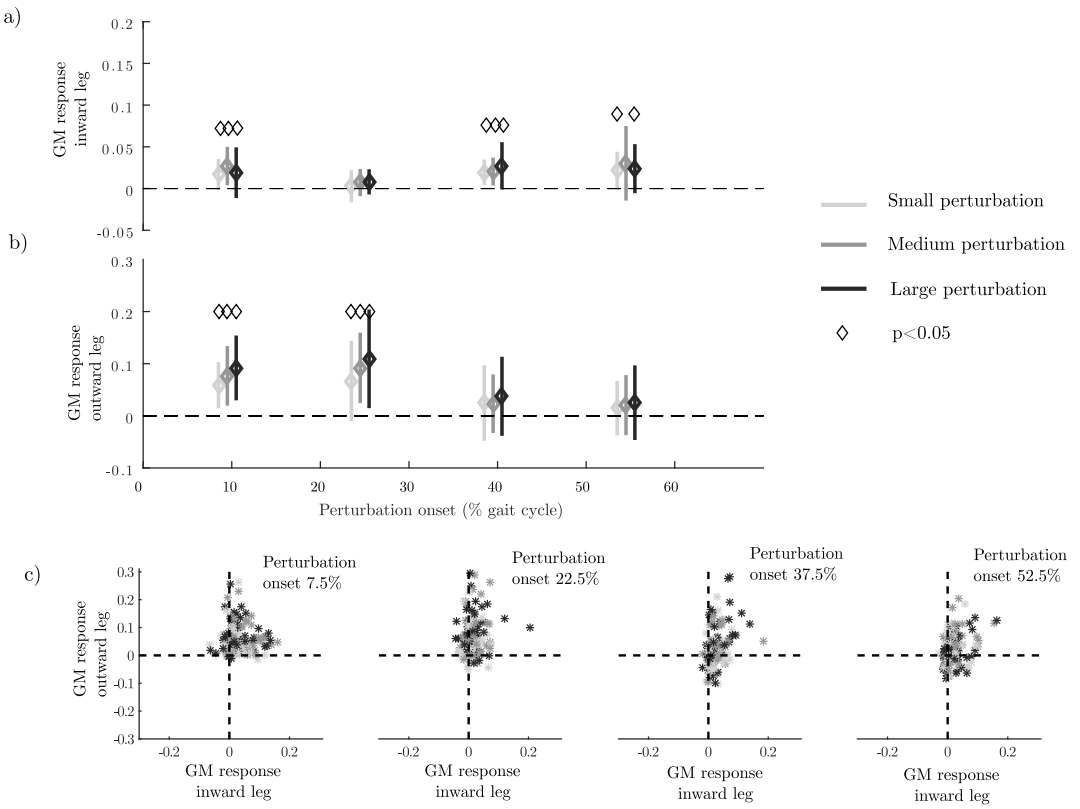

Figure 5.3: **Modulation of bilateral GM activity in response to platform translation during the gait cycle.** Group mean ± standard deviation of the GM response of the inward (a) and outward leg (b) to the platform translation as a function of onset timing of the perturbation during the gait cycle. GM response significantly different from zero (i.e. unperturbed walking) is highlighted with a square ($p<0.05$). The relative change in GM activity of the inward versus outward leg in response to the perturbation of all perturbation trials for the four different timings of perturbation (c).

intercept for margin of stability for all perturbations timings (Figure 5.5 b-f) shows that the perturbation caused a loss of stability without active muscle response. Second, the passive effect of the perturbation force also influenced the foot position at heel strike (Figure 5.5). Stride width increased for perturbations during first double support and early single stance (Figure 5.5a, positive intercept), but decreased for perturbation during late single stance and second double support (Figure 5.5e, negative intercept). Third, inter-limb distance and foot height at mid-swing decreased for perturbation during second double support, which may cause inter-limb and ground-limb collision (Figure 5.5 g-h, negative intercept perturbation at 52.5% gait cycle).

When adding the perturbation force and the active response of the inward or outward GM to the forward simulation, we found that GM activity of both the inward and outward leg increased gait stability. However, the effect of the GM response on stride width, the margin of stability at heelstrike and inter-feet distance during mid swing varied during the gait cycle.

For perturbations with onset during first double support (7.5% gait cycle), when the outward leg is in swing and outward foot placement can be adjusted, the active response of the GM of both the inward and outward leg increased gait stability. We found that forward simulations driven by measured reactive activity of the stance and swing leg GM can explain the increase in measured stride width in subjects where an increase stance leg GM (Figure 5.4- left), swing leg GM (5.4- middle), swing leg GM (5.4- right) was measured with EMG. The significant positive correlation between (1) swing leg GM response, (2) stance leg GM response, and (3) stride width and margin of stability of all subjects and trials shows that activation of both muscles increased stride width and margin of stability at first heel strike after the perturbation (Figure 5.5ab), which is visualized by the positive slope of the linear regression in Figure 5.5. The steeper slope of the regression between outward GM activity and simulated stride width and margin of stability compared to the slope of the inward GM activity shows the stance leg GM has an greater potential to increase stride width (Figure 5.5a) and margin of stability (Figure 5.5b) for perturbations with onset during first double support. The adjustment of swing foot position, and increase in stride width, was significantly slower following activation of the stance leg GM (latency: 0.36s $\pm$ 0.03 STD) compared to the swing leg GM (latency: 0.26s $\pm$ 0.03 STD) ($p<0.001$). In addition, the negative slope of the regression between outward GM activity and foot height shows that reactive swing leg GM activity decreased foot height during mid swing (Figure 5.5c), whereas stance leg GM activity increased foot height (Figure 5.5c, positive slope inward GM).

For perturbations with onset during early single stance (22.5% gait cycle), when the outward leg is in swing, the active response of the GM activity of the outward leg and not inward leg increased gait stability. The positive slope of the regression between outward GM activity, stride width and margin of stability shows that reactive outward GM activity increased step width and margin of stability. No active response of the inward GM was measured for this timing of perturbation and therefore did not contribute to gait stability (Figure 5.3).

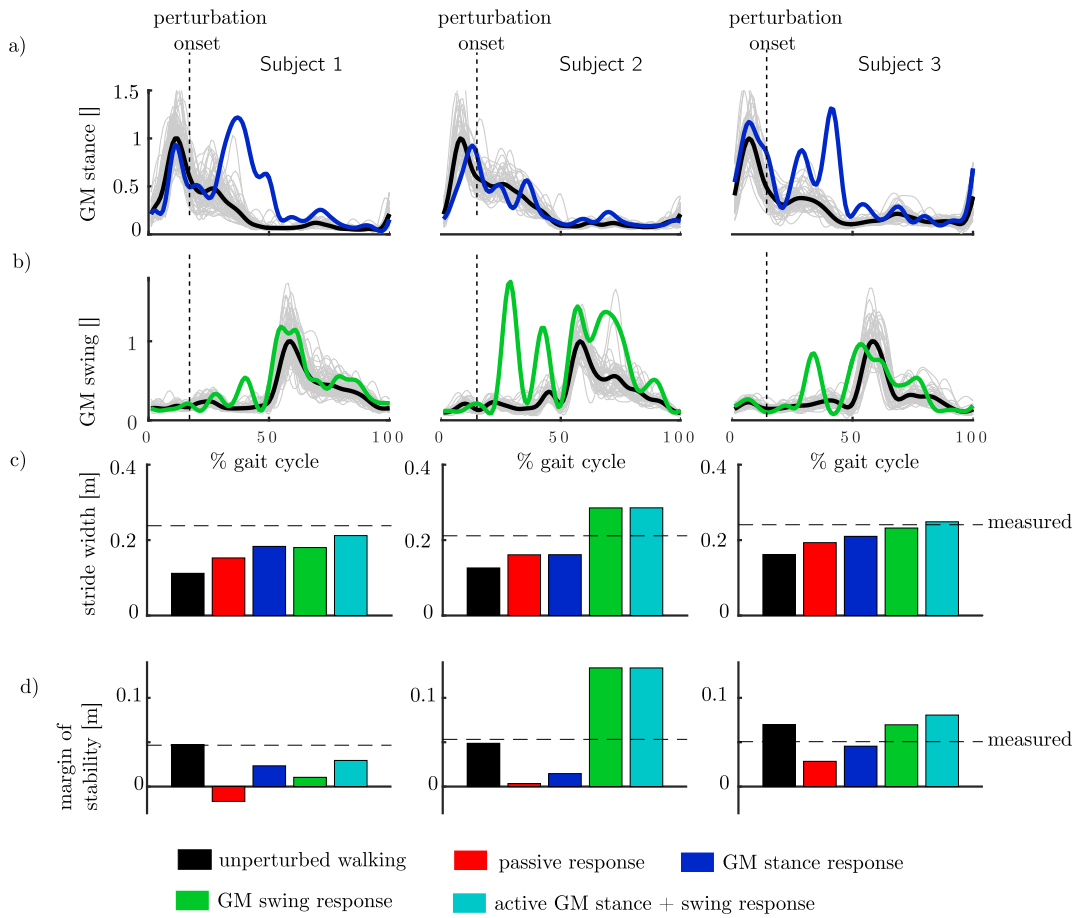

Figure 5.4: **Active and passive response to perturbation during first double support (7.5% gait cycle) for subjects using the GM activity of the inward (stance) leg, outward (swing) leg and a combination of both.** Simulated change in stride width and margin of stability for a subjects using mainly the stance leg GM (subject 1), the swing leg GM (subjects 2) or a combination of both (subject 3). The average measured muscle activity of the stance (a) and swing (b) leg GM during unperturbed walking is shown in black (all unperturbed gait cycles in gray) and after perturbation in blue for the stance leg and green for the swing leg. The vertical black dotted line represents perturbation onset. The stride width (c) and simulated margin of stability(d) at first heelstrike after perturbation is shown for unperturbed walking (black), passive response (red), active response stance leg GM (blue), active response swing leg GM (green) and combined response of stance and swing leg GM (cyan).

For perturbations with onset during second double support (52.5% gait cycle), when the inward leg transitions from stance to swing, the measured increase in GM activity of the inward leg prevented inter-limb collision but decreased the margin of stability. The negative slope of the regression between inward GM activity and margin of stability shows inward GM activity reduced the margin of stability (Figure 5.5f). The positive slope of the regression between inward GM activity and inter-feet distance shows that reactive GM activity increased inter-feet distance during mid swing (Figure 5.5h, positive slope) and therefore prevents inter-limb collision caused by the perturbation force (Figure 5.5h, negative intercept). No active response of the outward GM was measured for this timing of perturbation and therefore did not contribute to gait stability (Figure 5.3).

Discussion

We quantified the effect of bilateral GM activity in response to lateral platform translations on the mechanics of reactive control of gait stability. In accordance with previously published results [17], we found that reactive GM activity and stepping strategy are modulated during the gait cycle. In simulation, we confirmed the hypothesis that the potential of the GM of the inward and outward leg to adjust lateral foot placement and to prevent collisions during swing varies during the gait cycle. This explains the observed modulation in bilateral GM activity.

The measurements of perturbed walking showed that reactive GM activity and stepping strategy are modulated during the gait cycle [17]. The onset timing perturbation had a significant effect on the kinematics and reactive bilateral GM activity. The kinematic strategy shifted from an outward to an inward stepping strategy when the onset timing of the perturbation was later in the gait cycle (Figure 5.2). Lateral translations of the stance leg with onset during first double support resulted in an outward stepping strategy, characterised by an increase in stride width and an increase in GM activity of both the inward and outward leg. Perturbations during second double support resulted in an inward stepping strategy, characterised by a decrease in stride width and increased GM activity of the inward leg.

Results from the simulated passive response showed that the platform translation perturbed stability during all phases of the gait cycle and that an active response is needed to control gait stability. All perturbations caused a decrease in margin of stability (Figure 5.5, negative intercept MOS). In addition, the mechanical demands imposed by the perturbation change during the gait cycle, because the inward and outward leg transition between stance and swing phase. For perturbation early in the gait cycle, lateral foot placement of the outward leg is needed to compensate for the instability caused by the perturbation (i.e. outward stepping [18]). For perturbations late in the gait cycle, the outward leg is in stance phase and medial foot placement of the inward leg is therefore needed to prevent a fall (i.e. inward stepping [18]). In addition, perturbations during second double support in the absence of active muscle responses reduce inter-feet distance, which may cause inter-limb collision. The

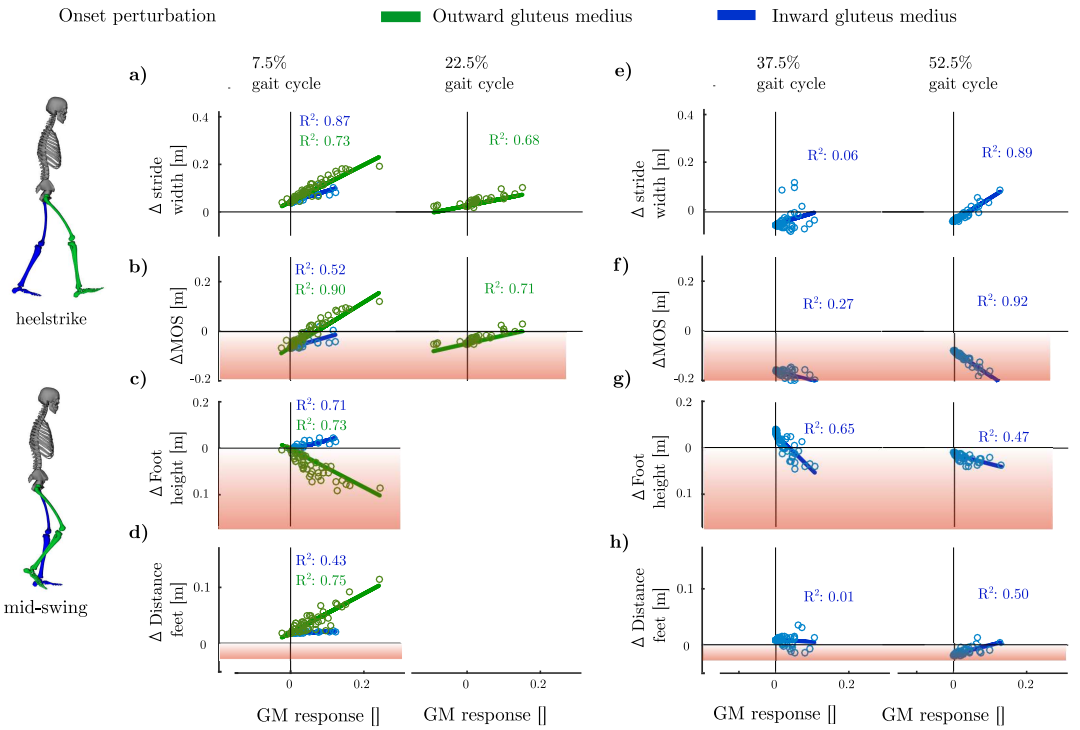

Figure 5.5: **Influence of bilateral GM activity on stability and swing foot position as a function of perturbation onset timing.** Linear regression between (a) stride width, (b) margin of stability, (c) foot height and (d) inter-feet distance during mid swing and GM activity of the inward (blue line) and outward leg (green line). Each dot represents the results of the active response simulation driven by measured EMG activity of the outward (green) and inward (blue) gluteus medius muscle of a single trial and single subject. The intercept of each regression shows the effect of the perturbation on the outcome variable without an active muscle response (i.e. passive response simulation. The slope of the regression shows the potential of the reactive muscle activity (i.e. active response) to adjust the four outcome variables. The stride width and margin of stability was evaluated at first heelstrike of the outward leg for the perturbations with onset at 7.5% and 22.5% of the gait cycle, and at first heelstrike of the inward leg for the perturbations with onset at 37.5% and 52.5% (i.e. since the outward leg is already on the ground). The red areas indicate when there is a potential loss of stability: (b,f) negative margin of stability (c,g) ground-foot collision during midswing (d,h) inter-feet collision during mid swing. The regression was only computed when a significant GM response of the inward or outward leg was observed (Figure 3). In addition, the results at mid-swing for perturbations with onset at 22.5% of the gait cycle were not visualised since the perturbation onset coincides with mid-swing.

changes in mechanical demands imposed by the perturbation suggest that modulation of reactive muscle activity is needed to control balance.

In simulation, we showed that the potential of the inward and outward leg GM to increase the margin of stability and to prevent collisions varies during the gait cycle (Figure 5.5, slope regression). Comparison between the simulated passive and active response shows the isolated effect of GM activity on the kinematics of gait stability. Our simulation results suggest that the potential of the muscle to control stability is different in stance versus swing phase and for the outward versus inward leg. Indeed, as hypothesized by Hof et al. [17, 19], reactive swing leg GM activity abducts the hip during swing phase and therefore controls outward position of the foot, which increases inter-feet distance during mid swing and stride width at heelstrike. This is true for both the outward and inward leg during their respective swing phases but more outward foot placement increases stability in the case of the outward leg (in line with outward stepping strategy) and decreases stability in case of the inward leg (counteracting inward stepping strategy). The contribution of the stance leg GM response to the stride width and margin of stability is more complex (Figure 5.6). Reactive GM activity of the stance has been observed by [17, 19, 22] but its contribution to gait stability was unknown. In simulation, we showed that an isolated increase in activity of the stance leg GM increases the stance leg hip abduction moment. The increased hip abduction moment tilts the pelvis upwards and increases the swing leg hip adduction angle (Figure 5.6c). Consequently, the swing leg hip abductor muscles (i.e. contra-lateral GM) stretch and generate more force for the same activation due to the altered position on the force length and force velocity relation of the Hill type muscle, therefore additionally increasing the swing leg hip abduction moment (Figure 5.6d). Through this mechanism, activity of the stance leg GM is mechanically coupled to pelvis and swing leg orientation, and supports lateral foot placement of the contra-lateral leg (Figure 5.6e).

Our simulations demonstrated changes in mechanical demands imposed by the perturbation and the changing potential of the GM to control stability throughout the gait cycle, suggesting that modulation of reactive GM activity is needed to control gait stability. Indeed, the experimentally observed changes GM responses and kinematics during the gait cycle shows that the subjects modulated reactive GM activity. Hence, the combination of the experimentally observed GM responses with simulation results show that reactive GM activity was modulated during the gait cycle to compensate for the changes in mechanical demands imposed by the perturbation and changes in muscle potential to control stability throughout the gait cycle.

During first double support (7.5% gait cycle), inward and outward GM are agonists in the control of stride width and inter-feet distance and considerable inter-subject variability in reactive GM activity was observed. Using forward simulations of the active response, we found that the isolated response of both inward and outward GM resulted in more lateral placement of the outward foot and an increased margin of stability at first heel strike after the perturbation (Figure 5.5). This is in agreement with the measured increase in stride width

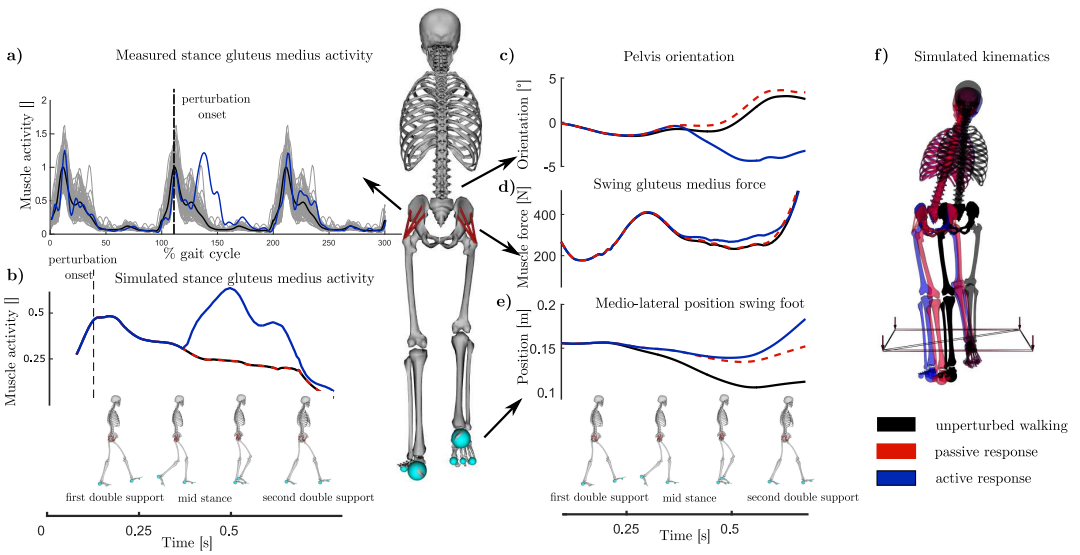

Figure 5.6: **Medio-lateral foot placement controlled by stance leg GM (GM) activity in perturbations with onset during first double support.** Stance leg GM activity was increased after perturbation (blue) compared to unperturbed walking (gray) (a). The isolated effect of stance leg GM response on walking kinematics was evaluated by comparing three forward simulations; (1) unperturbed walking (black), (2) passive response (red) and (3) active response (blue). The increase stance leg GM activity (b) and force tilts the pelvis upwards in the frontal plane (c) which stretches the swing leg hip abductors and therefore increases the swing leg GM force for the same activation (d). The resulting increase in swing leg hip abduction moment rotates the swing leg outwards and therefore increases the stride width (e). The resulting increase in stride width at heelstrike is shown in pane f.

for subjects that used only the stance leg gluteus medius (Figure 5.4-left), swing leg gluteus medius (Figure 5.4-middle) or a combination of both (Figure 5.4-right). The measured inter-subject variability in reactive GM activity of the inward (stance) versus outward (swing) leg suggests that subjects used the redundancy in strategies, due to the agonistic function of bilateral GM, differently. On the one hand, the swing leg muscle has a higher potential to increase stride width (Figure 5.5b, slope linear regression) and has a smaller delay between activity and adjustment of swing foot position compared to the stance leg GM. The swing leg GM response may therefore be a safer strategy to control foot placement. On the other hand, the response of the swing leg GM decreases foot height, and therefore requires activity of other muscles to increase foot height and prevent ground contact during mid swing. Therefore, use of stance leg GM might reduce the need to coordinate multiple muscles, thereby possibly simplifying control. Hence, the between-subjects variability in the use of stance versus swing leg GM for perturbations early in the gait cycle might reflect a trade-off between efficient foot placement and the need to coordinate multiple muscles.

For perturbations during early single stance (22.5% gait cycle) when the inward leg is in stance and the outward leg is in swing, GM response of the outward leg and not the inward leg contributes to gait stability. The absence of stance leg GM is probably due to the larger time delay between reactive muscle activity and adjustment of swing foot position for the stance leg GM strategy compared to the swing leg GM strategy. For perturbations with onset during early single stance when the outward leg already transitioned into swing, a reactive response of the stance leg GM might be too slow to adjust contra-lateral swing foot position sufficiently before heel strike. In response to perturbations, when solely the swing leg GM has the potential to control gait stability, only swing leg and not stance leg GM is used.

For perturbations during second double support (52.5% gait cycle), the observed GM activity of the inward leg is needed to prevent inter-limb collision, although it counteracts inward foot placement. Indeed, the measured decrease in stride width and increase in margin of stability reflects a successful inward strategy when perturbation onset was at 52.5% of the stride (Figure 5.2 b-d). The significant increase in the GM activity of the inward leg, which transitions from stance to swing, suggests that this muscle contributes to the inward strategy. However, in simulation the increase in muscle activity caused an increase in stride width and a decrease in margin of stability (Figure 5.5ef), therefore counteracting the measured inward stepping strategy. Differences between the simulated passive and active response to the perturbation suggest that the main function of the reactive GM activity of the inward leg is to prevent collision of the swing foot with the stance leg during mid-swing (Figure 5-h, negative intercept perturbation at 52.5%).

Several limitations should be considered when interpreting these results. First, the simulations of unperturbed walking did not exactly track measured marker positions and ground reaction forces. The errors originated from dynamic inconsistencies in the measured kinematics and external forces due to measurement and modelling errors. These errors can mainly be attributed to soft tissue artefacts, simplified representation of the trunk and head by a single rigid

body, and inaccuracies in the foot-ground contact model. However, tracking errors were small and we therefore suggest that they do not influence our conclusions. Second, EMG signals only give qualitative information about muscle activity and therefore the method used to scale EMG signals might have influenced the estimated magnitude of GM muscle activity. Since we used the EMG-based estimates of GM activity to drive these forward simulations, scaling inaccuracies will have influenced the reactive muscle force and therefore the simulated change in stride width, foot height and margin of stability. However, EMG scaling inaccuracies only affect the magnitude of the stepping strategy but not the relation (i.e. slope of the regression) between reactive muscle activity and the outcome variables. Therefore, the main conclusions are not sensitive to EMG scaling errors (Figure 5.5). Third, simulations are sensitive to modeling choices and model parameters. However, results from a sensitivity analysis showed that the modelling assumptions had only a small influence on the simulated stride width and margin of stability and did therefore not influence the trends between changes in reactive GM response, stride width and margin of stability after perturbation (Supplementary Section 5 Online).

The simulation method introduced in this paper has several advantages over induced acceleration analysis, which has been predominantly used to quantify the contribution of an isolated muscle to walking kinematics. The present forward simulation method evaluates the accumulated effect of a perturbation and reactive muscle response on kinematic variable, whereas induced acceleration analysis evaluates the instantaneous contribution of a muscle to the measured kinematics.

Conclusion

In conclusion, this study showed that the modulation of reactive bilateral GM activity in response to a medio-lateral perturbation of walking during the gait cycle reflects the phase dependent muscle potential to control the margin of stability and prevent inter-limb collision. Using forward simulations, it was possible to establish causal relations between the observed GM response to a perturbation and kinematic strategies for control of gait stability. First, these results showed that an increase in stance or swing leg GM activity causes an outward foot placement and therefore compensates for the stability loss caused by a lateral translation of the stance leg early in the gait cycle. Second, GM activity of the inward leg in response to a platform translation late in the gait cycle (i.e. during push-off) prevents collision between the swing foot and stance leg, although it counteracts inward foot placement. This study provides important insights in the muscle coordination of reactive control of stability during walking and proposes a novel method to quantify the contribution of the external perturbation force and the active muscle response to gait stability.

Chapter 6

Increased sensory noise and not muscle weakness explains changes in non-stepping postural responses following stance perturbations in healthy elderly

Maarten Afschrift, Ilse Jonkers, Sabine Verschueren, Friedl De Groote

Published in *Gait & Posture*

Abstract

The response to stance perturbations changes with age. The shift from an ankle to a hip strategy with increasing perturbation magnitude occurs at lower accelerations in older than in young adults. This strategy shift has been related to age-related changes in muscle and sensory function. However, the effect of isolated changes in muscle or sensory function on the responses following stance perturbations cannot be determined experimentally since changes in muscle and sensory function occur simultaneously. Therefore, we used predictive simulations to estimate the effect of isolated changes in (rates of change in) maximal joint torques, functional base of support, and sensory noise on the response to backward platform translations. To evaluate whether these modeled changes in muscle and sensory function could explain the observed changes in strategy; simulated postural responses with a torque-driven double inverted pendulum model controlled using optimal state feedback were compared to measured postural responses in ten healthy young and ten healthy older adults. The experimentally observed peak hip angle during the response was significantly larger (5°) and the functional base of support was smaller (0.04m) in the older than in the young adults but peak joint torques and rates of joint torque were similar during the recovery. The addition of noise to the sensed states in the predictive simulations could explain the observed increase in peak hip angle in the elderly, whereas changes in muscle function could not. Hence, our results suggest that strength training alone might be insufficient to improve postural control in elderly.

Keywords: Postural control, simulation, aging

Introduction

In elderly, falls are the leading cause of accidental death and injury admissions to hospitals [103]. Postural control deficits contribute to the increased incidence of falls [104] but the influence of specific age-related changes in the neuro-muscular system on postural control is not well understood.

Healthy young and older adults use a different strategy in response to a perturbation of standing. With increasing perturbation magnitude, both young and older adults shift from an ankle to a hip strategy and eventually from a non-stepping to a stepping strategy [20, 26]. But this shift in strategy occurs at lower perturbation magnitudes in older than in young healthy adults [20, 96, 104].

Age-related changes in perturbed standing balance have been related to changes in muscle function. First, overall muscle weakness has been correlated with impaired postural control, with especially weakness of distal lower limb muscles limiting non-stepping balance control [43]. In addition, muscular effort to control posture increases in elderly [105]. Second, the rate of force development decreases with age, however its effect on balance control is unclear [20,44]. Third, a decrease in functional base of support (FBOS) has been correlated with impaired postural control [20, 79]. Older adults with a decreased FBOS use a heel-rise and stepping strategy for smaller perturbations of balance compared to healthy controls [20].

Age-related changes in perturbed standing balance have also been related to changes in sensory function. The decline of the somatosensory system in elderly causes a decrease in position and movement sense [48–51] and sensory loss has been related to declined postural control [52–55]. For example, individuals with peripheral nerve dysfunction, such as patients with diabetic peripheral neuropathy, are at greater risk of falling [55]; patients with somatosensory loss rely on a hip rather than an ankle strategy for postural corrections [54]; and the compensatory muscle activity in response to a perturbation decreases when plantar skin sensory input is inhibited by hypothermia [52].

Dynamic simulations of perturbed standing balance have been used to investigate the selection of an ankle or hip strategy. Kuo et al. have shown that the capability to accelerate the center of mass, and hence to stabilize posture, is larger for hip versus ankle strategies and for stepping versus non-stepping strategies [95,106]. We recently found that hip strategies minimize center of mass movement whereas ankle strategies are energetically more efficient [77, 107]. Since age-related changes in muscle and sensory function occur simultaneously, their individual contributions to postural control are hard to determine experimentally. In contrast, predictive simulations of balance allow investigating the effect of isolated changes in muscle or sensory function on postural control.

Here, we used our recently developed framework for predictive simulations of perturbed standing balance [107] to investigate the effect of isolated age-related changes in the neuro-musculoskeletal system on the postural response to a backward support surface translation.

Specifically, we assessed how either a decrease in muscle function or an increase in sensory noise influenced the predicted postural response. Simulated responses were compared to measured responses in a group of healthy young and older adults without a history of falling to evaluate whether the modeled changes in muscle and sensory function could explain the increased occurrence of hip strategies in the older versus young adults.

Methods

Experiments

Ten healthy young (21 ± 2 STD (standard deviation) years) and ten healthy older adults (67 ± 3 STD years) without history of falling participated in the study. KU Leuven's commission of medical ethics approved the experimental protocol. Participants provided written, informed consent prior to participating.

Subjects stood at stance width equal to their shoulder width on a moving platform (Carenbase, Motekforce Link, Netherlands). Subjects were informed that the platform would randomly move in multiple directions and were instructed to maintain stability without stepping. We analyzed perturbed standing in response to backward platform translations (0.16m total excursion) administered within three blocks of randomized perturbations in anterior-posterior and medio-lateral directions with respectively fast, medium and slow acceleration profiles (1.1 m/s^2, 0.8 m/s^2 and 0.6 m/s^2)peak acceleration). These acceleration profiles elicited a wide range of postural responses. Two trials per acceleration profile were analyzed, resulting in six trials per subject. In order to measure the FBOS, subjects were asked to lean maximally anteriorly and posteriorly with their trunk. The maximal excursion of the center of pressure (COP) with respect to the ankle defined the FBOS. Whole-body motion was recorded with an extended plug in gait marker set (58 makers) [89] at 100Hz using a an 7-camera Vicon motion capture system. Ground reaction forces were collected at 1000 Hz from two AMTI force plates.

Experimental data processing

Experimental data was analyzed in OpenSim [68] using a scaled skeletal model with 23 degrees of freedom (Gait2392model). Joint kinematics were calculated from the recorded marker trajectories using a Kalman smoothing algorithm [74]. Joint kinetics were calculated using OpenSim's Inverse Dynamics tool. For each subject, peak hip flexion angles, COP excursions, peak joint torques and torque rates during the first two seconds of the postural response (i.e. the time required to return to quiet standing) were averaged over all trials of each acceleration profile. Additionally, the minimal distance between the COP during the postural response and the anterior bound (COP moves forward in response to backward translation) of the FBOS was computed.

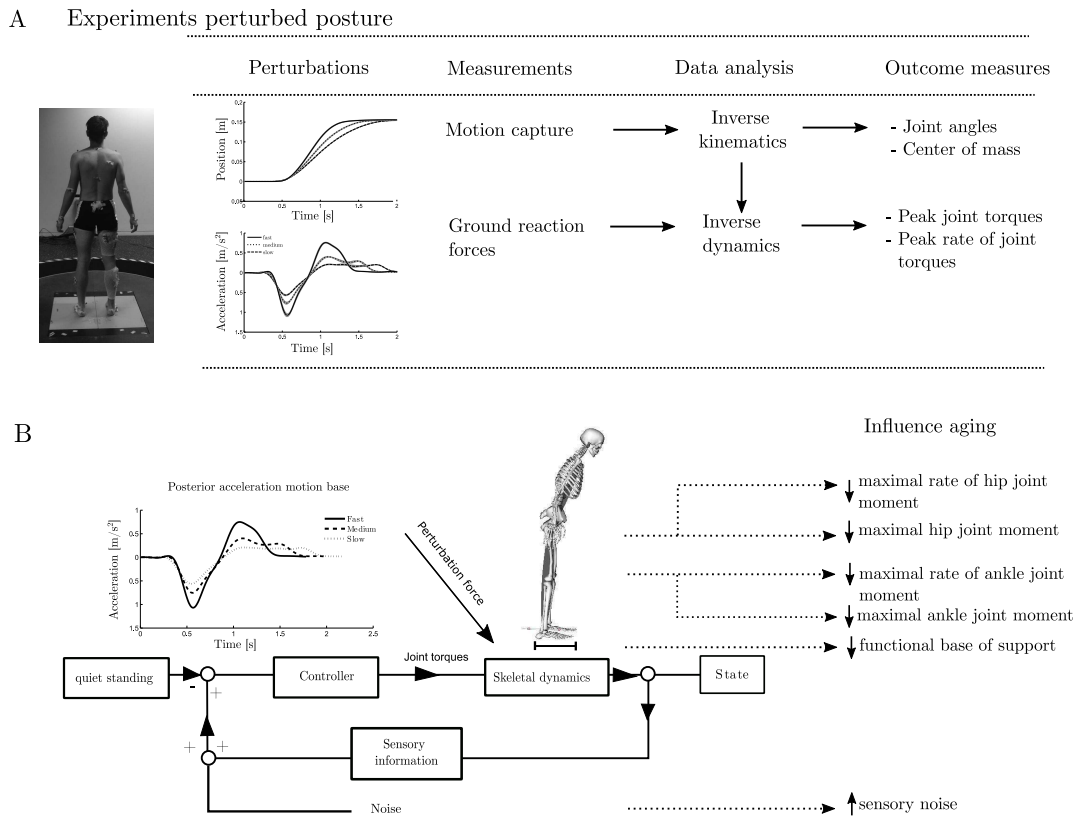

Figure 6.1: **Methods overview.** Pane A: Processing workflow of experimental data collected during the response to a stance perturbation by means of a posterior platform translation with three different acceleration profiles. Joint angles and center of mass locations during the postural response were determined from the motion capture data. Joint kinematics were combined with ground reaction forces to compute joint torques. Pane B: neuromechanical model to simulate postural responses. The feedback control model is similar to the model of [13]. In the sensory information block returns the full state of the model (ankle and hip joint angles and angular velocities) with or without additive noise. The sensed state is compared to the desired state corresponding to quiet standing. The error on the desired state is multiplied by a feedback gain matrix (eight feedback gains) in the controller to compute the ankle and hip joint torques. The different acceleration profiles of the platform as a function of time were approximated by cubic splines and imposed as external forces acting on the skeletal model. Age-related changes were induced to the simulations by a stepwise decrease of (1) the FBOS, (2-3) the maximal ankle and hip joint torque, (4-5) the maximal rates of change in ankle and hip torque (6) and by a stepwise increase of the additive white Gaussian noise on the state (sensory information block).

Predictive simulation of postural responses

Predictive simulations of the response to backward translations at each acceleration profile were generated based on a torque driven linearized double inverted pendulum model with optimal full state feedback. Nominal model parameters describe a healthy adult (for details see [90]). Parameters describing sensory and muscle function in the model were then varied to reflect age-related changes in the neuro-musculoskeletal system and corresponding simulations were generated (figure 6.1). The feedback gains of ankle and hip angles and velocities were selected by minimizing the weighted sum of postural instability and effort over the first two seconds of the response [13]. Postural instability and effort were modeled by the time integral of respectively the squared displacement of the extrapolated center of mass with respect to reference (perturbation onset), and joint power squared. We have previously shown that this model can describe the full range of ankle and hip strategies by changing the relative weighting of effort and instability in the cost function [107]. In this study, we selected the weight such that an ankle strategy, similar to the strategy measured in healthy young subjects, was predicted for the nominal model and then kept the weight constant in all consequent simulations. Therefore, changes in the predicted strategy can be solely attributed to changes in the parameters describing the neuro-musculoskeletal systems. Compliance of the simulation with physiological and mechanical constraints was imposed. First, COP movement was restricted to the measured FBOS. Second, simulated initial and final joint angles and joint torques were constrained based on the corresponding experimental values. Finally, stability of the resulting closed-loop system was imposed (online supplement, 5.3). Resulting dynamic optimization problems were solved with the direct collocation software GPOPS II. For more details on the predictive simulations, see the online supplement and [107].

To assess the effect of muscle function, a single parameter at a time was altered in the model and the corresponding simulation was generated. Age-related changes in muscle function were modeled by a stepwise decrease in the FBOS, maximal ankle and hip joint torques, and maximal ankle and hip joint torque rates starting from the nominal parameters [90]. Parameters were decreased until no feedback gains resulting in a response that satisfied all constraints could be found. To assess the effect of age-related changes in sensory information, white Gaussian noise was added to the sensed states in the feedback model. The modelled sensory noise is a simplified representation of the integrated sensory information of the visual, vestibular and somatosensory system. To avoid the simulation of responses that were tuned towards a specific noise signal, feedback gains that minimized the cost function for multiple random noise signals simultaneously were computed. Due to the strong increase in computational time when solving the dynamic optimization problems for an increasing number of random noise signals, the number of noise signals was limited to four. To assess the influence of selecting four noise signals, the optimization procedure was repeated for 15 sets of four randomly generated noise signals. The noise magnitude was increased in steps of 0.1 degrees and 0.1 degrees/s] until no feasible response could be found.

Outcome measures and statistical analysis

We evaluated the difference in measured postural responses between young and older adults based on (1) peak hip flexion angle, indicative of the use of a hip strategy, (2) center of pressure excursion as a percentage of the FBOS (3) maximal ankle and hip joint torque, and (4) maximal ankle and hip joint torque rate (Table 1). A mixed repeated measures Anova model was used in SPSS to evaluate the influence of aging and perturbation magnitude on the outcome measures. An independent sample t-test was used to compare the measured FBOS in the young and older adults. We evaluated simulated peak hip flexion angle as a function of the modified parameter in the neuro-musculoskeletal model and compared the parameter values at which a change in simulated peak hip angle occurred with the corresponding values measured during the response in both young and older adults.

Results

Descriptive statistics

The kinematic response of young and older adults to backward support surface translations was significantly different. None of the young subjects used a stepping or heel rise strategy. In contrast, in response to perturbations with respectively medium and fast acceleration profiles two and four older adults used a heel rise or stepping strategy (Table 1). Whereas the peak hip angles increased significantly with perturbation magnitude in both groups ($p<0.001$) (Table1), this increase was larger for older than young adults ($p=0.002$) (Table1).

	Slow		Medium		Fast	
	Young	Older	Young	Older	Young	Older
succeeded	10/10	10/10	10/10	8/10	10/10	6/10
Peak hip angle [deg]	4.1 (3.6) ⋆	8.7 (3.8) ⋆	9.0 (4.8) ⋆	14.3 (9.8) ⋆	11.5 (5.9) ⋆	14.8 (6.1) ⋆
COP in FBOS [%]	0.85 (0.08) ⋆	1.10 (0.1) ⋆	0.97(0.03) ⋆	1.15(0.09) ⋆	1.01(0.05) ⋆	1.15(0.05) ⋆
Peak T_a [Nm/kg]	0.62 (0.09)	0.63 (0.05)	0.74(0.11)	0.68(0.05)	0.76 (0.1)	0.69 (0.06)
Peak T_h [Nm/kg]	0.23 (0.08)	0.32(0.09)	0.30 (0.06)	0.30 (0.11)	0.40 (0.12)	0.41 (0.12)
Peak $\dot{T}_a$[Nm/kgs]	1.55 (0.27)	1.56 (0.25)	1.88(0.37)	1.64 (0.17)	2.2 (0.53)	2.02 (0.3)
Peak $\dot{T}_h$[Nm/kgs]	1.16 (0.38)	1.29(0.36)	1.47 (0.30)	1.31 (0.37)	1.97 (0.60)	1.99 (0.50)

Table 6.1: **Descriptive statistics of kinematics and kinetics during the response to the backward support surface translations in the young and older adults.** Significant differences between the young and older adults are highlighted with ⋆ for $p<0.01$. Peak T_{ankle} and peak T_{hip} represent respectively the maximal ankle plantarflexion and hip extension torque during the postural response. Peak $\dot{T}_{ankle}$ and peak $\dot{T}_{hip}$ represent respectively the maximal rate of change in ankle plantarflexion and hip extension torque during the postural response.

Although the measured FBOS was significantly smaller for older than for young adults, maximal joint torques and joint torque rates during the response to support surface translations were not significantly different. Older adults had a smaller FBOS (0.13 +/- 0.1 m) than

younger adults (0.17 +/- 0.1 m) (p=0.002). Peak ankle and hip joint torques during the postural responses increased significantly with perturbation magnitude (p<0.001) but were not different between young and older adults. Peak ankle and hip joint torque rates increased significantly with perturbation magnitude (p<0.001) but were not different between young and older adults (Table 1). The extreme anterior position of the COP relative to the anterior bound of the FBOS scaled with perturbation magnitude (p=0.001) and was significantly higher in older compared to young subjects (p=0.001).

Influence of age-related changes on the predicted postural response

Model parameters describing muscle function could be reduced to values below the experimentally observed values without change in the predicted response strategy. More specifically, simulated peak hip angles did not change when the variables that describe muscle function at the hip joint (peak hip torque and torque rate) were reduced below the values we measured during the response in both groups (Figure 6.3C, D). Simulated peak hip flexion angles increased when the FBOS was decreased below 0.1m, which corresponds to 59% and 76% of the measured FBOS in older and young adults respectively (Figure 6.2). Simulated peak hip flexion angles increased when the maximal ankle joint torque was decreased below 0.65 Nm/kg, which corresponds to 85% and 94% of the maximal observed ankle torque in respectively young and older subjects during the postural response (Figure 6.3, A). Simulated peak hip angles increased when the maximal rate of change in ankle joint torque was decreased below 0.35 Nm/kgs, which corresponds to 16% of the average values measured in both young and older adults during the response (Figure 6.3, B).

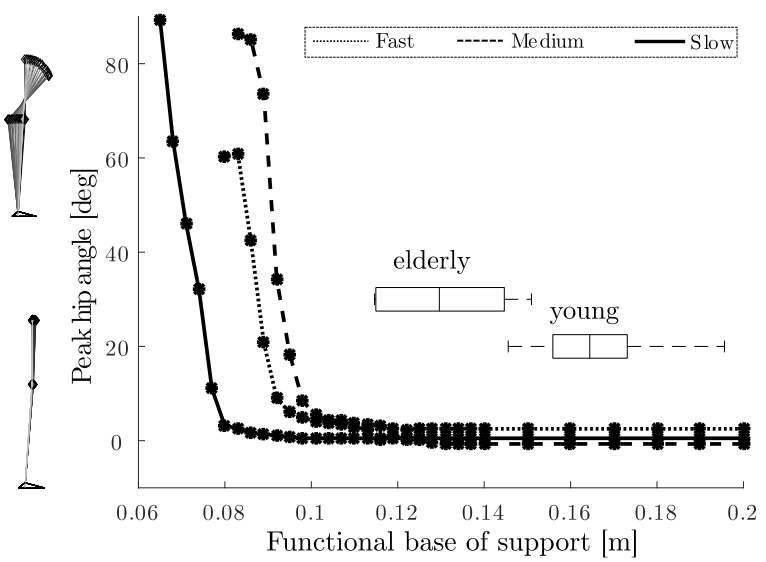

Figure 6.2: **Influence of decreased FBOS on the predicted postural response.** Each dot represents the predicted peak hip angle as a function of the FBOS for the perturbations with high, medium, and low acceleration. The box plot indicate the measured FBOS in respectively the young and older adults

Even small amounts of noise on the sensed states (ankle and hip angles and angular velocities) increased the simulated peak hip angle (figure 6.4). The increase in peak hip angle was quasi linear. No feasible response could be found when the standard deviation of the noise on the joint angles exceeded 0.9°. Furthermore, we verified that the observed shift of peak hip angles with sensory noise was due to a change in the optimal feedback gains and not to the effect of sensory noise on the joint angle trajectories (online supplement).

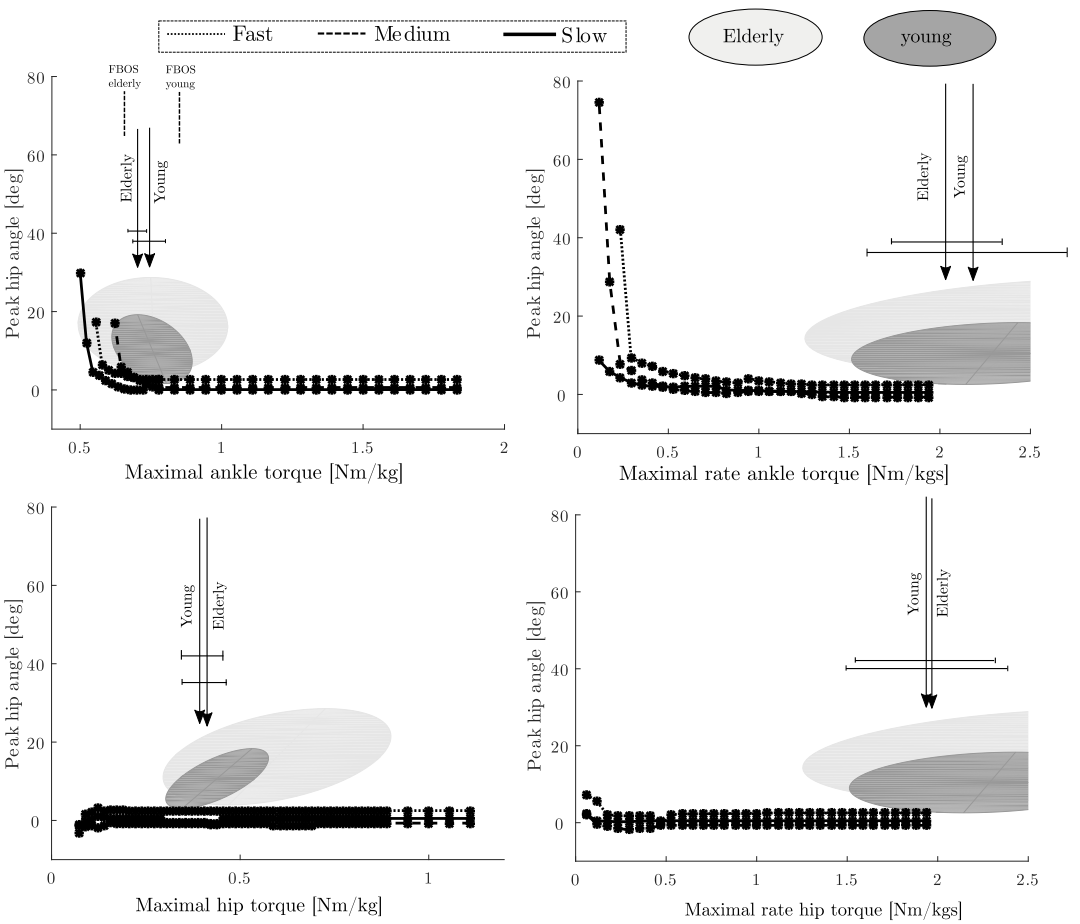

Figure 6.3: **Influence of changes in muscle function on the predicted postural response.** Each dot represents the predicted peak hip angle as a function of (A) the maximal ankle plantarflexion torque, (B) the maximal rate of change in ankle torque, (C) maximal hip flexion and extension torque, and (D) the maximal rate of change in hip torque. The vertical arrows and horizontal lines indicate respectively the peak values with standard deviation measured in the young and older adults during the response (table 1). The dark and light gray ellipses represent respectively the cloud of data points measured in young and older adults. The black dotted vertical line in Pane A represents the maximal ankle plantarflexion torque that does not violate the constraint that the COP should be within the measured average FBOS in the young and older adults.

Discussion

The main aim of the study was to identify the individual contribution of age-related changes in either muscle or sensory function to changes in non-stepping postural control in response to a backward surface translation. By modeling sensory noise we could explain the experimentally observed increase in peak hip flexion angle in older versus young adults. In contrast, changes in the variables that describe muscle function, including the FBOS, could not explain the experimentally observed increase in hip angle in a population of community-dwelling older adults without history of falling.

Our experimental data confirmed that older adults have a smaller FBOS and more often use a hip or stepping strategy in response to backwards platform perturbations while standing compared to young adults [20, 79]. However, the peak ankle and hip torque as well as the peak ankle and hip torque rates during the measured postural responses were not different in young versus older adults.

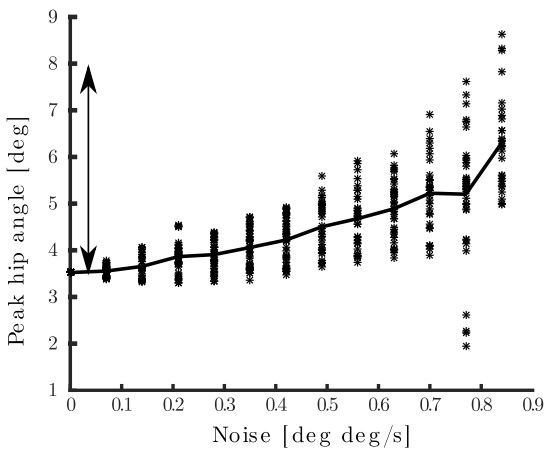

Figure 6.4: **Influence of sensory noise in the feedback system on the predicted postural response.** The predicted peak hip angles increased with sensory noise amplitude. Each dot represents a separate predictive simulation. For each noise amplitude, the simulation was repeated 15 times to assess the influence of optimizing the strategy based on a finite number of random noise signals. The vertical arrow represent the measured average difference in peak hip angle between the young and older adults

The modeled changes in muscle function do not explain the observed shift towards a hip strategy in our population of elderly without history of falling. The predicted strategy only shifted towards a hip strategy when the FBOS, the maximal hip torque, or maximal ankle and hip torque rates were decreased far below experimentally observed values during the postural response in both older and young adults. More specifically, a change in postural response strategy was only predicted when the modeled peak hip joint torques, or ankle and hip torque rates were decreased to about a third of the corresponding measured values in the older adults (Figure 6.3, B C D). A decrease of the peak ankle torque to a value below the measured value in both young and older adults during the postural response changed the

predicted strategy. However, the measured peak ankle torque during the postural response was not different between young and older adults and hence a deficit in ankle torque generation does not explain the observed differences between both groups. It is important to note that the measured peak ankle torque does not reflect the strength of subject but is limited by the non-stepping requirement. The measured FBOS was smaller in the older than in young adults but was in both populations markedly larger than the FBOS that introduces a shift towards a hip strategy in the predictive simulation. Furthermore, in the older adults, the center of pressure even moved slightly beyond the boundaries of the FBOS during the measured postural responses (Table 1). Therefore, our simulations suggest that the observed decrease in FBOS in the older adults cannot fully explain the observed shift towards a hip strategy.

Changes in ankle muscle function had a larger effect on the simulated response than changes in hip muscle function. The simulated shift in strategy occurred when the ankle and hip torque were respectively limited to 39% and 11% of the nominal values. Therefore, our simulation results confirms that weakness of distal rather than proximal lower limb muscles causes a shift towards a hip strategy [43], but only in patients with severe weakness. Although we did not observe differences in peak joint torques during the postural responses between our healthy young and older populations, such differences might be present in older adults with weakness or a history of falling.

Small levels of sensory noise can explain the observed shift in postural strategy with aging. Adding small levels of sensory noise to ankle and hip joint positions and velocities was sufficient to elicit a shift from ankle to hip strategies in the simulated responses. Additionally, an increase in peak hip angle was also found when noise was added to the joint angles or angular velocities separately (online supplement). The magnitude of the change in peak hip angles in the simulations with sensory noise is similar to the observed change in peak hip angle between young and older adults (figure 6.4). However, direct measurements of sensory noise are impossible and no experimental measures are therefore available for comparison to the simulated sensory noise. Nevertheless, there is evidence that the proprioceptive system deteriorates with aging [48]. In addition, the predicted changes in peak hip angle were comparable to changes in postural response strategy when sensory function was experimentally impaired by galvanic vestibular stimulation [108] or somatosensory loss [54]. We did not find feasible strategies for noise levels larger than 0.9°. This is considerably lower than previously described variability in joint position sense at the elbow in an arm position-matching task (being of 3.4°) and the variability in dynamic position sense tasks at the ankle joint (being up to 2.5°) [49]. This discrepancy might be due to task-related differences as well as specific modeling assumptions. First, we assume full state feedback as a simplified representation of the integrated sensory information of the visual, vestibular, and somatosensory system whereas position sense tasks only assess part of the sensory system. Second, our model is torque driven whereas muscle dynamics might provide inherent stability [92]. Finally, the limited number of degrees of freedom might have limited the capability of the model to cope with noise. It is likely that the allowable noise levels would increase when modeling arm swinging or lumbar bending.

Although our predictive simulations enabled us to assess cause effect relations between changes in the neuro-musculoskeletal system and the postural response strategy, several limitations can have influenced our results. First, the different age-related changes occur simultaneously and their combined effect influences postural control in aging. Second, some arm swinging was observed during the response to the perturbations that might explain the observed differences between the functional base of support and the excursion of the center of pressure during the experiments. Arm swing was not modelled in the predictive simulation and therefore the model might underestimate the capability to control balance compared to the experiments where arm swing was allowed. Third, the model was not able to predict the increase in peak angle with increased perturbation magnitudes for both the young and older adults (table 1). The predicted peak hip angle did not change with perturbation magnitude for the measured values of the FBOS and parameters that describe muscle function (Figure 6.2-6.3). This suggest that the increase in peak hip angle may be related to a shift in objective of the movement [107] rather than a limitation on strength or FBOS. Finally, only sensory noise was considered whereas signal dependent motor (efferent) noise will also influence postural control [109] and could be influenced by aging [48].

Conclusion

Noise in the sensory system but not reduced muscle function or a smaller functional base of support could explain the observed shift in postural strategy towards a hip strategy in healthy older versus young adults following a backward support surface translation. Hence, our results suggest that strength training alone might be insufficient to improve postural control in elderly. Alternative fall prevention strategies, such as proprioceptive training [31] or the use of sensory cues in the environment, should therefore be explored.

Chapter 7

Increased use of stepping strategy in response to medio-lateral perturbations in the elderly relates to altered reactive tibialis anterior and not gluteus medius activity

Maarten Afschrift, Robert van Deursen, Friedl De Groote, Ilse Jonkers

Under review in Gait & Posture

Abstract

The influence of aging on the active control of balance in response to perturbations in the frontal plane during walking is not well explored. We used an extensive gait perturbation protocol to test if reactive control to perturbations differs with aging. We hypothesized that alterations in reactive muscle activity of the tibialis anterior and gluteus medius will cause an age-related shift from lateral ankle to stepping strategy in the reactive control of balance. A treadmill-based perturbation protocol imposed medio-lateral platform translations and a sudden increase or decrease in belt speed of two different magnitudes. Perturbation were applied during different phases of the gait cycle. Motion capture and electromyography of the tibialis anterior, gluteus medius, soleus and gastrocnemius measured the response to the different perturbations in a group of eighteen young (age 21 $\pm$ 2 std) and ten older adults (age 71 $\pm$ 4 std). Only for a small subset of more challenging perturbations, reactive muscle activity and kinematic strategies differed between young and older subjects. When perturbation magnitude increased, the older adults relied more on a stepping strategy for inward directed frontal plane perturbations and for sagittal plane perturbation just before heelstrike. Tibialis anterior activity increased less in the older compared to the young subjects. Using simulations, we related tibialis anterior activity control to the outward center of pressure movement in the stance foot and confirmed therefore its contribution to the lateral ankle strategy. We conclude that deficient tibialis anterior activity, and not gluteus medius activity, predisposes elderly to use stepping strategies more than the lateral ankle strategies in response to more challenging perturbations. This finding suggests that current rehabilitation targets for fall prevention in elderly needs to also focus on ankle muscle reactivity.

Introduction

Falling is a major threat to the steadily growing population of elderly. Elderly are more at risk of falling, especially during walking [99]. The failure to maintain gait stability in the presence of a perturbation can result in a loss of balance, which may lead to a fall. Reactive control of balance in response to a perturbation relies on adjustment in muscle activity and joint kinematics to return to a steady-state walking pattern after perturbation [17, 19, 22]. Knowledge of the age-related differences in reactive muscle activity and kinematics in response to perturbations might help to understand the deficits in the control of balance during walking in elderly and in defining therapeutic targets to prevent falls.

The two main mechanisms for balance control are stepping and lateral ankle strategy [31]. Both strategies adjust the position of the center of pressure (COP) with respect to the position of the extrapolated center of mass (Xcom), which accounts for both the position and velocity of the center of mass) [18]. During the stepping strategy, the COP location is controlled by adjusting the medio-lateral and anterior-posterior foot placement as observed in response to mechanical and visual perturbations [18, 19, 22, 35]. Activity of the gluteus medius has been related to medio-lateral foot placement and is therefore considered to be the main contributor to the stepping strategy [17, 19, 22]. In the lateral ankle strategy, the COP location in the stance foot is adjusted by generating a torque around the ankle joint through reactive tibialis anterior, soleus or peroneus muscle activity [18, 31, 32].

The influence of aging on reactive balance control has mainly been investigated during sagittal plane perturbations [21, 35, 46, 60]. Older subjects need more steps to return to a stable gait pattern and have an increased center of mass movement after sagittal plane perturbations [21, 35].

However, the influence of aging on walking balance control in the frontal plane is largely unexplored. This despite the fact that walking is mainly unstable in the frontal plane and therefore requires more active frontal than sagittal plane control [30, 100, 110]. The important role of the tibialis anterior in the lateral ankle strategy and the role of the gluteus medius in the stepping strategy suggests that altered function of these muscles could cause deficits in frontal plane balance control in the elderly. During perturbed standing, reduced tibialis anterior strength has already been related to a shift from ankle towards stepping strategy in the elderly [20, 111]. Other experimental studies of standing stability suggest that hip abductor (i.e. gluteus medius) strength limits postural control performance in response to medio-lateral perturbations in the elderly [45]. In addition, decreased hip abductor strength was found to be a predictor of future falls risk [112] and to be larger in fallers as compared to non-fallers [42].

Currently, it remains unclear how aging affects balance control in the frontal plane and if altered reactive activity of the tibialis or gluteus medius are related to deficits in the control of balance during walking. We hypothesize that, comparable to standing balance control, elderly will shift earlier from a lateral ankle to stepping strategy in reactive control of gait [20, 111]

and that his can be related to a reduced magnitude of tibialis anterior or gluteus medius reactive activity. To test this hypothesis, gait was perturbed in a group of young and elderly subjects in medio-lateral and anterior-posterior direction during different phases of the gait cycle.

Method

Kinematics and muscle activity in response to medio-lateral or anterior-posterior perturbations with onset during different phases of the gait cycle were measured. 18 healthy young (age 21 +/- 2 std) and 10 older adults (age 71 +/- 4 std) without a history of falling, participated in the study. The experimental protocol was approved by the ethics committee of the School of Healthcare Sciences, Cardiff University. All participants gave written informed consent before participating in the study.

Perturbation protocol

Subjects first adapted to the split-belt treadmill (Grail, MotekForceLink) by walking two minutes at a speed of 1.1 m/s and were then exposed to three perturbation sessions with five minutes rest in between. A perturbation session consisted of 32 unique perturbations imposing two different perturbation magnitudes in four directions applied at four different instants in the gait cycle (Figure 7.1). Medio-lateral perturbations were induced by a sudden platform translation to the left or right and anterior-posterior perturbations were induced by a sudden increase or decrease in the speed of both belts. The direction of loss of stability defined the perturbation direction (i.e an increased belt speed caused the subject to fall forward and is considered a forward perturbation). All perturbations were applied immediately after left heelstrike (7.5% gait cycle, first double support), during early midstance (22.5% gait cycle), late midstance (37.5% gait cycle) or push-off (52.5% gait cycle, second double support).

Measurements and data analysis

Kinematics in response to the perturbations were recorded at 200Hz by 12 Vicon T20 cameras (Vicon, Oxford) measuring the trajectories of 48 retroflective markers of an extended plug-in gait marker protocol. Ground reaction forces were collected on a split-belt treadmill with a sampling frequency of 1000Hz (MotekForceLink). Ground reaction forces and 3D marker coordinates were filtered using a 4th order low-pass Butterworth filter (cutoff frequency: 8Hz). Muscle activity of the left and right gluteus medius, gastrocnemius, soleus and tibialis anterior was measured using surface electromyography (EMG) (Bortec Octopus 8 channel EMG) at 1000Hz. EMG data were filtered with a second order IIR notch filter to remove the electric hum and a 4th order recursive Butterworth band pass filter (cutoff frequencies of 20-400Hz). Subsequently, the filtered signals were rectified and a linear envelope was created with a 4th order recursive Butterworth low-pass filter (cutoff frequency: 20 Hz).

Left and right heel strikes were determined from the ground reaction forces. The muscle

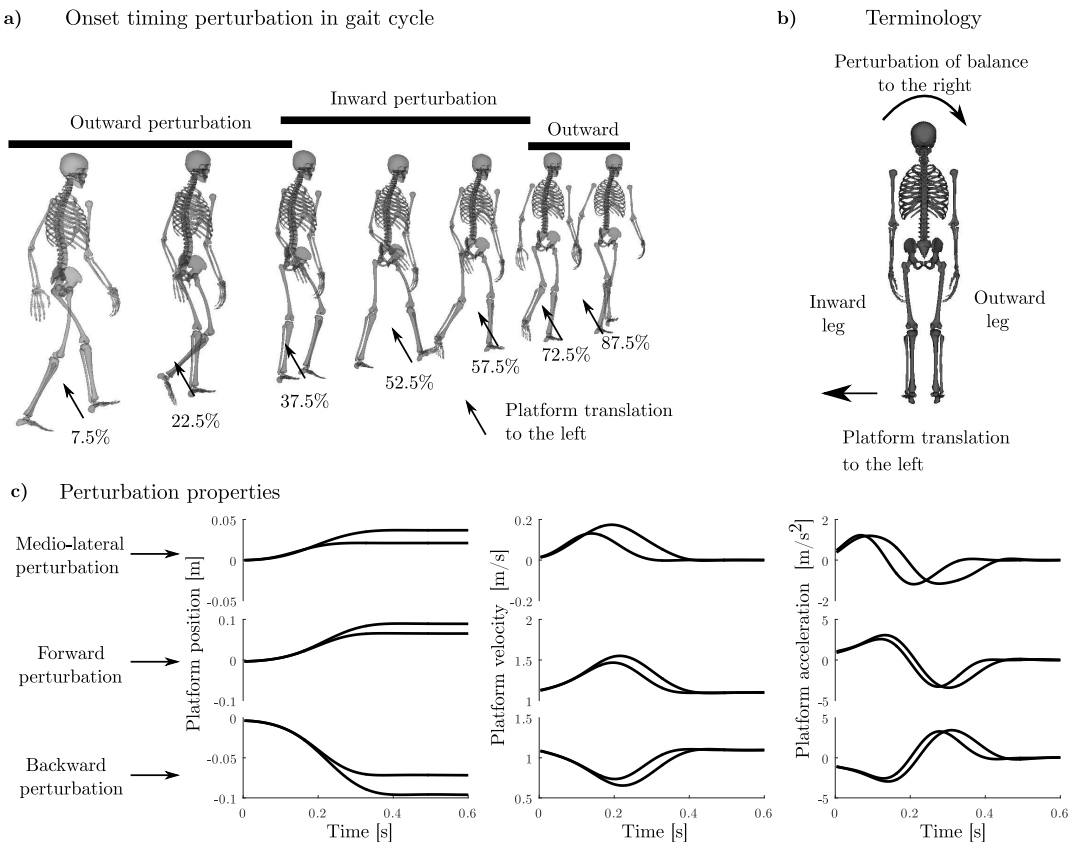

Figure 7.1: **Overview perturbation protocol.** The perturbation was applied during different phases of the gait cycle (Pane A). When assuming symmetry between the left and right leg, the perturbation in the sagittal plane at 7.5% and 52.5% are similar (i.e. both perturbations start just after heelstrike of the left and right leg respectively). In addition, when assuming symmetry, platform translations to the right at 7.5%, 22.5% and 37.5% of the gait cycle can be discussed as platform translations to the left at 57.5%, 72.5% and 87.5% of the gait cycle. We will refer to the right leg as outward leg and left leg as inward leg. A platform translation to the left causes a loss of stability to the right that is counteracted by either outward placement of the right foot hence termed the outward leg, or inward (cross-over) placement of the left foot, hence termed the inward leg (Pane B). Similarly, platform translations to the left during left stance are referred to as outward perturbations and platform translations to the left during right stance are referred to as inward perturbations (Pane A). The position, velocity and acceleration profile of the medio-lateral, forward and backward perturbations is shown in pane C

response to a perturbation was determined by subtracting the muscle activity during nominal walking from the activity after perturbation. To this aim, processed EMG data average over the last 60 gait cycles during the two minutes of unperturbed walking, and processed EMG data of the gait cycle after the perturbation were interpolated to 1000 data points. The muscle response was then quantified as the time integral of the difference in muscle activity during the first 300ms after perturbation onset.

A generic musculoskeletal model with 23 degrees of freedom was scaled to the subject's anthropometry and was used to calculate foot and center of mass kinematics from the recorded marker trajectories in OpenSim [68, 74]. Stride width was computed as the average frontal plane distance between the left and right ankle joint center during double support. The position of the Xcom was computed based on the position and velocity of the center of mass relative to the position of the ankle joint center at heel strike [6]. The movement of the COP was computed as the average distance between the COP and the ankle joint center 150 to 300ms after the perturbation (i.e. first 150ms removed due to noise caused by inertia of the moving force plates, see limitations).

Symmetry between the left and right side was assumed in the analysis of the medio-lateral perturbations to simplify the discussion. Hence, lateral platform translations to the right at 7.5%, 22.5% and 37.5% of the gait cycle were discussed as platform translations to the left at 57.5%, 72.5% and 87.5% of the gait cycle (Figure 7.1).

Outcome measures and statistical analysis

A generalized linear mixed effect model was used to evaluate the effect of the different perturbations and age groups on stride width, stride length and margin of stability during the first three heelstrikes after perturbation compared to nominal walking and on the reactive muscle activity during the first 300ms after perturbation. A variable intercept was used to account for inter-subject differences in nominal walking. Bonferroni correction for multiple comparisons was used. A two-sided confidence interval with an alpha level of 0.05 was used for all statistical tests.

Secondary analysis using model-based simulation

For muscles with different response in young and older adults, we evaluated the effect of reactive muscle activity on COP movement using our recently developed forward simulation workflow [113]. This allows evaluating the effect of an individual muscle response on the kinematics, which is impossible in the experimental approach where reactive activity of multiple muscles determine the COP movement. In addition, this method allows to discriminate between the effect of perturbation force and the contribution of reactive muscle activity to the movement of the COP. Hence, this approach establishes causal relations between an isolated muscle response and the COP movement. Details on the simulation method can be found in the appendix on simulation of walking balance control.

Results

Measurements: Medio-lateral perturbations:

In both age groups, onset timing of the medio-lateral perturbation had a significant effect on stride width, margin of stability, COP motion and reactive muscle activity (Figure 7.2, 7.4) for the large perturbations. Large perturbations with onset early in the gait cycle (7.5-22.5 %) caused an increase in stride width (i.e. outward stepping strategy) (Figure 7.2b,$F(1,1210)=318$, $p<0.001$), decrease in stride length (7.2a, $F(1,1210)=534$, $p<0.001$), medial position of the COP in the stance foot (Figure 7.5a, i.e. ankle strategy) and a medial [$F(1,1210)=89.0$, $p<0.001$] and forward [$F(1,1210)=327$, $p<0.001$] position of the Xcom compared to unperturbed walking (Figure 7.2cd). Perturbation with onset between 52% and 77% of the gait cycle, decreased stride width (Figure 7.2b, $F(1,1210)=655$, $p<0.001$), lateral position of the COP (i.e. ankle strategy) in the stance foot (Figure 7.5a, $p<0.001$) and a lateral position of the Xcom with respect to the foot [$F(1,1210)=202$, $p<0.001$] at the first step but did not change stride length [$F(1,1210)=1.44$, $p=0.302$] and sagittal plane Xcom position [$F(1,1210)=1.702$, $p=0.192$] (Figure 7.2). Foot placement and margin of stability normalised on or after step 2 (Figure 7.2).

In contrast, reactive muscle activity and foot placement differed between the young and older subjects in response to the inward directed perturbations with large amplitude (i.e. 37.5 - 72.5% of the gait cycle). Older adults relied more on an inwards stepping strategy, characterized by the reduced stride width at first heelstrike after perturbation compared to young adults (Figure 7.2b, $F(1,1210)=15.2$, $p<0.001$). In addition, stability decreased in the elderly, characterized by a decreased medio-lateral [$F(1,1210)=11.5$, $p=0.007$] and anterior-posterior [$F(1,1210)=17.2$, $p<0.001$] distance between Xcom and the foot at heelstrike for the perturbation at 37.5 and 52.5% of the gait cycle (Figure 7.2cd). For these perturbations, no difference in reactive gluteus medius activity was found between the young and older adults (Figure 7.4a, $F(1,7384)=0.597$, $p=0.44$), but older adults increased reactive activity of the tibialis anterior less (Figure 7.4a, $F(1,6872)=6.93$, $p=0.008$). Foot placement differed most for inward directed perturbation with onset just before heelstrike between the young and the elderly (i.e. 37.5% of gait cycle, Figure 7.6). The relation between age-related changes in tibialis anterior activity, movement of the feet, COP and COM is visualised in detail for a representative trail of a young and older subject (Figure 7.6.

Measurements: Anterior posterior perturbation

In both age groups, forward perturbations increased stride length [$F(1,1031)=231$, $p<0.001$] (Figure 7.3) and increased soleus [$F(1,4049)=28{,}6$, $p<0.001$] and gastrocnemius [$F(1,3886) = 144$, $p<0.001$] muscle activity of the stance leg (Figure 7.4). Backward perturbations decreased stride length (Figure 7.3, $F(1,1030)=266$, $p<0.001$) and in gastrocnemius [$F(1,3885) = 17.4$, $p<0.001$] and soleus [$F(1,3593)=26.7$, $p<0.0001$] activity of the stance leg (Figure 7.4),

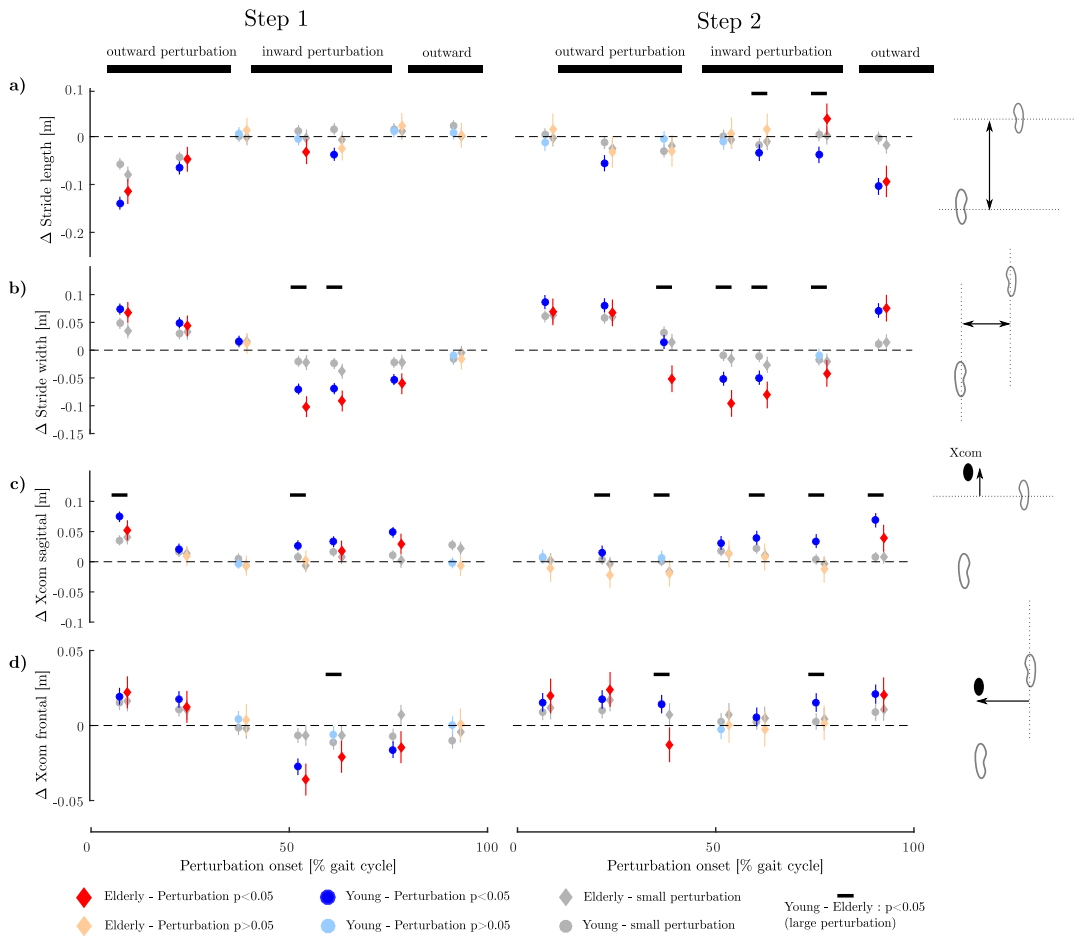

Figure 7.2: **Change in stride length (a), stride width (b), sagittal margin of stability (c) and frontal margin of stability (d) at first and second heelstrike after perturbation compared to unperturbed walking.** The dot represents the average change in outcome variable and the vertical line the confidence interval. The response to the large perturbation is shown in color (blue= young, red=elderly) and the response to the small perturbation is shown in gray. Responses significantly different from unperturbed walking are shown in bright colors for the large perturbation. Significant differences between the young and elderly for the large perturbations were highlighted with a black horizontal line. A small offset in onset timing of the perturbation was added to the data of the elderly for visualization purposes. Note that the first step is at heelstrike of the outward (i.e. right) leg for the perturbations with onset between 0%-40% of the gait cycle. The outward leg is in stance phase for perturbations with onset between 40-90% of the gait cycle, and the first step is therefore analyzed at heelstrike of the inward (i.e. left) leg.

but increased tibialis anterior activity of the stance leg (Figure 7.4, F(1,4059)=214, p<0.001). Foot placement and margin of stability normalised on or after step 2 (Figure 7.2).

In contrast, reactive muscle activity and foot placement differed between the young and older subjects in response to backward and forward perturbations at 37.5% of the gait cycle (i.e. perturbation onset just before heelstrike) (Figure 7.3, 7.4). Older adults reduced stride length more than younger adults in response to the backward perturbation [F(1,1030)=28.49, p <0.001] and increased stride length more in response to the forward perturbation (Figure 7.3, F(1,1031) = 26.91, p<0.001). In the elderly, forward position of the Xcom increased in response to backward perturbations with onset at 37.5% of the gait cycle (F(1,1030)=100, p<0.001), which is significantly different from the young subjects [F(1,1030)=374, p<0.001].

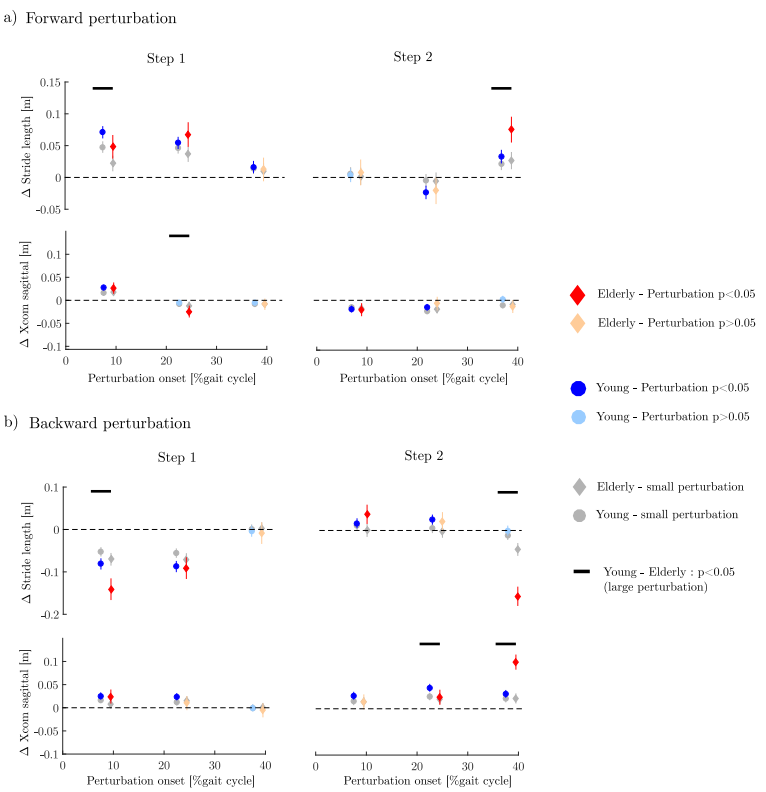

Figure 7.3: **Change in stride length and sagittal MOS at first and second heelstrike after belt acceleration (a) and belt deceleration (b) compared to unperturbed walking.** The dot represents the average change in stride length and MOS and the vertical line the confidence interval. The response to the large perturbation is shown in color (blue= young, red=elderly) and to the small perturbation is shown in gray. Responses significantly different from unperturbed walking are shown in bright colors. Significant differences between the young and elderly for the larg perturbations are highlighted with a black horizontal line. A small offset in onset timing of the perturbation was added to the data of the elderly for visualization purposes (i.e horizontal distance between red and blue data points). No changes in stride width and medio-lateral margin of stability were observed after perturbation compared to unperturbed walking and are therefore added to the online supplement.

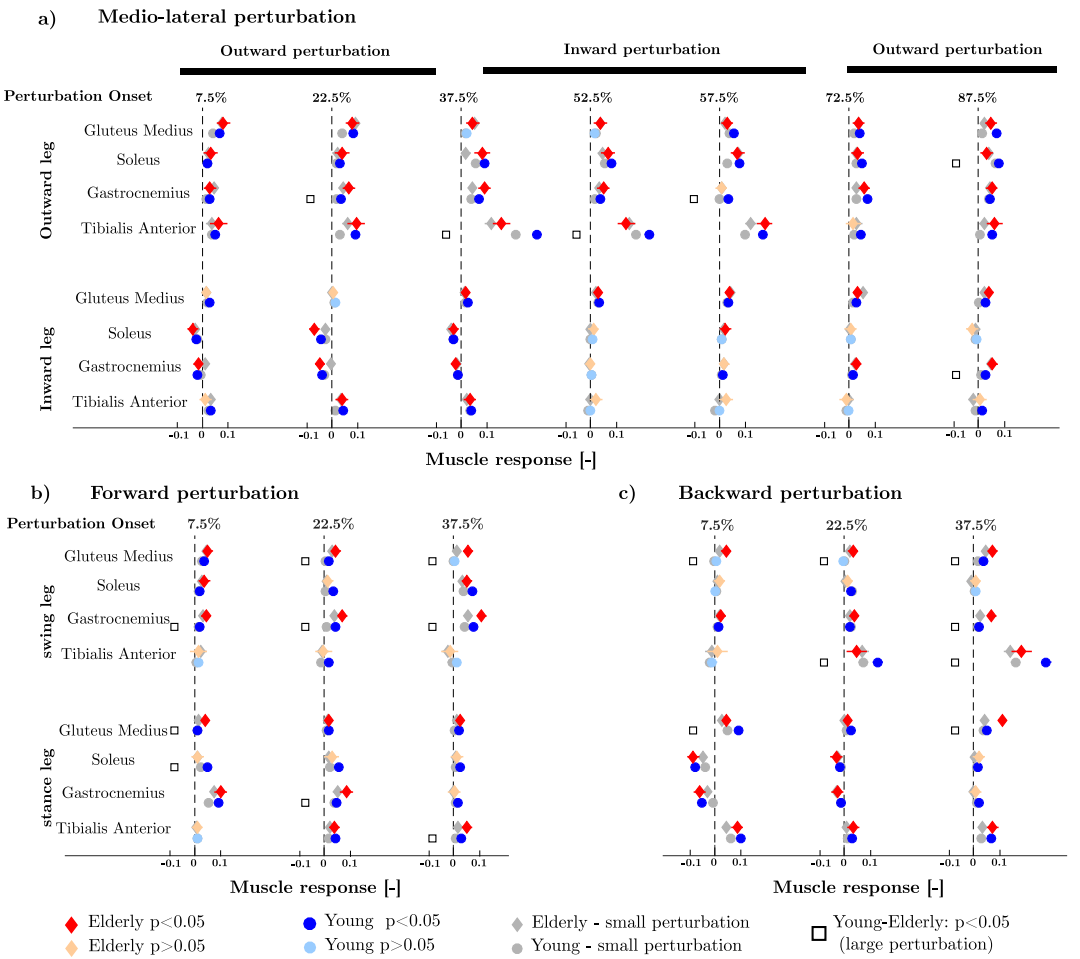

Figure 7.4: **Reactive muscle activity in response to the perturbation (0-300ms).** The muscle response to a sudden medio-lateral platform translation (a), increase (b) and decrease (c) in belt speed is shown as a function of the onset timing of the perturbation during the gait cycle. The dot represents the average muscle response and the horizontal line the confidence interval. The activity in response to the large perturbation is shown in color (young = blue, elderly = red) and to the small perturbation is shown in gray. Muscles responses significantly different from zero are shown in bright colors for the large perturbations. Significant differences between the young and elderly for the large perturbations were highlighted with a black square.

Simulation: influence tibialis anterior activity on medio-lateral position COP

To discriminate between the effect of perturbation force and the contribution of multiple muscles to the ankle strategy and therefore the movement of the COP (Center Of Pressure), we evaluated the isolated effect of reactive tibialis anterior activity on COP movement in simulation for each individual trail measured in the differetn subjects. Since the reactive tibialis anterior activity is believed to contribute to a lateral shift of the COP in the stance foot [32], we evaluated the isolated contribution of the measured tibialis anterior activity to the simulated shift in COP position for the perturbations at 37.5% of the gait cycle where a large increase in both tibialis anterior activity and COP shift was measured. A significant correlation was found between magnitude of the tibialis anterior response of the stance leg in the all the measured perturbation trails and simulated lateral movement of the COP in the stance foot in response to the inward directed perturbation ($p<0.01$, $R^2=0.86$, Figure 7.5).

Discussion

This is the first study that evaluated how aging influences the response to multi-directional perturbations of different amplitudes and in different phases of the gait cycle. When perturbation magnitude increased, older adults relied more on a stepping strategy for sagittal plane perturbations applied just before heelstrike and for inward directed frontal plane perturbations (Figure 7.2-7.3). We found that reduced reactive activity of the tibialis anterior and not gluteus medius may contribute to the shift in balance control strategy in the elderly. In simulation, we showed that the tibialis anterior has an important contribution to the lateral ankle strategy, which confirms the observed relation between reduced reactive tibialis anterior activity and increased occurrence the inward stepping strategy in the elderly (Figure 7.2b).

Foot placement differed only for a subset of the perturbations between young and older subjects. In the frontal plane, only the large inward perturbation caused an increase in inward stepping in the elderly (Figure 7.2). In the sagittal plane, only the large forward and backward perturbations with onset just before heelstrike (i.e. 37% of the gait cycle) caused larger respectively a larger increase and decrease in foot placement in the elderly (Figure 7.3). This shows that when perturbation magnitude increased, the older subjects shifted from an ankle towards a stepping strategy for a subset of the perturbations, whereas the young subjects did not or less. This shift in kinematics strategy is consistent with the shift from ankle toward hip and stepping strategies at lower perturbation magnitudes in standing balance control in elderly [20, 111].

Decreased reactive tibialis anterior activity in older adults may explain the shift from ankle toward stepping stategy in response to inward directed perturbations. Whereas, both young

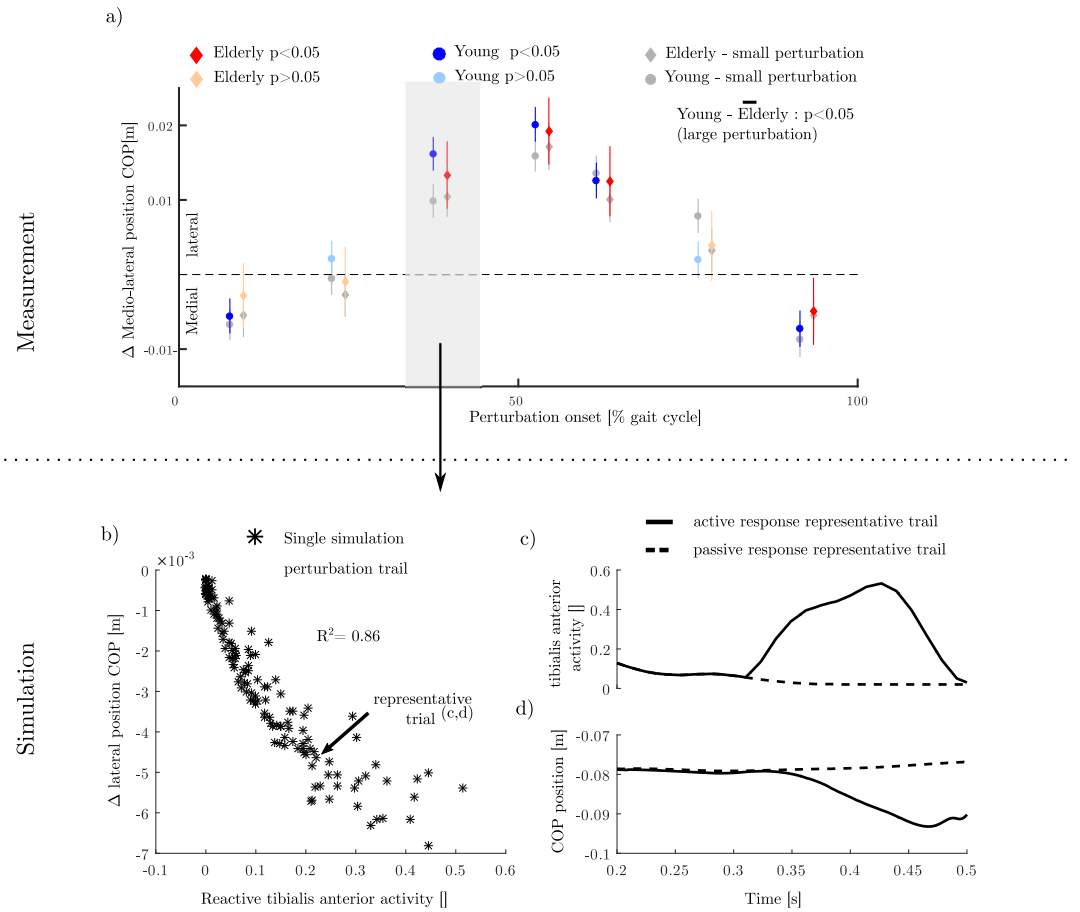

Figure 7.5: **Measured and simulation COP movement in the foot.** The measured medio-lateral shift of the COP in the stance foot, which characterizes the use of an ankle strategy, changes from a medial to a lateral shift when the medio-lateral perturbation onset varied during the gait cycle (pane a). The response to the large perturbation is shown in color (blue= young, red=elderly) and to the small perturbation is shown in gray. Responses significantly different from unperturbed walking are shown in bright colors. Significant differences between the young and elderly for the large perturbations are highlighted with a black horizontal line. The effect of tibialis anterior activity on COP movement in the stance foot was simulated for perturbations with onset at 37.5% of the gait cycle (pane b). A significant positive correlation was found between average reactive tibialis anterior activity and average lateral movement of the COP in the foot ($p<0.001$, $R^2=0.86$) during the first 300 ms after perturbation (pane b). The reactive tibialis anterior activity (pane c) and simulated movement of the COP (pane d) was plotted as a function of time for one representative trial.

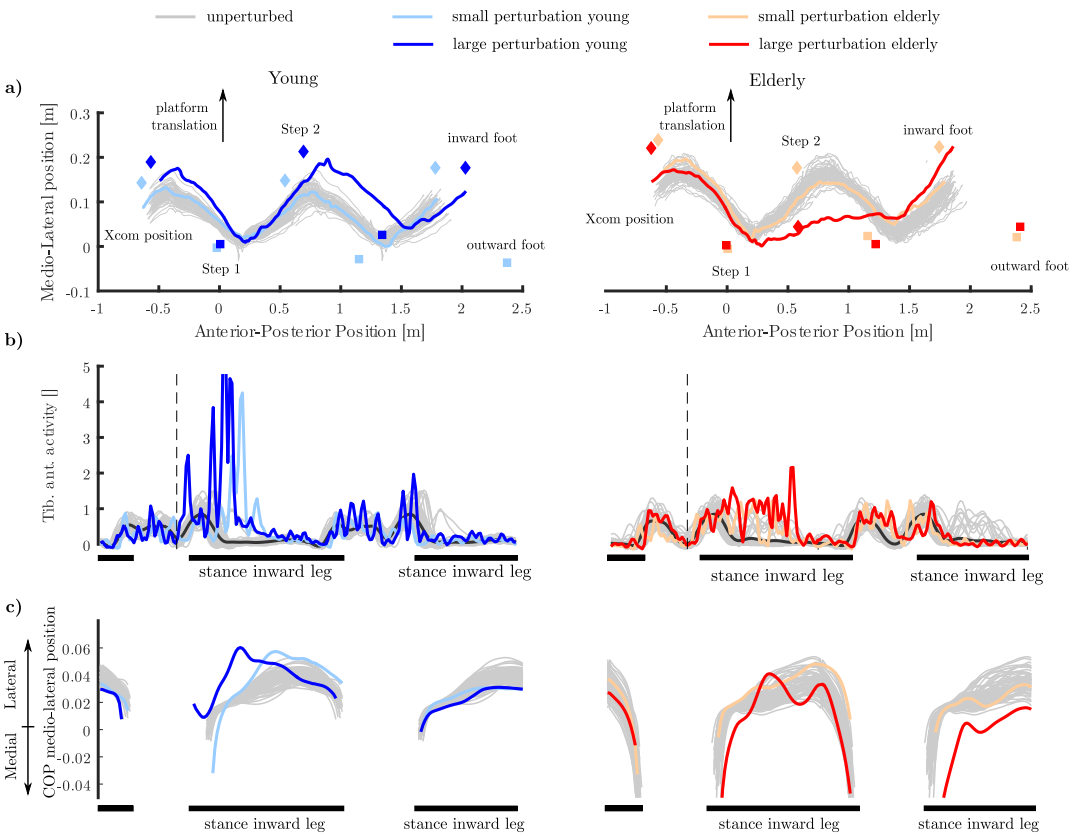

Figure 7.6: **Comparison between representative young and older subjects for perturbations with onset at 37.5% of the gait cycle.** Position of the Xcom with respect to the foot (Pane a), reactive tibialis anterior activity (pane b) and COP motion in the foot (Pane c) is shown for one representative young and older subject. The differences in reactive tibialis anterior activity and stepping strategy between the two selected subjects are represent the average changes found when comparing the young and older subjects (figure 2, 4, x). Reference walking data is shown in gray, response to the small perturbation in light colors (young= blue, elderly=red) and response to the large perturbation in bright colors.

and older adults, increased tibialis anterior activity in response to small inward directed perturbations, for increasing perturbation magnitude, older adults failed to increase tibialis anterior activity (Figure 7.4) and the associated lateral movement of the COP (Figure 7.5). In contrast, elderly increased the adjustment of foot placement indicative of a stepping strategy (Figure 7.2). The observed relation between reduced tibialis anterior activity, decreased lateral movement of the COP in the foot and increased use of inward stepping strategy in the elderly is visualized for a representative trail in (Figure 7.6) an suggests that reactive tibialis anterior activity controls the lateral ankle strategy. Indeed, using forward simulations, the tibialis anterior activity was causally related to lateral movement of the COP in the foot, therefore confirming the correlations between tibialis anterior activity and COP position derived from experiments [32] (Figure 7.5). This suggests that reactive activity of the tibialis anterior is required to move the COP in the foot, and that a failure to generate timely and sufficient tibialis anterior activity necessitates adjustment of the COP position through a stepping strategy. Therefore, our results indicate that altered reactive tibialis anterior activity explains the increase in occurrence of stepping strategies in the older adults, for perturbations in the frontal and sagittal plane.

Similar as in standing balance control [20], altered tibialis anterior strength in the elderly may limit the ability to use a lateral ankle strategy in the elderly. Additionally, age-related changes in proprioception [48] may decrease sensory acuity [49], which may induce poor detection of the perturbation and increase reaction time. Alternatively, the preference for the stepping strategy in the elderly might relate to a preference of a more robust control approach to cope with altered sensorimotor function or fear of falling. The stepping strategy is more robust against perturbations compared to the lateral ankle strategy as the potential COP excursion is larger in a stepping strategy compared to a lateral ankle strategy where it is constrained by the borders of the foot. To this end, predictive simulations of perturbed walking, similar to our previous work in perturbed standing, may in future elucidate to what extent altered tibialis anterior function versus altered control goals (e.g. robustness versus efficiency) contribute to the earlier change towards a stepping strategy in the elderly [63, 111].

In contrast to our hypothesis, reactive activity of the gluteus medius and kinematics of outward stepping, that is mainly controlled by the reactive gluteus medius activity[6], was not different between the young and older adults. In addition, the positive margin of stability and increased stride width at the first step after perturbations shows that the outward stepping strategy, was successful in both the young and older subjects. Our results therefore reject the hypothesis that deficits in gluteus medius function affect the control of balance in the elderly.

Several limitations should be considered when interpreting the results. First, the magnitude of the perturbation was limited to platform translation of 5 cm in medio-lateral direction and 10 cm in anterior posterior direction. Increasing perturbation magnitudes may reveal additional age-related changes in reactive control of balance during walking. Nevertheless, our study showed that for perturbations with limited amplitude, age-related changes in reactive control

of balance occur first in inward directed and not outward directed perturbations, which is related to altered tibialis anterior activity and not gluteus medius activity. Second, despite its important role in the lateral ankle strategy [32], the reactive activity of the peroneus muscle was not measured in this study. However, Hof et al. showed that the peroneus muscle mainly contributes to the lateral ankle strategy in response to outward directed perturbations [32], for which we did not find any differences in kinematic responses between the young and elderly. Therefore, also no differences in reactive peroneus activity between young and elderly are expected. Third, force plate inertial components in a moving surface were estimated according to [114], and combined with the kinematics of the motion base to correct the measured ground reaction forces and moments during acceleration of the motion base. Nevertheless, these corrections might have influenced the location of the COP (Figure 7.5). Finally, only healthy older adults without a fall history were included.

Conclusion

In conclusion, elderly presented the shift from ankle toward stepping strategies in response to inward directed perturbations and perturbations in the sagittal plane with onset before heel strike during gait and this could be related to altered tibialis anterior, but not gluteus medius reactive activity. Hence, our results suggest that gait perturbations paradigms for training of reactive recovery responses might benefit from an increased focus on this subset of perturbations and focus on reactive tibialis anterior activity [115].

Chapter 8

General discussion

The aim of this thesis was to identify to which extent changes in sensory and muscle function contribute to the observed differences in balance control in perturbed standing and walking in elderly. This goal was studied in two main objectives. Firstly, we identified which neuromechanical factors can explain the observed kinematic responses to perturbations of standing and walking in healthy young adults (Study 1 and 2). Secondly, we evaluated the influence of aging on balance control during standing and walking. The insights gained in this PhD thesis contribute to a better understanding of the role of aging in balance control and might aid in the design of fall prevention training and rehabilitation by allowing us to define specific therapeutic targets. This discussion starts with a summary of the hypotheses, results and specific conclusions of the individual studies. Next, the overarching insights gained in this PhD thesis will be discussed. Finally, the limitations of the work and suggestions for future research will be formulated.

Specific conclusions

Objective 1: To identify which neuromechanical factors can explain the experimentally observed kinematic responses to perturbations of standing and walking in healthy adults.

In standing balance control, it was unclear whether and how effort minimization influences the selection of a postural response in the continuum of ankle and hip strategies to a perturbation. In study 1, we evaluated if an optimal feedback control model can predict the measured postural responses to a backward support surface translation in a group of young subjects. Other researchers previously showed that feedback control models that minimize effort can predict reactive muscle activity in response to a backward surface translation [58], but it was unclear if this task level goal can also predict the kinematics of ankle and hip strategies. We therefore evaluated if the relative importance of minimizing effort versus postural instability can explain the continuum of the observed postural responses.

Hypothesis study 1: The relative importance of minimizing effort versus postural instability can explain the continuum of observed postural responses.

In this study, experimental motion data was collected in ten healthy young adults in response to backward support surface translations during standing. An inverse analysis of the experimental data was used to evaluate the correlation between estimates of effort and use of ankle and hip strategies. Forward simulations with a simple feedback model were then used to evaluate if the relative importance of minimizing mechanical work versus postural instability could explain the continuum of measured ankle and hip strategies. In addition, the ability of center of mass feedback to track the measured postural responses was tested. Finally, the validity of the model to predict the postural response following a change in the perturbation conditions was tested.

We confirmed our hypothesis and showed that the selection of a non-stepping postural response in the continuum of ankle and hip strategies can be explained by the trade-off between minimizing energy consumption and postural instability. The finding that minimizing center of mass movement results in a hip strategy was recently confirmed in another simulation study on standing balance control [77]. However, in contrast with our results, Versteeg et al. found that an effort-related objective (i.e. minimizing muscle stress) also resulted in a hip strategy and not an ankle strategy. Discrepancies between the results presented in this work and the result of Versteeg et al. might be related to the level of detail in the neuromechanical model. Versteeg et al. used a complex musculoskeletal model that accounts for 3D movement and muscle dynamics but did not incorporate feedback control. In ongoing work, we found that simulations with a more complex musculoskeletal model confirmed the results presented in this PhD thesis. Minimizing effort results in ankle strategies in a planar muscle-driven model with ankle, knee, hip and lumbar joint degrees of freedom and full state feedback. Discrepancies in simulation results might therefore be related to the modelling of

feedback.

The similarity between the predicted and measured kinematics in response to the perturbation suggests that this neuromechanical model can be used in future "what-if" studies evaluating the influence of age-related changes in sensorimotor function on the control of balance. In addition, the neuromechanical model was able to predict the shift in postural response when the base of support was decreased, indicating that the model can be used to predict postural responses in new experimental conditions. Indeed, the predicted gradual shift from an ankle towards a hip strategy with decreasing base of support is in accordance with the observed postural response in experimental studies of balancing on a narrow beam [26].

In walking balance control, the mechanisms driving the modulation of reactive muscle activity were unclear. Modulation of reactive gluteus medius activity was observed during perturbed walking and is thought to play an important role in balance control [17]. However, the insights on the contribution of reactive muscle activity to balance control were limited because it is hard to identify the individual contribution of individual muscle action to the mechanics of balance control. Therefore, in study 2, we developed a forward simulation of perturbed walking to evaluate the contribution of reactive stance and swing leg gluteus medius activity to balance control during different phases of the gait cycle.

Hypothesis study 2: The potential of the stance and swing leg gluteus medius to (1) adjust lateral foot placement and (2) prevent collisions during swing varies during the gait cycle and explains the observed modulation in stance and swing leg gluteus medius activity.

In study 2, reactive muscle activity (EMG) and kinematics (motion capture) were measured in response to medio-lateral platform translations with onset during different phases of the gait cycle in 18 healthy young subjects. We showed in simulation that the influence of these perturbations on the inter-foot distance (i.e. risk for inter-limb collision) and the margin of stability changes during the gait cycle. Hence, altered timing of the perturbations imposed different mechanical demands to balance control of walking. In addition, we showed in simulation that the contribution of the gluteus medius activity to adjustment of foot placement and to inter-limb distance varies during the gait cycle, which is caused by changes in muscle moment arm, muscle length/velocity, and body and ground contact configuration. This confirmed the hypothesis that the potential of the gluteus medius to adjust lateral foot placement and to prevent inter-limb collisions during swing varies during the gait cycle. Hence, imposing the experimentally observed gluteus medius responses to the forward simulation reveals that gluteus medius activity is modulated during the gait cycle to compensate for the changes in mechanical demands imposed by the perturbation and changes in muscle potential to control stability throughout the gait cycle.

Futhermore, reactive muscle activity was causally related in simulation to the kinematics of balance control during gait. This enabled identifying the underlying mechanisms behind the already previously reported experimentally derived correlations between reactive muscle activity and balance control kinematics. First, we showed that reactive swing leg gluteus

medius activity causes hip abduction and therefore controls outward foot placement. Hence, the simulation results confirmed the strong positive correlation between swing leg gluteus medius activity and outward foot placement derived from experiments [17,19,22]. In addition, we were able to explain the contribution of reactive activity of the stance leg gluteus medius to balance control: stance leg gluteus medius activity was found to cause an upward tilt of the pelvis, thereby stretching the hip abductor muscles of the swing leg and contributing to outward foot placement. Reactive activity of the stance leg gluteus medius was observed by several researchers [17, 19], but its contribution to the kinematics of balance control was unknown.

The methodological developments in study 2 extend the current state-of-the-art of forward simulations of walking in different ways. Only a few studies used direct collocation methods to solve forward simulations of walking efficiently [71, 80, 116]. The direct collocation approach is not sensitive to integration noise and allows an implicit formulation of the musculoskeletal dynamics. To the best of our knowledge, this is the first study that combined forward simulations with experimental results on reactive muscle activity during perturbed walking. Therefore, the most unique feature of this study is the combination of state-of-the-art optimization and simulation techniques with experimental data on perturbed walking in a single workflow to evaluate the individual effect of a perturbation force and measured reactive muscle activity on balance control during walking.

Objective 2: To evaluate the influence of aging on the dominant neuromechanical factors affecting balance control during standing and walking in the elderly.

In standing balance control, it is unclear how age-related changes in sensory and muscle function contribute to the increased occurrence of hip and stepping strategies in the elderly. Decreased muscle strength in the older adults was suggested to contribute to these observations [20]. However, since multiple age-related changes in the sensorimotor system occur simultaneously, it is hard to identify the individual contribution of muscle or sensory function to balance control. Therefore, in study 3, we introduced age-related changes in musculoskeletal constraints (i.e. maximal joint torque, rate of change in joint torque and size of the base of support) and sensory noise into the neuromechanical model to evaluate their effects on the model response. This analysis allows evaluating the effect of isolated changes in muscle and sensory function on standing balance control and may be informative for defining efficient therapeutic targets for balance control.

Hypothesis study 3: Noise in the sensory system and not reduced muscle function or a smaller functional base of support can explain the observed shift in postural strategy from an ankle towards a hip strategy in healthy older versus young adults following a backward support surface translation.

In this study, standing balance was perturbed in 10 healthy older adults using the same

perturbation protocol as in study 1. In accordance with previous studies [5, 20], we found that the older adults relied more on a hip strategy than the young subjects to control balance during perturbed standing. In simulation, an increase in hip strategies was predicted when sensory noise was added to the simulation, similar to the experimentally observed increase in hip strategies in the elderly. In contrast, we had to decrease maximal joint torque, rate of change in joint torque and functional base of support far below the values measured in the elderly before a shift from ankle to hip strategy was predicted. This observation indicates that noise in the sensory information could explain the observed increased use of a hip strategy in the elderly, whereas changes in muscle function could not. Therefore, our results suggest that fall prevention that rely on isolated strength training programs only may not be the most efficient intervention to improve standing balance control in the elderly. The addition of proprioceptive training or sensory cues in the environment seems important to deliver efficient training programs.

In balance control during walking, it remained unclear how aging influences the reactive muscle activity and kinematics in response to perturbations. The influence of aging on balance control was mainly investigated in the sagittal plane [21,46,60], whereas balance control in the frontal plane was largely unexplored. This is remarkable, given the finding that walking mainly needs active control in the frontal plane. In healthy young subjects, reactive activity of the gluteus medius and tibialis anterior was reported in response to frontal plane perturbation [18, 32]. This suggests that both muscles have an important contribution in the control of balance during walking. In study 4, we evaluated how aging influences the control of balance in response to sagittal and more importantly frontal plane perturbations during walking. In addition, forward simulations were used to evaluate if changes in balance control can be explained by altered reactive muscle activity of the tibialis anterior and gluteus medius.

Hypothesis study 4: Elderly shift earlier from a lateral ankle to a stepping strategy in response to a perturbation during walking, which can be related to concurrent alterations in reactive muscle activity of the tibialis anterior or gluteus medius.

To test this hypothesis, a blended experimental-simulation approach was used in which the perturbation protocol of study 2 was also used in a group of older adults and combined with forward simulations of perturbed walking. Reactive muscle activity and kinematic strategies differed between the young and older adults but only for a small subset of the perturbations. When perturbation magnitude increased, the older adults relied more on a stepping strategy for inward directed perturbations and for sagittal plane perturbations with onset just before heelstrike. Tibialis anterior activity increased less in the older compared to the young subjects. In simulation, we showed that reactive tibialis anterior controls the movement of the center of pressure in the foot and therefore contributes to a lateral ankle strategy. Hence, the reduced reactive tibialis anterior activity is related to the shift from ankle towards stepping strategies in the elderly. In contrast to our hypothesis, reactive activity of the gluteus medius was not different between the young and older adults. Hence, this finding suggests that current rehabilitation targets for fall prevention in elderly should especially target ankle muscles. In

addition, our results suggests that gait perturbation paradigms for training of reactive recovery responses might benefit from a focus on both sagittal and frontal plane perturbations.

General discussion and conclusions

A blended experimental and simulation approach contributes to innovative insights in the neuromechanics of balance control

In experimental studies on reactive balance control, age-related changes in muscle strength, reaction times, and sensory acuity are often correlated with measurements of kinematics and derived stability measures. These correlations are used to identify the changes in sensorimotor function that limit the ability to control balance in the elderly [9, 20, 45, 46]. However, this method provides only limited insights in the underlying mechanisms, especially when the different age-related changes are interdependent. For example, age-related decrease in muscle strength and decrease in number of motor units are both directly related to motor noise, which makes it hard to evaluate whether strength or noise, or a combination of both, contributes most to balance control deficits in the elderly [117]. In addition, the age-related changes in muscle and sensory function occur simultaneously and are therefore hard to control individually in experiments with humans. This complicates the identification of causal relations between aging and balance control. Hence, evaluation of the isolated contribution of the different interdependent age-related changes on balance control is needed to define specific therapeutic targets.

In this PhD, we showed that a blended simulation and experimental approach can be used to untangle the contribution of interdependent age-related changes in the musculoskeletal and sensory systems to altered control of balance (Figure 8.1). In the simulation framework developed in this PhD, a simplified version of the musculoskeletal system, sensory system and control system was described mathematically (Figure 2.1). Hence, when evaluating these equations in a forward simulation, there is a direct relation between the properties of the different subsystems and the simulated reactive muscle activity/ joint torque and kinematic strategies for balance control. When combined with experimental data, this simulation framework allows evaluating if predictive simulations with isolated changes in sensory and muscle function result in a similar kinematic pattern as observed in the experiments. More specifically, in study 3 we showed in simulation that the addition of sensory noise resulted in a similar hip strategy as observed in the elderly in response to a backward surface translation during standing, whereas limitations on muscle strength did not. Hence, the main advantage of this method is that the different age-related changes can be controlled individually in simulation.

Similarly, it is hard to untangle the contribution of individual muscles to altered control of balance since muscles respond simultaneously to a perturbation. However, insight in the relative importance of different muscles to control of balance would be useful to identify the most important muscles for fall prevention training [17, 20, 22, 32]. In addition, the perturbation force also influences the observed kinematics, which further complicates the identification of the contribution of a single muscle to the kinematics of balance control. Therefore, the

blended experimental and simulation approach was also used in study 2 and 4 to evaluate to which extent observed reactive activity of a single muscle can explain the observed kinematic strategy (study 2-4). More specifically, we evaluated if changes in reactive gluteus medius and tibialis anterior activity could explain the observed kinematic strategies in young and older subject in response to medio-lateral perturbations. We found that both stance and swing leg gluteus medius activity controls outward foot placement and tibialis anterior activity controls the position of the center of pressure in the foot.

Despite the clear advantage of this blended experimental and simulation approach, this method only allows testing if specific age-related changes (i.e. sensory noise and muscle weakness) can explain the observed kinematics and reactive muscle activity. We cannot exclude that age-related changes that where not modelled (e.g. increased reaction time) could produce similar results. In addition, the simulation approach is sensitive to modelling assumptions and therefore depends on the validity of the model. These limitations are discussed in more detail below.

Evaluating the musculoskeletal mechanics and neural control as an integrated neuromechanical system provides innovative insights in balance control

Human movement, and in particular balance control during standing and walking, emerges from the interaction between neural control actions and the mechanical structure of the musculoskeletal system. The complexity of both the neural and musculoskeletal systems makes it hard to study the interaction between both systems. Biomechanical studies typically analyze human movement using inverse simulation techniques that account for the highly non-linear and complex dynamics of the musculoskeletal system, but only reconstruct the measured movement [68]. Therefore, limited insight in the neural control of the musculoskeletal system is provided. The neural control and resulting muscle activity that underlies human movement is typically analyzed in motor control studies. As such multiple spinal and supra-spinal feedback and feed-forward control mechanisms have been identified, but these often neglect the complexity of the musculoskeletal system. Therefore, the contribution of passive dynamics to human movement and the influence of musculoskeletal dynamics on feedback control is often neglected. Using a neuromechanics approach, human movement is analyzed as the combined action of both the neural and musculoskeletal system. The results of this PhD thesis suggest that (simplified) neuromechanical models, that combine principles on the neural control of movement and biomechanics, can provide new insights in the control of movement and balance control.

In standing balance control, a simplified neuromechanical model was used to analyze the influence of task-level goals (study 1), sensory function (study 2) and muscle function (study 2) on the kinematic strategies for standing balance control. Using this method, we showed that both neural and mechanical constraints influence balance control. However, when ap-

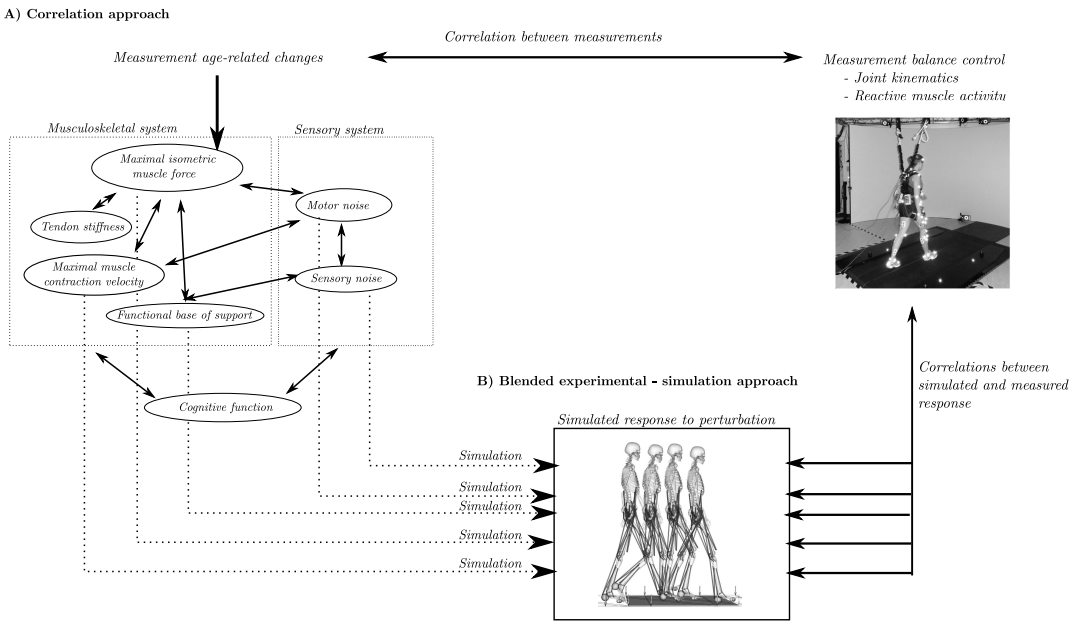

Figure 8.1: **Comparison between the correlation-based and blended experimental and simulation-based approaches to identify the influence of age-related changes in the musculoskeletal and sensory system on balance control.** In the correlation-based approach (a), individual measurements of age-related changes in the musculoskeletal and sensory systems are correlated with age-related changes in joint kinematics and reactive muscle activity in response to a perturbation. Since, the different age-related changes are interrelated, it is hard to evaluate the isolated contribution of the different age-related changes to balance control. In the blended experimental and simulation approach, used in this thesis, each age-related change can be introduced in the neuromechanical model separately and the resulting effect at the level of kinematics can be predicted in simulation. Comparison between the predicted and measured response allows evaluating which age-related changes can explain the measured responses best. Hence, using this approach, the isolated effect of the different age-related changes on balance control kinematics can be identified, thereby decoupling the effect of the interdependent age-related changes. However, note that the conclusions derived from the blended experimental and simulation approach are sensitive to modelling assumptions

plied to aging, we showed that only age-related changes in task-level goals and changes in sensory noise could predict the age-related shift from ankle toward hip strategy. We had to decrease the maximal joint torques and rate of joint torques (i.e. musculoskeletal constraints) far below the values measured in the elderly before a shift from ankle to hip strategy was predicted. Hence, by integrating the musculoskeletal and sensory system into a feedback-controlled torque-driven double inverted pendulum, we could evaluate the influence of both neural and musculoskeletal constraints on balance control and provided an explanation for the age-related shift in kinematic strategy. Note that a very simplified neuromechanical model, without muscle dynamics, sensory integration and state estimation, was used to simulate standing balance control. The insights gained are however only valid within the modelled complexity of the neuromechanical model. The inclusion of sensory integration and state estimation in the neuromechanical model might reduce the sensitivity to noise, thereby making it more robust to sensory noise.

In walking balance control, we showed that measurements of muscle activity (i. e. EMG) in combination with detailed models of the musculoskeletal system provided additional insight in balance control during walking. Our results suggest that reactive gluteus medius activity during walking is modulated by the nervous system to account for the changes in the effect of reactive muscle activity on the mechanics of balance control during the gait cycle. More specially, we showed that the relation between reactive muscle activity and the skeletal dynamics changes during a gait cycle due to changes in body and ground contact configuration, and muscle configuration (i.e. muscle tendon length, velocity and moments arms). As a result, the muscle's potential to control balance varies during the gait cycle. Furthermore, we showed that the influence of the medio-lateral platform translation on the inter-foot distance (i.e. inter-limb collision) and the movement of the center of mass with respect to the base of support changes during the gait cycle. The combined effect of changes in the muscle potential to control balance and the changes in mechanical demands imposed by the perturbation suggests that modulation of reactive muscle activity is needed to control balance. Hence, our results suggest that the changes in the musculoskeletal system during a gait cycle are represented in the nervous system (i.e. internal model) resulting in an efficient control of reactive gluteus medius activity.

In contrast to the simulations of standing balance control, we were not able to model feedback mechanisms for walking balance control but used measured reactive muscle activity to drive the musculoskeletal model. This is mainly related to the additional challenge that walking is the result of both feedback and feedforward control, whereas control of perturbed standing is mainly the result of feedback and therefore simpler to model [12,14,15]. A recently published paper on a neuromechanical model of perturbed walking with feedback control seems to be promising, since it is able to reconstruct joint kinematics in response to various perturbations during walking [63,118]. Detailed neuromechanical models that account for both feedforward and feedback control mechanisms are needed to evaluate if reduced reactive tibialis anterior activity and increased occurrence of stepping strategy in the elderly, observed in study 4, can be related to changes in muscle or sensory function.

Older adults select a more robust strategy to control balance during standing and walking

In perturbed standing and walking, elderly shifted for lower perturbation magnitudes towards a strategy with an increased ability to compensate for internal and external perturbations, hence more robust against perturbations. In standing balance control, elderly shifted for lower perturbation magnitudes from an ankle towards a hip strategy than the young subjects (study 3). The hip strategy is more robust against perturbations, since (1) all subjects shifted from an ankle towards a hip strategy when perturbations were more challenging, (2) hip strategies were predicted when minimizing instability and are less sensitive to noise and to changes in feedback gains (study 1 and 3). In balance control during walking, the older adults relied more on a stepping strategy compared to the young subjects for a subset of the perturbations (study 4). The stepping strategy is more robust against perturbations compared to the lateral ankle strategy as the potential COP excursion is larger in a stepping strategy compared to a lateral ankle strategy where it is constrained by the borders of the foot.

The shift in strategy in both standing and walking might relate to constraints in the musculoskeletal system such as the decreased muscle strength and decreased functional base of support in the elderly. However, in standing balance control, we showed that ankle strategy is still feasible when constraining the joint torques and rate of joint torques based on the values measured in the elderly (study 2). Since we were not able to execute predictive simulations of perturbed walking, we could not evaluate whether limitations in strength cause a decrease in reactive tibialis anterior activity and increased use of stepping strategy in perturbed walking. Nevertheless, our results suggest that, at least in standing balance control, musculoskeletal constraints in isolation cannot explain the age-related shift in strategy.

The shift in strategy in both standing and walking could be related to altered sensory function. In standing balance control, we showed in simulation that sensory noise can explain the observed shift from an ankle towards hip strategy (study 2). In walking balance control, it remains unknown if the increased use of a stepping strategy can be explained by altered sensory function. Similarly as in standing balance control, increased sensory noise might predispose elderly to select a more robust automatic response that is less sensitive to the noise in the feedback system [48, 49]. In standing balance control, we found that the optimal feedback gains resulted in a more stable hip strategy when sensory noise was added to the predictive simulation (Figure 11.10. This is consistent with reaching tasks in an unstable force field where studies showed that endpoint stiffness of the arm increased when the environmental instability increased, resulting in a more stable reaching movement (i.e. less sensitive to perturbations) [8]. These findings suggest that a similar strategy might be used during perturbed walking in the older adults. They might select automatic feedback gains that are more robust against sensory noise and perturbations, resulting in a more stable kinematic strategy. Besides increased sensory noise, the shift towards a more robust strategy in the elderly might also be related to an increase in time delay between the perturbation onset and reactive muscle activity. Van den Bogert et al. showed that the response time is a

critical factor in balance control, since instability of the musculoskeletal system increases over time after perturbation due to the action of gravity [119]. Therefore, increased response time might explain the need for a more robust strategy in the elderly. Decreased sensory acuity, increased neural transmission delay due to loss of myelination, and age-related decrease in cognitive resources might delay the selection of an appropriate response [9, 59].

Therapeutic approaches aiming at fall prevention might benefit from an increased focus on sensory function, in addition to strength training

The results of study 3 suggest that strength training alone might be insufficient to prevent falls in the elderly. Alternative fall prevention strategies, such as proprioceptive training or the use of sensory cues in the environment, should be explored. We believe that an increased focus on sensory function in addition to strength training might improve fall prevention training.

In contrast to this statement, several studies showed that strength training is an effective training modality to reduce fall risk in the elderly based on randomized controlled trials (review: [120, 121]). Strength training increases maximal muscle forces and therefore contributes to balance control when high forces are required [21]. However, some studies suggested that strength training alone is not specific enough to induce change in neuromuscular capacity to control balance and to prevent falls [122]. Nowadays, training protocols that focus on whole body movement and the control of balance in particular are being developed and tested [121]. A recent study showed that balance training restored vestibular orientation in the elderly [123]. Since it is highly unlikely that this can be attributed to structural changes in the vestibular system, it is assumed that balance training improves the state estimation and therefore decreases the influence of sensory noise [123]. Similarly, perturbation-based training was shown to be effective in promoting balance recovery mechanisms [124]. In addition, a recent review of randomized control trials for balance training showed that perturbation-based training that challenges balance control, have a larger effect on fall prevention than strength training alone [121]. Hence, these studies are consistent with our finding that sensory noise influences balance control in the elderly and indicate that the inclusion of exercises that potentially improves state estimation might be of added value to strength training for fall prevention.

Besides the potential improvement in state estimation, perturbation training could be used to guide the elderly to select automatic balance control strategies that are more robust against perturbations. Given the influence of increased internal noise in the elderly on balance control, it might be counter-productive to train older adults to switch towards the more efficient, but less robust, ankle strategy as used by the young subjects. Perturbation training could benefit fall prevention by learning the elderly to select feedback gains in the automatic response that are more robust against external perturbations and internal noise. Our results indicate that the healthy elderly automatically switched towards more robust kinematic strategies.

Limitations

This thesis contributes to a better understanding of the influence of aging on the control of balance during standing and walking. However, the findings should be interpreted in the context of some specific limitations.

Limitations related to the experimental protocol

The older adults that were recruited were relatively young, without a history of falling and without major injuries in the last six months. Therefore, we did not recruit frail elderly that are most at risk for falling [1]. In addition, the sample of older adults is relatively small and may be biased by the fact that they volunteered to participate in a perturbation study, which makes it less likely that they have fear of falling. Perturbation experiments of walking and standing in a group of elderly with a history of falling are needed to evaluate if the conclusions from this thesis can be extrapolated to the incidence of falling in the elderly. The studies on standing balance control (study 3) and walking balance control (study 4) need to be repeated in frail elderly with a history of falling to evaluate if sensory noise, and not muscle weakness, still explains observed changes in standing balance control and if changes in walking balance control are still mainly related to altered tibialis anterior and not gluteus medius activity.

In the study on perturbed walking, the muscle activity measured with surface EMG was limited to a small set of superficial muscles. Additional information on the activity of the peroneus muscle, which contributes to the lateral ankle strategy [32], could provide additional insight in the effect of aging on balance control in perturbed walking.

We could not test experimentally if differences in muscle and sensory function between the subjects and between the young and older cohorts were correlated with changes in perturbed standing and walking kinematics as we did not use a standardized test to evaluate muscle and sensory function. Muscle strength could be measured with maximal voluntary isometric torque [125], motor noise could be measured with force matching tasks [117], and proprioception and sensory noise could be measured with (dynamic) position sense tasks [49]. Correlations between sensorimotor function and stability-related outcome measures of the perturbation experiment could have had additional value in evaluating the validity of the simulation results presented in study 3.

Currently, it remains unclear if the observation that sensory noise, and not muscle weakness, explains the differences in balance control between the young and older adults still holds when the perturbation causes a fall. Additional experiments with increased perturbation magnitudes or different types of perturbations are needed to evaluate if increased sensory noise also has a role in increased fall risk or if it only explains the shift in balance control strategy. Nevertheless, the perturbation magnitudes used in this study were sufficient to trigger a wide range of balance recovery responses in perturbed standing and walking and

were therefore adequate to tests if aging influences the control of balance.

Besides changes in the musculoskeletal and sensory system, reduced cognitive function might also explain to some extent the observed changes in balance control in the elderly compared to the young subjects. Reduced cognitive function in the elderly was related to a reduced ability to react promptly to a perturbation, which is important in balance control [119]. A recent study showed that reaction time during walking increased in the elderly when a stepping task involved decision making [62]. The reactive muscle activity to a perturbation is not a local reflex, but is assumed to be a long latency reflex which is modulated by supra-spinal structures, and may therefore be affected by constraints in cognitive function [14]. In addition, it was suggested that the increase in internal noise in the elderly results in an increased need for attention resources for state estimation (i.e. processing sensory information). Older adults might therefore rely less on automatic and more on cognitive processing of sensory information [59]. Quantification of the reaction time (i.e. time between perturbation onset and onset of reactive muscle activity) might provide insights into the role of increased reliance on cognitive processing and its role in balance control in the elderly. Unfortunately, due to the high variability in background muscle activity during unperturbed walking, we were not able to compute the reaction time in study 3 and 4. The addition of standardized tests to quantify reaction time and cognitive function could be used to model age-related changes in reaction time and cognitive function, and to evaluate their influence on balance control.

Limitations related to simulations of perturbed standing

The results from the simulations of perturbed standing might be influenced by limitations in the neuromechanical model. Both the neural control and musculoskeletal system were strongly simplified by modelling it as a torque-driven double inverted pendulum model with full state feedback. The effect of muscle dynamics, neural time delay, sensory integration and state estimation were therefore neglected in the simulation. Aspects of muscle dynamics, more specifically muscle force-length and, force-velocity relation, tendon stiffness and short-range stiffness, provide resistance to the perturbation and will therefore inherently increase stability [72, 92, 98]. Including sensory integration and state estimation will decrease the influence of sensory noise on the sensory systems and the resulting motor command, and therefore decrease the influence of sensory noise on the control of balance. Furthermore, the current model cannot differentiate between sensory noise from the visual, vestibular and somatosensory systems. In addition, other studies showed that center of mass acceleration feedback can reconstruct reactive muscle activity in response to a perturbation [58, 76]. More specifically in study 1, the results that feedback from center of mass kinematics is insufficient to reconstruct hip strategies might be induced by neglecting the muscle dynamics, neural time delay and center of mass acceleration feedback. In addition, in study 3, the level of sensory noise in the elderly was unknown and the predicted levels of noise that caused a shift from ankle towards hip strategy might be higher when sensory integration and state-esimation was modelled.

We showed that the relative importance of minimizing postural instability versus effort can explain the continuum of ankle and hip strategies observed during perturbed standing. Other task goals may produce similar results and we can therefore not exclude that the subjects used different task-level goals during balance control.

We showed that increased sensory noise and not muscle weakness can explain the shift in postural response observed in the elderly, but we did not investigate other contributing factors (study 2). Other factors that were not tested, are an increase in neural delay [60] and signal-dependent motor noise [109]. In addition, we evaluated the similarity between the predicted postural response in terms of joint kinematics. Given the muscle redundancy, multiple muscle activation and therefore changes in feedback system could generate the same kinematic response to the perturbation. Hence, the comparison between the predicted and simulated postural response in terms of reactive muscle activity instead of joint kinematics might provide additional insights in the validity of the model to predict the response to increased sensory noise.

Limitations related to simulations of perturbed walking

Due to the complex musculoskeletal dynamics and the limited modelling of neural control in neuromechanical models of walking, we were not able to simulate the influence of sensory noise and muscle weakness on balance control during perturbed walking. Predictive simulations of perturbed walking are computationally expensive and result in motions that reconstruct only the basic patterns of joint kinematics and muscle activity observed during normal walking [126]. Nevertheless, a recently published paper on a neuromechanical model of perturbed walking with feedback control seems to be promising, since it was able to reconstruct joint kinematics in response various perturbations during walking [118].

We found that the reactive gluteus medius activity needs to be varied (i.e. modulated) by the nervous system to cope with changes in muscle function during the gait cycle. However, the underlying neural mechanisms that cause changes in reactive tibialis anterior and gluteus medius activity during the gait cycle remain unknown. Hof et al. assumed feedback and discussed the changes in reactive gluteus medius activity as gain modulation. However, the changes in reactive muscle activity can be the result of (1) constant feedback gains but varying states that are input to the feedback loop or (2) gain modulation by the nervous system. We can therefore not conclude that the changes in reactive muscle activity during the gait cycle result from gain modulation.

Future work

Increase detail in the neuromechanical models

An increase in the level of detail of the musculoskeletal dynamics and neural control of movement is needed to develop more representative predictive models that allow to represent all the different age-related changes in the musculoskeletal system, sensory system, sensory integration and cognitive processing and to study their effect on human movement.

Since cognitive function is a risk factor for falls, the implementation of cognitive processing and how it is affected by aging might be needed to predict the influence of aging on balance control. Quantification of the reaction time in dual-task paradigms [59] and experiments on adjustment of movement in tasks that involve decision making [127] could be used to create models that incorporate a neural time delay that depends on the cognitive load of a task. The age-related changes in cognitive function might then be (partially) modelled by an increased time-delay for a given cognitive load.

Modelling of the sensory integration and state estimation of the internal model is needed to gain more insight in the effect of aging of the different sensory systems on balance control. In this work, general noise on the integrated sensory signal was modelled, which limits our insight in the relative contribution of the age-related noise in the visual, vestibular and somatosensory system. We believe that a comprehensive model that describes the interaction between the different sensory systems is needed to advance our insights into the influence of aging of the sensory system on balance control [10]. The integration of sensory information and state estimation of the internal model could be modelled with a Kalman filter [8,109]. The Kalman filter describes the state estimation based on the internal model and accounts for integration of noisy sensory information. Therefore, this can provide additional insights in the influence of aging on sensory reweighting. Simultaneous measurements of the influence of aging on visual, vestibular and somatosensory function and balance control are needed to validate such a comprehensive model.

Predictive simulation of perturbed walking

The implementation of sensorimotor noise and feedback control in predictive simulations of walking is needed to evaluate the effects of age-related alterations in muscle and sensory function on balance control during walking. Computational problems in the incorporation of the complex musculoskeletal dynamics of walking into stochastic optimal control limits simulations of walking to noise-free systems. In addition, feedback control is not incorporated in the predictive simulations of walking, except for the models of Geyer et al. [63, 118]. In future work, similar perturbation protocols as the one used in study 3 and 4 might be used to generate rich datasets for identification of the feedback control mechanisms in walking. For example, one could test if the reactive gluteus medius activity observed in study 3 can be

reconstructed with center of mass position, velocity and acceleration feedback, similar as in standing balance control [58].

Another factor that limits the use of predictive simulations of walking is the computation time. Predictive simulations of gait are computationally expensive [126], which makes it time consuming to develop the neuromechanical models and identify the age-related changes in muscle and sensory function that affect balance control most in a sensitivity analysis. Efficient computational tools, such as neural networks for surrogate modelling of muscle geometry and automatic differentiation for analytical computation of the derivatives are currently being developed and applied to predictive simulations of human movement [128]. Furthermore, modelling of the neural constraints by muscle synergies and feedback control might reduce the size of the optimal control problem [16].

Sensory noise in the elderly

Additional experimental studies are needed to evaluate if increased sensory noise not only explains but also causes the increased occurrence of hip strategies in the elderly. Therefore, measurements of sensory noise in the elderly, such as tests to evaluate the sense of position and velocity of the joints during movement (i.e. dynamic position sense [49]), should be incorporated in the neuromechanical model to evaluate the influence of sensory noise. Subject specific levels of sensorimotor noise, based on standardized measurements, could be included into the neuromechanical model. In addition, the predictive validity of the neuromechanical model to simulate reactive muscle activity and balance control kinematics in experiments where sensory noise is imposed should be tested. Potential perturbations paradigms to evaluate the isolated effect of sensory noise on balance control are sudden changes in the visual field in a virtual reality environment, muscle vibration or galvanic stimulation. The measured response to the backward support surface translation could be measured with and without the additional noise to evaluate if a similar shift from ankle towards hip strategy is observed.

Is it possible to desensitize the elderly to sensory noise?

The positive effect of perturbation and balance training on balance control, without dedicated strength training, suggests that the age-related neural deficits can be improved by training [121]. This in combination with our result that internal noise may explain the changes in control of balance in the elderly suggests that an improved state estimation and the selection of feedback gains (i.e. strategy) that are robust to noise might explain the effectiveness of perturbation training. Additional research on the mechanisms that result in improved balance control following perturbation training is needed. Randomized control trials could be used to gain insight in the extent to which extent state estimation improves during a perturbation training period and if these measures relate to a change in balance control.

Assistance of balance control

Current neuromechanical models for balance control in combination with datasets on perturbed standing and walking can be used in the development of biomimetic controllers for assistive devices such as exoskeletons. Several studies suggested that the use of exoskeletons is currently limited by the lack of knowledge on human-robot interaction [129,130]. Exoskeleton assistance of balance control is mainly based on robotic strategies that do not take into account the balance control strategies used by the human. Hence, this control forces the operator in a trajectory and therefore potentially resists instead of assists human movement. In collaboration with the robotics group at KU Leuven, I designed a bio-inspired controlled for a lower limb exoskeleton to assist standing balance based on the feedback gains identified in study 1 and 3. We will evaluate whether the assistive torques, generated by the bio-inspired controller are in better agreement with the human joint kinetics compared to popular robot controllers. In the future, similar feedback mechanisms might be identified in perturbed walking using the dataset study 2 and 4 to develop bio-inspired controllers for (exoskeleton) assistance of balance during walking.

Chapter 9

Dankwoord

Bedankt !

Na een fantastische periode als doctoraatsstudent is het zover. Met het schrijven van mijn dankwoord rond ik mijn thesis af. Veel mensen hebben me de afgelopen jaren geholpen, gemotiveerd en geïnspireerd. Daarom heb ik geprobeerd om enkele woorden van dank op papier te zetten.

Ik zal beginnen met FWO en bijgevolg de belastingbetaler. Bedankt om mijn onderzoek te ondersteunen. Ik hoop dat mijn doctoraat niet enkel een leuke oefening was, maar dat het ook een stapje voorwaarts is in de richting meer kennis. Ook een woord van dank voor alle proefpersonen in Leuven en Cardiff om vrijwillig deel te nemen aan mijn experimenten.

Maar natuurlijk wil ik vooral de mensen bedanken die me persoonlijk hebben geholpen. Dankzij de vele collega's was er altijd wel iets te beleven in en rond gebouw de Nayer. Collega's van de Ugent, jullie lessen en begeleiding tijdens mijn masterthesis en het uitwisselen van papers heeft mijn interesse in biomechanica aangewakkerd. Zonder jullie was ik nooit aan mijn doctoraat in Leuven begonnen. Ook bedankt voor de ondersteuning tussen het afronden van mijn master thesis en het begin van mijn doctoraat. Collega's van het MIRAD project, bedankt om altijd de tijd te nemen tijdens de vergaderingen om dingen uit te leggen. Dit was heel waardevol, zeker in het begin van mijn doctoraat, en heb ik altijd enorm gewaardeerd. Collega's van de onderzoeksgroep, het was een plezier om samen met jullie papers te bespreken, papers te schrijven, nieuwe simulatie-tools te coderen, op conferenties en summerschools te gaan en ga zo maar door. Maar zonder de gezamenlijke sportactiviteiten was mijn doctoraat nooit zo snel voorbij gevlogen. Wat begon met enkele keren te gaan lopen met Sam liep snel uit de hand en resulteerde in trialton, trail-running, mtb'en, tennis, zwemmen, ping-pong en ga zo maar door. Het was een plezier om samen met jullie deze intellectuele en fysieke uitdagingen aan te gaan.

Familie en andere vrienden mogen natuurlijk ook niet ontbreken in mijn dankwoord. Weekendjes, avonden op café en sportactiviteiten met jullie hebben altijd voor de nodige ontspanning gezorgd. Maar ook bedankt voor de inhoudelijke hulp. Opa en Oma voor het nalezen van mijn Nederlandse samenvatting. Adriaan voor het maken van de schitterende tekening op mijn kaft. Mijn voetballer-fietsvrienden voor de discussies tijdens de langere trainingen.

Mijn tactiek om zo weinig mogelijk namen neer te schrijven (want dan kan je niemand vergeten) moet ik stilaan laten varen. Er zijn enkele mensen die ik persoonlijk moet bedanken.

Als eerste wil ik mijn juryleden en voorzitter bedanken. Filip, Benedicte, Sabine, Jean-Jacques en Lena voor het nalezen en verbeteren van mijn doctoraat. Jullie constructieve feedback op de verschillende evaluatiemomenten tijdens mijn doctoraat heeft me zeker vooruitgeholpen. Thank you Prof. Lena Ting for you critical review of my thesis and all your research on neuromechanics of balance control. Your work inspires me and it is an honour to receive your feedback and comments.

Daarnaast wil ik natuurlijk mijn (co-)promotoren Ilse, Friedl en Joris persoonlijk bedanken

voor de vlotte samenwerking. Jullie hebben me altijd geïnspireerd en gemotiveerd zonder de druk van deadlines. Ilse, eerst en vooral bedankt om in me te geloven, mij aan te nemen op het MIRAD project en mij te ondersteunen bij projectaanvragen. Zonder deze steun was er in elk geval geen doctoraat geweest. Daarnaast wil ik je vooral bedanken om me wegwijs te maken in de biomechanica-simulatie wereld en voor jouw hulp bij het schrijven van papers. Herinner je nog de draft van mijn eerste paper? Dan weet je ook dat ik veel van je heb geleerd. Friedl, bedankt voor de vele inhoudelijke discussies op journal clubs, conferenties en optimalisatie meetings. Zonder jouw ideeën had dit doctoraat er helemaal anders uitgezien. Daarnaast vooral bedankt om altijd geduldig de tijd te nemen om mij de complexere simulatie en optimalisatie technieken uit te leggen. Dit heb ik altijd heb gemist in mijn opleiding als bewegingswetenschapper. Bedankt om me niet op mijn honger te laten zitten en veel succes met het opleiden van andere bewegingswetenschappers. Robert, officieel ben je dan wel geen promotor maar jou wil ik ook zeker bedanken. Bedankt voor het warme ontvangst in Cardiff. Zonder jouw hulp en ervaring was er geen sprake van de studies rond evenwichtscontrole tijdens wandelen. Het was fijn om samen te werken.

Vake, Moeke, Pieter, Jorre, Katrien en Rune. Bedankt voor alle gezellige momenten als familie samen. Jullie geven me de zekerheid die ik nodig heb om ook door te bijten in lastigere momenten. Vake en Moeke, bedankt om me alle kansen te geven in mijn studies, me altijd te steunen en fier te zijn op de dingen die ik doe.

Tenslotte Sofie, bedankt om samen met mij te werken, te genieten en te dromen. Ik kijk al uit naar alle nieuwe uitdagingen die ons te wachten staan.

Chapter 10

Appendices

Appositions

- Large benchmark datasets are needed to validate predictive neuromechanical models, enabling to predict the influence of pathologies and rehabilitation interventions on human movement.
- Applying the open-source concept to both software, datasets and study results can accelerate the field of human movement sciences, especially the context of university research paid by the taxpayer.
- The difference between the capabilities required for a task and the capability of the neuromechanical system is a valuable parameter to evaluate the deficits in activities of daily living in patient populations and can be used in the control of assistive devices.

Bijstellingen

- Er is een nood aan rijke benchmark datasets om voorspellende simulaties met neuromechanische modellen te valideren om zo de invloed van pathologieën en revalidatie-interventies op het menselijke bewegen te voorspellen.
- Het toepassen van het open-source concept op software, datasets en resultaten kan het onderzoek in het menselijke bewegen versnellen, zeker in de context van academisch onderzoek betaald door de belastingbetaler.
- Het verschil tussen de gewrichtsmomenten die nodig zijn voor het uitvoeren van een taak en de maximale gewrichtsmomenten van het neuromechanische systeem is een waardevolle parameter om beperkingen in het uitvoeren van activiteiten van het dagelijkse leven te evalueren en kan gebruikt worden in de controle van ondersteunende apparaten.

Professional career Maarten Afschrift

Maarten received his MSc. degree in human movement sciences at Ghent University, Belgium, 2012. From 2013, he is a PhD researcher at the Department of Movement Sciences, KU Leuven. He worked two years on a multidisciplinary IWT-SBO projects that aimed at assisting human posture and locomotion with a robotic exoskeleton. Since October 2014, he worked as an FWO-aspirant fellow on the topic of this PhD. During his PhD, he gained extensive experience in measurements and dynamic simulations of human locomotion and balance control. He spent several months in the School of Healthcare Sciences at Cardiff University during two research stays to develop an extensive protocol to perturb gait stability.

Maarten taught the practical session on biomechanics in the first year undergraduate students of rehabilitation sciences. He assisted in writing and teaching of a course on scientific programming for the research master in human movement sciences. In addition, Maarten

coached several master students in rehabilitation, movement sciences and biomedical engineering during their master thesis.

Scientific acknowledgments

This research was funded by the IWT-SBO project Mirad (2013-2014) and by an FWO-aspriant fellowship (2014-2018).

Personal contribution

The author of this manuscript was responsible for data collection, data analysis and interpretation, and writing of all chapters included in this PhD thesis.

Conflict of interest

We can confirm that there are no conflicts of interest of any of the authors.

List of publications

Articles in internationally reviewed academic journals

- Afschrift M., Pitto L., Aerts W., van Deursen R., Jonkers I., De Groote F. (2018) Modulation of gluteus medius activity reflects the potential of the muscle to meet the mechanical demands during perturbed walking. Scientific Reports.
- Afschrift M., De Groote F., Verschueren S., Jonkers I. (2018). Increased sensory noise and not muscle weakness explains changes in non-stepping postural responses following stance perturbations in healthy elderly. Gait & Posture, 5, 122-127.
- Afschrift M., Jonkers I., De Schutter J., De Groote F. (2016). Mechanical effort predicts the selection of ankle over hip strategies in non-stepping postural responses. Journal of Neurophysiology, 116 (4), 1937-1945.
- Afschrift M., De Groote F., De Schutter J., Jonkers I. (2014). The effect of muscle weakness on the capability gap during gross motor function: a simulation study supporting design criteria for exoskeletons of the lower limb. Biomedical engineering online, 13, 111.
- Lambrecht S., Harutyunyan A., Tanghe K., Afschrift M., De Schutter J., Jonkers I. (2017). Real-Time Gait Event Detection Based on Kinematic Data Coupled to a Biomechanical Model. Sensors, 17 (4), 671-684.

Articles under review in internationally reviewed academic journals

- Afschrift M., van Deursen R., De Groote F., Jonkers I. (2018) Increased use of stepping strategy in response to medio-lateral perturbations in the elderly relates to altered reactive tibialis anterior and not gluteus medius activity. Gait & Posture.
- Vantilt J., Tanghe K., Afschrift M., Bruijnes A., Junius K., Geeroms J., Aertbeliën E., De Groote F., Lefeber D., Jonkers I., De Schutter J. (2018) Model-based Control for Exoskeletons with Series Elastic Actuators evaluated on Sit-to-stand Movements. Journal of NeuroEngineering and Rehabilitation.

Meeting abstracts presented at scientific conferences

- Afschrift M., Pitto L., Van Deursen R., De Groote F., Jonkers I. (2018). Modulation of hip abductor muscle activity reflects the potential of the muscle to control balance during perturbed walking. Dynamic Walking. Florida, 21-24 May 2018.
- Afschrift M., De Groote F., Jonkers I. (2017). Increased sensory noise explains age-related changes in postural resposnes to perturbations of standing. Neural control of movement. Dublin, 2-5 May.
- Afschrift M., De Groote F., Van Deursen R., Jonkers I. (2017). Gluteus medius activity in the stance leg controls contralateral foot placement in perturbed walking. Congress of the International Society of Biomechanics. Brisbane, Australia, 23-27 July 2017.
- Afschrift M., Jonkers I., De Groote F. (2016). The Influence of age-related changes on non-stepping balance control: a simulation study. Neuromechanics. Heidelberg, 4-6 October 2016.
- Afschrift M., Jonkers I., De Groote F. (2016). Effort minimization predicts ankle over hip strategie. Biomechancis and neural control of movement. Mt. Sterling, 12-17 June.
- Afschrift M., De Groote F., Jonkers I. (2015). A feedback controller to predict the postural control in response to a perturbation. International society of biomechanics. Glasgow, 12-15 July 2015.
- Afschrift M., De Groote F., Verschueren S., Jonkers I. (2014). The influence of weakness on posture control. European scientific society for clinical gait and movement analysis. Rome, 29 September - 4 October.
- Afschrift M., De Groote F., De Schutter J., Jonkers I. (2014). The effect of muscle weakness on the capability gap during gross motor function. World congress of biomechanics. Boston, 6-11 July 2014.
- Afschrift M., De Groote F., De Schutter J., Jonkers I. (2014). Quantifying the assistance that is needed to perform activities of daily living in the presence of muscle weakness. Dynamic walking. Zurrich, 10-13 July 2014.

Bibliography

[1] T. E. Lockhart, "An integrated approach towards identifying age-related mechanisms of slip initiated falls," *International Society of Electrophysiological Kinesiology*, vol. 18, pp. 205–217, apr 2008.

[2] P. Kannus, J. Parkkari, S. Koskinen, S. Niemi, M. Palvanen, M. Järvinen, and I. Vuori, "Fall-induced injuries and deaths among older adults," *Journal of the American Medical Association*, vol. 281, pp. 1895–1899, may 1999.

[3] M. E. Tinetti, M. Speechley, and S. F. Ginter, "Risk Factors for Falls among Elderly Persons Living in the Community," *New England Journal of Medicine*, vol. 319, pp. 1701–1707, dec 1988.

[4] I. Melzer, N. Benjuya, and J. Kaplanski, "Postural stability in the elderly: A comparison between fallers and non-fallers," *Age and Ageing*, vol. 33, no. 6, pp. 602–607, 2004.

[5] F. B. Horak, "Postural orientation and equilibrium: what do we need to know about neural control of balance to prevent falls?," *Age and ageing*, vol. 35 Suppl 2, pp. ii7–ii11, sep 2006.

[6] a. L. Hof, M. G. J. Gazendam, and W. E. Sinke, "The condition for dynamic stability.," *Journal of biomechanics*, vol. 38, pp. 1–8, jan 2005.

[7] J. Pratt, J. Carff, S. Drakunov, and A. Goswami, "Capture point: A step toward humanoid push recovery," in *Proceedings of the 2006 6th IEEE-RAS International Conference on Humanoid Robots, HUMANOIDS*, pp. 200–207, 2006.

[8] D. W. Franklin and D. M. Wolpert, "Computational mechanisms of sensorimotor control," nov 2011.

[9] D. L. Sturnieks, R. St George, and S. R. Lord, "Balance disorders in the elderly," 2008.

[10] R. J. Peterka, "Sensorimotor Integration in Human Postural Control," *The Journal of Neurophysiology*, vol. 88, pp. 1097–1118, sep 2002.

[11] M. Kawato, "Internal models for motor control and trajectory planning," dec 1999.

[12] H. van der Kooij, E. van Asseldonk, and F. C. T. van der Helm, "Comparison of different methods to identify and quantify balance control.," *Journal of neuroscience methods*, vol. 145, pp. 175–203, jun 2005.

[13] S. Park, F. B. Horak, and A. D. Kuo, "Postural feedback responses scale with biomechanical constraints in human standing.," *Experimental brain research*, vol. 154, pp. 417–27, feb 2004.

[14] L. H. Ting, K. W. van Antwerp, J. E. Scrivens, J. L. McKay, T. D. J. Welch, J. T. Bingham, and S. P. DeWeerth, "Neuromechanical tuning of nonlinear postural control dynamics.," *Chaos (Woodbury, N.Y.)*, vol. 19, p. 026111, jun 2009.

[15] A. Kuo, "An optimal control model for analyzing human postural balance.," jan 1995.

[16] E. Burdet, D. W. Franklin, and T. Milner, "Book Review : Human Robotics : Neuromechanics and Motor Control," vol. 7, no. 2, p. 2309729, 2014.

[17] A. L. Hof and J. Duysens, "Responses of human hip abductor muscles to lateral balance perturbations during walking," *Experimental Brain Research*, vol. 230, no. 3, pp. 301–310, 2013.

[18] a. L. Hof, S. M. Vermerris, and W. a. Gjaltema, "Balance responses to lateral perturbations in human treadmill walking.," *The Journal of experimental biology*, vol. 213, pp. 2655–64, aug 2010.

[19] B. L. Rankin, S. K. Buffo, and J. C. Dean, "A neuromechanical strategy for mediolateral foot placement in walking humans.," *Journal of neurophysiology*, vol. 112, pp. 374–83, jul 2014.

[20] M. Fujimoto, W.-L. Hsu, M. H. Woollacott, and L.-S. Chou, "Ankle dorsiflexor strength relates to the ability to restore balance during a backward support surface translation.," *Gait & posture*, vol. 38, pp. 812–7, sep 2013.

[21] M. Pijnappels, M. F. Bobbert, and J. H. Van Dieën, "Push-off reactions in recovery after tripping discriminate young subjects, older non-fallers and older fallers," *Gait and Posture*, vol. 21, pp. 388–394, jun 2005.

[22] H. E. Stokes, J. D. Thompson, and J. R. Franz, "The Neuromuscular Origins of Kinematic Variability during Perturbed Walking," *Scientific Reports*, vol. 7, no. 1, 2017.

[23] N. C. Duclos, L. Maynard, J. Barthelemy, and S. Mesure, "Postural stabilization during bilateral and unilateral vibration of ankle muscles in the sagittal and frontal planes.," *Journal of neuroengineering and rehabilitation*, vol. 11, p. 130, jan 2014.

[24] L.-J. Hsu, P. V. Zelenin, G. N. Orlovsky, and T. G. Deliagina, "Effects of galvanic vestibular stimulation on postural limb reflexes and neurons of spinal postural network.," *Journal of neurophysiology*, vol. 108, pp. 300–13, jul 2012.

[25] G. Nashner, Lewis M. and McCollum, L. M. Nashner, G. McCollum, and G. Nashner, Lewis M. and McCollum, "The organization of human postural movements: A formal basis and experimental synthesis," *Behavioral and Brain Sciences*, vol. 8, no. 01, pp. 135–150, 1985.

[26] F. B. Horak and L. M. Nashner, "Central programming of postural movements: adaptation to altered support-surface configurations.," *J Neurophysiol*, vol. 55, pp. 1369–1381, jun 1986.

[27] A. L. Adkin, J. S. Frank, M. G. Carpenter, and G. W. Peysar, "Postural control is scaled to level of postural threat," *Gait and Posture*, vol. 12, pp. 87–93, 2000.

[28] S. M. Henry, J. Fung, and F. B. Horak, "EMG responses to maintain stance during multidirectional surface translations.," *Journal of neurophysiology*, vol. 80, no. 4, pp. 1939–1950, 1998.

[29] A. Kuo, "Control model of human posture strategy selection," *Proceedings of 17th International Conference of the Engineering in Medicine and Biology Society*, vol. 2, pp. 1223–1224, 1995.

[30] S. M. O'Connor and A. D. Kuo, "Direction-Dependent Control of Balance During Walking and Standing," *Journal of Neurophysiology*, vol. 102, no. 3, pp. 1411–1419, 2009.

[31] H. Reimann, T. D. Fettrow, E. D. Thompson, P. Agada, B. J. McFadyen, and J. J. Jeka, "Complementary mechanisms for upright balance during walking," *PLoS ONE*, vol. 12, no. 2, 2017.

[32] A. L. Hof and J. Duysens, "Responses of human ankle muscles to mediolateral balance perturbations during walking," *Human Movement Science*, vol. 57, pp. 69–82, feb 2018.

[33] K. Karamanidis, A. Arampatzis, and L. Mademli, "Age-related deficit in dynamic stability control after forward falls is affected by muscle strength and tendon stiffness," *Journal of Electromyography and Kinesiology*, vol. 18, pp. 980–989, dec 2008.

[34] E. I. McIntosh, J. L. Zettel, and L. A. Vallis, "Stepping Responses in Young and Older Adults Following a Perturbation to the Support Surface During Gait," *Journal of Motor Behavior*, pp. 1–11, 2016.

[35] D. Martelli, F. Aprigliano, P. Tropea, G. Pasquini, S. Micera, and V. Monaco, "Stability against backward balance loss: age-related modifications following slip-like perturbations of multiple amplitudes," *Gait & Posture*, 2017.

[36] T. J. Doherty, "Invited review: Aging and sarcopenia.," *Journal of applied physiology (Bethesda, Md. : 1985)*, vol. 95, pp. 1717–27, oct 2003.

[37] Y. Aoyagi and R. J. Shephard, "Aging and Muscle Function," dec 1992.

[38] S. V. Brooks and J. A. Faulkner, "Skeletal muscle weakness in old age: underlying mechanisms," *Medicine and Science in Sports and Exercise*, vol. 26, p. 432, apr 1994.

[39] L. Larsson, X. Li, and W. R. Frontera, "Effects of aging on shortening velocity and myosin isoform composition in single human skeletal muscle cells.," *The American journal of physiology*, vol. 272, no. 2 Pt 1, pp. C638—-49, 1997.

[40] L. Stenroth, J. Peltonen, N. J. Cronin, S. Sipila, and T. Finni, "Age-related differences in Achilles tendon properties and triceps surae muscle architecture in vivo," *Journal of Applied Physiology*, vol. 113, pp. 1537–1544, nov 2012.

[41] D. G. Thelen, "Adjustment of Muscle Mechanics Model Parameters to Simulate Dynamic Contractions in Older Adults," *Journal of Biomechanical Engineering*, vol. 125, no. 1, p. 70, 2003.

[42] M. Inacio, A. S. Ryan, W. N. Bair, M. Prettyman, B. A. Beamer, and M. W. Rogers, "Gluteal muscle composition differentiates fallers from non-fallers in community dwelling older adults," *BMC Geriatrics*, vol. 14, p. 37, dec 2014.

[43] C. G. C. Horlings, U. M. Küng, B. G. M. van Engelen, N. C. Voermans, G. J. D. Hengstman, a. J. van der Kooi, B. R. Bloem, and J. H. J. Allum, "Balance control in patients with distal versus proximal muscle weakness.," *Neuroscience*, vol. 164, pp. 1876–86, dec 2009.

[44] C. D. Hall, M. H. Woollacott, and J. L. Jensen, "Age-related changes in rate and magnitude of ankle torque development: implications for balance control.," *The journals of gerontology. Series A, Biological sciences and medical sciences*, vol. 54, pp. M507–M513, oct 1999.

[45] M. Arvin, J. H. Van Dieën, G. S. Faber, M. Pijnappels, M. J. Hoozemans, and S. M. Verschueren, "Hip abductor neuromuscular capacity: A limiting factor in mediolateral balance control in older adults?," *Clinical Biomechanics*, vol. 37, pp. 27–33, aug 2016.

[46] M. Pijnappels, J. C. E. van der Burg, N. D. Reeves, and J. H. van Dieën, "Identification of elderly fallers by muscle strength measures," *European Journal of Applied Physiology*, vol. 102, pp. 585–592, mar 2008.

[47] J. H. Pasma, D. Engelhart, A. C. Schouten, H. van der Kooij, A. B. Maier, and C. G. Meskers, "Impaired standing balance: The clinical need for closing the loop," may 2014.

[48] S. W. Shaffer and A. L. Harrison, "Aging of the Somatosensory System: A Translational Perspective," *Physical Therapy*, vol. 87, no. 2, pp. 193–207, 2007.

[49] S. Verschueren, S. Brumagne, S. Swinnen, and P. Cordo, "The effect of aging on dynamic position sense at the ankle," *Behavioural Brain Research*, vol. 136, no. 2, pp. 593–603, 2002.

[50] T. M. Herter, S. H. Scott, and S. P. Dukelow, "Systematic changes in position sense accompany normal aging across adulthood," *Journal of NeuroEngineering and Rehabilitation*, vol. 11, no. 1, p. 43, 2014.

[51] S. U. Ko, E. Simonsick, N. Deshpande, and L. Ferrucci, "Sex-specific age associations of ankle proprioception test performance in older adults: Results from the Baltimore Longitudinal Study of Aging," *Age and Ageing*, vol. 44, no. 3, pp. 485–490, 2015.

[52] A. M. C. Germano, D. Schmidt, and T. L. Milani, "Effects of hypothermically reduced plantar skin inputs on anticipatory and compensatory balance responses," *BMC Neuroscience*, vol. 17, p. 41, dec 2016.

[53] D. J. Goble, J. P. Coxon, A. Van Impe, M. Geurts, M. Doumas, N. Wenderoth, and S. P. Swinnen, "Brain Activity during Ankle Proprioceptive Stimulation Predicts Balance Performance in Young and Older Adults," *Journal of Neuroscience*, vol. 31, no. 45, pp. 16344–16352, 2011.

[54] F. B. Horak, L. M. Nashner, and H. Diener, "Postural strategies associated with somatosensory and vestibular loss," *Experimental Brain Research*, vol. 82, no. FEBRUARY 1990, pp. 167–177, 1990.

[55] J. B. Dingwell, J. S. Ulbrecht, J. Boch, M. B. Becker, J. T. O'Gorman, and P. R. Cavanagh, "Neuropathic gait shows only trends towards increased variability of sagittal plane kinematics during treadmill locomotion," *Gait and Posture*, vol. 10, no. 1, pp. 21–29, 1999.

[56] D. C. Roden-Reynolds, M. H. Walker, C. R. Wasserman, and J. C. Dean, "Hip proprioceptive feedback influences the control of mediolateral stability during human walking," *Journal of Neurophysiology*, vol. 114, pp. 2220–2229, oct 2015.

[57] P. J. Stapley, L. H. Ting, M. Hulliger, and J. M. Macpherson, "Automatic postural responses are delayed by pyridoxine-induced somatosensory loss.," *The Journal of neuroscience : the official journal of the Society for Neuroscience*, vol. 22, pp. 5803–5807, jul 2002.

[58] D. B. Lockhart and L. H. Ting, "Optimal sensorimotor transformations for balance.," *Nature neuroscience*, vol. 10, pp. 1329–36, oct 2007.

[59] M. P. Boisgontier, I. A. M. Beets, J. Duysens, A. Nieuwboer, R. T. Krampe, and S. P. Swinnen, "Age-related differences in attentional cost associated with postural dual tasks: Increased recruitment of generic cognitive resources in older adults," sep 2013.

[60] M. Pijnappels, M. F. Bobbert, and J. H. Van Dieën, "How early reactions in the support limb contribute to balance recovery after tripping," *Journal of Biomechanics*, vol. 38, pp. 627–634, mar 2005.

[61] A. M. Schillings, "Stumbling Over Obstacles in Older Adults Compared to Young Adults," *Journal of Neurophysiology*, vol. 94, no. 2, pp. 1158–1168, 2005.

[62] A. S. Oliveira, M. S. Reiche, C. I. Vinescu, S. A. H. Thisted, C. Hedberg, M. N. Castro, and M. G. Jørgensen, "The cognitive complexity of concurrent cognitive-motor tasks reveals age-related deficits in motor performance," *Scientific Reports*, vol. 8, p. 6094, dec 2018.

[63] S. Song and H. Geyer, "Predictive neuromechanical simulations indicate why walking performance declines with ageing," *Journal of Physiology*, vol. 596, pp. 1199–1210, apr 2018.

[64] S. Kim, F. B. Horak, P. Carlson-Kuhta, and S. Park, "Postural feedback scaling deficits in Parkinson's disease.," *Journal of neurophysiology*, vol. 102, pp. 2910–20, nov 2009.

[65] S. Kim, C. G. Atkeson, and S. Park, "Perturbation-dependent selection of postural feedback gain and its scaling," *Journal of Biomechanics*, vol. 45, no. 8, pp. 1379–1386, 2012.

[66] R. J. Peterka, K. D. Statler, D. M. Wrisley, and F. B. Horak, "Postural compensation for unilateral vestibular loss," *Frontiers in Neurology*, vol. SEP, p. 57, 2011.

[67] a. D. Kuo and F. E. Zajac, "Human standing posture: multi-joint movement strategies based on biomechanical constraints.," 1993.

[68] S. L. Delp, F. C. Anderson, A. S. Arnold, P. Loan, A. Habib, C. T. John, E. Guendelman, and D. G. Thelen, "OpenSim: open-source software to create and analyze dynamic simulations of movement.," *IEEE transactions on bio-medical engineering*, vol. 54, pp. 1940–50, nov 2007.

[69] F. E. Zajac, "Muscle and tendon: properties, models, scaling and application to biomechanics and motor control," *critical review in biomedical engineering*, vol. 17, no. 4, pp. 359–410, 1989.

[70] M. A. Sherman, A. Seth, and S. L. Delp, "Simbody: Multibody dynamics for biomedical research," in *Procedia IUTAM*, vol. 2, pp. 241–261, 2011.

[71] M. Ackermann and A. J. van den Bogert, "Optimality principles for model-based prediction of human gait.," *Journal of biomechanics*, vol. 43, pp. 1055–60, apr 2010.

[72] F. De Groote, A. L. Kinney, A. V. Rao, and B. J. Fregly, "Evaluation of Direct Collocation Optimal Control Problem Formulations for Solving the Muscle Redundancy Problem," *Annals of Biomedical Engineering*, vol. 44, pp. 2922–2936, oct 2016.

[73] F. C. Anderson and M. G. Pandy, "Static and dynamic optimization solutions for gait are practically equivalent.," *Journal of biomechanics*, vol. 34, pp. 153–61, feb 2001.

[74] F. De Groote, T. De Laet, I. Jonkers, and J. De Schutter, "Kalman smoothing improves the estimation of joint kinematics and kinetics in marker-based human gait analysis.," *Journal of biomechanics*, vol. 41, pp. 3390–8, dec 2008.

[75] B. R. Umberger, "Stance and swing phase costs in human walking," *Journal of The Royal Society Interface*, vol. 7, no. 50, pp. 1329–1340, 2010.

[76] T. D. J. Welch and L. H. Ting, "A Feedback Model Reproduces Muscle Activity During Human Postural Responses to Support-Surface Translations," *J Neurophysiol*, vol. 99, pp. 1032–1038, 2007.

[77] C. S. Versteeg, L. H. Ting, and J. L. Allen, "Hip and ankle responses for reactive balance emerge from varying priorities to reduce effort and kinematic excursion: A simulation study," *Journal of Biomechanics*, vol. 49, no. 14, pp. 3230–3237, 2016.

[78] L. H. Ting, S. A. Chvatal, S. A. Safavynia, and J. Lucas Mckay, "Review and perspective: Neuromechanical considerations for predicting muscle activation patterns for movement," 2012.

[79] M. King, J. Judge, and L. Wolfson, "Functional base of support decreases with age," *Journal of gerontology*, vol. 49, no. 6, pp. 258–63, 1994.

[80] A. J. Van Den Bogert, D. Blana, and D. Heinrich, "Implicit methods for efficient musculoskeletal simulation and optimal control," in *Procedia IUTAM*, vol. 2, pp. 297–316, Elsevier Masson SAS, 2011.

[81] A. Wächter and L. T. Biegler, "On the implementation of an interior-point filter line-search algorithm for large-scale nonlinear programming," *Mathematical Programming*, vol. 106, pp. 25–57, mar 2006.

[82] A. V. Rao, D. a. Benson, C. Darby, M. a. Patterson, C. Francolin, I. Sanders, and G. T. Huntington, "GPOPS II: A MATLAB Software for Solving Multiple-Phase Optimal Control Problems Using hp–Adaptive Gaussian Quadrature Collocation Methods and Sparse Nonlinear Programming," *ACM Transactions on Mathematical Software*, vol. 37, no. 2, pp. 1–39, 2010.

[83] M. A. Patterson, M. J. Weinstein, and A. V. Rao, "An efficient overloaded method for computing derivatives of mathematical functions in MATLAB," *ACM Transactions on Mathematical Software*, vol. 39, pp. 17:1–17:36, apr 2013.

[84] C. F. Runge, C. L. Shupert, F. B. Horak, and F. E. Zajac, "Ankle and hip postural strategies defined by joint torques.," *Gait & posture*, vol. 10, pp. 161–70, oct 1999.

[85] a. V. Alexandrov, a. a. Frolov, and J. Massion, "Biomechanical analysis of movement strategies in human forward trunk bending. I. Modeling.," *Biological cybernetics*, vol. 84, no. 6, pp. 425–434, 2001.

[86] T. D. J. Welch and L. H. Ting, "Mechanisms of Motor Adaptation in Reactive Balance Control," *PLoS ONE*, vol. 9, no. 5, p. e96440, 2014.

[87] C. Assaiante and B. Amblard, "An ontogenetic model for the sensorimotor organization of balance control in humans," *Human movement science*, vol. 9457, no. 94, pp. 13–43, 1995.

[88] J. L. McKay and L. H. Ting, "Optimization of muscle activity for task-level goals predicts complex changes in limb forces across biomechanical contexts.," *PLoS computational biology*, vol. 8, jan 2012.

[89] R. B. Davis Iii, S. Õunpuu, D. Tyburski, and J. R. Gage, "A gait analysis data collection and reduction technique," 1991.

[90] S. L. Delp, J. P. Loan, M. G. Hoy, F. E. Zajac, E. L. Topp, J. M. Rosen, and A. N. D. J. M. Rosen, "An interactive graphics-based model of the lower extremity to study orthopaedic surgical procedures.," *IEEE transactions on bio-medical engineering*, vol. 37, no. 8, pp. 757–67, 1990.

[91] T. D. J. Welch and L. H. Ting, "A feedback model explains the differential scaling of human postural responses to perturbation acceleration and velocity.," *Journal of neurophysiology*, vol. 101, no. 6, pp. 3294–309, 2009.

[92] C. T. John, F. C. Anderson, J. S. Higginson, and S. L. Delp, "Stabilisation of walking by intrinsic muscle properties revealed in a three-dimensional muscle-driven simulation.," *Computer methods in biomechanics and biomedical engineering*, vol. 16, pp. 451–62, apr 2013.

[93] B. I. Prilutsky, "Coordination of two- and one-joint muscles: functional consequences and implications for motor control.," *Motor control*, vol. 4, no. 1, pp. 1–44, 2000.

[94] L. H. Ting and J. L. McKay, "Neuromechanics of muscle synergies for posture and movement.," *Current opinion in neurobiology*, vol. 17, pp. 622–8, dec 2007.

[95] A. D. Kuo and F. E. Zajac, "A biomechanical analysis of muscle strength as a limiting factor in standing posture," *Journal of Biomechanics*, vol. 26, pp. 137–150, 1993.

[96] W. L. Hsu, L. S. Chou, and M. Woollacott, "Age-related changes in joint coordination during balance recovery," *Age*, vol. 35, no. 4, pp. 1299–1309, 2013.

[97] I. D. Loram, C. N. Maganaris, and M. Lakie, "The passive, human calf muscles in relation to standing: The short range stiffness lies in the contractile component," *Journal of Physiology*, vol. 584, no. 2, pp. 677–692, 2007.

[98] L. Cui, E. J. Perreault, H. Maas, and T. G. Sandercock, "Modeling short-range stiffness of feline lower hindlimb muscles.," *Journal of biomechanics*, vol. 41, pp. 1945–52, jan 2008.

[99] W. P. Berg, H. M. Alessio, E. M. Mills, and C. Tong, "Circumstances and consequences of falls in independent community-dwelling older adults," *Age and Ageing*, vol. 26, pp. 261–8, jul 1997.

[100] S. H. Collins and A. D. Kuo, "Two independent contributions to step variability during over-ground human walking.," *PloS one*, vol. 8, p. e73597, jan 2013.

[101] T. McGeer and McGeer, "Passive dynamic walking," apr 1990.

[102] A. L. Hof, "The equations of motion for a standing human reveal three mechanisms for balance.," *Journal of biomechanics*, vol. 40, pp. 451–7, jan 2007.

[103] W. Hayes, E. Myers, S. Robinovitch, A. Van Den Kroonenberg, A. Courtney, and T. McMahon, "Etiology and prevention of age-related hip fractures," *Bone*, vol. 18, pp. S77–S86, jan 1996.

[104] N. B. Alexander, N. Shepard, M. J. Gu, and A. Schultz, "Postural control in young and elderly adults when stance is perturbed: kinematics.," *Journal of gerontology*, vol. 47, pp. M79–M87, may 1992.

[105] T. Cattagni, G. Scaglioni, D. Laroche, V. Gremeaux, and A. Martin, "The involvement of ankle muscles in maintaining balance in the upright posture is higher in elderly fallers," *Experimental Gerontology*, vol. 77, pp. 38–45, 2016.

[106] B. E. Maki and W. E. McIlroy, "Control of rapid limb movements for balance recovery: age-related changes and implications for fall prevention.," *Age and ageing*, vol. 35 Suppl 2, pp. ii12–ii18, sep 2006.

[107] M. Afschrift, I. Jonkers, J. De Schutter, and F. De Groote, "Mechanical effort predicts the selection of ankle over hip strategies in nonstepping postural responses," *Journal of Neurophysiology*, vol. 116, no. 4, pp. 1937–1945, 2016.

[108] J. Inglis, C. Shupert, F. Hlavacka, and F. Horak, "Effect of galvanic vestibular stimulation on human postural responses during support surface translations," *Journal of Neurophysiology*, vol. 73, no. 2, 1995.

[109] H. Van Der Kooij and R. J. Peterka, "Non-linear stimulus-response behavior of the human stance control system is predicted by optimization of a system with sensory and motor noise," *Journal of Computational Neuroscience*, vol. 30, pp. 759–778, jun 2011.

[110] A. D. Kuo, "Stabilization of Lateral Motion in Passive Dynamic Walking," *The International Journal of Robotics Research*, vol. 18, pp. 917–930, sep 1999.

[111] M. Afschrift, F. De Groote, S. Verschueren, and I. Jonkers, "Increased sensory noise and not muscle weakness explains changes in non-stepping postural responses following stance perturbations in healthy elderly," *Gait and Posture*, vol. 59, pp. 122–127, 2018.

[112] M. J. Hilliard, K. M. Martinez, I. Janssen, B. Edwards, M. L. Mille, Y. Zhang, and M. W. Rogers, "Lateral Balance Factors Predict Future Falls in Community-Living Older Adults," *Archives of Physical Medicine and Rehabilitation*, vol. 89, pp. 1708–1713, sep 2008.

[113] M. Afschrift, R. VanDeursen, I. Jonkers, and F. De Groote, "Modulation of gluteus medius activity reflects the potential of the muscle to meet the mechanical demands during perturbed walking [under review]," *Nature Scientific reports*, 2018.

[114] R. Preuss and J. Fung, "A simple method to estimate force plate inertial components in a moving surface," *Journal of Biomechanics*, vol. 37, no. 8, pp. 1177–1180, 2004.

[115] M. H. Gerards, C. McCrum, A. Mansfield, and K. Meijer, "Perturbation-based balance training for falls reduction among older adults: Current evidence and implications for clinical practice," *Geriatrics & Gerontology International*, vol. 17, pp. 2294–2303, dec 2017.

[116] A. J. Meyer, I. Eskinazi, J. N. Jackson, A. V. Rao, C. Patten, and B. J. Fregly, "Muscle Synergies Facilitate Computational Prediction of Subject-Specific Walking Motions," *Frontiers in Bioengineering and Biotechnology*, vol. 4, p. 77, oct 2016.

[117] N. B. Singh, N. König, A. Arampatzis, and W. R. Taylor, "Age-related modifications to the magnitude and periodicity of neuromuscular noise," *PLoS ONE*, vol. 8, p. e82791, dec 2013.

[118] S. Song and H. Geyer, "Evaluation of a Neuromechanical Walking Control Model Using Disturbance Experiments," *Frontiers in Computational Neuroscience*, vol. 11, p. 15, mar 2017.

[119] A. J. Van den Bogert, M. J. Pavol, and M. D. Grabiner, "Response time is more important than walking speed for the ability of older adults to avoid a fall after a trip," *Journal of Biomechanics*, vol. 35, no. 2, pp. 199–205, 2002.

[120] M. K. Karlsson, H. Magnusson, T. Von Schewelov, and B. E. Rosengren, "Prevention of falls in the elderly - A review," mar 2013.

[121] C. Sherrington, Z. A. Michaleff, N. Fairhall, S. S. Paul, A. Tiedemann, J. Whitney, R. G. Cumming, R. D. Herbert, J. C. Close, and S. R. Lord, "Exercise to prevent falls in older adults: An updated systematic review and meta-analysis," 2017.

[122] U. Granacher, T. Muehlbauer, L. Zahner, A. Gollhofer, and R. W. Kressig, "Comparison of traditional and recent approaches in the promotion of balance and strength in older adults," may 2011.

[123] I. K. Wiesmeier, D. Dalin, A. Wehrle, U. Granacher, T. Muehlbauer, J. Dietterle, C. Weiller, A. Gollhofer, and C. Maurer, "Balance training enhances vestibular function and reduces overactive proprioceptive feedback in elderly," *Frontiers in Aging Neuroscience*, vol. 9, p. 273, aug 2017.

[124] C. McCrum, M. H. G. Gerards, K. Karamanidis, W. Zijlstra, and K. Meijer, "A systematic review of gait perturbation paradigms for improving reactive stepping responses and falls risk among healthy older adults," *European Review of Aging and Physical Activity*, vol. 14, p. 3, dec 2017.

[125] N. B. Singh, N. König, A. Arampatzis, M. O. Heller, and W. R. Taylor, "Extreme Levels of Noise Constitute a Key Neuromuscular Deficit in the Elderly," *PLoS ONE*, vol. 7, p. e48449, nov 2012.

[126] T. W. Dorn, J. M. Wang, J. L. Hicks, and S. L. Delp, "Predictive simulation generates human adaptations during loaded and inclined walking.," *PloS one*, vol. 10, p. e0121407, jan 2015.

[127] Z. Potocanac and J. Duysens, "Online adjustments of leg movements in healthy young and old," 2017.

[128] A. Motte dit falisse, G. Serrancoli, J. Gillis, C. Dembia, I. Jonkers, and F. De Groote, "A framework to solve optimal control problems using automatic differentiation of multibody dynamics in OpenSim," in *International symposium on computer simulation in biomechanics*, (Brisbane), 2017.

[129] R. W. Jackson, C. L. Dembia, S. L. Delp, and S. H. Collins, "Muscle–tendon mechanics explain unexpected effects of exoskeleton assistance on metabolic rate during walking," *The Journal of Experimental Biology*, vol. 220, pp. 2082–2095, jun 2017.

[130] J. Zhang, P. Fiers, K. A. Witte, R. W. Jackson, K. L. Poggensee, C. G. Atkeson, and S. H. Collins, "Human-in-the-loop optimization of exoskeleton assistance during walking," *Science*, vol. 356, pp. 1280–1283, jun 2017.

[131] A. J. van den Bogert, T. Geijtenbeek, O. Even-Zohar, F. Steenbrink, and E. C. Hardin, "A real-time system for biomechanical analysis of human movement and muscle function," *Medical & Biological Engineering & Computing*, vol. 51, pp. 1069–1077, oct 2013.

Chapter 11

Appendix simulation standing balance control

Glossary

com	center of mass
COP	center of pressure
J	segment moment of inertia
$\mathbf{K}$	feedback gains
$\mathbf{K}_0$	guess of initial feedback gains optimization
$\mathbf{x}$	model state
l	segment length
l_c	distance from the joint to the center of mass
m	segment mass
$\mathbf{q}$	ankle and hip joint angle
$\dot{\boldsymbol{q}}$	ankle and hip joint velocity
$\mathbf{T}$	ankle and hip joint moment
$\hat{\mathbf{T}}$	measured ankle and hip joint moments
w	weight a number between 0 and 1
$\mathbf{x}_{qs}$	state during quiet standing
$\ddot{x}_{platform}$	horizontal acceleration of the motion base
$\hat{\mathbf{x}}$	Experimental state, i.e. ankle and hip joint angles and angular velocities
$X\,com$	extrapolated center of mass position

Dynamics double inverted pendulum model

The dynamics equations of the double inverted pendulum model with feedback control were adopted from Park et al. [13]. Skeletal dynamics were linearised around the vertical axis. In order to improve the readability of this appendix, the dynamic equations reported by Park et al. were repeated in this section [13].

Equations of motion

The equation of motion of the linearised double inverted pendulum model can be written as follows.

$$\boldsymbol{M}\begin{bmatrix}\ddot{q_a}\\ \ddot{q_h}\end{bmatrix} = \boldsymbol{G}\begin{bmatrix}\dot{q_a}\\ \dot{q_h}\end{bmatrix} + \begin{bmatrix}T_a\\ T_h\end{bmatrix} + \boldsymbol{P}(t) \tag{11.1}$$

Where q_a and q_h are the ankle and hip joint angles respectively,T_a and T_h are the ankle and hip joint moments.

$$\boldsymbol{M} = \begin{bmatrix} J_1 + m_1 l_{c1}^2 + m_2 l_1^2 + m_2 l_1 l_{c2} + J_2 + m_2 l_1 l_{c2} + m_2 l_1 l_{c2}^2 & J_2 + m_2 l_1 l_{c2} + m_2 l_{c2}^2 \\ m_2 l_1 l_{c2} + J_2 + m_2 l_{c2}^2 & J_2 + m_2 l_{c2}^2 \end{bmatrix} \tag{11.2}$$

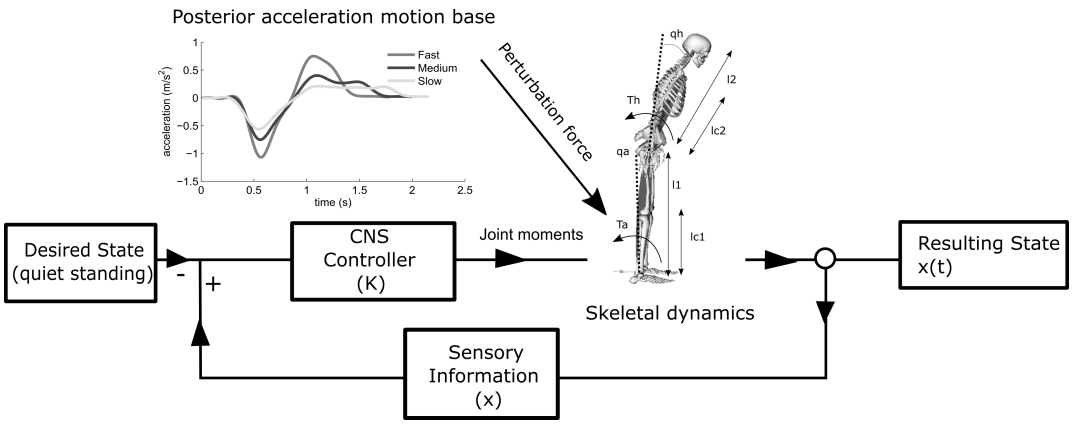

Figure 11.1: **Feedback control model:** The feedback control model is similar to the model of Park et al. [13]. In the sensory information block, either the full state of the model (ankle and hip joint angles and angular velocities) or only the center of mass position and velocity was used. The sensory information is compared to the desired state of quiet standing. The error on the desired state is multiplied by a feedback gain matrix K to compute the ankle and hip joint torque (eight feedback gains for full state feedback and four feedback gains for center of mass feedback). The different acceleration profiles of the platform as a function of time were approximated by cubic splines and imposed as external forces acting on the skeletal model.

$$\boldsymbol{G} = \begin{bmatrix} m_1 g l_{c1} + m_2 g l_1 + m_2 g l_{c2} & m_2 g l_{c2} \\ m_2 g l_{c2} & m_2 g l_{c2} \end{bmatrix} \tag{11.3}$$

$$\boldsymbol{P}(t) = - \begin{bmatrix} m_1 l_{c1} + m_2 l_1 + m_2 l_{c2} \\ m_2 l_{c2} \end{bmatrix} \ddot{x}_{platform}(t) \tag{11.4}$$

where $\ddot{x}_{platform}$ is the acceleration of the platform,m is the segment mass, l is the segment length, l_c is the distance from the joint to the center of mass, J is the segment moment inertia. The model parameters were derived from the scaled OpenSim models that were used to analyse the experimental data (figure: 11.1).

State-variable form

The equations of motion (equation:11.1) can be written in state-variable form where the state consists of the joint angles and angular velocities.

$$\boldsymbol{x} = \begin{bmatrix} q_a & q_h & \dot{q_a} & \dot{q_h} \end{bmatrix}^T \tag{11.5}$$

The joint moments T_a and T_h are the result of feedback and can be written as

$$\begin{bmatrix} T_a \\ T_h \end{bmatrix} = -\boldsymbol{K}\boldsymbol{D}(\boldsymbol{x} - \boldsymbol{x_{qs}}) \tag{11.6}$$

Where $\boldsymbol{x_{qs}}$ is the state during quiet standing ($\boldsymbol{x_{qs}} = \begin{bmatrix} 0 & 0 & 0 & 0 \end{bmatrix}^T$) and $\mathbf{K}$ the feedback gains.

1. In the case of full state feedback:

$$\boldsymbol{K} = \begin{bmatrix} k_{11} & k_{12} & k_{13} & k_{14} \\ k_{21} & k_{22} & k_{23} & k_{24} \end{bmatrix} \tag{11.7}$$

$$\boldsymbol{D} = \boldsymbol{I} \tag{11.8}$$

   Where I is a $4x4$ identity matrix.

2. In the case of center of mass feedback:

$$\boldsymbol{K_{com}} = \begin{bmatrix} k_{11} & k_{12} \\ k_{21} & k_{22} \end{bmatrix} \tag{11.9}$$

$$\boldsymbol{D} = \begin{bmatrix} \frac{l_{c1}m_1 + l_1 m_2 + l_{c2}m_2}{m_1 m_2} & \frac{l_{c2}m_2}{m_1 m_2} & 0 & 0 \\ 0 & 0 & \frac{l_{c1}m_1 + l_1 m_2 + l_{c2}m_2}{m_1 m_2} & \frac{l_{c2}m_2}{m_1 m_2} \end{bmatrix} \tag{11.10}$$

Hence the dynamics of the model in state-variable form.

$$\dot{\boldsymbol{x}}(t) = \boldsymbol{A}\boldsymbol{x}(t) - \boldsymbol{B}\boldsymbol{K}\boldsymbol{D}(\boldsymbol{x}(t) - x_{qs}) + \boldsymbol{C}(t) \tag{11.11}$$

with:

$$\boldsymbol{A} = \begin{bmatrix} 0 & 0 & 1 & 0 \\ 0 & 0 & 0 & 1 \\ \boldsymbol{M}^{-1}\boldsymbol{G} & 0 & 0 \\ & & 0 & 0 \end{bmatrix}, \boldsymbol{B} = \begin{bmatrix} 0 & 0 \\ 0 & 0 \\ \boldsymbol{M}^{-1} \end{bmatrix}, \boldsymbol{C} = \begin{bmatrix} 0 \\ 0 \\ \boldsymbol{M}^{-1}\boldsymbol{P} \end{bmatrix}$$

Optimization

The direct collocation optimal control software GPOPS II was used to find the optimal states and feedback gains ($\mathbf{K}$) for the tracking simulation and the predictive simulations [82]. The dynamic optimization problem was formulated according to the generic GPOPS framework. The optimization parameters are the feedback gains ($\mathbf{K}$).

Tracking simulation

In the tracking simulation, the feedback gains ($\mathbf{K}$) were optimized to minimize the difference between the measured and predicted joint angles (equation 11.12).

$$f = \int_{t_0}^{t_{end}} (\hat{\boldsymbol{x}} - \boldsymbol{x})^2 dt \tag{11.12}$$

where t_0 is the start of the perturbation, $t_e nd$ 1 second after the end of the perturbation and $\hat{\boldsymbol{x}}$ is the model state computed with the motion capture data at t_0.

Predictive simulation

In the predictive simulation, the feedback gains (**K**) were optimized to minimize the weighted sum of the extrapolated center of mass movement(Xcom) and the mechanical work. The value of w determines the relative weight between both parts of the instability-effort objective function.

$$J(K) = \int_{t_0}^{t_{end}} [w(Xcom - Xcom_0)^2 + (1-w) \sum_{i}^{nDOF} (\dot{q}_i T_i)^2] dt \tag{11.13}$$

With Xcom the extrapolated center of mass and $Xcom_0$ the initial position of the Xcom prior to perturbation. $\dot{\boldsymbol{q}}$ is a vector containing the ankle and hip angular velocities and $\boldsymbol{T}$ is a vector containing the ankle and hip joint moments. Xcom was calculated using the equations of Hof et al. [102].With *com* the horizontal position of the whole body center of mass, $\dot{com}$ the horizontal velocity of the center of mass and l the distance between the ankle joint and the whole-body center of mass during normal standing.

$$Xcom(t) = com(t) + \frac{\dot{com}(t)}{\sqrt{g/l}} \tag{11.14}$$

A second objective function is the weighted sum of the deviation from upright posture and postural instability. This objective function was used to investigate whether effort explains ankle strategy as good as upright posture and is similar to the function proposed by Kuo et al. [15]. We will refer to this function as the instability-upright objective function.

$$J(K) = \int_{t_0}^{t_{end}} [w(Xcom - Xcom_0)^2 + (1-w)\boldsymbol{q}] dt \tag{11.15}$$

Constraints

Constraints were added to make the simulation physiologically and mechanically more realistic.

1. Dynamic Constraint:
   - Skeletal dynamics were imposed by a dynamic constraint.

$$\dot{\boldsymbol{x}}(t) = \boldsymbol{A}\boldsymbol{x}(t) - \boldsymbol{B}\boldsymbol{K}\boldsymbol{D}(\boldsymbol{x}(t) - x_{qs}) + \boldsymbol{C}(t) \tag{11.16}$$

2. Path Constraints:
   - The ankle and hip joint moments were constrained between maximal moment generating capacities around the joints.

$$T_{min} \leq -\boldsymbol{K}(\boldsymbol{x} - \boldsymbol{x_{qs}}) \leq T_{max} \tag{11.17}$$

With T_{max} and T_{min} respectively the maximal moment and minimal moment that can be generated around the joints. The moment generating capacities around the ankle and hip joint were imposed as follows:

(a) Constraint on maximal hip joint moment: ($T_{max} = 150Nm$ and $T_{min} = -150Nm$)

(b) Constraint on maximal ankle joint moment:

$$T_{max} = m(\ddot{com}_y + g)COP_{max} \tag{11.18}$$

$$T_{min} = m(\ddot{com}_y + g)COP_{min} \tag{11.19}$$

where COP_{max} and COP_{min} are respectively the maximal and minimal displacement of the COP during the measurements of the function base of support(FBOS), m is the mass of the subject and $\ddot{com}_y$ is the vertical acceleration of the center of mass.

- Constraint on maximal rate of change in joint moments:

$$-250Nms^{-1} \leq -\boldsymbol{K}(\boldsymbol{x} - \boldsymbol{x_{qs}} \leq 250Nms^{-1} \tag{11.20}$$

- The initial joint angles, angular velocities and joint moments could not deviate too much from the experimental data to model the anticipatory feed-forward control in the simulation.

$$\hat{x}(t_0) = x_(t_0) \tag{11.21}$$

$$\hat{T}(t_0) - 10Nm \leq -\boldsymbol{K}\boldsymbol{x}(t_0) \leq \hat{T}(t_0) + 10Nm \tag{11.22}$$

- The final state of the model was constrained as well, where $\boldsymbol{\Delta x}$ is the maximum deviation from experimentally measured the final state.

$$\boldsymbol{\Delta x} = \begin{bmatrix} 0.1rad & 0.1rad & 0.3rad/s & 0.3rad/s \end{bmatrix} \tag{11.23}$$

$$\hat{\boldsymbol{x}}(t_{end}) - \boldsymbol{\Delta x} \leq \boldsymbol{x}(t_{end}) \leq \hat{\boldsymbol{x}}(t_{end}) + \boldsymbol{\Delta x} \tag{11.24}$$

Stability Constraint

Fourth, the feedback gains were constrained to result in a stable closed-loop system. A closed-loop system is stable if the real parts of the eigenvalues are negative. In a stable system, the predicted joint angles approach a constant value as time approaches infinity. Therefore, an additional constraint was imposed that constraints the ankle and hip joint angles within the boundaries of normal standing after 20s of simulation starting from six different initial body configurations.

$$\begin{bmatrix} -0.1rad & -0.05rad \end{bmatrix} < \begin{bmatrix} q_a(t=20) & q_h(t=20) \end{bmatrix} < \begin{bmatrix} 0.1rad & 0.05rad \end{bmatrix} \tag{11.25}$$

The real parts of the eigenvalues of the system matrix were calculated afterwards to evaluate if this constraint resulted in a stable system. The real parts of the four eigenvalues of the system matrix are negative for the selected predictive simulations (figure 11.2). This indicates that the stability constraint works.

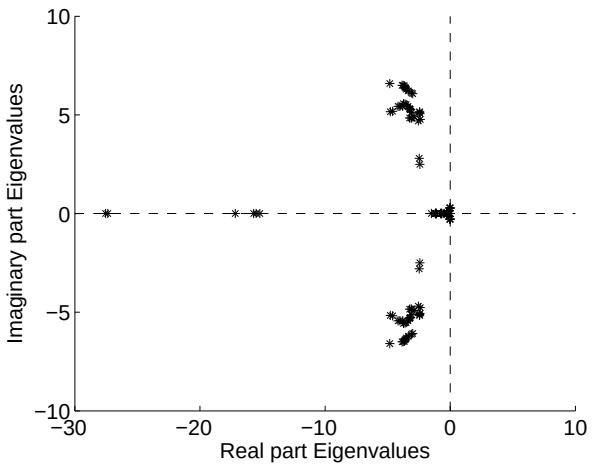

Figure 11.2: **Stability constraint:** Each dot represent one of the four eigenvalues for the multiple predictive simulations of one trial.

Additional results predictive simulation

Predicted joint moments

The predicted joint kinetics were evaluated for the two postural responses that were selected in figure 3 in the paper. The predicted joint moments are in the same order of magnitude as the measured joint moments (calculated with inverse dynamics). The predicted knee joint moment is the internal moment needed to keep the knee locked in the simulation. The small difference between the predicted and measured knee joint moments shows that the predictive simulations with a locked knee joint are physiologically realistic.

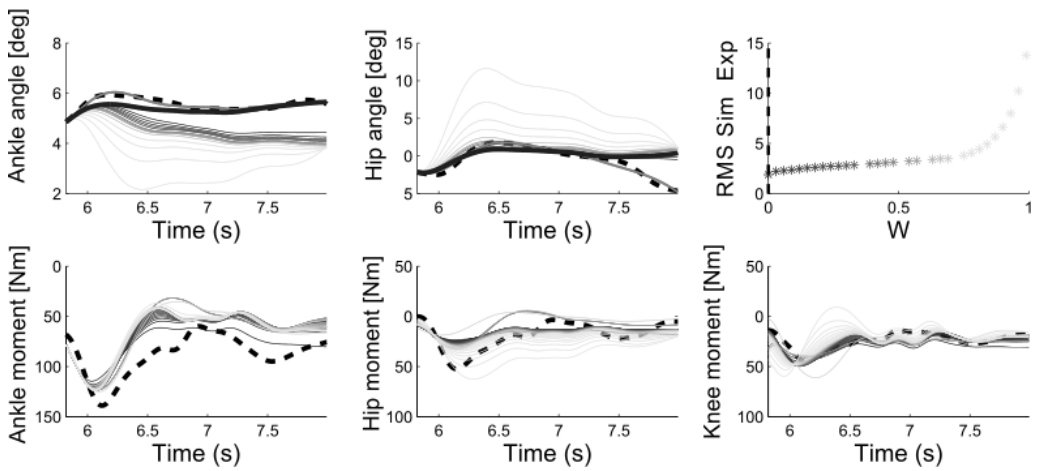

Figure 11.3: **Prediction ankle strategy.** This figures shows the measured and the predicted joint kinematics and kinetics for a trial with a typical ankle strategy. The black dashed line represents the experimental results. The blue lines represent the predicted joint kinematics and kinetics for different values of w. The red line represent the results of the tracking simulation.

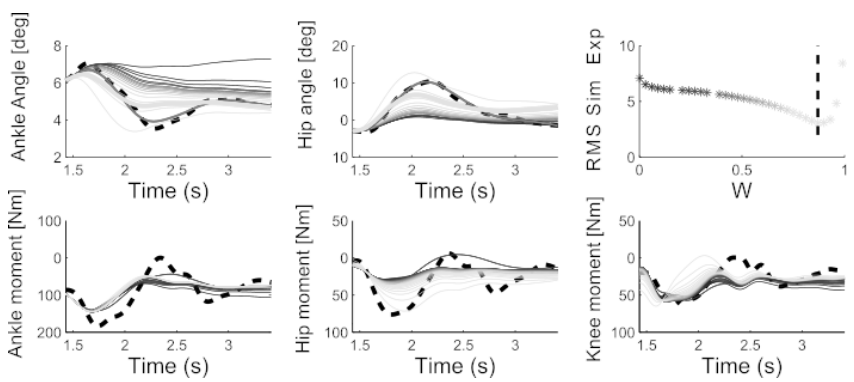

Figure 11.4: **Prediction hip strategy.** This figures shows the measured and the predicted joint kinematics and kinetics for trial with a typical hip strategy. The black line represents the experimental results. The blue lines represent the predicted joint kinematics and kinetics for different values of w. The red line represents the results of the tracking simulation.

Note that the peak plantarflexion moment is higher in the typical hip strategy compared to the typical ankle strategy. This seems to be contra-intuitive. However, the increase in peak ankle joint torque in the typical hip strategy compared to the typical ankle strategy is influenced by the platform acceleration. The typical hip strategies occurred in the trials with higher platform accelerations compared to the trials with ankle strategies. Runge et al. found the same relationship between perturbation amplitude and ankle joint moment [84]). They found that the ankle joint moment increases when the perturbation amplitude increases. Therefore, the use of a measured hip strategy, in both the kinematic and kinetic description of the hip strategy, does not necessarily causes a decrease in ankle joint moment when the perturbation conditions vary. This example shows the influence of confounding variables in

experimental measurement. The joint kinetics were clearly influenced by the perturbation condition in our experimental data and in the study of Runge et al [84]. With our predictive model we were able to investigate the difference between ankle and hip strategies when the perturbation condition remains invariant.

Sensitivity initial guess

The sensitivity of the optimal values to the initial guess was investigated using 150 simulations with random initial feedback gains. The random feedback gains were selected using latin hypercube sampling in matlab in an interval between -5 and 5 times the optimal feedback gains computed with the hot start optimization. As described in the paper, a hot start of the initial feedback gains was computed using the measured joint angles and joint moments. For each joint, the feedback gains were computed by solving the linear set of equations expressing that the measured joint moment need to equal the measured state times the feedback gains. This over determined system of equations is solved for K_0 in a least squares sense.

$$\hat{x}_i \boldsymbol{K_0} = \hat{T}_i \tag{11.26}$$

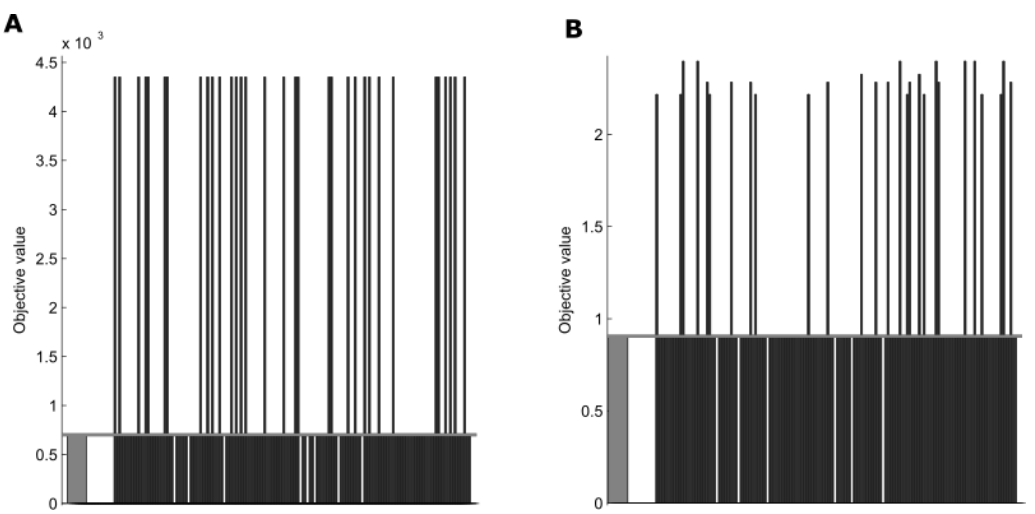

Figure 11.5: **Sensitivity of the optimization results to the initial feedback gains.** The red bar shows the optimal objective value for the optimization were the initial feedback gains were computed using the experimental joint kinematics and kinetics (i.e. hot start method). The blue lines show the optimal objective values for the random initial feedback gains. The figure on the left hand side shows the results for the tracking simulation (A) and the figure on the right hand side for the predictive simulation (B).

The variation in the objective value after optimization shows that the results are sensitive to the initial guess. However, the optimization starting from the hot start initial feedback gains results always in the lowest optimal objective value. This suggests that the true minimum is found when the hot start method is used in the optimization.

Sensitivity Postural response

The sensitivity of the predicted postural response to changes in the optimal feedback gains was investigated. The optimal feedback gains were varied individually to 10% in steps of 1%. Subsequently, the predicted kinematics and the eigenvalues of the system matrix were calculated. The predicted ankle strategy were sensitive to changes in the feedback gains. Especially changes in the joint position feedback gains resulted in an unstable system (figure 11.6, table 11.1). The predicted hip strategies (minimizing postural instability) were less sensitive to changes in the feedback gains (figure 11.9) than the predicted ankle strategies (figure 11.7) and mixed strategies (figure 11.8). This sensitivity analysis emphasizes previous findings and our results that the hip strategy is a more stable postural response. Furthermore, the results from this sensitivity analysis suggest that hip strategies are more robust to perturbations.

Table 11.1: Minimal change in optimal feedback gains (expressed as a %) that resulted in an unstable system for the predicted ankle, mixed and hip strategies: the > 10% indicates that a 10% deviation did not result in an unstable system.

	K11	K12	K13	K14	K21	K22	K23	K24
Ankle strategy	2%	3%	>10%	>10%	2%	2%	>10%	>10%
Mixed strategy	2%	4%	>10%	>10%	2%	2%	>10%	>10%
Hip strategy	4%	>10%	>10%	>10%	7%	>10%	>10%	>10%

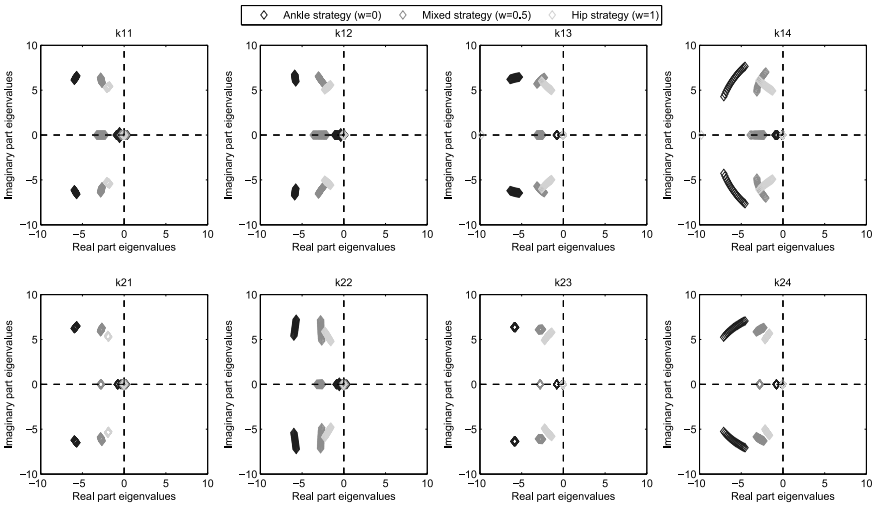

Figure 11.6: **Eigenvalues of the system matrix for the predicted ankle (red), mixed (blue), hip (magenta) strategies with 10% of variation in the optimal feedback gains.** Each subplot shows the influence of the variation in the individual feedback gain on the eigenvalues of the system matrix. High sensitivities are identified by large changes in eigenvalues. This analysis shows that the predicted ankle strategies are more sensitive to changes in the feedback gains compared to the mixed and hip strategy. Furthermore, the analysis shows that change of the gain of ankle torque relative to ankle position can result in unstable motion (positive real parts of eigenvalues, FB gain k11) confirms previous research [13].

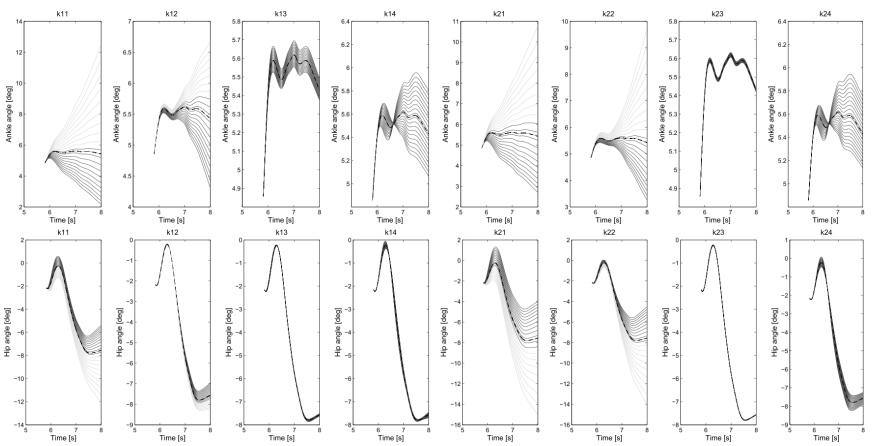

Figure 11.7: **Sensitivity of an ankle strategy (w=0) to variations in the feedback gains.** The black-red dotted line shows the result of the optimization. The blue and green lines show the predicted ankle and hip angle and angular velocity with variations in feedback gains with 10% in steps of 1%. Each feedback gain was varied individually and shown in a different column. The blue lines are stable strategies (real part eigenvalues are negative) the green lines are unstable strategies (real parts eigenvalues are 0 or positive).

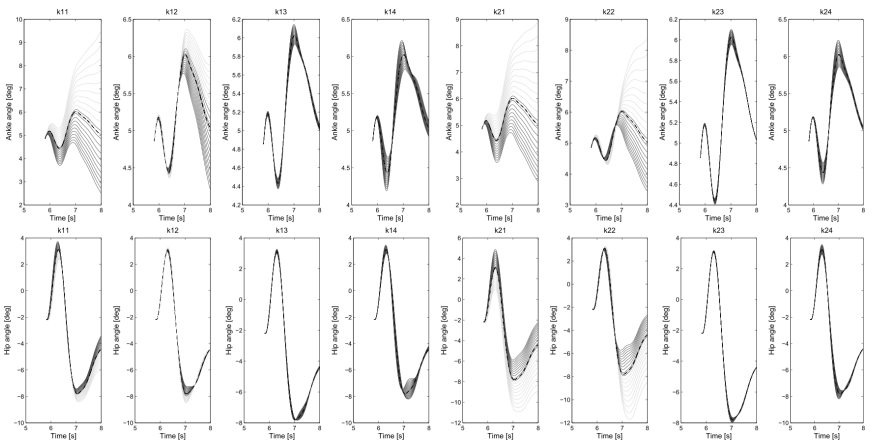

Figure 11.8: **Sensitivity of a mixed strategy (w=0.5) to variations in the feedback gains.** The black-red dotted line shows the result of the optimization. The blue and green lines show the predicted ankle and hip angle and angular velocity with variations in feedback gains with 10% in steps of 1%. Each feedback gain was varied individually and shown in a different column. The blue lines are stable strategies (real part eigenvalues are negative) the green lines are unstable strategies (real parts eigenvalues are 0 or positive).

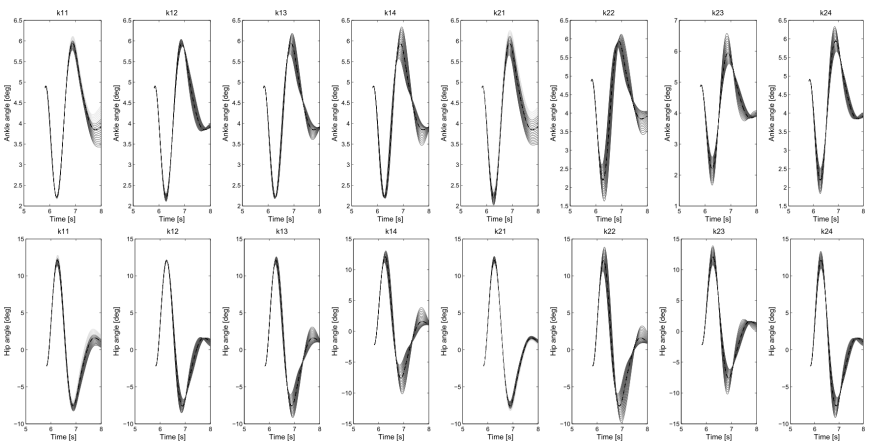

Figure 11.9: **Sensitivity of a hip strategy (w=1) to variations in the feedback gains.** The black-red dotted line shows the result of the optimization. The blue and green lines show the predicted ankle and hip angle and angular velocity with variations in feedback gains with 10% in steps of 1%. Each feedback gain was varied individually and shown in a different column. The blue lines are stable strategies (real part eigenvalues are negative) the green lines are unstable strategies (real parts eigenvalues are 0 or positive).

Influence of sensory noise on optimal feedback gains

To verify that the higher peak hip angles in the presence of noise resulted from a change in strategy and not from the effect of noisy sensory signals, we evaluated (1) whether feedback gains changed as a function of the noise level (figure 11.10), and (2) whether these changes also resulted in increased peak hip angles in the absence of sensory noise (figure 11.11).

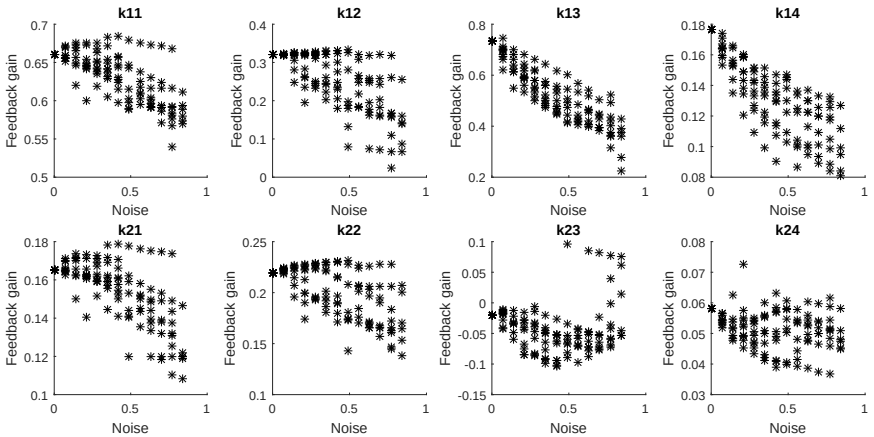

Figure 11.10: **Influence sensory noise on optimal feedback gains.** The optimal feedback gains decreased with sensory noise amplitude. Each dot represents a separate predictive simulation. For each noise amplitude, the simulation was repeated 15 times to assess the influence of optimizing the strategy based on a finite number of random noise signals. The feedback gains were scaled as in [13]

.

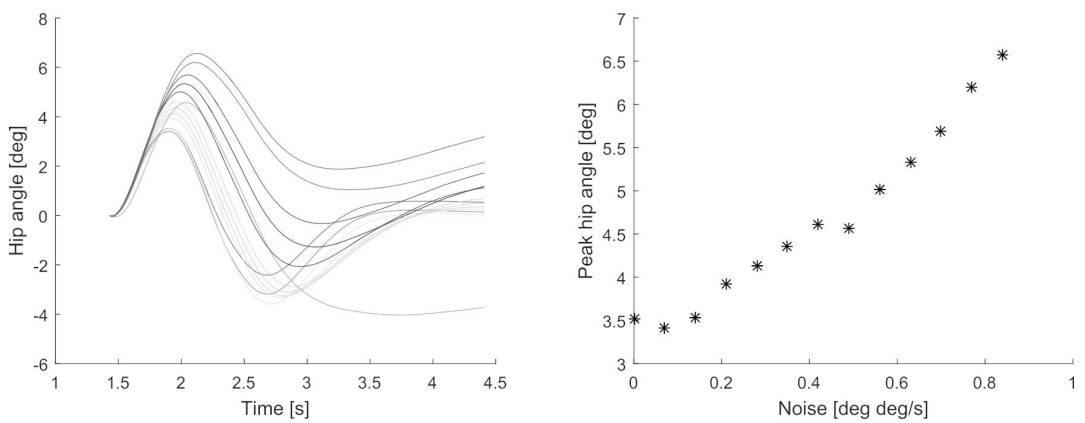

Figure 11.11: The left figure shows the predicted hip angle as a function of time for a forward simulation of the noise-free system with optimal feedback gains for the different levels of noise. The colors represent the level of noise that was used to determine the optimal feedback gains. The graph on the right shows the peak hip angle as a function of the noise level for which the feedback gains were optimized

.

Joint angle and angular velocity noise seperatly

An increase in peak hip angle was also found when noise was added to the joint angles or angular velocities separately (figure 11.12). But for the noise levels that were used when adding sensory noise to both angles and angular velocities, noise on the joint angles had a larger effect on the peak hip joint angle than noise on the joint velocities

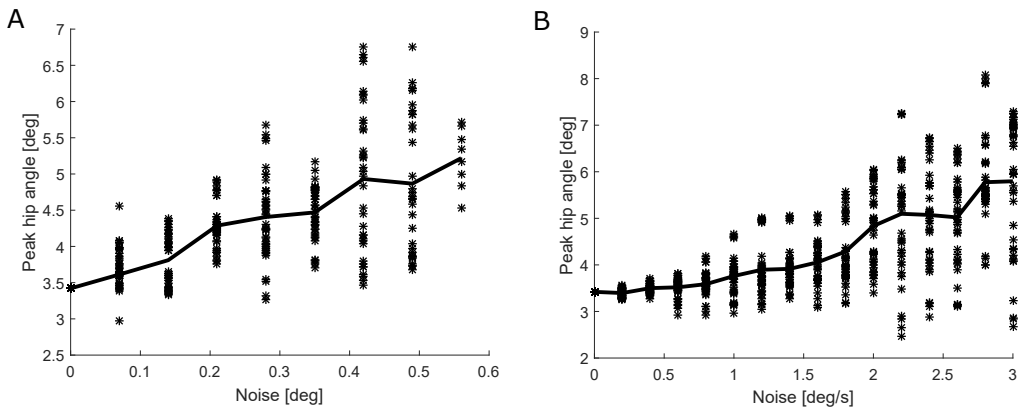

Figure 11.12: **The peak hip angle as a function of sensory noise on joint angles (A) and angular velocity (B) separately.** Each dot represents a separate predictive simulation. For each noise amplitude, the simulation was repeated 10 times to assess the influence of optimizing the strategy based on a finite number of random noise signals.

.

Experiments

Marker set

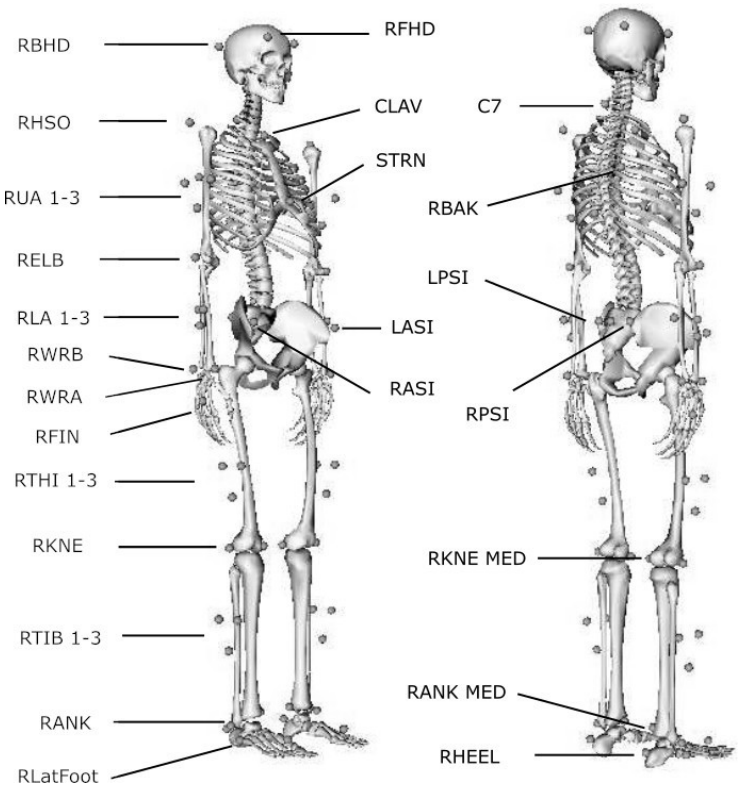

Figure 11.13: Motion capture markers visualised on the musculoskeletal model used in the inverse analysis

Head markers		
RFHD	Right front head	Located approximatly over the right temple
RBHD	Right back head	Placed on the back of the head

Torso markers		
C7	7th Cervical vertebrae	Spinous process of the 7th cervical vertebrae
T10	10th Thoracic Vertebrae	Spinous Process of the 10th thoracic vertebrae
CLAV	Clavicle	Jugular notch where the clavicles meet the sternum
STRN	Sternum	Xiphoid process of the Sternum
RBAK	Right Back	Placed in the middle of the right scapula

Arm Markers

RHSO	Right shoulder marker	Placed on the acromio-clavicular joint
RUA 1-3	Right upper arm cluster	Upper arm between the elbow and shoulder marker
RELB	Right elbow	Lateral epicondyle
RLA 1-3	Right lower arm cluster	Lower arm between the elbow and wrist
RWRA	right wrist	Right wrist bar thumb side
RWRB	right wrist	Right wrist bar pinkie side
LFIN	Left fingers	Dorsum of the hand below the second metacarpal

Pelvis

RASI	Right ASIS	Right anterior superior iliac spine
RPSI	Right PSIS	Right posterior superior iliac spline

Leg Markers

RTHI 1-3	Right femur cluster	Lower lateral surface of the thigh
RKNE	Right knee	Lateral epicondyle of the right knee
RKNE MED	Right knee	Medial epicondyle of the right knee
LTIB 1-3	Right tibial cluster	Lateral side of the shank
RANK	Right ankle	Lateral malleolus
RANK MED	Right ankle	Medial malleolus
RLatFoot	Right foot	tuberositas ossis metatarsi

Chapter 12

Appendix simulation walking balance control

Musculoskeletal model

OpenSim's gait2392 model was used to simulate musculoskeletal dynamics during walking. The model was scaled to the anthropometry and mass of the subjects based on the anatomical marker positions and ground reaction forces during a static trial (i.e. subjects is standing upright). As described below, several adjustments were made to the model.

Passive forces

Passive joint moments were added to the ankle, knee, hip and lumbar joints to simulate ligament forces. Passive joint torques were modeled as coordinate limit forces in OpenSim (Equation 12.1). Coefficients were selected for each joint and were based on [73] (Table 12.1).

$$P = k_1 e^{k_2(q-\theta_2)} + k_3 e^{k_4(q-\theta_1)} - c\dot{q} \tag{12.1}$$

where P is the passive joint torque, q is the joint angle and $\dot{q}$ is the angular velocity.

	k_1 $[Nm]$	k_2 $[-]$	k_3 $[Nm]$	k_4 $[-]$	$\theta_1[rad]$	$\theta_2[rad]$	c $[Nms]$
ankle PF	-12	15	11.03	-11.33	2.4	0.13	0.025
knee	-12	15	4	-15	0.74	0.52	0.025
hip flexion	5	5.05	3	-10	-0.47	1.81	0.025
hip adduction	-5	15	5	-15	-0.52	0.26	0.025
hip rotation	-5	15	5	-15	-0.52	0.52	0.025
lumbar flexion	-5	30.7	5	-20	0.52	0.17	0.025
lumbar adduction	-5	20.36	5	-20.36	-0.35	0.35	0.025
lumbar rotation	-5	20.36	5	-20.36	-0.35	0.35	0.025

Table 12.1: Coefficients passive joint torques

Muscle moment arms

Computation speed in the forward simulations was increased by approximating muscle tendon length - joint angle relationships with polynomial functions. Coefficients were estimated by minimzing the difference between the muscle tendon length computed with the polynomial approximation an OpenSim's Muscle Analysis Tool. The order of the polynomial was increased stepwise until the difference between the muscle tendon length and moment arms computed with the polynomial approximation and OpenSim's Muscle Analysis Tool was smaller than 1.5 mm for the kinematics observed during normal and perturbed during walking [131].

Moment arms were computed as the partial derivative of the muscle-tendon length to the selected degree of freedom (equation 12.2).

	r [m]	k $[Nm^{\frac{2}{3}}]$	c $\frac{s}{m}$
Heel	0.035	15	1
Toes	0.015	5	1

Table 12.2: Parameters contact model

$$dM_j = \frac{\partial L_{MT}}{\partial q_j} \tag{12.2}$$

where dM_j is the moment arm of the muscle for the joint angle q_j, L_{MT} is the muscle tendon length. Muscle tendon velocity was computed as the product of the moment arm and the angular velocity (Equation 12.3)

$$V_{MT} = \sum_{j=1}^{N_{dof}} \frac{\partial L_{MT}}{\partial q_j} \dot{q}_j \tag{12.3}$$

where V_{MT} is the muscle-tendon velocity and N_{dof} the number of degrees of freedom spanned by the muscle.

Ground contact model

Ground contact forces were simulated with a spring-damper based contact model. Contact geometry was modelled by one contact sphere at the heel and three at the metatarsal heads (Figure 12.1). Vertical reaction force F_y acting on each sphere was computed based on the indentation and indentation velocity of the contact sphere in the ground [70].

$$F_y = (10^6 k \sqrt{r}(y-r)^3)(1 + c\dot{y}) \tag{12.4}$$

where k is the stiffness parameter, r is the radius of the sphere, y is the indentation of the sphere in the ground, c is the damping parameter and $\dot{y}$ is the indentation velocity of the sphere in the ground. Details on the contact parameters are shown in table 12.2 .

Friction forces (F_x and F_z) were computed as a function of the vertical ground reaction force and the horizontal velocity of the contact sphere.

$$F_x = F_y tanh(10\dot{x}) \tag{12.5}$$

$$F_z = F_y tanh(10\dot{z}) \tag{12.6}$$

where F_x and F_z is the friction force in respectively anterior-posterior and medio-lateral direction, $\dot{x}$ and $\dot{z}$ are respectively the velocity of the contact sphere in the anterior-posterior and medio-lateral direction.

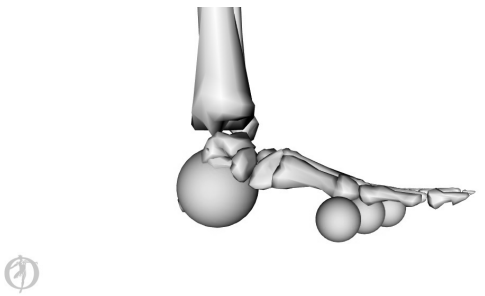

Figure 12.1: Location of the four contact spheres on the foot

Tracking skeletal dynamics

We created a model-based simulation of unperturbed walking by tracking the experimental data for a gait cycle of unperturbed walking. First, we solved for the joint torques that, when input to the skeleton dynamics, minimized the difference between simulated and measured movement (details below). Next, we solved for the muscle excitations that produced these joint torques by solving the muscle redundancy problem (see section 3).

We used the model described in section 1 and replaced the muscle-tendon actuators by joint actuators. Hence, model inputs were the joint torques and the model's state ($\boldsymbol{x}$) consisted of the generalized coordinates ($\boldsymbol{q}$) and velocities ($\dot{\boldsymbol{q}}$).

$$\boldsymbol{x} = \begin{bmatrix} \boldsymbol{q} & \dot{\boldsymbol{q}} \end{bmatrix} \tag{12.7}$$

Model inputs (joint torques) were optimized to minimize the difference between the measured and simulated marker positions, ground reaction forces and joint torques:

$$J = \int_{t_0}^{t_{end}} \|(\boldsymbol{p} - \hat{\boldsymbol{p}}\|_2^2 + w_1 \sum_{j}^{nF} (\boldsymbol{F_j} - \hat{\boldsymbol{F}}_{\boldsymbol{j}})^2 + w_2 \|\boldsymbol{T} - \hat{\boldsymbol{T}}\|_2^2 dt \tag{12.8}$$

where t_0 is the time of left heelstrike and t_{end} the time of the consecutive left heelstrike, $\boldsymbol{p}$ is the vector containing the 3D marker coordinates of all 48 markers on the skeletal model, $\hat{\boldsymbol{p}}$ is a vector with the corresponding measured marker coordinates, $\boldsymbol{F}$ and $\hat{\boldsymbol{F}}$ are vectors containing respectively the simulated and measured ground contact forces and moments and nF equals two (ground reaction force under left and right foot). $\hat{\boldsymbol{T}}$ is a vector containing the inverse dynamic joint torques based on the measured kinematics and ground reaction forces, $\boldsymbol{T}$ is a vector containing the corresponding simulated joint torques.

The optimization was subject to skeleton dynamics. We solved this dynamic optimization problem using direct collocation. To improve the numerical condition of the resulting non-linear programming problem, we first reformulated the optimization problem as described below.

Problem formulation

First, we used an implicit formulation of skeleton dynamics [116]. To this aim, we introduced joint accelerations $\boldsymbol{u_{\ddot{q}}}$ as additional controls, simplifying the dynamic equations:

$$\frac{d\dot{\boldsymbol{q}}}{dt} = \boldsymbol{u_{\ddot{q}}} \tag{12.9}$$

Skeleton dynamics were then imposed by a path constraint:

$$\boldsymbol{T_{ID}} = f(\boldsymbol{q}, \dot{\boldsymbol{q}}, \boldsymbol{u_{\ddot{q}}}) \tag{12.10}$$

Second, we defined the kinematic chain with the foot as a floating base, the position and orientation of the model was described by 6 degrees of freedom between the foot and the ground. By choosing the foot instead of the pelvis as a floating base, we obtained a more direct relation between the model's states (kinematics of the foot) and the ground reaction forces, which improved convergence of the optimization problem. As a consequence, we had to define seperate kinematic chains for the left and right leg, which were coupled at the pelvis [116]. Each chain had a reduced pelvis segment with a mass and inertia that equalled half of the mass and inertia of the original pelvis segment. We introduced forces $\boldsymbol{F_p}$ and moments $\boldsymbol{M_p}$ acting on the right reduced pelvis as additional controls. Reaction forces and moments were applied on the left reduced pelvis.

We then added additional path constraints to impose that the two reduced pelvises had the same kinematics. For both models, skeleton dynamics was evaluated through OpenSim's Inverse Dynamics Tool during the optimization. The residual forces and moments (i.e. external forces and moments) computed with inverse dynamics were constrained to be equal to the ground reaction forces computed with the contact model implemented in Matlab.

Summary optimal control problem

In summary, we solved the following dynamic optimization problem through direct collocation:

1. **State:**
$$\boldsymbol{x} = \begin{bmatrix} \boldsymbol{q} & \dot{\boldsymbol{q}} \end{bmatrix} \tag{12.11}$$

2. **Controls:**
$$\boldsymbol{u} = \begin{bmatrix} \boldsymbol{u_{\ddot{q}}} & \boldsymbol{F_p} & \boldsymbol{M_p} & \boldsymbol{T} \end{bmatrix} \tag{12.12}$$

3. **Dynamic constraints:**
$$\dot{\boldsymbol{x}} = \begin{bmatrix} \dot{\boldsymbol{q}} & \boldsymbol{u_{\ddot{q}}} \end{bmatrix} \tag{12.13}$$

4. **Path constraints:**

- Input joint torques should equal the inverse dynamics torques computed based on the model's kinematics.

$$\begin{bmatrix} \boldsymbol{T_{ID}} & \boldsymbol{F_{ground-foot}} \end{bmatrix} = f_{ID}(\boldsymbol{q}, \dot{\boldsymbol{q}}, \boldsymbol{u_{\ddot{q}}}, \boldsymbol{F_p}, \boldsymbol{M_p}) \tag{12.14}$$

- Residual forces and moments at the foot from OpenSim's Inverse Dynamics Tool $F_{ground-foot}$ should equal the forces and moments computed based on the contact model.

$$\boldsymbol{F_{ground-foot}} - \boldsymbol{F_{contact}}(\boldsymbol{q}, \dot{\boldsymbol{q}}) = 0 \tag{12.15}$$

- Position and orientation of the pelvis in the left and right model should be equal

$$\boldsymbol{P_{PelvisLeft}}(\boldsymbol{q}) = \boldsymbol{P_{PelvisRight}}(\boldsymbol{q}) \tag{12.16}$$

where $\boldsymbol{F_p}$ and $\boldsymbol{M_p}$ are the forces and torques to simulate the action of one model on the other, $\boldsymbol{T_{ID}}$ is a vector containing the inverse dynamics torques, $\boldsymbol{F_{ground-foot}}$ is a vector containing the residual inverse dynamics forces and moments, $\boldsymbol{F_{contact}}$ is vector containing the ground reaction forces and moments computed with the ground contact model, $\boldsymbol{P_{PelvisLeft}}$ and $\boldsymbol{P_{PelvisRight}}$ are vectors containing the position and orientation of the left and right pelvis in the ground.

Implementation

The direct collocation software GPOPS II was used to formulate the non-linear programming problem, which was solved using IPOPT. Inverse dynamics and the computation of the marker locations was solved using the OpenSim libraries trough a Mex file. Computation time was decreased by distributing the collocation points between multiple cores using OpenMPI. The ground contact forces and moments were computed in Matlab.

Tracking results

The root-mean square error of the tracking simulation of unperturbed walking was 0.03 cm for the marker positions, 29N for the ground reaction forces and 6.7 Nm for the joint torques. The tracking of the ground reaction forces (Figure 12.2) and joint torques (Figure 12.3) is shown for one representative trial.

Tracking muscle dynamics

In a second step, the muscle excitations that generate the inverse dynamic joint torques were computed using dynamic optimization. We modified the dynamic optimization approach proposed by [72] to include tracking of the gluteus medius activity (measured with electromyography). The objective function contains a part that minimizes muscle excitations

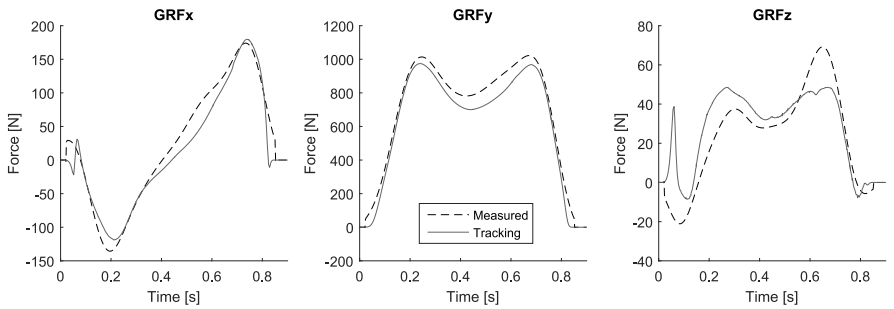

Figure 12.2: Measured ground reaction forces (black dotted) versus simulated ground reaction forces (gray) for one representative trial of the tracking simulations.

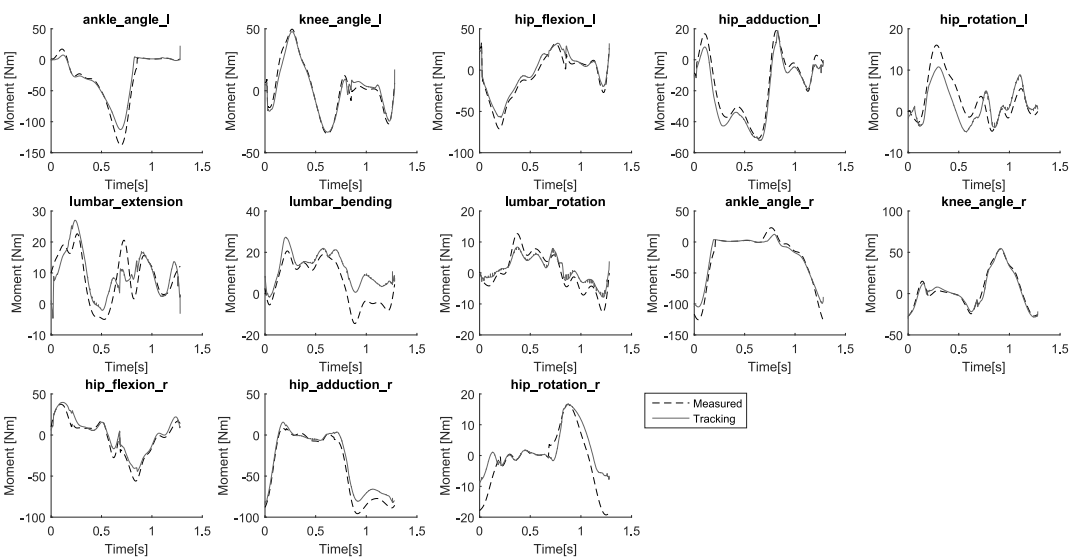

Figure 12.3: Estimated joint torques from the measured ground reaction forces and kinematics with inverse dynamics (black dotted) versus simulated joint torques (gray) for one representative trial of the tracking simulations.

squared, a second part the minimizes the differences between the measured and simulated excitations of the gluteus medius and a third part that minimizes the torque generated by ideal torque actuators (i.e. reserve actuators according to OpenSim terminology) (Equation 12.17).

$$J = \int_{t_0}^{t_{end}} \sum_{i}^{nMus} e_i^2 + w_1(s\hat{e}_{GM} - e_{GM})^2 + w_2 \sum_{j}^{nDOF} e_{Tj} T_{max} dt \tag{12.17}$$

where nMus=92 is the number of muscles in the model, e_i is the simulated excitation of muscle i, $\hat{e}_{GM}$ is the processed EMG of the gluteus medius, s is an optimization variable and scales the EMG from voltage to muscle excitations, e_{GM} is the simulated excitation of the gluteus medius, $Tmax$ equals 150Nm and is the reserve actuator of degree of freedom j, e_{Tj} is the activation of the reserve actuator of DOF k. Note that the weight w_2 is high to penalize the use of the reserve actuators.

The reserve actuators were added to guarantee feasibility in the presence of fast changes in joint torques in the tracking simulation that can not be generated by the muscles.This objective function was minimized subject to dynamic constraints following from muscle activation and contraction dynamics and to path constraints imposing that the model's actuators (muscles, passive torque, reserve actuators) should produce the inverse dynamics joint torques. In this case, the inverse dynamics joint torques were the result of the tracking simulation described in section 2. Reserve actuator torques did not exceed 2 Nm in the simulation. Joint torques resulting from the muscles, passive forces and reserve actuators were imposed to be equal to the joint torques from tracking the skeletal dynamics. The tracking of the gluteus medius activity in one representative trail can be found in Figure 12.4.

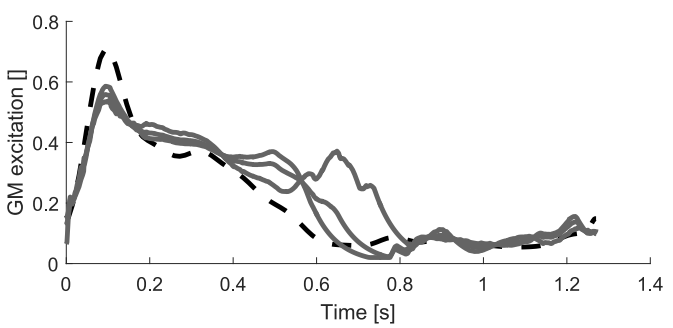

Figure 12.4: Measured (black dotted) and simulated activity of the bundles of the gluteus medius (gray) in one representative trial.

The source code of the muscle redundancy solver can be found on the simtk project optcntrlmuscle.

Forward simulation

The initial state and simulated muscle excitations from the tracking simulations were used to reconstruct the unperturbed walking in a forward simulation. The passive response to the perturbation was simulated by imposing the platform translation as an external force in the forward simulation of unperturbed walking. The active response was simulated by imposing the perturbation force and adding the measured muscle response to the perturbation (i.e. the difference between measured activity during unperturbed walking and after perturbation) to the muscle excitations from the tracking simulation of unperturbed walking. Muscle and skeletal dynamics were evaluated implicitly and integrated with a fully implicit integrator in Matlab (ode15i, absolute tolerance 10^{-5}). A time scaling factor (w) of 10^4 was used to improve the numerical condition (Equation 12.18)).

$$\tilde{t} = wt \tag{12.18}$$

$$\tilde{\boldsymbol{q}} = \boldsymbol{q} \tag{12.19}$$

$$\tilde{\dot{\boldsymbol{q}}} = \frac{\dot{\boldsymbol{q}}}{w} \tag{12.20}$$

$$\tilde{\ddot{\boldsymbol{q}}} = \frac{\ddot{\boldsymbol{q}}}{q^2} \tag{12.21}$$

Sensitivity analysis

Stiffness contact model

The sensitivity of the simulated active and passive response to contact model properties was evaluated by modifying the stiffness of the contact model in the tracking and forward simulation. The stiffness k was stepwise increased in the tracking simulation of one representative trial (Equation 12.4). The results from the tracking simulation and the modified contact model were used in the forward integration of the passive and active response. The stiffness had only a small influence on the simulated ground reaction forces in the tracking simulation and had only a limited effect on the simulated stride width and margin of stability in the active and passive response (Figure 12.5). Since the contact stiffness had only a small influence on the simulation results, we selected a relatively low stiffness value $k = 10$ to decrease the stiffness of the differential equations.

Lower bounds on activity

It has been hypothesized that muscle co-contraction is used as a strategy to control balance during walking by increasing the joint stiffness [22]. The influence of this co-contraction strategy on the simulated passive response was evaluated by constraining the minimal muscle activity in the muscle redundancy solver. The minimal muscle activity was increased stepwise in the muscle redundancy solver. The stride width and margin of stability at first heelstrike

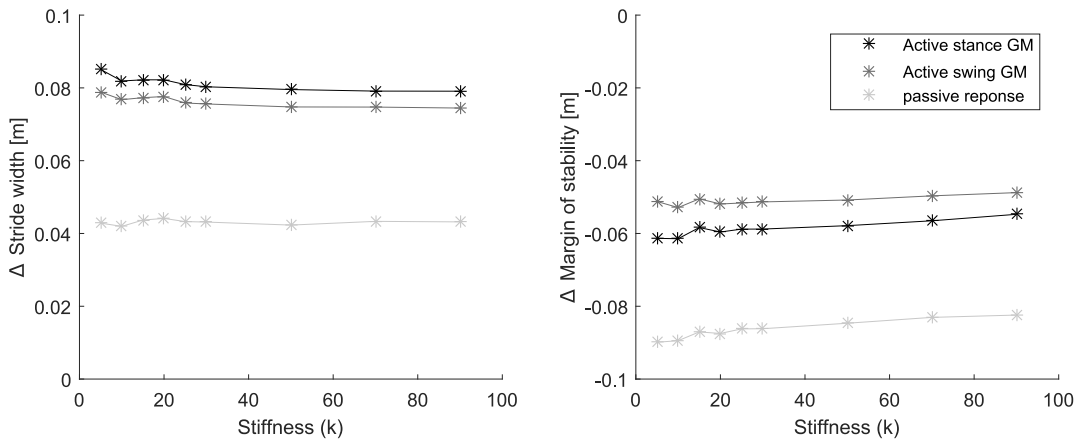

Figure 12.5: Influence stiffness of the contact model on stride width and margin of stability in the simulated active (blue and green) and passive (red) response to the perturbation.

after perturbation was computed in the passive and active response using forward simulations for the different levels of minimal muscle activity. Stride width decreased with increased muscle activity and a small change in the margin of stability was found in the active and passive response simulations (Figure 12.6).

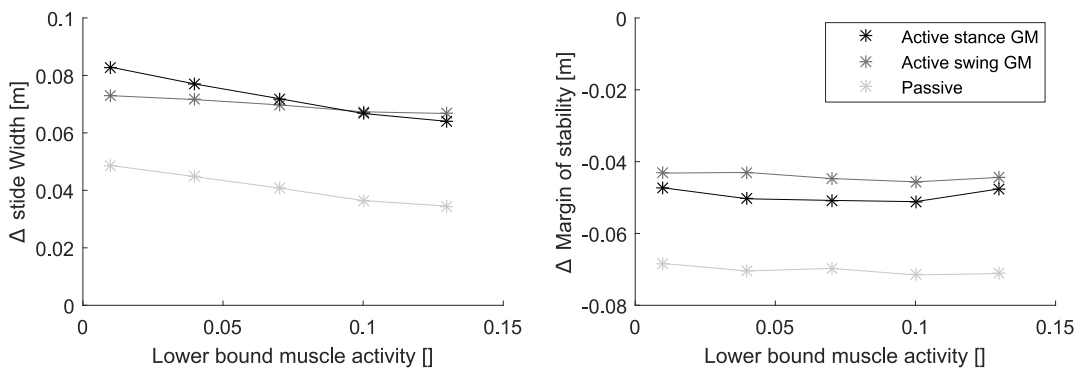

[H]

Figure 12.6: Influence of lower bound on muscle activity on stride width and margin of stability in the simulated active (blue and green) and passive (red) response to the perturbation.

Chapter 13

The effect of muscle weakness on the capability gap during gross motor function: a simulation study supporting design criteria for exoskeletons of the lower limb

Maarten Afschrift, Friedl De Groote, Joris De Schutter, Ilse Jonkers

Published in *BioMedical Engineering OnLine*

Abstract

Background: Enabling persons with functional weaknesses to perform activities of daily living (ADL) is one of the main challenges for the aging society. Powered orthoses, or exoskeletons, have the potential to support ADL while promoting active participation of the user. For this purpose, assistive devices should be designed and controlled to deliver assistance as needed (AAN). This means that the level of assistance should bridge the capability gap, i.e. the gap between the capabilities of the subjects and the task requirements. However, currently the actuators of exoskeletons are mainly designed using inverse dynamics (ID) based calculations of joint moments. The goal of the present study is to calculate the capability gap for the lower limb during ADL when muscle weakness is present, which is needed for appropriate selection of actuators to be integrated in exoskeletons.

Methods: A musculoskeletal model (MM) is used to calculate the joint kinematics, joint kinetics and muscle forces of eight healthy subjects during ADL (gait, sit-to-stand, stand-to-sit, stair ascent, stair descent). Muscle weakness was imposed to the MM by a stepwise decrease in maximal isometric force imposed to all muscles. Muscle forces were calculated using static optimization. In order to compensate for muscle weakness, ideal moment actuators that represent the motors of an exoskeleton in the simulation were added to deliver AAN required to perform the task.

Results: The ID approach overestimates the required assistance since it relies solely on the demands of the task, whereas the AAN approach incorporates the capabilities of the subject. Furthermore, the ID approach delivers continuous support whereas the AAN approach targets the period where a capability gap occurs. The level of muscle weakness for which the external demands imposed by ADL can no longer be met by active muscle force production, is respectively 40%, 70%, 80% and 30%.

Conclusions: The present workflow allows estimating the AAN during ADL for different levels of muscle weakness, which can be used in the mechatronic design and control of powered exoskeletons. The AAN approach is a more physiological approach than the ID approach, since the MM accounts for the subject-specific capabilities of the user.

KeyWords: Assistance as needed, muscle weakness, design criteria, exoskeleton, musculoskeletal model, simulation

Introduction

Enabling persons with functional weaknesses to perform activities of daily living (ADL) is one of the main challenges for the aging society. It will be crucial for the welfare of our society to maintain the mobility and activity of the population as long as possible. Powered orthoses, or exoskeletons, have the potential to support ADL while promoting active participation of the user. This is essential to maintain neuromotor function and prevent disuse [1]. For this purpose, assistive devices should be designed and controlled to deliver the level of assistance needed for a specific individual during a specific motor activity. This level of assistance should bridge the capability gap, i.e. the discrepancy between the motor capabilities of the subject and the task requirements [2]. The motor capabilities are the joint moments that the subject is able to generate through coordinated muscle action. The task requirements are the external moments and powers that are imposed to the joints during the task execution. Hence, quantification of the capability gap is needed for appropriate selection of actuators to be integrated in lower-limb exoskeletons.

Currently, the actuator selection for assistive devices is mainly based on inverse dynamics (ID) calculations of joint moments and joint powers [3–5]. This method only accounts for the task requirements and assumes continuous support, despite the actual level of assistance required by the patient. Therefore, this method leads to overdimensioning of the actuators if the users have some remaining muscle function. As a first step towards defining assistance as needed (AAN), Carmichael et al. introduced the concept of a task model [6] that determines the task requirements and a strength model [7] that determines the motor capabilities of a person in reaching and lifting tasks. Using both these models, the required assistance for the upper limb can be calculated. However, assistance to support motor functions of the lower limb during ADL has not yet been evaluated using these concepts. Furthermore, the study of Carmichael et al. only considers assistance of the end effector (i.e. the hand). However, most lower limb exoskeletons are designed to support the function of the individual joints. Hence, the capability gap needs to be defined at the joint level in different ADL.

The purpose of the present study is to identify the capability gap during ADL. More specifically, we will investigate to what extent the task requirements can no longer be met if different levels of muscle weakness are present. To do so, the force generating capacities of the muscles in a musculoskeletal model (MM) will be modified to reflect different levels of weakness. Inherently, these models account for bi-articular muscle action and their inter-joint coupling as well as for the influence of the kinematic state on the force-generating capacities of the muscles. This approach allows quantifying the capability gap depending on the specific task requirements imposed by the ADL. The capability gap can then be expressed in terms of the joint moment deficits, for use in the mechatronic design of assistive devices. Furthermore, based on the task requirements and the capability gap for different levels of muscle weakness, critical tasks (i.e. the tasks that impose the highest demands) for a specific degree of freedom (DOF) can be identified and identify the critical threshold of muscle weakness that will interfere with ADL task execution.

In general, we hypothesize that the working envelope for the AAN design requirements in the presence of muscular weakness will differ substantially from the design requirements defined using the classic ID approach.

Methods

Experimental data

Eight healthy subjects (61 ± 8 kg, 23 ± 3 years) provided written informed consent in accordance with the ethical committee of UZ Leuven to participate in this study. Each subject performed the selected ADL three times (Figure 1). The selected ADL are: sit-to-stand, stand-to-sit, gait, stair ascent, stair descent. The sit-to-stand movement is measured at self-selected speed in four conditions: a chair height of 100% knee height and 120% knee height, with and without hand support. A crutch of 75 cm height is used in the hand support condition. The gait data is measured overground at self-selected speed and on a split-belt treadmill at 3 and 5 km/h. The stair ascent and descent is measured using a staircase with 20 cm height and 40 cm width for each step. Motion data is collected with 10 Vicon cameras, sampled at 100 Hz. Ground reaction forces are measured using three force plates (Amti), sampled at 1000 Hz. The muscle activity of the rectus femoris, vastus lateralis, biceps femoris medialis, tibialis anterior, soleus and gastrocnemius lateralis are measured with surface electromyography (EMG, zero wire, Aurion, It), sampled at 1000 Hz. The SENIAM EMG placement protocol was used [8]. The EMG data were band-pass filtered (20-400 Hz), rectified and low pass filtered with a cutoff frequency of 10 Hz.

Modeling and simulation

Opensim 3.1 is used for the dynamic simulations of human movement [9]. A generic musculoskeletal model (MM) with 23 degrees of freedom (DOF) and 92 musculotendon actuators was scaled to match the anthropometry and weight of the subject (name MM: 3DGaitModel2392) [10]. The scaled model reproduced the measured motion of the markers by means of an inverse kinematics algorithm that minimizes the squared distances between the measured markers and the markers on the scaled model. The motion of the model and the external forces from the force plates were used to calculate the joint moments with inverse dynamics (Opensim 3.1). The joint moments were normalized to the body mass of the subject. Muscle forces were calculated using the dedicated static optimization in Opensim. The goal function of the optimization solves the muscle redundancy problem by minimizing the sum of muscle activation squared.

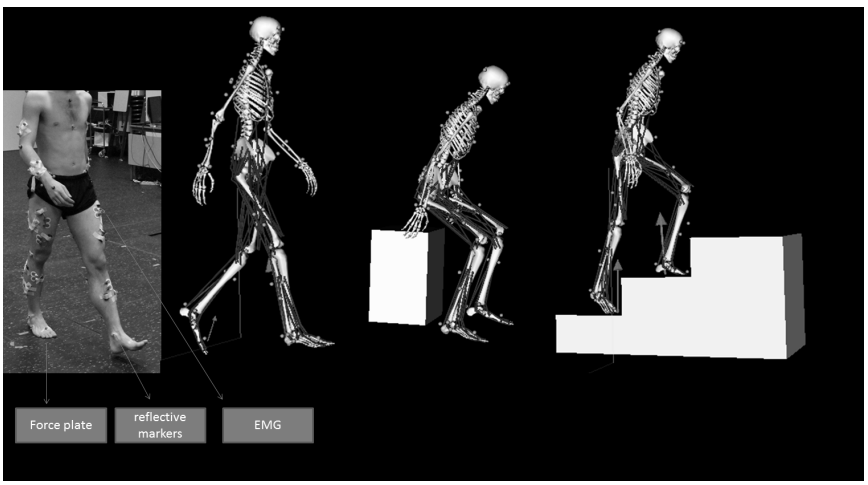

Figure 13.1: **Experimental set-up.** The left picture shows a subject during the experiments. Reflective markers were mounted on anatomical location of the subject to capture the motion with 10 infrared cameras. Muscle activity of 14 muscles is measured with surface electromyography. Ground reaction forces between the feet and the ground are measured with three force plates. These measurements are used with a generic musculoskeletal model in opensim to calculate the joint kinematics and kinetics during sit-to-stand, stand-to-sit, gait, stair ascent and stair descent.

Simulation of muscle weakness

The simulations of muscle weakness were performed by a stepwise decrease of the maximal isometric force of the muscles in the MM ranging from 0 to 100% in steps of 10%. Decreasing the maximal isometric force of a muscle scales the force-length and force-velocity curves of the Hill-type muscle model. We assume an identical reduction in maximal isometric forces for all the muscles [11]. To compensate for muscle weakness, ideal moment actuators were added to the joints, which represent the motors of an exoskeleton in the simulation that would be available to deliver the assistance that is needed to successfully perform the task. The cost function of the static optimization, that minimizes the summed squared muscle activations, was supplemented with an additional term to account for the ideal moment actuators:

Constraint function:

$$\tau_k = \sum_{t=1}^{nMA} \tau_{k,t}^0 a_t + \sum_{m=1}^{N} \left[a_m f(F_m^0, l_m, v_m) \right] r_{m,k} \tag{13.1}$$

Objective function:

$$J = \sum_{t=1}^{nMA} (a_t)^2 + \sum_{m=1}^{N} (a_m)^2 \tag{13.2}$$

We assigned an optimal moment of $\tau_(t,k)^0 = 1$ Nm to the ideal moment actuators, therefore making them costly to use (i.e. high activations are required to use this actuator). Hence, actuation by muscles is preferred over actuation by the ideal moment actuators

nMa	Number of ideal moment actuators
k	The selected specific DOF of the MM
$\tau^0_{k,t}$	Optimal moment of the ideal moment actuator on the DOF k
a_t	Activation of the ideal moment actuator
N	Number of muscles in the MM
a_m	Activation of the muscle
F^0_m	Maximal isometric force of the muscle
l_m	Length of the muscle
V_m	Velocity of the muscle fiber
$r_{m,k}$	Moment arm of the muscle ont the DOF k

Table 13.1: Terminology

Representation of the results

The analysis of the simulation results mainly focused on the sagittal plane joint moments, since for the tasks studied, these moments clearly exceed the joint moments required in other movement planes. For each subject the task requirements and capability gaps were calculated for the different ADL. The task requirements, i.e. the joint moments and joint powers imposed by the task to the joints, were calculated with inverse dynamics in Opensim. The maximal task requirement is identified as the maximal joint moment observed during the spectrum of ADL analyzed in this study. The capability gap is calculated by subtracting the joint moment generated by the muscle actuators in the MM (motor capability) from the joint moment imposed by the task (task requirements) and corresponds to the joint moment generated by the ideal moment generators. The capability gap for the different ADL was calculated for the different levels of muscle weakness. The maximal capability gap reflects the maximal joint moment deficit observed during the spectrum of ADL analyzed in this study. The maximal capability gap was calculated for each level of muscle weakness.

Statistical analysis

The task requirements and capability gaps were compared for the different ADL and DOF using repeated measures Anova (significance threshold 5%). A Tukey's hsd post hoc test is used for pairwise comparison (significance threshold 5%). A two-sided Wilcoxon sign rank test with a significance threshold 5% was used to statistically test the differences in joint moments due to speed during gait and due to chair height and hand support during sit-to-stand. Comparing the measured EMG with calculated muscle activity is a method to validate the simulations [12]. Therefore, to check the validity of the simulation, the time series of the simulated muscle activations and the muscle activity, measured with EMG, were compared using a spearman correlation (Table1).

Results

Task requirements during ADL

	Gait	Stair ascent	Stair descent	Sit-to-stand	Stand-to-sit
Rectus femoris	-0.09	0.44**	0.40**	-0.35	-0.35
Vastus lateralis	0.28**	0.83**	0.30**	0.89**	0.89**
Biceps femoris medialis	0.82**	0.49**	0.36**	0.93**	0.46**
Tibialis anterior	0.83**	0.66**	0.09	0.61**	0.35**
Soleus	0.66**	0.63**	0.22*	0.97**	0.73**
Gastrocnemius	0.76**	0.87**	0.25**	0.19*	0.15
* p<0.05 **p<0.01					

Table 13.2: **Correlation between measured muscle activity and simulated muscle activation:** This table presents the spearman correlation coefficients for the correlation between measured muscle activity and simulated muscle activation.

The task requirements differ between ADL and joints (Figure 2). Based on the task requirements we can specify the maximal task requirements in terms of joint moments (Figure 3) and joint powers (Figure 4). At the ankle joint, the stair ascent task imposes the highest net plantarflexion moment (1.68 ± 0.09 Nm/kg, p<0.05) whereas gait imposes the highest dorsiflexion moment (0.11 ± 0.02 Nm/kg, p<0.05). At the knee joint, the stair ascent and descent tasks impose the highest extensor moment (1.30 +/-0.30 Nm/kg, 1.31 +/- 0.25 Nm/kg, p¡0.05) whereas the stair ascent and gait tasks impose the highest flexor moment (0.40 +/- 0.06 Nm/kg, 0.42 ± 0.13 Nm/kg, p<0.05). At the hip joint, the stair ascent task imposes the highest extensor moment (0.91 ± 0.25 Nm/kg, p<0.05) whereas gait imposes the highest flexor moment (0.63 ± 0.10 Nm/kg, p<0.05). In general, considering the selected ADL, the ankle plantarflexion moments are highest (p<0.01).

The maximal task requirements in terms of joint power are shown in Figure 4. The highest positive ankle power is present during stair ascent (4.66 ± 0.63 W/kg) and the highest negative power is present during stair descent (3.74 ± 0.95W/kg). For the knee joint, stair ascent imposes the highest positive power (2.91 ± 0.39 W/kg), whereas stair descent imposes the highest negative power (3.64 ± 0.58 W/kg). For the hip joint, stair ascent (1.73 ± 0.49 W/kg) and gait (1.33 ± 0.42 W/kg) impose the highest positive power, whereas stand-to-sit imposes the highest negative power (1.26 ± 0.41 W/kg). In general, considering the ADL, the ankle joint positive power and the ankle joint and knee joint negative power are highest.

Capability gap

Figure 5 illustrates the main differences between the ID and AAN approaches during a stair ascent task for 70% muscle weakness. Firstly, the ID approach requires a higher assistive ankle moment (1.53 Nm/kg) compared with the capability gap in the AAN approach (0.68

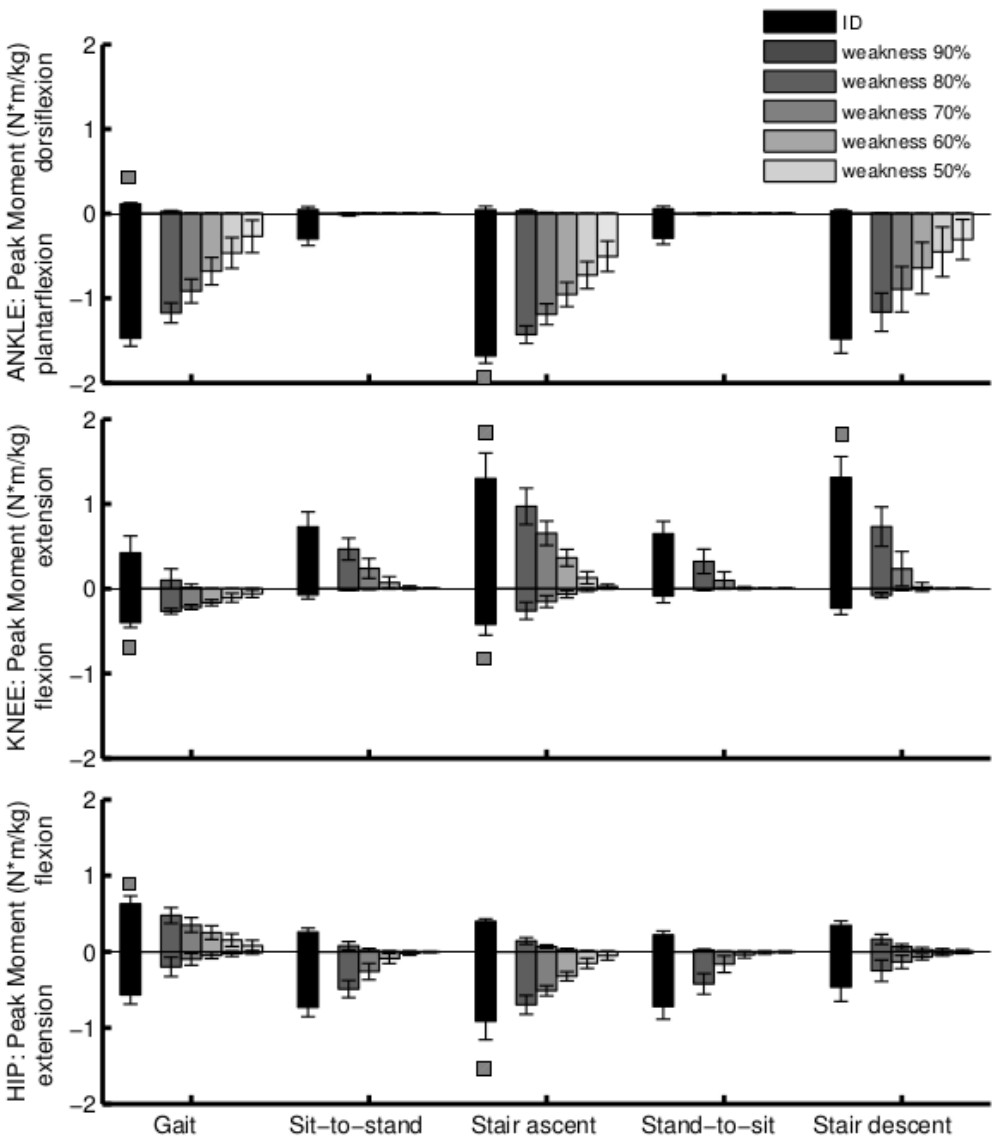

Figure 13.2: **Task requirements and capability gaps during ADL.** The task requirements for the ADL are shown in black (task requirements). The capability gaps for the different levels of muscle weakness are shown in gray. Gait is measured at self-selected speed and the sit-to-stand and stand-to-sit movements are measured with a chair of 100% knee height. The peak ID moment for the DOF were compared between the different movements using one way repeated measure Anova. A Tukey's hsd test is used for pairwise comparison when the one way repeated measures Anova test was significant significance threshold 5%). For the selected DOFs, the movement with the highest task requirements is marked with a gray square ($p<0.05$).

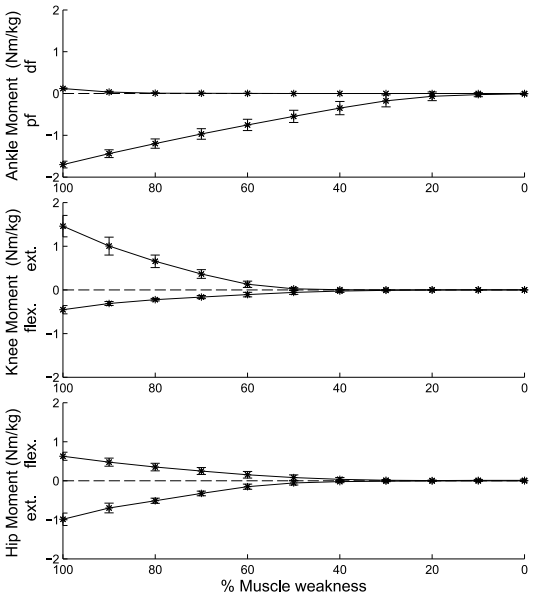

Figure 13.3: **Maximal task requirements and maximal capability gaps in terms of joint moments.** The maximal task requirements are the joint moments when 100% of muscle weakness is present. The maximal capability gap is shown as a function of the level of muscle weakness.

Nm/kg). Secondly, the ID approach delivers continuous support whereas the AAN approach targets the period where a capability gap occurs (i.e. 55%-65% of the stair ascent cycle). Figure 6 illustrates the influence of an increasing level of muscle weakness on the capability gap during stair ascent. Both the timing and the magnitude of the capability gap depend on the level of muscle weakness.

Figure 2 illustrates the capability gap for different ADL and different levels of muscle weakness. For example in the presence of 70% muscle weakness, no ankle dorsiflexion moment deficit is found. The highest plantarflexion capability gap occurs during stair ascent (0.96 $\pm$ 0.14 Nm/kg, $p<0.05$). For the knee joint, the highest knee extensor capability gap occurs during stair ascent (0.36 $\pm$ 0.09 Nm/kg, $p<0.05$) and the highest knee flexion capability gap occurs during gait (0.16 $\pm$ 0.03 Nm/kg, $p<0.05$). For the hip joint, the highest extensor capability gap occurs during stair ascent (0.32 $\pm$ 0.06 Nm/kg, $p<0.05$) and the highest flexion capability gap during gait (0.25 $\pm$ 0.09 Nm/kg, $p<0.05$).

A capability gap is found from 30% of muscle weakness onwards: from this level the ankle plantarflexion function during stair ascent and stair descent becomes insufficient and ideal moment generators assist. During gait, a capability gap is found when 40% of muscle weakness is present, and plantarflexion function is lacking. The sit-to-stand and stand-to-sit movements are less affected by overall muscle weakness: the knee and hip extension functions are only impaired when 70% of muscle weakness is present for the sit-to-stand task and when 80% of muscle weakness is present for the stand-to-sit task.

The capability gap differs significantly depending on the specific DOF: the ankle plantarflexion

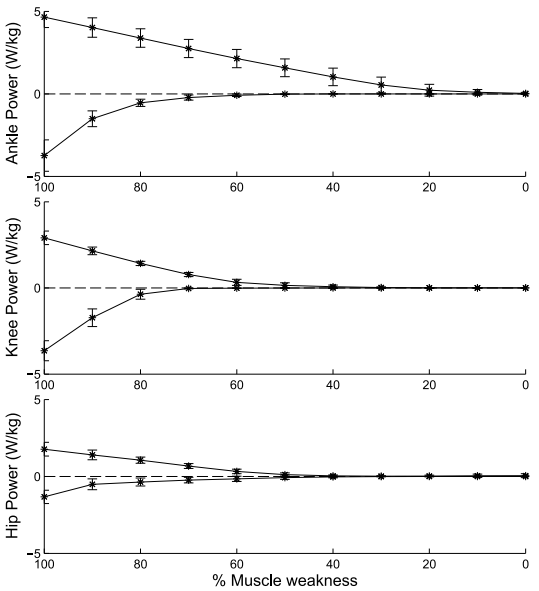

Figure 13.4: **Maximal task requirements and maximal capability gaps in terms of joint powers.** The maximal task requirements are the joint powers when 100% of muscle weakness is present. The maximal capability gap is shown as a function of the level of muscle weakness.

function is impaired from 30% weakness onwards, whereas the dorsiflexion function is only impaired when 90% weakness is present. For the knee and hip joint, the knee flexion/extension and hip flexion/extension functions are impaired during ADL from 50% muscle weakness onwards.

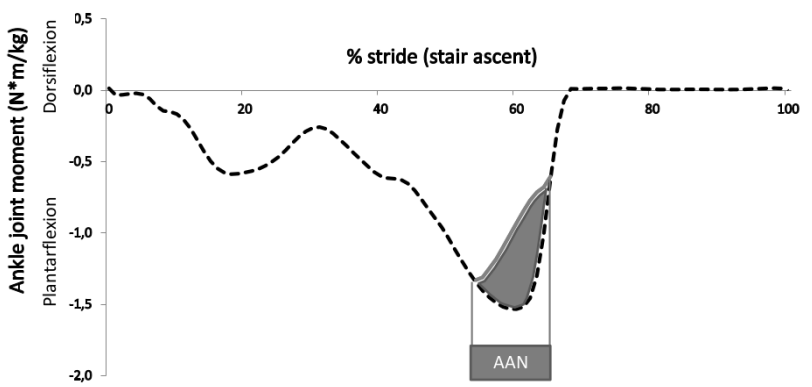

Figure 13.5: **Plantarflexion capability gap during stair ascent.** The difference between the net moment imposed by the task to the joint (task requirements, black dashed line) and the joint moment generated by the muscles (capability, gray solid line) equals the capability gap (gray area). The capability gap is the external assistance that is needed to perform the task. In this case, the capability is calculated with a MM presenting 70% muscle weakness.

Based on the capability gaps for the ADL, we can specify the maximal capability gap for the

different DOF in term of joint moments (Figure 3) and joint powers (Figure 4). These figures show the maximal moment and power assistance that is needed to perform the ADL for the different levels of muscle weakness.

When inducing more strenuous activities, the task requirements for several DOF increase (Figure 7). For example increasing the walking speed from 3km/h to 5km/h causes an increase in the task requirements for all the DOF.

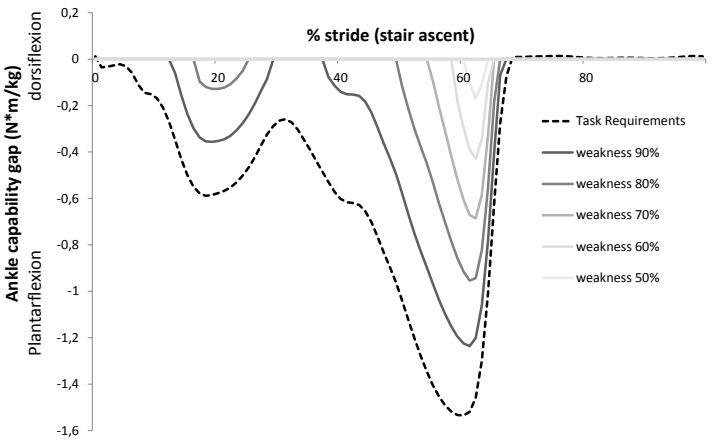

Figure 13.6: **Influence of muscle weakness on the plantarflexion capability gap during stair ascent.** The net ankle joint moment (task requirements, black dotted line) and the capability gap for different levels of muscle weakness (grey solid lines) are shown during a stair ascent stride. Both the level and timing of the capability gap increases when the level of weakness increases.

Discussion

The aim of the present study was to identify the capability gap during ADL when muscle weakness is present. We hypothesized that the AAN paradigm based on an MM differs substantially from the classic ID approach. The findings of the study can be used to define the specifications of the actuators to be integrated in powered assistive devices. Similar to the study of Carmichael et al. [2], we have used an MM to confront the force generating capacities of subjects when different levels of muscle weakness were introduced. This study explores the capability gap of the lower limbs during gross motor function related to typical ADL. Based on the capability gap; the level of assistive moments for each DOF can then be specified. The maximal capability gap in terms of moment or power can be used to select the actuators of an assistive device. Furthermore, the joint moment capability gap for a given ADL can be used to provide assistance as needed during the task execution through appropriate control of the assistive device.

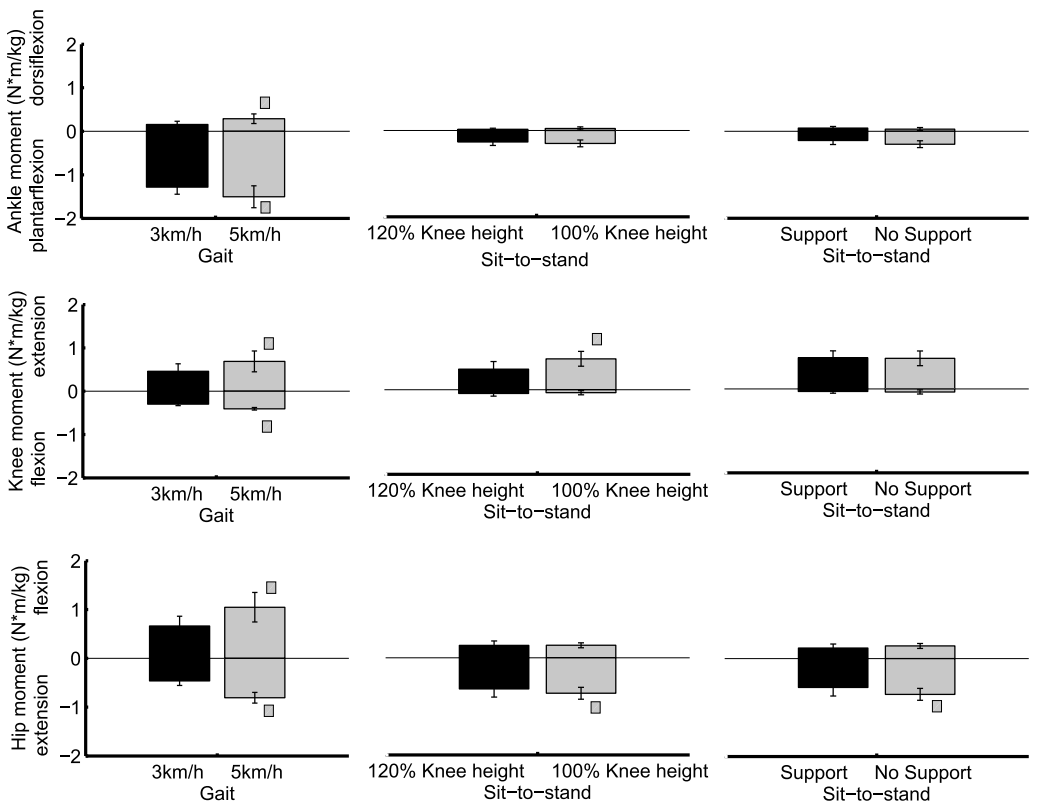

Figure 13.7: **The influence of more strenuous activities on the task requirements.** Increasing the gait speed (3km/h vs. 5km/h) causes an increase in the task requirements. There is an increase in net plantarflexion moment ($p<0.01$), dorsiflexion moment ($p<0.05$), knee extension moment ($p<0.05$), knee flexion moment ($p<0.01$), hip flexion moment ($p<0.01$) and hip extension moment ($p<0.01$). Increasing the chair height from 100% knee height to 120% knee height decreases the net knee extension and hip extension moment ($p<0.05$, $p<0.05$). The use of hand support causes a decrease in peak hip extension moment ($p<0.05$). The peak joint moments were compared using a wilocoxon sign rank test. The significant differences between the conditions are marked with a gray square.

Comparison between the ID approach and the AAN approach

Our findings confirm a substantial capability gap that depends on the specific ADL task and the level of muscle weakness. The capability gap is determined based on a joint moment deficit, illustrated in Figure 5. This figure emphasizes the difference between the ID approach and the AAN approach. The ID approach overestimates the required assistance as it relies solely on the demands of the task, whereas the AAN approach incorporates the capabilities of the subject. To date, several exoskeletons are designed based on a percentage of the peak joint moments that are calculated with the ID approach [13]. This method assumes that the capability of the subject is a constant percentage of the peak moment calculated with ID (Figure 8a). However, not only the task requirements, but also the angle dependency of the moment generating capacity around the joint and the task requirements of the adjacent joints will affect the capability gap. The use of MM–based dynamic simulations accounts for the force-length properties of the muscle fibers and for the change in moment arm of the muscle with the joint angle. Therefore, the moment generating capacity of the subject is not constant, but varies in magnitude during the motor task in the AAN approach and affects the capability gap (Figure 5 + Figure 8b). This causes a substantial difference between required assistance in the AAN approach and the (scaled) ID approach.

Capability gap during ADL

The simulation of muscle weakness allows us to identify to what extent the MM is able to cope with muscle weakness. The capability gaps are analyzed for the ankle and knee in the sagittal plane and for the hip in the sagittal, frontal and transversal plan. The MM is able to perform stair ascent until 30% of muscle weakness is present, which is caused by a plantarflexion capability gap. The tolerance of the MM-model to muscle weakness, i.e. level of muscle weakness for which the external demands imposed by gait, sit-to-stand, stand-to-sit and stair descent can no longer be met by active muscle force production, is respectively 40%, 70%, 80% and 30%. The tolerance level reported for gait agrees with previously reported simulation results [14]. The tolerance level for the sit-to-stand movement is comparable to the experimental results from Hughes et al [15]. In the presence of a reduction of 63% in maximal isometric force, elderly had to deliver 97% of their available strength to rise from the chair. Despite this agreement with experimental work, the tolerance level of 70% of muscle weakness for the sit-to-stand movement is somewhat surprising as difficulties in executing sit-to stance maneuvers are frequent in the elderly population [15]. These results indicate that in the elderly population, instability and inadequate coordination strategies more than muscle strength impair task execution when rising from a chair, as previously suggested by [16].

Several factors influence the assistance that is needed to perform ADL. Firstly, the level of muscle weakness determines the timing and the magnitude of the capability gap (Figure 6). Secondly, the magnitude of the capability gap varies between the tasks and the joints. The

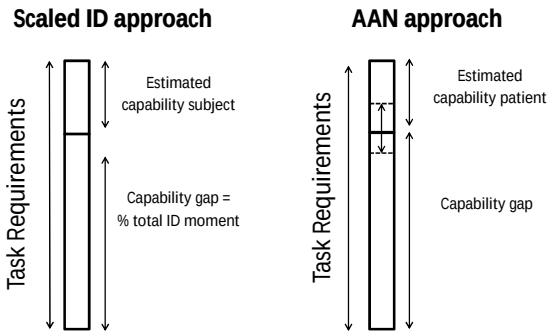

Figure 13.8: **Scaled ID approach versus AAN approach.** The scaled ID approach uses an estimation of the capability of the subject, which is the constant scaling factor of the peak task requirement. The AAN approach estimates the capability of the subject using an MM. Due to the musculotendon properties and the coupling between joints in the MM, the relative capability with regards to the ID moment varies with the kinematics and the task requirements at the other joints. Therefore the capability varies in time during ADL.

plantarflexion has the highest maximal capability gap for all the DOF. This is caused by the high plantarflexion moments that are imposed during stair ascent (1.70 Nm/kg). These results emphasize the importance of plantarflexion assistance in powered exoskeletons, in particular during stair ascent when muscle weakness is present. Furthermore, the high angular velocity during push off in combination with the high plantarflexion joint moments causes high positive joint powers. Therefore, generating sufficient plantarflexion moment and power will be an important challenge in the design of lower limb exoskeletons.

The crucial activity for the dorsiflexion capability gap is gait. Despite the relative small dorsiflexion moment deficits during gait, assisting this DOF is important for patients with drop foot gait. Our results show that there is only 0.11 (+/-0.02) Nm/kg dorsiflexion moment required to assist persons with total central paralysis of the dorsiflexion muscles during the selected ADL. However, the required dorsiflexion moment increases with gait speed (Figure 7).

In contrast with the ankle, the directional dominance of the assistance is less clear at the knee and hip joint: at the knee a slight dominance of knee extension assistance is confirmed whereas at the hip both flexion and extension require similar assistance. Furthermore, the level of weakness tolerated before introducing the moment generators is substantially higher at the knee and hip.

Limitations

The aforementioned results should be interpreted and used within the limitations of the methodology. Firstly, to assess the validity of the simulations, we have calculated the correlation between the simulated muscle activations and the measured muscle activity (Table1). These results indicate that the simulated muscle activation of all the mono-articular muscles correlates significantly with the measured activity. It is known that the activity of the bi-articular rectus femoris (RF) is less well predicted in the simulation [17]. Secondly, we assume in our simulation that persons perfectly adapt to an assistive moment, i.e. subjects are assumed not to oppose the induced external moment by increasing their antagonistic muscle activity or change the joint kinetics pattern. Indeed, experiments with single joint powered exoskeletons have shown that there is no difference in joint kinetics with and without assistance in healthy subjects [18, 19]. Furthermore, there is no difference in antagonistic muscle activity but a decrease in agonistic muscle activity when walking with a powered exoskeleton [20, 21]. Therefore, the assumption seems to be valid. Thirdly, the current workflow assumes that the MM represents the subject specific impairments of user/patient. It is known that aging and pathologies cause changes in musculotendon properties and activation dynamics [22]. In order to estimate the capability for these populations, the MM should ideally be adjusted towards the target population. Fourthly, the presented results rely on one specific objective function. However, the influence of the cost function on the capability gap is limited. The capability gap is the moment deficit when muscles maximally contribute to the desired motion. Therefore the influence of the cost function, which merely defines the muscle force distribution and not the overall level of agonistic muscle activity, on the moment deficit is small. Lastly, this study does not account for the stabilization of joints, fatigue, potential losses in body mass due to weakness and it assumes that the kinematics remain constant despite the presence of muscle weakness.

Application of the results

Within the limitations of the study, the results can be used in the design of assistive devices that support ADL. Elderly and patients with sarcopenia have a reduction in maximal isometric force that ranges between 20%-40% [11]. Our results suggest that in these cases solely an assistive plantarflexion moment is required to perform ADL (Figure 3). However, this study does not include the influence of fatigue on the capability gap of the individual subject. An additional knee flexion/extension and hip flexion/extension moment is required when the level of muscle weakness increases to 50%. In the study of Stevens-Lapsley et al. , there is a reduction of 50 $\pm$20% in maximal isometric force in persons with severe Parkinson disease, with 68% of the patients with severe Parkinson disease have 70% or less reduction in maximal isometric knee extensor moment [23]. Assuming an upper limit of body mass that equals 92.9 kg [23], Figure 3-4 can then be used to determine the design requirements of an exoskeleton that is able to assist this population in ADL: The exoskeleton should be able to deliver peak moments of 89.1 Nm (254 W) at the ankle joint, 33.4 Nm (72.5 W) at the knee joint and 29.7

Nm (63.17W) at the hip joint. Furthermore, the present simulation workflow can be used to select the actuators of an assistive device with specific design criteria. The relative cost of the ideal moment actuators at the hip, knee, and ankle will influence bi-articular muscle action and therefore the capability gap at the joints. Therefore, the relative costs can be optimized for specific design criteria. For example, one could increase the cost of using the ideal moment actuator at the ankle joint in order to minimize the actuator size at the ankle (at the cost of increasing the size at the knee and hip).

Further directions

Although the added value of the current results is without question, future work should concentrate on forward simulations that allow changes in the motor strategy during the task. For example, changing the strategy to stand up from a chair influences the kinematics and peak joint moments [24]. Hughes et al. described a difference in chair rise strategy in the functionally impaired elderly in order to increase their stability [16]. On the one hand, these differences in motor strategies could influence the required assistance during ADL. On the other hand, exoskeletons are designed to increase the physical performance of the user, in order to achieve or exceed a healthy motor function.

The current study provides sufficient proof-of-concept to consider the design of targeted functional protocols that allow tuning the control settings for the exoskeleton to the functional limitations in terms of muscle weakness of individual subjects. This AAN control will promote active participation of the user which is essential to prevent disuse and promote neuromotor rehabilitation.

Conclusion

The combination of experimental measurements with an MM enables the identification of the capability gap during ADL when muscle weakness is present. Both the magnitude and timing of the assistance in this AAN approach differs substantially from the classic ID approach. This AAN is a more physiological approach, since it accounts for the capabilities of the operator which are modeled in the MM. The results can be used, within the limitations of the methodology, in the mechatronic design and control of an assistive device.

References

1. Kaelin-lang A, Sawaki L, Cohen LG: Role of Voluntary Drive in Encoding an Elementary Motor Memory. 2005:1099–1103.

2. Carmichael MG, Liu D: Estimating Physical Assistance Need Using a Musculoskeletal Model. 2013, 60:1912–1919.

3. Skelton J, Wu S: Design of a Powered Lower-Extremity Orthosis for Sit-to-Stand and Ambulation Assistance. 2013, 7(September):1–2.

4. Tsukahara A, Kawanishi R, Hasegawa Y, Sankai Y: Sit-to-Stand and Stand-to-Sit Transfer Support for Complete Paraplegic Patients with Robot Suit HAL. Adv Robot 2010, 24:1615–1638.

5. Bleex EE, Zoss AB, Kazerooni H, Chu A: Biomechanical Design of the Berkeley Lower. Trans Mechatron 2006, 11:128–138.

6. Carmichael MG, Liu D: A task description model for robotic rehabilitation. Conf Proc Annu Int Conf IEEE Eng Med Biol Soc IEEE Eng Med Biol Soc Conf 2012, 2012:3086–9.

7. Carmichael MG, Liu D: Towards using Musculoskeletal Models for Intelligent Control of Physically Assistive Robots. 2011:8162–8165.

8. Hermens HJ, Freriks B, Disselhorst-Klug C, Rau G: Development of recommendations for SEMG sensors and sensor placement procedures. J Electromyogr Kinesiol 2000, 10:361–374.

9. Delp SL, Anderson FC, Arnold AS, Loan P, Habib A, John CT, Guendelman E, Thelen DG: OpenSim: open-source software to create and analyze dynamic simulations of movement. IEEE Trans Biomed Eng 2007, 54:1940–50.

10. Hamner SR, Seth A, Delp SL: Muscle contributions to propulsion and support during running. J Biomech 2010, 43:2709–16.

11. Doherty TJ: Invited review: Aging and sarcopenia. J Appl Physiol Bethesda Md 1985 2003, 95:1717–27.

12. Crowninshield RD: Use of Optimization Techniques to Predict Muscle Forces. J Biomech Eng 1978, 100:88–92.

13. Cenciarini M, Dollar AM: Biomechanical considerations in the design of lower limb exoskeletons. IEEE Int Conf Rehabil Robot Proc 2011, 2011:5975366.

14. Van der Krogt MM, Delp SL, Schwartz MH: How robust is human gait to muscle weakness? Gait Posture 2012, 36:113–9.

15. Hughes M a, Myers BS, Schenkman ML: The role of strength in rising from a chair in the functionally impaired elderly. J Biomech 1996, 29:1509–13.

16. Hughes M a, Schenkman ML: Chair rise strategy in the functionally impaired elderly. J Rehabil Res Dev 1996, 33:409–12.

17. Duysens J, De Groote F, Jonkers I: The flexion synergy, mother of all synergies and father of new models of gait. Front Comput Neurosci 2013, 7(March):14.

18. Kao P-C, Lewis CL, Ferris DP: Invariant ankle moment patterns when walking with and without a robotic ankle exoskeleton. J Biomech 2010, 43:203–9.

19. Lewis CL, Ferris DP: Invariant hip moment pattern while walking with a robotic hip exoskeleton. J Biomech 2011, 44:789–93.

20. Galle S, Malcolm P, Derave W, Clercq D De: Gait & Posture Adaptation to walking with an exoskeleton that assists ankle extension. Gait Posture 2013:1–5.

21. Sawicki G: Mechanics and energetics of level walking with powered ankle exoskeletons. J Exp Biol 2008:1–2.

22. Thelen DG: Adjustment of Muscle Mechanics Model Parameters to Simulate Dynamic Contractions in Older Adults. J Biomech Eng 2003, 125:70.

23. Stevens-Lapsley J, Kluger BM, Schenkman M: Quadriceps muscle weakness, activation deficits, and fatigue with Parkinson disease. Neurorehabil Neural Repair 2012, 26:533–41.

24. Yoshioka S, Nagano A, Himeno R, Fukashiro S: Computation of the kinematics and the minimum peak joint moments of sit-to-stand movements. Biomed Eng Online 2007, 6:26.